Optimization of Polyphenols Extraction Using Response Surface Methodology and Application of Near Infrared Spectroscopy to Phenolic Content Analysis of Pine Bark

by

Nana Sarfo Agyemang Derkyi

A Thesis submitted to the Department of Chemical Engineering,

Kwame Nkrumah University of Science and Technology

In partial fulfillment of the requirements for the degree of

DOCTOR OF PHILOSOPHY

Faculty of Chemical and Materials Engineering

College of Engineering

April 2010

DECLARATION

I hereby declare that this submission is my own work towards the PhD and that, to the best of my knowledge, it contains no material previously published by another person nor material which has been accepted for the award of any other degree of the University, except where due acknowledgement has been made in the text.

Nana Sarfo Agyemang Derkyi
…… …….. ……
(PhD Candidate)

Certified by:

Nana (Dr.) Baah Boakye
…… …….. ……
(Supervisor)

Mrs. Zsuzsanna Momade
…… …….. ……
(Head of Department)

DEDICATION

This dissertation is dedicated to my lovely wife Afua Adutwumwaa and sweet children Nana Osei, Nana Baah and Maame Abenaa and also to the loving and cherished memories of my father, Nana Boadu Kwadwo II, my mother, Obaapanyin Abena Konama, my father in-law, Mr. Kofi Acheampong Ameyaw and my good friend Harry Agudetse who we recently lost. Finally, to my late supervisor Ing. Dr. Benjamin Adu Amankwa who after all the work had been done did not live to see the defense of the thesis. You all will be forever missed!

ABSTRACT

The utilization of pine bark for processing water resistant phenol-formaldehyde adhesive for plywood production encounters difficulties due to the very high reactivity of the formaldehyde condensable phenolics and other un-intended compounds (sugars) extracted into solution, as well as time consuming and costly chemical analysis. The potential of near infrared reflectance spectroscopy (NIRS) for rapidly and accurately determining the polyphenolic contents in *Pinus caribaea* bark extracts was assessed by means of multivariate calibration techniques. To optimize the polyphenol content, four different solvents (aqueous acetone, aqueous ethanol, aqueous NaOH and water) were used in the extractions. Batch experiments were performed at different solvent concentrations, time, temperature and liquid-solid ratio. Mathematical polynomial models were proposed to identify the effects of individual interactions of these variables on the extraction of polyphenols and optimum content using response surface methodology (RSM). The optimized conditions were used to extract polyphenols which were used in the formulation of resol resins for plywood manufacture. The first derivative spectra with PLS regression were found to provide the best prediction of the tannin content and Stiasny number of pine bark with a SECV = 0.14 and 1.26 and r^2 = 0.97 and 0.95 respectively. The predicted values were thus highly correlated with costly measured values of tannin content and Stiasny number. The highest extraction model efficiency (78.98%) was observed for aqueous extraction when only tannin content was maximized in the numerical optimization process. This corresponded to optimum extraction conditions of 69°C extraction temperature, 126 min extraction time and 23:1 liquid-solid ratio. The RSM model that gave a high tannin content (18.85%) with a corresponding good quality resin (shear strength = 2.4 MPa, 10% delamination) was found for aqueous ethanol extraction when the objective function was to maximize both the tannin content and Stiasny number and minimize the sugar content simultaneously.

Table of Contents

ABSTRACT iv

List of Tables ix

List of Figures x

ACKNOWLEDGEMENTS xiii

CHAPTER ONE 1

INTRODUCTION 1

1.1 Extraction of Phenolics for Phenol-Formadehyde Resins 1

1.1.1 Availability of raw material 1

1.1.2 Use of near infrared spectroscopy (NIRS) to rapidly determine phenolic contents 2

1.1.3 Extraction of phenolic compounds 3

1.1.4 Utilization of phenolic extracts in phenol-formadehyde resins 4

1. 2 Extraction Process Optimization 6

1.3 Response Surface Methodology 8

1.4 Research Problem 11

1.5 Objectives 12

CHAPTER TWO 13

LITERATURE REVIEW 13

2.1 Modeling Chemical Properties using Near Infrared Spectroscopy (NIRS) 13

2.1.1 Near infrared spectrum 14

2.1.2 Chemometric calibration 14

2.1.3 Spectral pretreatment 16

2.1.4 Robustness of model 16

2.2 Solid-Liquid Extraction 16

2.2.1 Mechanism of extraction 17

2.2.2 Methods of operation 18

2.2.3 Extraction equipment 19

2.2.4 Design of an extraction process 19

2.2.4.1 Process and Operating Conditions 19
2.2.4.2 Extractor-Sizing Calculations 21
2.2.5 Mass transfer 25
2.2.6 Material balances 27
2.2.7 Application of solid-liquid extraction modeling 29
2.3 Optimization 31
2.3.1 Optimization methods 31
2.3.2 Response surface methodology 32
2.3.2.1 Analysis of a First-Order Response Surface 34
2.3.2.2 Analysis of a Second-Order Response Surface 34
2.3.2.3 Designs for Fitting Second-Order Model 35
2.4 Tannins 36
2.4.1 Extraction of tannins 38
2.4.2 Chemistry of condensed tannins 39
2.4.3 Hydrolysis of tannins 41
2.5 Phenol-formaldehyde resins 42
2.5.1 Addition Reaction 43
2.5.2 Condensation Reaction 45
2.6 Naturally Derived Phenolic Resins 48
2.6.1 Reactivity of pine bark tannins 49
2.6.2. Development of tannin production technologies 50
2.6.3. Factors favouring or limiting commercial production of tannins 51
2.7 Plywood Manufacture 53
CHAPTER THREE 55
MATERIALS AND METHODS 55
3.1. Chemometric Calibration of Phenolic Quantities in Pine Bark 55
3.1.1. Materials 55

3.1.2. Extraction procedure 55
3.1.3 Chemical Analysis of Pine Bark Extract 56
3.1.3.1. Total phenolics determination 56
3.1.3.2. Tannin content determination 56
3.1.3.3. Stiasny reaction 56
3.1.4. Near Infrared Spectra Aquisition 57
3.1.5. Chemometric Calibration 57
3.2. Optimization of Extraction Process Parameters 59
3.2.2. Experimental Design 59
3.2.3. Extraction Process 59
3.2.3.1. Single Factor Experiments 60
3.2.3.2. Response Surface Methodology 62
3.3. Accelerated Solvent Extraction (ASE) 65
3.4. Formulation of Tannin-Formaldehyde Adhesive for Plywood Manufacture 66
3.4.1. Materials 66
3.4.2. Resin Processing 66
3.4.3. Effect of Extraction Conditions on Resin Quality 67
3.4.4. Viscosity and Pot Life Determination 69
3.4.5. Panel Preparation 69
3.4.6. Adhesive Bond Evaluation 69
3.5. Statistical Analysis 70
CHAPTER FOUR 71
RESULTS AND DISCUSSIONS 71
4.1 Calibration of chemical properties 71
4.2 Optimization of Phenolic Extraction 80
4.2.1 Results from single factor extraction experiments 80
4.2.1.1 Selection of solvent concentration range 80

4.2.1.2 Selection of liquid-solid ratio range 81
4.2.1.3 Selection of extraction time range 82
4.2.1.4 Selection of extraction temperature range 83
4.2.1.5 Selection of Extraction stage 84
4.2.2.1 Optimum extraction conditions based on maximizing tannin content 86
4.2.2.2 Optimum extraction conditions based on minimizing sugar content 106
4.2.2.3 Optimum extraction conditions based on maximizing Stiasny number 126
4.2.2.4 Optimum extraction conditions based on tannin content, sugar content and Stiasny number simultaneously 145
4.2.2.5 Verification of optimal extraction conditions 148
4.2.2.6 Efficiencies of the models 148
4.3 Effect of phenolic extraction condition on resin quality 152
CHAPTER FIVE 158
CONCLUSIONS AND RECOMMENDATIONS 158
5.1 Conclusion 158
5.2 Recommendations 160
REFERENCES 161
APPENDICES 171

List of Tables

Table 2.1: Some models and parameters used in solid-liquid extraction……29
Table 3.1: Coded and real values of solvent extractions…….....63
Table 3.2: Resins prepared from tannins extracted at various optimized conditions……...68
Table 4.1: Descriptive statistics for tannin content and Stiasny number of *P. caribaea* bark……71
Table 4.2: PLS regression calibration developed for polyphenol content, tannin content and Stiasny number……...74
Table 4.3: Comparison of experimental and predicted values using Box-Behnken design for four independent variables on the content of tannin from aqueous acetone extraction……87
Table 4.4: Comparison of experimental and predicted values using Box-Behnken design for four independent variables on the content of tannin from aqueous ethanol extraction……...92
Table 4.5: Comparison of experimental and predicted values using Box-Behnken design for four independent variables on the content of tannin from aqueous NaOH extraction.……..... 97
Table 4.6: Comparison of experimental and predicted values using Box-Behnken design for four independent variables on the content of tannin from water extraction……..102
Table 4.7: Comparison of experimental and predicted values using Box-Behnken design for four independent variables on the sugar content from aqueous acetone extraction……107
Table 4.8: Comparison of experimental and predicted values using Box-Behnken design for four independent variables on the sugar content from aqueous ethanol extraction……112
Table 4.9: Comparison of experimental and predicted values using Box-Behnken design for four independent variables on the sugar content from aqueous NaOH extraction…….117
Table 4.10: Comparison of experimental and predicted values using Box-Behnken design for three independent variables on the sugar content from water extraction ……122
Table 4.11: Comparison of experimental and predicted values using Box-Behnken design for four independent variables on the Stiasny number from aqueous acetone extraction……127
Table 4.12: Comparison of experimental and predicted values using Box-Behnken design for four independent variables on the Stiasny number from aqueous ethanol extraction……132
Table 4.13: Comparison of experimental and predicted values using Box-Behnken design for four independent variables on the Stiasny number from aqueous NaOH extraction…….136
Table 4.14: Comparison of experimental and predicted values using Box-Behnken design for three independent variables on the Stiasny number from water extraction……141
Table 4.15: Optimized conditions for aqueous acetone extraction with both predicted and actual values…….149
Table 4.16: Optimized conditions for aqueous ethanol extraction with both predicted and actual values…….150

Table 4.17: Optimized conditions for aqueous NaOH extraction with both predicted and actual values……150
Table 4.18: Optimized conditions for water extraction with both predicted and actual values……150
Table 4.19: Optimization model efficiencies of solvent extraction process……..151

List of Figures

Figure 2.1: Composition diagrams for extraction calculations; (a) right-triangular diagram; (b) modified Ponchon-Savarit diagram…….25
Figure 2.2: Contour plot with a response surface for a process depending on temperature and pressure……..33
Figure 2.3: Central Composite Design for k = 2……..35
Figure 2.4: Hydrolyzable and condensed tannins……37
Figure 2.5: Rings A and B of tannin……40
Figure 2.6: Structure of condensed tannin……40
Figure 2.7: Phenol-formaldehyde polymer from its reactants……..42
Figure 2.8: Resonance structures of phenoxide ions in alkaline medium……44
Figure 2.9: Formation of intra-molecular hydrogen bonds……..44
Figure 2.10: Formation of a chelate ring structure under NaOH catalysis……...44
Figure 2.11: Addition reactions during resolesynthesis……...45
Figure 2.12: Formation of quinone methide intermediate under alkaline conditions……..46
Figure 2.13: Methylene bridge formation through quinone methide intermediates……46
Figure 2.14: Dimethylene ether bridge formation and its conversion to methylene bridge….47
Figure 2.15: Additional and unusual crosslink structures in cured resoles……..47
Figure 4.1: Near infrared diffuse reflectance spectra of *P.caribaea* bark……75
Figure 4.2: First derivative spectra of *P. caribaea* bark in selected wavelength region……..76
Figure 4.3a: NIR spectra of four *P.caribaea* bark samples showing different tannin contents……76
Figure 4.3b: NIR spectra of four *P.caribaea* bark samples showing different Stiasny numbers……...77
Figure 4.4a: Actual versus predicted values for calibration estimating polyphenol content...78
Figure 4.4b:Actual versus predicted values for calibration estimating tannin content ……...78
Figure 4.4c: Actual versus predicted values for calibration estimating Stiasny number ……79
Figure 4.5: RMSECV plotted against Rank for polyphenol content, tannin content and Stiasny number……..79
Figure 4.6: Effect of extraction solvent concentration on tannin content……80
Figure 4.7: Effect of liquid-solid ratio on tannin content……81
Figure 4.8: Effect of extraction time on tannin content……...82
Figure 4.9: Effect of extraction temperature on tannin content……...84
Figure 4.10: Effect of extraction stage on tannin content……85
Figure 4.11a: Response surface plot showing percentage tannin content from aqueous acetone extraction at varying extraction temperature and time…….89
Figure 4.11b: Response surface plot showing percentage tannin content from aqueous acetone extraction at varying temperature and solvent concentration……90
Figure 4.11c: Response surface plot showing percentage tannin content from aqueous acetone extraction at varying extraction time and solvent concentration……..90

Figure 4.12: Effect of individual variables on the content of tannin from aqueous acetone extraction……...91
Figure 4.13a: Response surface plot showing percentage tannin content from aqueous ethanol extraction at varying extraction temperature and time……94
Figure 4.13b: Response surface plot showing percentage tannin content from aqueous ethanol extraction at varying extraction temperature and concentration.…….95
Figure 4.13c: Response surface plot showing percentage tannin content from aqueous ethanol extraction at varying extraction temperature and liquid-solid ratio……95
Figure 4.14: Effect of individual variables on the content of tannin from aqueous ethanol extraction…….....96
Figure 4.15a: Response surface plot showing percentage tannin content from aqueous NaOH extraction at varying temperature and solvent concentration……99
Figure 4.15b: Response surface plot showing percentage tannin content from aqueous NaOH extraction at varying extraction temperature and time……100
Figure 4.15c: Response surface plot showing percentage tannin content from aqueous NaOH extraction at varying extraction time and solvent concentration……100
Figure 4.16: Effect of individual variables on the content of tannin from aqueous NaOH extraction……101
Figure 4.17a: Response surface plot showing percentage tannin content from water extraction at varying extraction time and liquid-solid ratio…….104
Figure 4.17b: Response surface plot showing percentage tannin content from water extraction at varying extraction time and temperature……104
Figure 4.17c: Response surface plot showing percentage tannin content from water extraction at varying extraction and liquid-solid ratio……105
Figure 4.18: Effect of individual variables on the content of tannin from water extraction……106
Figure 4.19a: Response surface plot showing percentage sugar content from aqueous acetone extraction at varying extraction time and solvent concentration…....110
Figure 4.19b: Response surface plot showing percentage sugar content from aqueous acetone extraction at varying extraction time and temperature……...110
Figure 4.19c: Response surface plot showing percentage sugar content from aqueous acetone extraction at varying extraction time and liquid-solid ratio……...111
Figure 4.20: Effect of individual variables on the sugar content from aqueous acetone extraction…….....112
Figure 4.21a: Response surface plot showing percentage sugar content from aqueous ethanol extraction at varying temperature and solvent concentration……...115
Figure 4.21b: Response surface plot showing percentage sugar content from aqueous ethanol extraction at varying extraction temperature and time……...115
Figure 4.21c: Response surface plot showing percentage sugar content from aqueous ethanol extraction at varying liquid-solid ratio and solvent concentration…….116
Figure 4.22: Effect of individual variables on the sugar content from aqueous ethanol extraction……...……...117
Figure 4.23a: Response surface plot showing percentage sugar content from aqueous NaOH extraction at varying temperature and solvent concentration……..120
Figure 4.23b: Response surface plot showing percentage sugar content from aqueous NaOH extraction at varying extraction temperature and time……....120
Figure 4.24: Effect of individual variables on the sugar content from aqueous NaOH extraction…….……...121
Figure 4.25a: Response surface plot showing percentage sugar content from water extraction at varying extraction temperature and time……...……124

Figure 4.25b: Response surface plot showing percentage sugar content from water extraction at varying extraction temperature and liquid-solid ratio…..…….124
Figure 4.25c: Response surface plot showing percentage sugar content from water extraction at varying liquid-solid ratio and extraction time……..….....125
Figure 4.26: Effect of individual variables on the sugar content from water extraction 126
Figure 4.27a: Response surface plot showing Stiasny number from aqueous acetone extraction at varying extraction time and liquid-solid ratio…….....130
Figure 4.27b: Response surface plot showing Stiasny number from aqueous acetone extraction at varying extraction temperature and liquid-solid ratio….……130
Figure 4.27c: Response surface plot showing Stiasny number from aqueous acetone extraction at varying extraction time and temperature……..……131
Figure 4.28: Effect of individual variables on the Stiasny number from aqueous acetone extraction…….....131
Figure 4.29a: Response surface plot showing Stiasny number from aqueous ethanol extraction at varying extraction time and temperature……..……..134
Figure 4.29b: Response surface plot showing Stiasny number from aqueous ethanol extraction at varying solvent concentration and liquid-solid ratio..…….…135
Figure 4.29c: Response surface plot showing Stiasny number from aqueous ethanol extraction at varying extraction temperature and liquid-solid ratio..……...135
Figure 4.30: Effect of individual variables on the Stiasny number from aqueous ethanol extraction…….....136
Figure 4.31a: Response surface plot showing Stiasny number from aqueous NaOH extraction at varying extraction temperature and solvent concentration……..139
Figure 4.31b: Response surface plot showing Stiasny number from aqueous NaOH extraction at varying extraction temperature and liquid-solid ratio…….…...139
Figure 4.32: Effect of individual variables on the Stiasny number from aqueous NaOH.. extraction……..……...140
Figure 4.33a: Response surface plot showing Stiasny number from water extraction at varying extraction temperature and time……..…….143
Figure 4.33b: Response surface plot showing Stiasny number from water extraction at varying extraction temperature and liquid-solid ratio…….…...143
Figure 4.33c: Response surface plot showing Stiasny number from water extraction at varying extraction time and liquid-solid ratio ...……144
Figure 4.34 Effect of individual variables on the Stiasny number from water extraction….145
Figure 4.35: Pot life against viscosity of resins……..156
Figure 4.36: Effect of extraction solvent and mode of extraction optimization on dry shear strength of plywood bond……...……...156
Figure 4.37: Effect of extraction solvent and mode of extraction optimization on wet shear strength of plywood bond……..157
Figure 4.38: Effect of extraction solvent and mode of extraction optimization on three cycle soak/dry tests for plywood bond delamination……....157

ACKNOWLEDGEMENTS

Wisdom and knowledge comes from the one who transcends man's understanding. To Him I give all the glory.

I appreciate the immense supervisory role of my late supervisor, Ing. Dr. B. Adu Amankwa. I would like to thank my advisors Dr. Daniel Sekyere and Dr. N. A. Darkwa for their guidance and support throughout this process. Indeed, you all encouraged me to explore all of my potentials and provided sound advice. I am also grateful to Nana (Dr.) Baah Boakye for supervising the work after the demise of Ing. Dr. B. Adu Amankwa. To the lecturers of the Department I say a very big thank you to you all. As a matter of actual fact, I appreciated your criticisms and wonderful suggestions made towards the progress of the study.

No one can accurately measure the sacrifices made by a beloved family and also get the response factors to be accurate. If you saw my wife beaming with smile, she had just finished an arduous task of being a wife or counting days when my long nights working would be over. As if that was not enough, she also spent time going through my thesis amidst her own tight schedule. Afua, I say bravo and a very big thank you for your prayers, support and understanding. And the children? there were times they will say 'please daddy stay home with us' but knowing what is at stake, they will give in and allow me to go. Nana Osei, Nana Baah and Maame Abena I thank you too for your consideration and prayers. The goodwill I have enjoyed and continue to enjoy through life's process is very much appreciated and for that I thank my family the Derkyi family and Ameyaw family.

I would like to express my appreciation to CIRAD-FORET for the use of the near infrared spectrometer and the accelerated solvent extractor. In particular, I would like to thank Henri Bailleres, Marie-France Thevenon, Gilles Chaix and Nabila Boutahar. Again, I wish to express my gratitude to the management and staff of Pledgetex Plywood limited and Bondplex for making their facilities available for the work. I am also grateful to the staff of CSIR-FORIG for their assistance and comments on my work, which was very helpful. In particular I thank Dr. A. A. Oteng-Amoako who urged me on to pursue a PhD, Wilson, Alhaji, Kofi, Kwame and indeed all the good numerous colleagues.

Finally, I am appreciative of the friendship we enjoyed together as course-mates, going through thick and thin to master the subjects and pass. Victor, Augustine, Asiedu and Owo I say thank you for the good relationships we shared together. Yaw, Abena, Charity, Nasta, Sky and all the friends I say thank you for your companionship and prayers.

CHAPTER ONE

INTRODUCTION

1.1 Extraction of Phenolics for Phenol-Formadehyde Resins

1.1.1 Availability of raw material

The bark and wood extracts of various commercially important trees contain polyphenolics which in the form of tannins can form condensation products with formaldehyde to produce wood adhesives. Such condensation products have been widely studied particularly with a view to obtain suitable adhesives for plywood and particle-board (Yazaki, 1983; Vazquez et al, 1987; Pizzi, 1994). These bark tannin and wood extracts are well known in the art and may be obtained, for example, by extraction from milled wood and bark in water in which the tannins tend to dissolve.

Research on wattle tannin-based adhesives started in the 1950s with the initial studies conducted by Dalton (1950 and 1953). Subsequent work by Plomley (1959 and 1966) demonstrated that wattle-bark tannins are suitable raw materials for plywood and particleboard adhesives production. Several attempts to partially replace phenol in phenol-formaldehyde resol-type resins with carbohydrates derived from wood have been reported in the literature (Conner *et al.,* 1986; Christiansen and Gillespie, 1986). Lignin, a residue from the pulp and paper industry and from wood acid hydrolysis, has also been used to partially replace phenol (Nimz, 1983; Sellers 1990; Roffael and Dix, 1991). In a new Japanese approach for partially replacing phenol in phenol-

formaldehyde (PF) resins, whole wood substance, instead of isolated fractions (i.e. carbohydrates, lignin, and tannins), is dissolved in phenol. The resulting material is used to prepare PF adhesives (Shiraishi *et al.,* 1987; Ono and Inoue, 1994; Pu *et al.,* 1994). Among suitable raw materials, tannins represent the best substitute for phenol in resin preparation. Tannin extracted from the bark of the black wattle tree *(Acacia mearnsii,* formerly *A. mollissima)* and quebracho *(Schinipisiss* spp.) is available commercially (Pizzi and Scharfetter ,1981; Drlje, 1975). It is the renewable resource that is most widely used in adhesive production. A considerable pool of tannins is also potentially available, from the bark of several pine *(Pinus radiata, P. patula, P. elliotti, P. taeda, P. pinaster, P. halepensis* etc.), hemlock (*Tsuga heterophylla*), Douglas-fir *(Pseudotsuga menziessi),* and spruce *(Picea* spp.) (Pizzi and Scharfetter, 1981). It is reported that Ghana has nearly one hundred tannin-containing tree species (Irvine, 1961). These species include *Acacia nilotica, Pinus caribaea, Azadiracta indica,* and *Tetrapleura tetraptera* which are also abundant in Ghana. Thus availability of raw material base for a polyphenol-formaldehyde resin could therefore be assured.

1.1.2 Use of near infrared spectroscopy (NIRS) to rapidly determine phenolic contents

Precise information on the composition and content of polyphenolic extracts is needed so that their performances in adhesive applications can be improved. One of the main problems affecting utilization of plant phenolics is the lack of information on contents and on the variability between tree species and between different parts of the tree. This makes it difficult to compute economic analysis of new phenolics.

Near infrared reflectance spectroscopy (NIRS) is a rapid, cheap, environmentally-friendly and non-destructive technique offering the potential for accurate and repeatable measurements of chemical constituents in organic materials (Norris, 1989; Norris *et al*., 1976; Williams, 1975).

Use of NIRS in chemical analysis has grown due to development of computers and specific software for analysis in analytical chemistry and in statistics. Traditionally, NIRS has been used to determine the composition of agricultural products, but today, it is also used in other areas, such as the oil industry, pharmaceuticals, polymers, food industry, and clinical laboratories (Hall and Pollard, 1992). The Association of Official Analytical Chemists (1995) recommends use of this technique for the analysis of phenolic compounds.

1.1.3 Extraction of phenolic compounds

Whenever extractives, particularly from pine bark, have been used for wood adhesives, difficulties have been encountered with low content of extracts, excessive viscosity and inconsistent quality of extractives from the bark (Yazaki,1985). One potential method of overcoming these problems has been fractionation of the extracts. Ultra-filtration methods have been found to be useful in overcoming problems relating to the excessive viscosity and inconsistent quality of the extractives from radiata pine bark (Yazaki and Hillis, 1980) and improvements in these methods have enabled effective fractionation of the extracts (Yazaki,1985). However, ultra-filtration processes are too expensive for the commercial production of wood adhesives from pine bark.

Accelerated solvent extraction (ASE) is an innovative extraction technique that combines elevated temperature and pressures with liquid solvents to achieve fast and efficient removal of analytes from various matrices (Dionex Technical Note 208, 1998). ASE has been demonstrated to be equivalent to existing extraction methodologies such as Soxhlet and automated Soxhlet for most analytes from solid and semisolid matrices. ASE is a more efficient form of liquid solvent extraction, so all of the principles inherent to that technique apply. To achieve efficient extraction, appropriate sample preparation techniques and operational parameters must be selected. It is normally very easy to transfer an existing solvent-based extraction method to ASE technology. The use of static cycles developed is to introduce fresh solvent during the extraction process, which helps to maintain a favourable extraction equilibrium. This effectively approximates dynamic extraction conditions without the need for troublesome flow restrictors to maintain pressure (Dionex Technical Note 208, 1998).

A low-cost technology for the production from pine bark of high content and uniform quality tannin extracts suitable for wood adhesives is still required. Extraction by refluxing was used in this work rather than soxhlet extraction or ASE because refluxing is a close approximation to industrial extractions rather than soxhlet extraction. Despite its high efficiency in extraction, ASE still remains a laboratory analytical method and currently it is difficult to set up large plants because of the very high pressure required. However, advantage was taken of its high efficiency to compare the efficiencies of various optimized extraction processes in this study.

1.1.4 Utilization of phenolic extracts in phenol-formadehyde resins

Phenol-Formaldehyde resins (PF) result from the polycondensation of phenol and formaldehyde. From a commercial standpoint, PF resins have been of prime importance since the early 1900's,

when they appeared as the first synthetically produced polymers (Pizzi, 1994). Empirical research and development has significantly contributed to the technological properties of PF. In fact, PF properties can be tailored for a variety of applications, including foundry resins, molding compounds and wood-based composite binders (Knop and Pilato, 1985). PF resins are weather durable. As a consequence they are utilized in exterior grade wood-based composites (Knop and Pilato, 1985; Sellers, 1985). Depending upon reagent ratios and catalyst type, two classes of adhesives have been developed. *Resoles* are produced from base catalyzed polymerization using excess formaldehyde. On the other hand, *Novolacs* are obtained from acid catalyzed polymerization using excess phenol. The manufacture of wood-based composites utilizes mainly resoles.

There have been several attempts to replace part of the petroleum-derived phenolic compounds in wood bonding adhesives with phenolic-type compounds obtained from renewable sources. Principal among these efforts is the development of adhesives from tannin contained in wood bark (Pizzi, 1983). Bark extracts are complex mixtures of organic compounds including tannins, lignin, cellulose, and other minor natural substances, together with chemicals used in the extraction process. The condensed tannins whose chemical structure is that of polyflavonoids (Pizzi, 1983) provide the possibility, of using them for replacing certain components of synthetic adhesives with the aim of both reducing manufacturing costs and possibly improving the final product.

Tannins from pine bark, like all the condensed tannins, consist of flavonoid units with varying degrees of condensation (Pizzi, 1983), which can be used for the preparation of bio-adhesives for

bonding wood. In the past, there has been considerable interest worldwide in the development of tannin wood adhesives as substitutes for wood adhesives derived from non- renewable resources, and in particular phenol and resorcinol which are derivatives from the petrochemical industry. Tannins from two hardwoods: wattle and quebracho, have been produced and used commercially for many years, but production of pine bark tannins has generally not been successful on a commercial scale (von Leyser and Pizzi, 1990). Pine bark, however, is a good source of natural polyphenolic compounds for wood adhesives. Many attempts have been made to utilize it as a wood adhesive (Yazaki, 1985).

There is potential for increased demand for use of more bonded wood products to cope with increasing variable resources, and thus more adhesives are needed especially from renewable resources. Thus, the technology when fully realized would provide a substantial means by which low-value tropical wood resources may be value-added. The full extent of the economic benefit will depend on the extent to which the process is employed and on the overall efficiency of the conversion processes with respect to the final cost analysis. Moreover, the creation of jobs within the forest sector provides a further economic benefit. Tannin use, however, has been limited by its high reactivity and viscosity, which causes short pot life, and by its lack of intermolecular crosslinking, causes weak adhesive bonds.

1. 2 Extraction Process Optimization

Presently, there are many research articles about optimization methods; the typical ones are based on calculus, numerical methods, and random methods. The calculus based methods have been intensely studied and are subdivided in two main classes: 1) the direct search methods find

a local maximum moving on a function over the relative local gradient directions and 2) the indirect methods usually find the local ends solving a set of non-linear equations, resultant of equaling the gradient from the object function to zero, i.e., by means of multidimensional generalization of the notion of the function's extreme points from elementary calculus give a smooth function without restrictions to find a possible maximum which is to be restricted to those points whose slope is zero in all directions. Both methods have been improved and extended.

Considering the diversity in composition of the natural sources of polyphenols, as well as the structure and physicochemical properties of these compounds, a universal extraction protocol is not conceivable, and specific processes must be designed and optimized for each phenolic source (Escribano-Bailon and Santos-Buelga, 2003; Pinelo *et al.,* 2005). Moreover, co-extraction of undesirable compounds such as sugars, fats, terpenes or pigments, must be avoided and has to be taken into account during the optimization of the process. Many factors contribute to the efficiency of solvent extraction, such as the type of solvent, the pH, the temperature, the number of steps, the liquid-to-solid ratio, and the particle size and shape of the plant matrix (Mafart and B´eliard, 1992).

Implementing process optimization helps to ensure that the extraction process is working as effectively as possible. Recently, some companies are creating mathematical models of their processes to better understand and review the interdependencies between process variables. Not only are these models able to obtain real-time data from throughout the process, but they also are able to make changes to process parameters in real-time. The design variables throughout

extraction processes are typically required for these mathematical models, and quantifying these values requires a solid understanding of the behavior of the individual variables and their performance over their respective operating ranges. For such programmes to be effective, it is essential that the models are accurate. Once process variability from these sources is identified and optimized, an accurate extraction process model can be derived. Available optimization tools make it possible to optimize the extraction process design variables. One such tool is the response surface methodology (RSM).

1.3 Response Surface Methodology

Classical optimization studies use the one-factor-at-a-time approach, in which only one factor is variable at a time while all others are kept constant. This approach is time-consuming and expensive. In addition, possible interaction effects between variables cannot be evaluated and misleading conclusions may be drawn. The response surface methodology (RSM) can overcome these difficulties, since it allows accounting for possible interaction effects between variables. If adequately used, this powerful tool can provide the optimal conditions that improve a process (Bas & Boyac, 2007).

The Response Surface Methodology (RSM) is a collection of mathematical and statistical techniques useful for the modeling and analysis of problems in which a response of interest is influenced by several variables and the objective is to optimize this response by searching for the optimum process conditions (Montgomery, 2005; Liyana-Pathirana and Shahidi, 2005; Rodriguez *et al*., 2007; Roldan *et al*., 2008). When treatments are from a continuous range of

values, then a Response Surface Methodology is useful for developing, improving, and optimizing the response variable. In this case, the response variable y, is expressed as

$y = f(x_1, x_2) + e$

where x_1 and x_2 are independent variables upon which the response y depends.

Thus the dependent variable y is a function of x_1, x_2, and the experimental error term, denoted as e. The error term e represents any measurement error on the response, as well as other type of variations not counted in f. It is a statistical error that is assumed to distribute normally with zero mean and variance s^2. In most RSM problems, the true response function f is unknown. In order to develop a proper approximation for f, the experimenter usually starts with a low-order polynomial in some small region. If the response can be defined by a linear function of independent variables, then the approximating function is a **first-order model**. A first-order model with 2 independent variables can be expressed as

$$y = b_0 + b_1x_1 + b_2 x_2 + e \qquad \textbf{(1.1)}$$

If there is a curvature in the response surface, then a higher degree polynomial should be used. The approximating function with squared variables is called a **second-order model**:

$$y = b_0 + b_1x_1 + b_2 x_2 + b_{11}x^2_{11} + b_{22} x^2_{22} + b_{12}x_1 x_2 + e \qquad \textbf{(1.2)}$$

In general all RSM problems use either one or a mixture of both of these models. In each model, the levels of each factor are independent of the levels of other factors. In order to get the most

efficient result in the approximation of polynomials the proper experimental design must be used to collect data. Once the data are collected, the *Method of Least Square* is used to estimate the parameters in the polynomials. The response surface analysis is performed by using the fitted surface. The **response surface designs** are types of designs for fitting response surface. Therefore, the objective of studying RSM can be accomplish by

1. understanding the topography of the response surface (local maximum, local minimum, ridge lines), and

2. finding the region where the optimal response occurs. The goal is to move rapidly and efficiently along a path to get to a maximum or a minimum response so that the response is optimized.

The analysis of a second-order model is usually done by computer software. The analysis of variance for fitting the data to the second-order and contour plots will help characterize the response surface.

The RSM optimization procedure is as follows (Oehlert, 2000);

1. Plan and run a factorial (or fractional factorial) design near or at the current operational variables.
2. Fit a linear model (no interaction or quadratic terms) to the data.

3. Determine path of steepest ascent (PSA) which is a quick way to move to the optimum conditions.
4. Run tests on the PSA until response no longer improves.
5. If curvature of surface is large go to step 6, else go to step 1.
6. Neighborhood of optimum - design, run, and fit (using least squares) a 2nd order model.
7. Based on 2nd order model - pick optimal settings of independent variables.

1.4 Research Problem

Fundamental research is still one of the challenges and offers opportunities for successful development of extraction technologies. As the technology and application for products have developed, so has knowledge and awareness of the technical and economical challenges to be addressed. The role that fundamental research can play in aiding successful commercialization of phenolic extraction includes raw material characterization and enhanced content of the product.

One of the main problems affecting the utilization of bark tannins in the manufacture of bio-adhesives is that the raw material (bark) from various sources, each time has to be analyzed for its chemical constituents in order to use it appropriately. However, the classical chemical methods of analysis are tedious, time-consuming and costly. There is therefore the need for a rapid and inexpensive method of determination.

In spite of the appearance of numerous research reports, bark tannins have not seen worldwide commercial applications and indeed is non-existing in Ghana. One of the main reasons is the low content (due to inappropriate extraction technologies) and high reactivity of these phenolic compounds. Current methods to increase the content also increase the content of sugars which

negatively affects the ability of phenolics to effect good bonding in wood panels. Again, detailed literature study showed that of the several process variables that affect the extraction of tannins from pine, only few have been studied by most researchers and in the cases where sizeable number of factors had been studied, they were varied one at a time (Vazquez et al., 1987), making it impossible to study the interaction effects. It therefore appears that, optimization of phenolic extraction from pine to content optimum formaldehyde condensable phenolics is limited.

1.5 Objectives

Based on the research problem defined, the objectives of the study were:

1. To rapidly determine the quantities of phenolics (suitable for adhesive applications) available in pine bark using near infrared spectroscopy.

2. To optimize the extraction of phenolics (suitable for phenol-formaldehyde adhesive in plywood production) from pine bark using response surface methodology.

CHAPTER TWO

LITERATURE REVIEW

2.1 Calibrating Chemical Properties using Near Infrared Spectroscopy (NIRS)

Over the last few years NIR spectroscopy together with the chemometric approach and multivariate data analysis has led to numerous applications for different fields of science and industry. There are several advantages of utilizing the NIR wavelength region: firstly, the rapidity of NIR measurements facilitates the collection of descriptive data and is a prerequisite for creating control systems working in real time. Secondly, since there is no need for sample preparation, the technique should be applicable to virtually any type of sample. From the early 1990s several parameters related to wood, have been estimated by NIR spectroscopy (Wright *et al.,* 1990; Michell, 1995; Schimleck *et al.,* 1998; Schwanninger and Hinterstoisser , 2001; Easty *et al.,* 1990; Schimleck *et al.,* 1997).

NIRS procedure is based on the vibrations of the C–H, N–H, and O–H functional groups of molecules. In NIRS applications, the spectrum of light that is reflected by a sample contains details on the chemical composition (i.e., number and nature of bonds present) of that material (Shenk and Westerhaus, 1991a). A statistical analysis is applied to test the intensity of the relationship between a particular absorbance and independent laboratory analysis of a constituent of interest. NIR analysis is thus an indirect method that estimates the composition of a sample by comparing spectra with samples of known composition (Shenk and Westerhaus, 1995). This step is known as the calibration procedure.

2.1.1 Near infrared spectrum

The NIR spectrum extends from 750 nm to 2500 nm (Osborne *et al*., 1993). Absorption bands observed in reflectance spectra of organic materials arise from overtones and combinations of vibrations of C-O, O-H, C-H, and N-H bonds. These absorption signals from the various constituents are similar and highly overlapping and no distinct absorption bands can be observed that can be directly related to the chemical abundance of a single wood constituent. The many overlapping signals result in a spectrum with broad peaks, making it difficult to interpret compared to the conventional mid-IR spectrum.

2.1.2 Chemometric calibration

The problem of difficult interpretation of NIR spectrum is overcome by employing chemometrics. Multivariate calibration focuses on finding relationships between one set of measurements, usually easily or cheaply acquired (as it is the case with NIR spectra), and other expensive or laborious measurements through mathematical treatment of the chemical property of interest. For the establishment of regression models from multivariate data, Partial Least Squares Projections to Latent Structures, PLS, is a very suitable projection method (Antti, 1999; Geladi, 2003).

In NIRS application, only a subset of the samples is used for the calibration, and the remaining samples used for the validation of the calibration equation. This second step is called the cross-validation procedure. During this cross-validation, the remaining samples for the original sample population are processed to validate the calibration equation. Finally, NIRS can be used in a laboratory for routine scanning of samples (routine analysis) which involves the application of

the calibration equations to determine component of interest (e.g. tannin content) of the unknown samples. However, before applying the calibration model to the unknown samples, it is checked that the spectra from the unknown sample belong to the same spectral population by calculating the Mahalanobis distance (Mahalonobis, 1936). Continuous monitoring of the routine analysis is necessary to ensure accurate results (Shenk *et al*., 1989).

The goal for every quantitative analytical spectroscopic measurement technique is to determine a certain system property – *Y* (%, concentration value) from some measured system parameter – *X* (spectral data). The individual parameters *X* and *Y* are written in matrix form. The spectral intensities, in the chosen frequency intervals, of the spectroscopic measurement are written point by point row-wise into the *X*-matrix. The spectral data for each measured sample correspond to one row in the matrix. The corresponding sample component concentration values are written in a similar way as the rows of the *Y*-matrix. Such a quantitative analysis requires calibration and analysis (prediction). During the calibration, known samples are used to establish a certain relationship between *X* and *Y* parameters and calibration function *b*. The most widely used method of calibration is Partial Least Squares (PLS) regression (Haaland and Thomas, 1998; Geladi and Kowalski, 1986; Beebe and Kowalski, 1987).

After the calibration, analysis of the system property *Y* is determined for new unknown samples by applying the calibration model to the measured properties *X*:

$Y = Xb$

in which the calibration function *b* is given by:

$b = (XTX)^{-1} XT\ Y$

where *T* is used to denote the transpose of the associated matrix.

Thus, the NIRS determination is based on the use of regression models between the spectral information of a set of samples and their reference values.

2.1.3 Spectral pretreatment

Spectral filtering together with other types of data pre-treatment is often essential for deriving a properly working multivariate calibration model. Traditional methods of pretreatments in order to remove variation in spectra not related to the investigated properties are base line correction, normalization, first and second order derivatives or Multiplicative Scatter Correction (MSC), to mention just a few.

2.1.4 Robustness of model

In order to find out how well the model is performing in making predictions, the model has to be validated. For internal cross-validation procedures one group at a time is kept out of the model before the model predicts it, whereas in external test-set validations a number of samples is kept out of the calibration model to use them solely for validating the predictive ability.

2.2 Solid-Liquid Extraction

Extraction is the removal of a soluble fraction, in the form of a solution, from an insoluble, permeable solid phase with which it is associated. The separation usually involves selective dissolution, with or without diffusion, but in the extreme case of simple washing it consists merely of the displacement (with some mixing) of one interstitial liquid by another with which it is miscible. The soluble constituent may be solid or liquid; and it may be incorporated within,

chemically combined with, adsorbed upon, or held mechanically in the pore structure of the insoluble material. The insoluble solid may be massive and porous; more often it is particulate and the particles may be openly porous, cellular with selectively permeable cell walls, or surface-activated. It is common practice to exclude from consideration as extraction the elution of surface-adsorbed solute. This process is treated instead as a special case of the reverse operation, adsorption. Also usually excluded is the washing of filter cakes, whether in situ or by re-slurrying and re-filtration. Because of its variety of applications and its importance to several ancient industries, extraction is known by a number of other names. Among those encountered in chemical engineering practice are leaching, solid-liquid extraction, lixiviation, percolation, infusion, washing, and decantation-settling. The stream of solids being extracted and the accompanying liquid is known as the underflow; in hydrometallurgy practice it is called pulp. The solid content of the stream is sometimes called marc (particularly by oil seed processors). The stream of liquid containing the extracted solute is the overflow. As it leaves the extraction process it has several optional names: extract, solution, lixiviate, leachate, or miscella.

2.2.1 Mechanism of extraction

The mechanism of extraction may involve simple physical solution or dissolution made possible by chemical reaction. The rate of transport of solvent into the mass to be leached, or of soluble fraction into the solvent, or of extract solution out of the insoluble material, or some combination of these rates may be significant. A membranous resistance may be involved. A chemical-reaction rate may also affect the rate of extraction. Inasmuch as the overflow and underflow streams are not immiscible phases but streams based on the same solvent, the concept of equilibrium for extraction is not the one applied in other mass-transfer separations. If the solute

is not adsorbed on the inert solid, true equilibrium is reached only when all the solute is dissolved and distributed uniformly throughout the solvent in both underflow and overflow (or when the solvent is uniformly saturated with the solute, a condition never encountered in a properly designed extractor). The practical interpretation of extraction equilibrium is the state in which the overflow and underflow liquids are of the same composition; on a *y*-*x* diagram, the equilibrium line will be a straight line through the origin with a slope of unity. It is customary to calculate the number of ideal (equilibrium) stages required for a given extraction task and to adjust the number by applying a stage efficiency factor, although local efficiencies, if known, can be applied stage by stage. Usually, however, it is not feasible to establish a stage or overall efficiency or an extraction rate index (e.g., overall coefficient) without testing small-scale models of likely apparatus. In fact, the results of such tests may have to be scaled up empirically, without explicit evaluation of rate or quasi-equilibrium indices (Perry, 1999).

2.2.2 Methods of operation

Extraction systems are distinguished by operating cycle (batch, continuous, or multibatch intermittent); by direction of streams (cocurrent, countercurrent, or hybrid flow); by staging (single-stage, multistage, or differential-stage); and by method of contacting (sprayed percolation, immersed percolation, or solids dispersion). In general, descriptors from all four categories must be assigned to stipulate a extraction system completely (e.g., the Bollman-type extractor is a continuous hybrid-flow multistage sprayed percolator). Whatever the mechanism and the method of operation, it is clear that the extraction process will be favored by increased surface per unit volume of solids to be leached and by decreased radial distances that must be traversed within the solids, both of which are favored by decreased particle size. Fine solids, on

the other hand, cause slow percolation rate, difficult solids separation, and possible poor quality of solid product. The basis for an optimum particle size is established by these characteristics.

2.2.3 Extraction equipment

It is classification by contacting method that provides the two principal categories into which extraction equipment is divided: (1) that in which the extraction is accomplished by percolation and (2) that in which particulate solids are dispersed into a liquid and subsequently separated from it. Each includes batch and continuous units. Materials which disintegrate during extraction are treated in equipment of the second class. A few designs of continuous machines fall in neither of these major classes.

2.2.4 Design of an extraction process

At the heart of an extraction plant design at any level-conceptual, preliminary, firm engineering, or whatever-is unit-operations and process design of the extraction unit or line. The major aspects that are particular for the extraction operation are the selection of process and operating conditions and the sizing of the extraction equipment.

2.2.4.1 Process and Operating Conditions

The major parameters that must be fixed or identified are the solvent to be used, the temperature, the terminal stream compositions and quantities, extraction cycle (batch or continuous), contact method, and specific extractor choice.

***a) Choice of Solvent*:** The solvent selected will offer the best balance of a number of desirable characteristics: high saturation limit and selectivity for the solute to be extracted, capability to produce extracted material of quality unimpaired by the solvent, chemical stability under process conditions, low viscosity, low vapor pressure, low toxicity and flammability, low density, low surface tension, ease and economy of recovery from the extract stream, and price. These factors are listed in an approximate order of decreasing importance, but the specifics of each application determine their interaction and relative significance, and anyone can control the decision under the right combination of process conditions.

***b) Temperature*:** The temperature of the extraction should be chosen for the best balance of solubility, solvent-vapor pressure, solute diffusivity, solvent selectivity, and sensitivity of product. In some cases, temperature sensitivity of materials of construction to corrosion or erosion attack may be significant.

***c) Terminal Stream Compositions and Quantities*:** These are basically linked to an arbitrary given: the production capacity of the extraction plant (rate of extract production or rate of raw-material purification by extraction). When options are permitted, the degree of solute removal and the concentration of the extract stream chosen are those that maximize process economy while sustaining conformance to regulatory standards.

***d) Extraction Cycle and Contact Method*:** As is true generally, the choice between continuous and intermittent operation is largely a matter of the size and nature of the process of which the

extraction is a part. The choice of a percolation or solids-dispersion technique depends principally on the amenability of the extraction to effective, sufficiently rapid percolation.

***e) Type of Reactor*:** The specific type of reactor that is most compatible (or least incompatible) with the chosen combination of the preceding parameters seldom is clearly and unequivocally perceived without difficulty, if at all. In the end, however, that remains the objective. As is always true, the ultimate criteria are reliability and profitability.

2.2.4.2 Extractor-Sizing Calculations

For any given throughput rate (which fixes the cross-sectional area and/or the number of extractors), the size of the units boils down to the number of stages required, actual or equivalent. In calculation, this resolves into determination of the number of ideal stages required and application of appropriate stage efficiencies. The methods of calculation resemble those for other mass-transfer operations, involving equilibrium data and contact conditions, and based on material balances.

***a) Composition Diagrams*:** In its elemental form, an extraction system consists of three components: inert, insoluble solids; a single non-adsorbed solute, which may be liquid or solid; and a single solvent. Thus, it is a ternary system, albeit an unusual one, as already mentioned, by virtue of the total mutual "insolubility" of two of the phases and the simple nature of equilibrium.

The composition of a typical system is satisfactorily presented in the form of a diagram. Those diagrams most frequently employed are a right-triangular plot of mass fraction of solvent against mass fraction of solute (Fig. 2.1a) and a plot suggestive of a Ponchon-Savarit diagram, with inerts taking the place of enthalpy (Fig. 2.1b). A third diagram, less frequently used, is a modified McCabe-Thiele plot in which the overflow solution (inerts-free) and the underflow solution (traveling out of a stage with the inerts) are treated as pseudo phases, the mass fraction of solute in overflow, *y,* being plotted against the mass fraction of solute in underflow, *x.* (An additional representation, the equilateral-triangular diagram frequently employed for liquid-liquid ternary systems, is seldom used because the field of extraction data is confined to a small portion of the triangle.) With reference to Fig. 2.1 (both graphs), *EF* represents the locus of overflow compositions for the case in which the overflow stream contains no inert solids. E^1 F^1 represents the overflow streams containing some inert solids, either by entrainment or by partial solubility in the overflow solution. Lines *GF, GL,* and *GM* represent the loci of underflow compositions for the three different conditions indicated on the diagram. In Fig. 2.1*a,* the constant underflow line *GM* is parallel to *EF,* the hypotenuse of the triangle, whereas *GF* passes through the right-hand vertex representing 100 percent solute. In Fig. 2.1*b,* underflow line *GM* is parallel to the abscissa, and *GF* passes through the point on the abscissa representing the composition of the clear solution adhering to the inert solids.

Compositions of overflow and underflow streams leaving the same stage are represented by the intersection of the composition lines for those streams with a tie line (*AC,* AC^1, *BD,* BD^1). Equilibrium tie lines (*AC, BD*) pass through the origin (representing 100 percent inerts) in Fig. 2.1*a,* and are vertical (representing the same inert-free solution composition in both streams) in

Fig. 2.1*b*. For non-equilibrium conditions with or without adsorption or for equilibrium conditions with selective adsorption, the tie lines are displaced, such as AC^1 and BD^1. Point C^1 is to the right of C if the solute concentration in the overflow solution is less than that in the underflow solution adhering to the solids. Unequal concentrations in the two solutions indicate insufficient contact time and/or preferential adsorption of one of the components on the inert solids. Tie lines such as AC^1 may be considered as "practical tie lines" (i.e., they represent actual rather than ideal stages) if data on underflow and overflow composition have been obtained experimentally under conditions simulating actual operation, particularly with respect to contact time, agitation, and particle size of solids. The illustrative construction lines of Fig. 2.1a have been made with the assumption of constant underflow. In the more realistic case of variable underflow, the points C, C^1, D, D^1 would lie along line GL. Like the practical tie lines, GL is a representation of experimental data.

***b) Algebraic Computation*:** This method starts with calculation of the quantities and compositions of all the terminal streams, using a convenient quantity of one of the streams as the basis of calculation. Material balance and stream compositions are then computed for a terminal ideal stage at either end of an extraction battery (i.e., at Point A or Point B in Fig. 2.1a), using equilibrium and solution-retention data. Calculations are repeated for each successive ideal stage from one end of the system to the other until an ideal stage which corresponds to the desired conditions is obtained. Any solid-liquid extraction problem can be solved by this method. For certain simplified cases it is possible to calculate directly the number of stages required to attain a desired product composition for a given set of feed conditions. For example, if equilibrium is attained in all stages and if the underflow mass rate is constant, both the equilibrium and

operating lines on a modified McCabe-Thiele diagram are straight, and it is possible to calculate directly the number of ideal stages, N, required to accommodate any rational set of terminal flows and compositions:

$$N = \frac{\log[(y_b - x_b)/(y_a - x_a)]}{\log[(y_b - y_a)/(x_b - x_a)]} \qquad \textbf{(2.1)}$$

Even when the conditions of equilibrium in each stage and constant underflow obtain, Eq. (2.1) normally is not valid for the first stage because the unextracted solids entering that stage usually are not premixed with solution to produce the underflow mass that will leave. This is easily rectified by calculating the exit streams for the first stage and using those values in Eq. (2.1) to calculate the number of stages required after stage 1.

***c) Graphical Method*:** This method of calculation is simply a diagrammatic representation of all the possible compositions in a extraction system, including equilibrium values, on which material balances across ideal (or, in some cases, non-ideal) stages can be evaluated in the graphical equivalent of the stage-by-stage algebraic computation. It normally is simpler than the hand calculation of the algebraic solution, and it is viewed by many as helpful because it permits visualization of the process variables and their effect on the operation. The modified Ponchon-Savarit or right-triangular plots (Fig. 2.1) are most convenient for extraction calculations. The techniques of graphical solution, in fact, are not unlike those for distillation and absorption (binary) problems using McCabe-Thiele, Ponchon-Savarit, and right-triangular diagrams and are similar to solvent-extraction (ternary) systems (McCabe et al., 1993; Treybal, 1980).

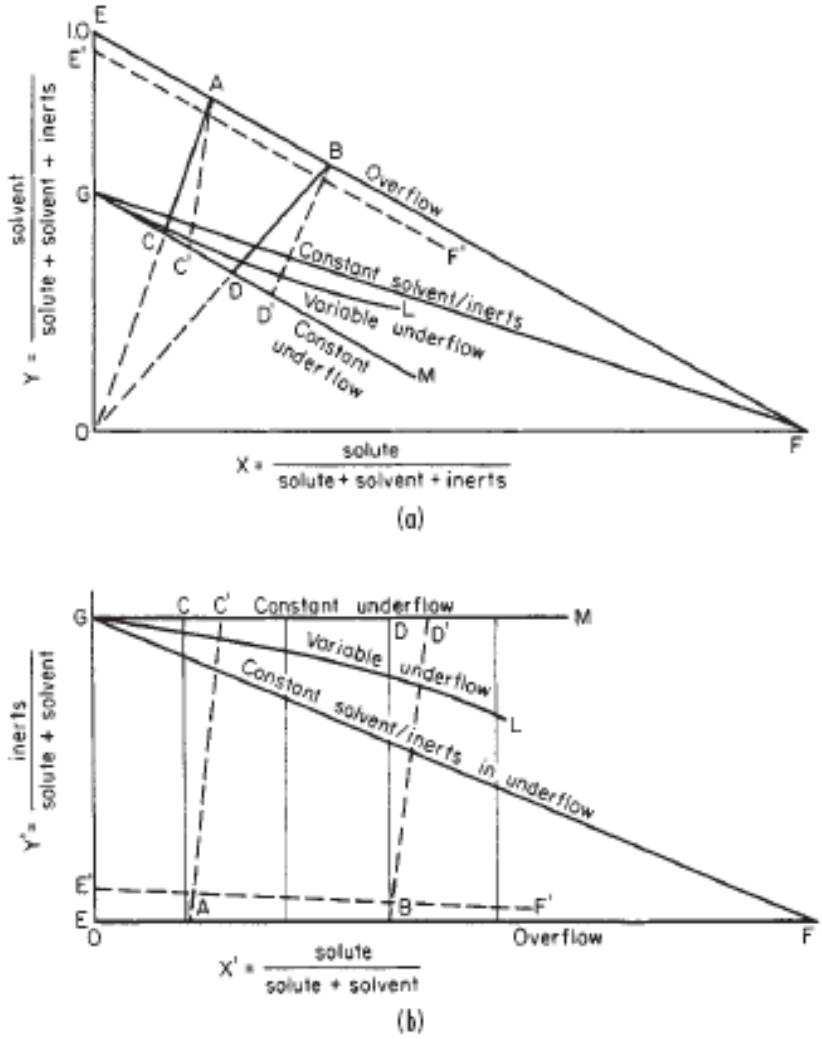


Figure 2. 1: Composition diagrams for extraction calculations: (a) right-triangular diagram; (b) modified Ponchon-Savarit diagram

Source: Perry's Handbook for Chemical Engineers, 7th ed.

2.2.5 Mass transfer

Mass transfer in solids is important in chemical and biological processing. Transport in solids can be classified into two types of diffusion; diffusion that can be considered to follow Fick's law and does not depend primarily on the actual structure of the solid, and diffusion in porous solids where the actual structure and void channels are important (Geankopolis, 1993).

Mass-transfer calculations involve transport properties, such as diffusivities, and other empirical factors that have been found to relate mass-transfer rates to measured "driving forces" in myriad geometries and conditions. The context of the problem dictates whether the fundamental or more applied coefficient should be used. One key distinction is that, whenever there is flow parallel to an interface through which mass transfer occurs, the relevant coefficient is an empirical combination of properties and conditions. Conversely, when diffusion occurs in stagnant media or in creeping flow without transverse velocity gradients, ordinary diffusivities may be suitable for solving the problem. In either case, it is strongly suggested to employ data, whenever available, instead of relying on correlations (Perry, 1999). Fick's first law relates flux of a component to its composition gradient, by employing the constant of proportionality, diffusivity. It can be written in several forms, depending on the units and frame of reference. Three that are related but not identical are

$$ {}_vJ_A = - D_{AB} \frac{dc_A}{dz} \quad \propto \quad {}_vJ_A = - cD_{AB} \frac{dx_A}{dz} \quad \propto \quad {}_vJ_A = - D_{AB} \frac{dw_A}{dz} \qquad \textbf{(2.2)} $$

The first equality (on the left-hand side) corresponds to the molar flux with respect to the volume average velocity, while the equality in the center represents the molar flux with respect to the molar average velocity and the one on the right is the mass flux with respect to the mass average velocity. These must be used with consistent flux expressions for fixed coordinates and for *NC* components, such as:

$$ N_A = {}_vJ_A + c_A \sum_{i=1}^{NC} N_i \bar{V}_i = {}_MJ_A + x_A \sum_{i=1}^{NC} N_i = \frac{{}_mJ_A + w_A \sum_{i=1}^{NC} n_i}{M_A} \qquad \textbf{(2.3)} $$

In each case, the term containing the summation accounts for *conveyance,* which is the amount of component *A* carried by the net flow in the direction of diffusion. Its impact on the total flux can be as much as 10 percent. In most cases it is much less, and it is frequently ignored.

Diffusivity D_{AB}, is defined by Fick's first law as the ratio of the flux to the concentration gradient, as in Eq. (2.2). It is analogous to the thermal diffusivity in Fourier's law and to the kinematic viscosity in Newton's law. These analogies are flawed because both heat and momentum are conveniently defined with respect to fixed coordinates, irrespective of the direction of transfer or its magnitude, while mass diffusivity most commonly requires information about bulk motion of the medium in which diffusion occurs. For liquids, it is common to refer to the limit of infinite dilution of *A* in *B* using the symbol, $D°_{AB}$. When the flux expressions are consistent, as in Eq. (2.3), the diffusivities in Eq. (2.2) are identical. As a result, experimental diffusivities are often measured under constant volume conditions but may be used for applications involving open systems. It turns out that the two versions are very nearly equivalent for gas-phase systems because there is negligible volume change on mixing. That is not usually true for liquids, however.

2.2.6 Material balances

Whenever mass-transfer applications involve equipment of specific dimensions, flux equations alone are inadequate to assess results. A material balance or continuity equation must also be used. When the geometry is simple, macroscopic balances suffice. The following equation is an overall mass balance for such a unit having *Nm* bulk-flow ports and *Nn* ports or interfaces through which diffusive flux can occur:

$$\frac{dM}{dt} = \sum_{i=1}^{N_m} m_i + \sum_{i=1}^{N_n} n_i A_{csi} \qquad \textbf{(2.4)}$$

where M represents the mass in the unit volume V at any time t; m_i is the mass flow rate through the ith port; and n_i is the mass flux through the ith port, which has a cross-sectional area of A_{csi}. The corresponding balance equation for individual components includes a reaction term:

$$\frac{dM_j}{dt} = \sum_{i=1}^{N_m} m_{ij} + \sum_{i=1}^{N_n} n_{ij} A_{csi} + r_j V \qquad \textbf{(2.5)}$$

For the jth component, $m_{ij} = m_i w_{ij}$ is the component mass flow rate in stream i; w_{ij} is the mass fraction of component j in stream i; and r_j is the net reaction rate (mass generation minus consumption) per unit volume V that contains mass M. If it is inconvenient to measure mass flow rates, the product of density and volumetric flow rate is used instead. In addition, most situations that involve mass transfer require material balances, but the pertinent area is ambiguous. Examples are packed columns for absorption, distillation, or extraction. In such cases, flow rates through the discrete ports (nozzles) must be related to the mass-transfer rate in the packing. As a result, the mass-transfer rate is determined via flux equations, and the overall material balance incorporates the stream flow rates m_i and integrated fluxes. In such instances, it is common to begin with the most general, differential material balance equations. Then, by eliminating terms that are negligible, the simplest applicable set of equations remains to be solved.

2.2.7 Application of solid-liquid extraction modeling

Solid-liquid extraction has been a major area of research in process engineering in recent years. Several authors have tried to model the extraction process of natural products under transient conditions using either Fick's second law with an effective or apparent diffusion coefficient or mass transfer coefficients**.** Most of the models assume uni-dimensional transport within a homogeneous solid, disregarding the fact that foods are highly heterogeneous at the microstructural level (Aguilera and Stanley; 1999**).** Application of Fick's law to experimental data allows the determination of the effective diffusivity from the slope of a plot of log (extent of extraction) versus time after assuming a specific geometrical shape for the product (usually sphere, slab or cylinder). The effective diffusivity D_{eff} encompasses mechanistic as well as microstructural effects. A summary of some models and solutions to mass transfer during solid-liquid extraction is presented in Table 2.1

Table 2. 1 Some models and parameters used in solid-liquid extraction

Author	**Year**	**Model used**	**Solution**
Aguilera *et al.*	1987	Mass transfer coefficient, one dimension.	Mass transfer coefficient dependant on concentration.
Fan *et al.*	1948	Fick's second law, one dimension	D corrected for moisture content.
Krasuk *et al.*	1967	Fick's second law, one dimension	D dependant on concentration.
Loncin	1980	Fick's second law, one dimension	Effective D.
Naessens *et al.*	1981	Fick's second law, one dimension	D dependant on concentration.

Osburn and Katz	1944	Fick's second law, one dimension	Effective D.
Patricelli *et al.*	1979	Mass transfer coefficient, one dimension.	2 different and separate situations (washing and diffusion).
Le Maguer and Yao	1995	Mass and volume balance equations, similar to Fick's first law, one dimension.	Correction by variable volume, concentration and macrostructural effects
Rastogi and Niranjan	1998	Fick's second law, rectangular parallelepiped	Binary diffusion with 2 Ds.
So and MacDonald	1986	Mass transfer coefficient, one dimension.	3 situations: washing, hindered and unhindered diffusion.
Zanderighi	1983	Fick's second law, one dimension	Effective D.
Zhang *et al.*	1984	Fick's second law, two dimensions.	Concentration dependant on D and the solid changed size.

Source; **Journal of Food Process Engineering (2001)**

The most common correction parameters introduced to accommodate structural effects in the diffusivity of porous solids are the tortuosity and the porosity. Tortuosity ***(τ)*** is a factor which compensates for the path through longer pores. This factor ranges between 1.5 and 5 (Gekkas, 1992). The other factor used, porosity *(ε),* is the ratio of volume of pores to the total volume (i.e. $\varepsilon < 1$). This approach leads to an effective diffusivity which is smaller than the diffusion coefficient of a diluted species in a solvent (Cussler, 1997):

$$D_{eff} = (\varepsilon/\tau) \times D \qquad \textbf{(2.6)}$$

2.3 Optimization

For three decades, many mathematical programming methods have been developed to solve optimization problems. However, until now, there has not been a single totally efficient and robust method to cover all optimization problems that arise in the different engineering fields.

Most engineering application design problems involve the choice of design variable values that better describe the behavior of a system. At the same time, those results should cover the requirements and specifications imposed by the norms for that system. This last condition leads to predicting what the entrance parameter values should be whose design results comply with the norms and also present good performance, which describes the inverse problem. Generally, in design problems the variables are discreet from the mathematical point of view. However, most mathematical optimization applications are focused and developed for continuous variables.

2.3.1 Optimization methods

Presently, there are many research articles about optimization methods; the typical ones are based on calculus, numerical methods, and random methods. The calculus based methods have been intensely studied and are subdivided in two main classes: 1) the direct search methods find a local maximum moving on a function over the relative local gradient directions and 2) the indirect methods usually find the local ends solving a set of non-linear equations, resultant of equaling the gradient from the object function to zero, i.e., by means of multidimensional generalization of the notion of the function's extreme points from elementary calculus give a smooth function without restrictions to find a possible maximum which is to be restricted to those points whose slope is zero in all directions. Both methods have been improved and

extended, however they lack robustness for two main reasons: 1) they have a local focus, since they seek the maximum in the analyzed point neighborhoods; 2) they depend on the existence of their derivative, which many spaces of practical parameters respect little the notion of having derivatives and smoothness. The real world has many discontinuities and noisy spaces that is why it is not surprising that the methods depending upon the restrictive requirements of continuity and existence of a derivative are unsuitable for all, but a very limited problem domain. A number of schemes have been applied in many forms and sizes. The idea is quite direct inside a finite search space or a discrete infinite search space, where the algorithms can locate the object function values in each space point one at a time. The simplicity of this kind of algorithm is very attractive when the numbers of possibilities are very small.

New optimization techniques are arriving daily, often stimulated by fascinating insights from other fields. Optimization methods are used everywhere in engineering, business and other fields. The process of optimization begins with a real problem, full of details and complexities, some relevant and some not. From this one extracts the essential elements to create a model, and chose an algorithm or solution technique to apply to it. Validation and sensitivity analysis are performed to test the robustness of the method.

2.3.2 Response surface methodology

Response Surface Methods are designs and models for working with continuous treatments when finding the optima or describing the response is the goal (Oehlert, 2000). The first goal for Response Surface Method is to find the optimum response. When there is more than one response then it is important to find the compromise optimum that does not optimize only one response (Oehlert, 2000). When there are constraints on the design data, then the experimental

design has to meet requirements of the constraints. The second goal is to understand how the response changes in a given direction by adjusting the design variables. In general, the response surface can be visualized graphically (Fig. 2.2). The graph is helpful to see the shape of a response surface; hills, valleys, and ridge lines. Hence, the function $f(x_1, x_2)$ can be plotted versus the levels of x_1 and x_2. In order to understand the surface of a response, graphs are helpful tools. But, when there are more than two independent variables, graphs are difficult or almost impossible to use to illustrate the response surface, since it is beyond 3-dimension, so the general mathematical solution for the location of the optimum point has to be used. For this reason, response surface models are essential for analyzing the unknown function *f*.

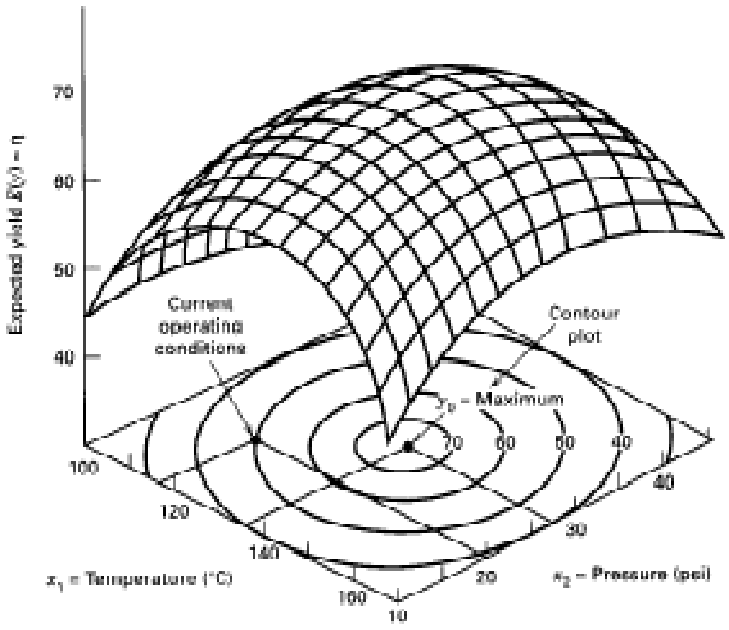


Figure 2. 2: A contour plot with a response surface for a process depending on temperature and pressure.

2.3.2.1 Analysis of a First-Order Response Surface

The relationship between the response variable *y* and independent variables is usually unknown. In general, the low-order polynomial model is used to describe the response surface *f*. A polynomial model is usually a sufficient approximation in a small region of the response surface. Therefore, depending on the approximation of unknown function *f*, either first-order or second-order models are employed. Furthermore, the approximated function *f* is a first-order model when the response is a linear function of independent variables. A first-order model with *N* experimental runs carrying out on *k* design variables and a single response *y* can be expressed as follows:

$$y_i = \beta_0 + \beta_1 x_{i1} + \ldots\ldots + \beta_k x_{ik} + \varepsilon_i \qquad (i = 1, 2, 3, \ldots\ldots.., N) \qquad \textbf{(2.7)}$$

The response *y* is a function of the design variables $x_1, x_2, \ldots, x_k$, denoted as *f*, plus the experimental error ε. A first-order model is a *multiple-regression* model and the β_i's are regression coefficients.

2.3.2.2 Analysis of a Second-Order Response Surface

When there is a curvature in the response surface the first-order model is insufficient. A second-order model is useful in approximating a portion of the true response surface with parabolic curvature. The second-order model includes all the terms in the first-order model, plus all quadratic terms like $\beta_{11}x_{1i}^2$ and all cross product terms like $\beta_{13}x_{1i}$. It is usually expressed as;

$$y = \beta_0 + \sum_{i=1}^{k} \beta_i x_i + \sum_{i=1}^{k} \beta_{ii} x_i^2 + \sum_{\substack{i=1 \\ i<j}}^{k-1} \sum_{j=2}^{k} \beta_{ij} x_i x_j + \varepsilon \qquad \textbf{(2.8)}$$

The second-order model is flexible, because it can take a variety of functional forms and approximates the response surface locally. Therefore, this model is usually a good estimation of the true response surface.

2.3.2.3 Designs for Fitting Second-Order Model

There are many designs available for fitting a second-order model. The most popular one is the *central composite design* (CCD). This design was introduced by Box et al. (1978). It consists of factorial points (from a 2^k design and 2^{k-q} *fractional factorial design*, where k is number of factors and q is number of design generators), central points, and axial points. CCD was often developed through a *sequential experimentation*. When a first-order model shows an evidence of *lack of fit*, axial points can be added to the quadratic terms with more center points to develop CCD. The number of center points n_c at the origin and the distance a of the axial runs from the design center are two parameters in the CCD design. The center runs contain information about the curvature of the surface, if the curvature is significant, the additional axial points allow for the experimenter to obtain an efficient estimation of the quadratic terms. Figure 2.3 illustrates the graphical view of a central composite design for $k = 2$ factors.

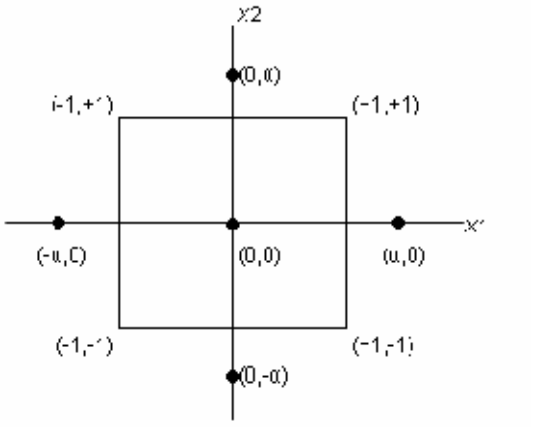


Figure 2. 3: Central Composite Design for k =2

There are couple of ways of choosing a and n_c. First, CCD can run in incomplete blocks. A block is a set of relatively homogeneous experimental conditions so that an experimenter divides the observations into groups that are run in each block. An incomplete block design may be conducted when all treatment combinations cannot be run in each block. In order to protect the shape of the response surface, the block effects need to be orthogonal to treatment effects. This can be done by choosing the correct a and n_c in factorial and axial blocks.

Also, a and n_c can be chosen so that the CCD is not blocked. If the precision of the estimated response surface at some point x depends only on the distance from x to the origin, not on the direction, then the design is said to be *rotatable* (Oehlert, 2000). When the rotatable design is rotated about the center, the variance of $\hat{y}$ will remain same. Since the reason for using response surface analysis is to locate unknown optimization, it makes sense to use a rotatable design that provides equal precision of estimation of the surface in all directions. The choice of a will make the CCD design rotatable by using either $\alpha = 2^{k/4}$ for the full factorial or $\alpha = 2^{(k-q)/4}$ for a fractional factorial.

2.4 Tannins

Tannins are plant phenolic compounds (Hagerman, 1988). They are preponderant in nature: foliage and bark of some trees may contain up to 40 % of tannin which makes up a significant portion of the forest carbon pools (Kraus et al., 2003). Bate-Smith and Swain (1962) defined tannins as 'water-soluble phenolic compounds having molecular weights between 500 and 3000, giving the usual phenolic reactions and having special properties such as the ability to precipitate alkaloids, gelatin and other proteins'. Haslam (1998) has more recently recommended the term

'polyphenol' for 'tannin' in an attempt to emphasize the multiplicity of phenolic groups characteristics of these compounds.

There are two types of tannin, namely, the condensable and the hydrolyzable (Godwin and Mercier, 1983). In the former, the benzene nuclei are joined to the larger complex by carbon linkages, while in the latter, they are joined by oxygen atoms. Most of the tannins in pine bark are condensed tannins (Fig. 2. 4), formed by polymerization of flavan-3-ols or flavan-3,4-diols. They are largely polymeric condensation products and cannot be hydrolyzed by acids or enzymes, but condense readily to high molecular-weight tannins. Hydrolyzable tannins on the other hand, decompose in water, with which they react to form other useful substances such as garlic acid, protocatechuic acid and sugar. Figure 2.4 shows some examples of the two types.

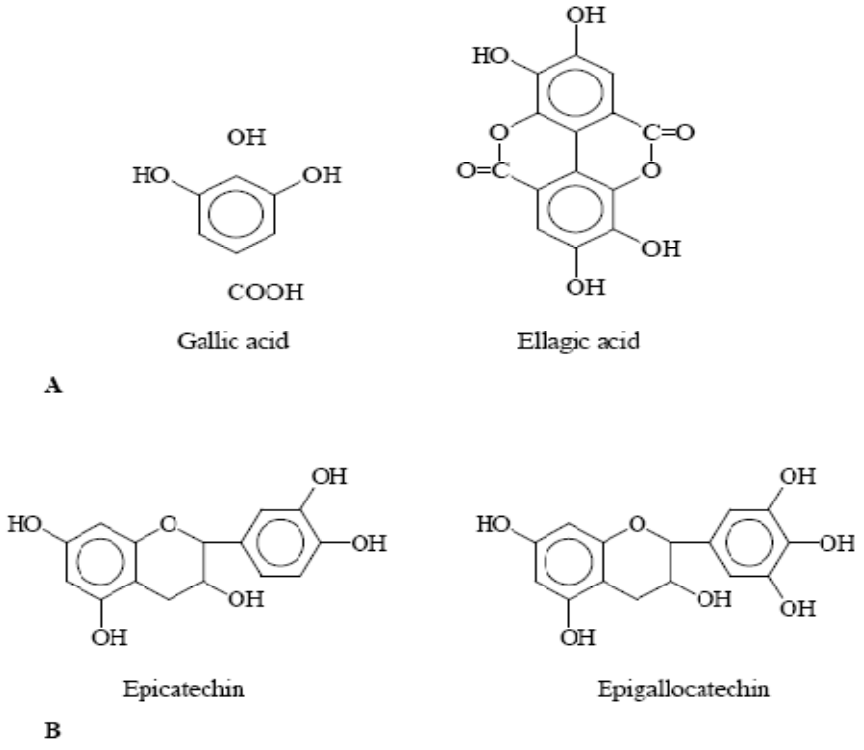


Figure 2. 4: Schematic illustration of tannins: A-hydrolysis products of hydrolysable tannins. B-flavonoid members of condensed tannins

Tannins have diverse uses (Austin, 1994). The traditional use is for rendering raw hides into leather. But they have also been employed industrially in denaturing alcohol; in aqueous solution for treating burns and protecting plant against dehydration and damage by animals; as mordants on dyeing; as antidote for metallic, alkaloid and glycoside poisons; and as reagents in photography. They are also added to mud in oil drilling operation to increase the viscosity and have been used for the manufacture of ink, rubber and plastics; for preventing sculling in hot waters; for ores flotation and water treatment; and by combining them with binding agents such as polyvinyl pyrrolidone (PVP) to clarify wine and beer. They are suitable for making wood adhesives.

2.4.1 Extraction of tannins

Although the potential for production of polyphenols from wood biomass for wood adhesives has long been realized, commercial production has not succeeded due to the high production costs associated with the appropriate quality of high extracts weight percentage recovery. Therefore many techniques have been developed attempting to increase the weight percentage recovery of wood polyphenols and improve their quality for wood adhesives. These techniques include water extraction with addition of chemicals, solvent extraction (Pizzi, 1994), and fractionation of extracts with ultra filtration (Yazaki, 1983).

Solvent extraction from a milled plant material includes first a swelling step consisting in the sorption of the solvent in the solid phase. This sorption is caused by osmotic forces, capillarity and solvation of the ions in the solid matrix. A portion of the solute contained in the damaged

plant material is extracted by leaching, and the solubilization by hydrolysis of another fraction of initially insoluble compounds may occur as well. The swelling step is followed by a diffusive phenomenon firstly inside the plant material and secondly through the outer layer that surrounds the plant particles (Mafart and B´eliard, 1992).

The choice of the most suitable solvent for the removal of polyphenolic extractives depends on the species under examination and the type of information required. Water is commonly used, particularly in commercial practice, to extract the cell contents. However, the nature of some polyphenols can change with increase in the age of the tissue, so that the water extraction does not always give accurate information on the amount of polyphenols present (Hathway, 1958). So, different solvent systems have been found for the extraction. Reduction of solvent use in extraction, enhanced selectivity, minimal energy consumption, fast operational time and increased weight percentage recovery for economical and environmental improvement are the main goals of Research and Development in extraction process.

2.4.2 Chemistry of condensed tannins

The tannin polyflavonoid consists essentially of 5-11 monoflavonoid units. In the monoflavonoid unit, two phenolic rings ‘A’ and ‘B’ (Fig. 2.5), are joined by a heterocyclic ring. Tannin, being phenolic, reacts with formaldehyde in a manner similar to that for the reaction of formaldehyde with phenol. However, unlike most synthetic phenolic compounds, tannin has a high reactivity towards formaldehyde, and is larger in size (Fig. 2.6). Therefore, during the condensation reaction of tannin with formaldehyde, especially at high temperatures, tannin-formaldehyde resoles become rapidly immobilized due to premature gelation as a result of its high reactivity

and molecular size. The result is that condensation does not go far enough to achieve the required adhesive properties. It can therefore be said that the size and the reactivity of the 'A' ring, are most probably responsible for the poor adhesive properties. In addition, the presence of non-tannin compounds such as gums, which are highly-branched polysaccharides, affects the properties of tannin-based adhesive, particularly its moisture resistance.

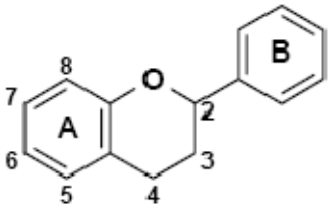


Figure 2. 5: Structural part of tannin showing rings A and B

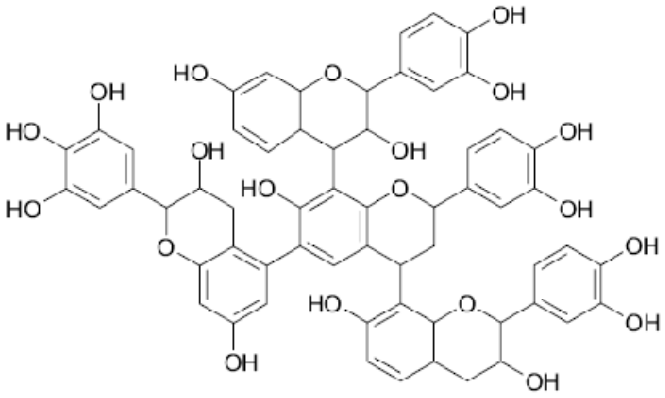


Figure 2. 6: Structure of condensed tannin

2.4.3 Hydrolysis of tannins

Caustic hydrolysis of tannin has been reported to cleave the interflavonoid bond and open the heterocyclic ring, joining the 'A' and 'B' rings of the flavonoid unit (Pizzi and Scharffeter, 1981). Acid hydrolysis has been shown to open the heterocyclic ring of polyflavonoids easily, with the formation of a carbo-cation which is capable of reacting with another nucleophile present. Pizzi and Stephanou (1992) reported an improvement in the performance of a non-fortified mimosa-tannin-based adhesive developed by subjecting tannin extracts to acetic anhydride and subsequent alkaline treatment. They suggested the following as probable reasons for the improved adhesive performance (Pizzi and Stephanou, 1992); (i) Cleavage of tannin interflavonoid bond. This results in smaller, more mobile tannin flavonoid compounds and therefore enhances the level of condensation with formaldehyde. (ii) Opening of the heterocyclic ring joining the 'A' and 'B' rings of tannin flavonoid compound leads to a more flexible compound, reduces the stiffness of the tannin molecules and consequently the brittleness of the adhesive. (iii) Hydrocolloid gums are hydrophilic and very viscous, even at moderate concentrations. The presence of these gums in tannin extract tends to promote high solution viscosity and poor moisture resistance of tannin-based adhesive. However, their corresponding sugars (of low molecular weight) do not have much effect on viscosities of solutions. The destruction of these gums will therefore improve moisture resistance of the resulting tannin-based adhesive. In addition, because of its reduced viscosity, penetration of adhesive into wood substrate will be enhanced.

2.5 Phenol-formaldehyde resins

Wood adhesives are polymeric materials that are capable of interacting physically or chemically, or both, with the surface of wood in such a manner that stresses are transferred between bonded members, hopefully without rupture of the adhesive or detachment of the adhesive from the wood. Adhesives and the physicochemical phenomenon of adhesion play an important role in more than 70% of all wood-based materials in use today (Marra, 1984).

Phenol-formaldehyde (PF) Resoles are polycondensation products of phenol (P) and formaldehyde (F) in an alkaline aqueous medium with excess formaldehyde (Figure 2.7). Formaldehyde is often used in the form of an aqueous solution during commercial production of PF resoles. The polymeric form of formaldehyde, paraformaldehyde, is rarely used in industrial processes due to its high cost. PF resoles used as wood binders are typically synthesized under 100 ^{o}C with a formaldehyde/phenol (F/P) ratio of 1.6 to 2.5, a final resin solids range of 40-60% and a final pH between 9 and 12 (Sellers, 1985).

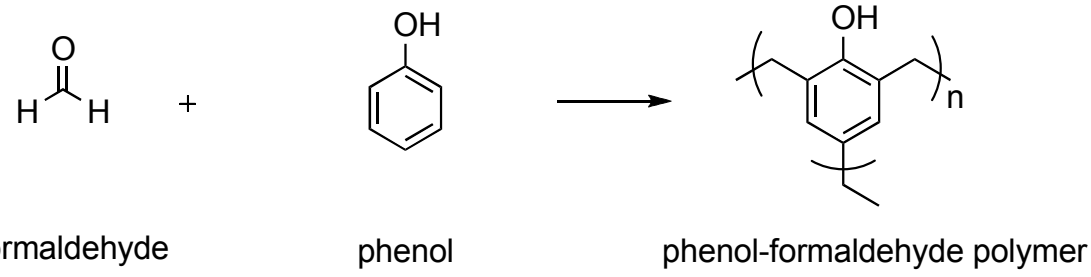


Figure 2. 7: Phenol-formaldehyde polymer from its reactants

The most commonly used catalyst in commercial resole preparation is sodium hydroxide (NaOH). Besides its catalytic effect, sodium hydroxide also improves the solubility of PF resoles in aqueous solution, which allows resoles to be synthesized with a high degree of advancement for fast curing, while maintaining good processability (Sellers, 1985). PF resole synthesis is a step growth polymerization comprising two steps: addition and condensation.

2.5.1 Addition Reaction

In an aqueous solution, formaldehyde is present in its hydrated form, methylene glycol (Walker, 1964). In an alkaline medium, phenols are deprotonated to form phenoxide ions as shown in Fig. 2.8. The electron rich ortho and para positions in phenoxide ions are susceptible to electrophilic aromatic substitution (often referred to as addition). Freeman and Lewis (1954) found that the para position is more reactive toward electrophilic aromatic substitution than is the ortho position. Also, the hydroxymethylation at the ortho positions was found to increase the reactivity of the para positions. This was explained by the formation of intra-molecular hydrogen bonds that lead to a higher negative charge on the para position (Figure 2.9). When sodium hydroxide is used as the catalyst, the formation of a chelate structure (Figure 2.10) is proposed which favors ortho-substitution (Caesar and Sachanen, 1948). Freeman and Lewis (1954) also found that the mono-substituted hydroxymethylated phenols (HMPs) react with methylene glycol to form di- and tri-substituted HMPs before the slower condensation reaction could occur. The formation of mono-, di- and tri- substituted HMPs is shown in Figure 2.11.

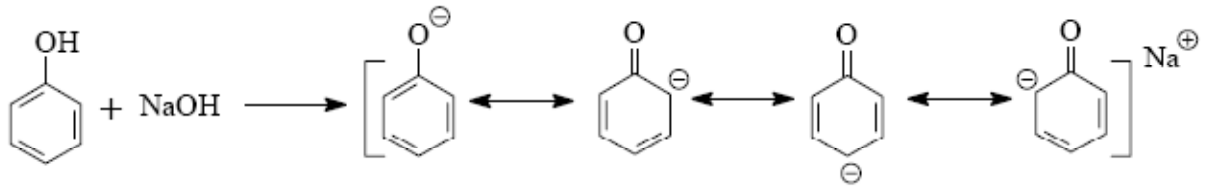


Figure 2. 8: Resonance structures of phenoxide ions in an alkaline medium

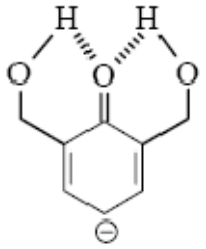


Figure 2. 9: Formation of intra-molecular hydrogen bonds after ortho-substitutions that activate the para position

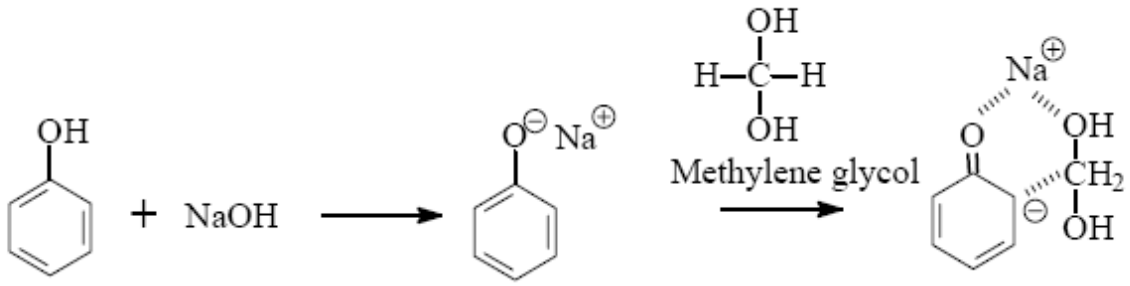


Figure 2. 10: Formation of a chelate ring structure under sodium hydroxide catalysis

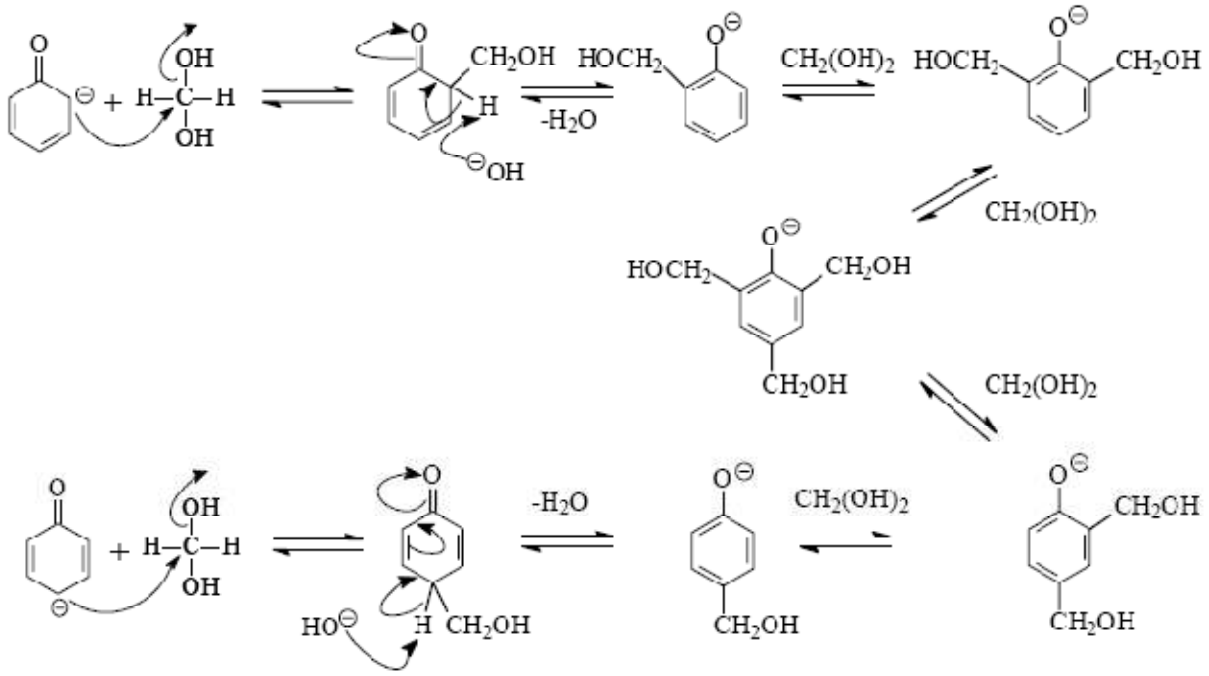


Figure 2.11: Addition reactions during resole synthesis: formations of mono-, di- and tri-substituted HMPs

2.5.2 Condensation Reaction

Overall, the step growth polymerization of HMPs is a water-producing condensation. However, as will be shown, this condensation occurs through electrophilic aromatic substitution. HMPs can be condensed to three stages, i.e. initial resoles (A stage), resitols (B stage) and resite (C stage) (Sellers, 1985). The initial resole (A stage) is a mixture of monomers and dimers of HMPs while the resite stage refers to the fully cured insoluble and infusible state (Marra, 1992). Commercial PF resoles used for wood bonding applications are usually condensed to B-stage with different molecular weights and molecular weight distributions suitable for various applications. It is generally agreed that HMPs condense through quinone methide (QM) intermediates. The formation of a quinone methide from HMP is shown in Figure 2.12. Quinone methides are strong

electrophiles and will readily substitute onto other electron rich phenoxides to form methylene bridges (Figure 2.13). Due to the high reactivity of para-hydroxymethyl groups in the condensation reaction, methylene bridges formed are mainly in the form of ortho-para (o,p) and para-para (p,p) bridges with the ortho-ortho (o,o) bridges rarely forming (Westler, 1986; Kim et al., 1997). The remaining hydroxymethyl groups are present predominantly on ortho positions in uncured resoles (Kim et al., 1997; Kim et al., 1980). In contrast to novolaks, dimethylene ether-type of bridges are scarce in resoles, and may only be present as short-lived intermediates that will convert to the more stable methylene linkages upon heating (Figure 2.14) (Kim *et al*., 1997; Kim *et al*., 1980; So and Rudin, 1990; Pizzi, 1994).

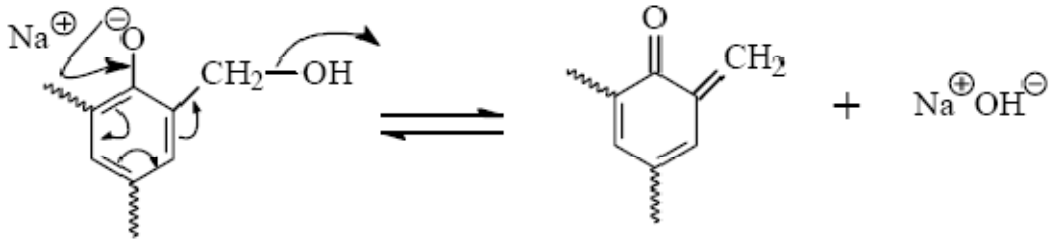


Figure 2. 12: Formation of quinone methide (QM) intermediate under alkaline conditions

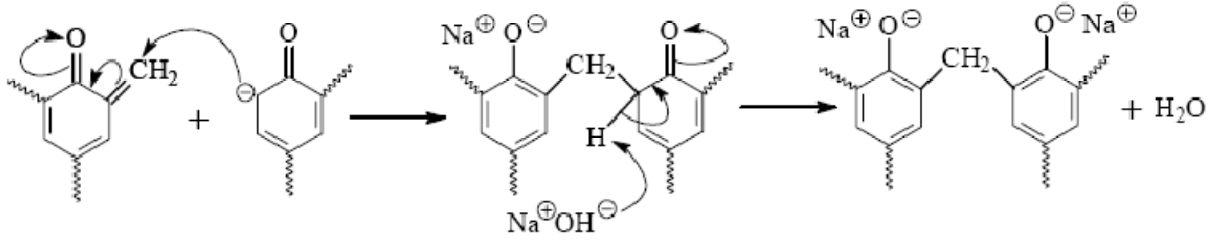


Figure 2. 13: Methylene bridge formation through quinone methide (QM) intermediates

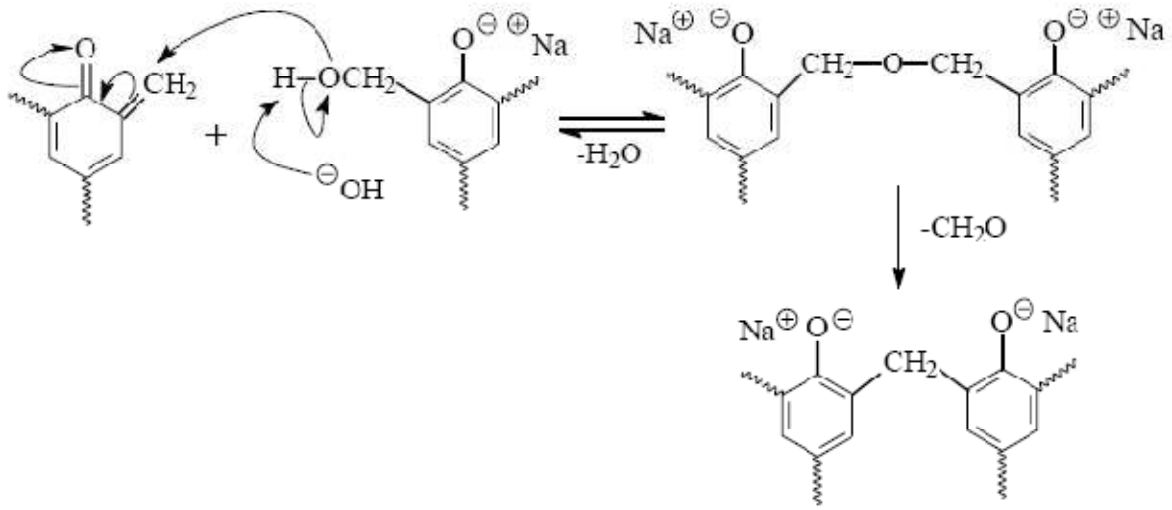


Figure 2. 14: Dimethylene ether bridge formation and its conversion to methylene bridge by releasing formaldehyde

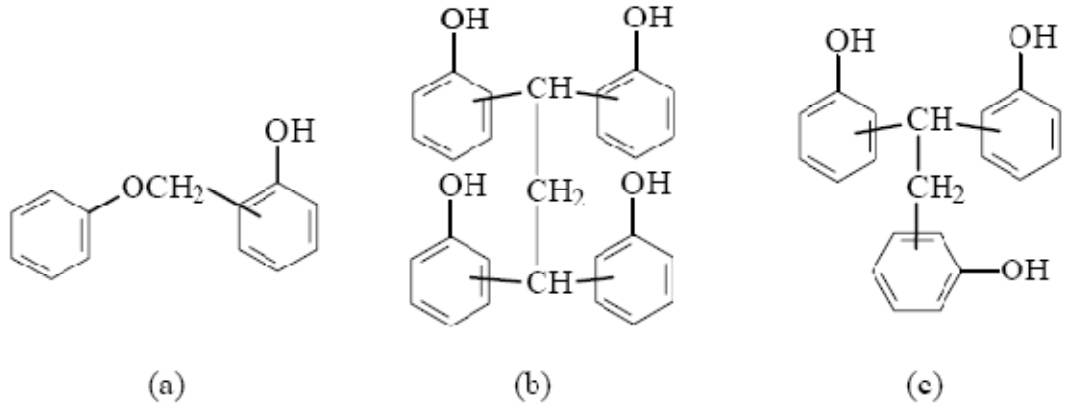


Figure 2. 15: Additional and unusual crosslink structures thought to be present in cured resoles (Maciel *et al.*, 1984)

By varying the reaction time, reaction temperature, catalyst type, and the ratio of formaldehyde to phenol, a number of adhesive systems with different characteristics can be produced (Knop and Scheib, 1979).

2.6 Naturally Derived Phenolic Resins

A number of natural phenolic-containing materials are available, including lignins and tannins. Many attempts with varying degrees of success have been made to use these materials either totally or partially for the production of wood adhesives (Pizzi 1994; Pizzi and Mittal, 1994). With the exception of cellulose, lignin is the most abundant polymeric material in the plant world. It is a complex, irregular polymer composed of phenyl propane (C9) units. Lignin is recovered mainly as a by-product of the pulping of wood for the production of paper, primarily by kraft pulping (an alkaline process) and to a lesser extent by sulfite pulping (an acid process). The substitution of lignin, particularly kraft lignin, for phenol in PF resins is the most studied use of lignin. This stems from the fact that lignin is phenolic in nature and, as such, is expected to undergo the same sorts of reactions that occur between formaldehyde and other phenolics. However, due to the fact that the aromatic ring of the lignin molecule is rather highly substituted and that any remaining sites can undergo reactions during the pulping process, there are few positions remaining for lignin to react with formaldehyde.

Sequential extraction of the bark of most coniferous and deciduous trees with water followed by aqueous alkali contents two fractions of polyphenols. These are commonly referred to as condensed tannins and hydrolyzable tannins, respectively. Hydrolyzable tannins have been used successfully as partial replacements for phenol in PF resin adhesives. However, their lack of a macromolecular structure, their low reactivity toward formaldehyde, and their limited worldwide production have led to minimal interest in these tannins as adhesive precursors (Pizzi, 1983). Condensed tannins, on the other hand, constitute more than 90% of the total world production of tannins and have generated considerable interest as precursors for adhesive production. Some of

these compounds can be reacted with formaldehyde or phenolic-formaldehyde prepolymers to produce suitable thermosetting resins for use in exterior conditions or for producing coldsetting, waterproof adhesives. Commercial extracts of western hemlock, Douglas fir, and redwood in North America were used in a limited capacity as sources of wood adhesives from about 1955 through 1975. Acacia bark tannin (wattle) is currently used in South Africa and South America as a source of wood adhesives. The large quantities of pine bark residues produced at wood-processing plants in North America, Australia, and New Zealand sparked research (especially following the oil crisis of the 1970s) on the use of tannin from these barks as "captive" sources of wood adhesives.

2.6.1 Reactivity of pine bark tannins

Pine bark tannin is more reactive toward formaldehyde than tannins from other sources. This limits the shelf life and assembly times of pine bark tannin adhesives. Condensed tannins and, importantly, even whole bark, can be "liquefied" in phenol with an acid catalyst. This process is referred to as phenolysis or phenolation because the phenol acts not only as the solvent but also as a reactant. The product can be used directly in the formulation of wood adhesives without having to first isolate the tannin (Santana *et al.,* 1995). The chemistry of the reactions that take place between phenol and tannin has been studied using catechin as a model. The results of these studies show that the reactions are very complex. The results suggest that, in part, the pyran rings of the tannin are opened and phenol is appended to the tannin structure.

Because pine tannins are highly reacting with formaldehyde, it is preferable for extracts to be reacted with a resol of low molecular weight and high methylol content, in which case the crosslinking molecules are larger and bonding stronger. The proposal of copolymerization of phenol and tannins with formaldehyde has the disadvantage of requiring close control of the reaction (Vazquez *et al.,* 1989). For large-scale industrial use, the physical and chemical properties of adhesives have to be suitably reproducible, which in the present context depends largely on the bark applied as well as on extraction and concentration processes (Vazquez *et al.,* 1987, 1989).

2.6.2. Development of tannin production technologies

The potential of bark as a raw material depends largely on the species of origin. Wattle tannins have been used commercially in South Africa since the 1970s, and extracts of Pine have been applied in New Zealand and Chile (yon Leyser, and Pizzi, 1990). However, over the last decade most research work in this area has been directed rather towards understanding the structure and chemistry of bark extract components than towards the development of new products and applications (Hemingway, 1981). Although the potential for production of pine bark tannins for wood adhesives has long been realized, commercial production has not succeeded due to the high production costs associated with the appropriate quality of high weight percentage recovery of extracts. Therefore, many techniques have been developed attempting to increase content of the pine bark tannins and to improve their quality for wood adhesives. These techniques include water extraction with addition of chemicals, solvent extraction (Yazaki, 1983) and fractionation of extracts with ultra filtration (Yazaki 1985, Pizzi, 1994). However, only the water extraction processes, with or without addition of chemicals, is relatively economically feasible.

Australian researchers have developed a pilot process which includes extraction in a counter-current hot water wash with high pressure filtration (Crammond and Wilcox, 1992). In a separate study in Australia, a laboratory process has been developed which has a four-stage squeeze extraction comprising two-stage hot water extraction, one-stage NaOH aqueous extraction, and one-stage hot water washing with sulphitation of the last two stages of extracts (Yazaki, and Collins1994). Different extraction processes have also been investigated in South Africa, Chile and New Zealand which include a counter-current water/methanol and metabisulphite/urea solution, sulphite solution (von Leyser and Pzzi, 1990) and vacuum belt counter-current sodium carbonate/sodium sulphite solution.

2.6.3. Factors favouring or limiting commercial production of tannins

Commercial potential of a process for the production of pine bark tannins will depend on several factors including availability of the bark resource, development of processing techniques, tannin product quality, size of the product market, production cost, and environmental concerns. According to Jingge and Maplesden (1998), issues favouring pine bark tannins are:

- Tannins are able to replace phenol and resorcinol, and can make aldehyde-free and zero emission adhesives.

- Tannins have a good environmental "image" compared with other phenolic adhesives. Strict regulations have been gazetted to decrease the proportion of synthetic phenol in

effluent waters from factories. Environmental concern is rising to limit formaldehyde emissions from wood products bonded with adhesives.

- There is potential for increased demand for use of more bonded wood products to cope with an increasingly variable resource, and thus more adhesives are needed especially from renewable resources.

- Fundamental knowledge of tannin extraction and adhesive formulation has been extended in the last two decades, and the technologies have been significantly improved for production and utilization of tannins.

The problems limiting commercialization of pine bark tannins are as follows:

- To achieve high weight percentage recovery and appropriate quality of tannins for wood adhesives production, the cost is high.

- The varying tannin properties caused by variability of bark sources necessitate development of different adhesive production systems.

- More technical difficulties are involved in replacing resorcinol with pine bark tannins than with wattle tannins; thus, more research is required to develop improved systems for production of pine bark tannin adhesives at competitive prices.

In Nigeria, where mangrove forests abound on the south coast, Ohunyon (1992) and Ohunyon and Ebewele (1992) have attempted to develop mangrove-tannin-based plywood adhesive. Their efforts were concentrated on using metal acetates to induce participation of the 'B' ring of the tannin flavonoid molecule in the tannin-formaldehyde condensation reaction. The 'B' ring is normally inert towards formaldehyde except at pH>8, when the reactivity of the 'A' ring towards formaldehyde becomes unacceptably high. High-level (55%) fortification with methylol phenol was found necessary to achieve good adhesive properties. Recent work on mangrove-tannin-based adhesive has shown that the level of adhesive fortification with either phenol or phenol-formaldehyde can be reduced drastically (to about 15%) by hydrolysis with sodium hydroxide and acetic anhydride (Sowunmi *et al.,* 1996).

2.7 Plywood Manufacture

Plywood is made from thin sheets of veneer that are cross-laminated and glued together with a hot-press. The wood veneer is literally peeled from the log as it is spun. Throughout the thickness of the panel, the grain of each layer is positioned in a perpendicular direction to the adjacent layer. There are always an odd number of layers in plywood panels so that the panel is balanced around its central axis. This strategy makes plywood stable and less likely to shrink, swell, cup or warp. However, the plywood may be the result of combination of the same material from a log or a tree or may be containing different species for different layers with a central symmetry. The plywood thus provides the entrepreneurs or researchers opportunity to try the best combinations from the economic angle (commercial) and from the functional angle (specialty). Such experimentation is more demanding for plantation species to economize the product and improves the quality. Plywood panels have been produced and marketed in Ghana

and other countries for many years. They are considered a material of choice in the building industry because of outstanding structural performance as defined by a high strength-to-weight ratio, excellent dimensional stability, and durability compared to other building material (Pease, 1994). Plywood typically consists of an uneven number of thin layers of wood veneers, called plies that are glued together into a panel. The individual plies are typically arranged in the panel so that their grains are perpendicular to one another (right angles of 90°). The 90° arrangement to one another improves the dimensional stability and makes the properties of the plywood more uniform along both the vertical and horizontal axes. The anisotropic nature of wood results in a tendency to swell less parallel to the grain than perpendicular to the grain and simultaneously gives wood greater strength parallel to the grain than perpendicular to the grain. Therefore, arranging individual plies at 90° to one another affords greater dimensional stability, decreases the tendency to split, and generally evens out the strength properties in all directions. If the grain angles were not varied then the plywood would have less dimensional stability and be much stronger along the grain axis but weaker perpendicular to the axis. The appearance of the final product can be improved if desired by applying a decorative surface veneer to give the final plywood a desired appearance. The final overall properties of the plywood depend on many factors, including the wood species, the quality of wood veneers, the order of placement of the veneer plies in the panel, the type and amount of adhesive applied, and the curing or pressing conditions.

CHAPTER THREE

MATERIALS AND METHODS

3.1. Chemometric Calibration of Phenolic Quantities in Pine Bark

3.1.1. Materials

Pine bark, obtained from 110 trees in plantation stands at Kumasi and Winneba metroplolis of Ghana, were dried at 40°C for 48 h in a convection oven, ground in a Wiley mill to 100 - 250 μm particle size, sealed in a plastic bag, and stored at room temperature until use. All chemicals used were of analytical grade, obtained from commercial suppliers (MRS Scientific representative in Kumasi, Ghana).

3.1.2. Extraction procedure

For each of the 110 trees, the phenolic compounds were extracted using 20 g of the dried powdered bark sample in soxhlet extraction. Extractions were carried out successively with 60% aqueous acetone (v/v) and 70% aqueous ethanol (v/v). Samples were heated to boiling until exhaustive extractions were achieved (indicated by absence of phenolics in the extraction solvent contained in the soxhlet). For each extract (20g/400ml), 0.1 ml was taken for total phenolics determination and the rest concentrated in vacuo to dryness. The residue was finally dried in an aerated oven at 60°C till constant weight was achieved. The dried crude extracts were used for tannin content and Stiasny number determinations. Each solvent extraction was run in duplicate.

3.1.3 Chemical Analysis of Pine Bark Extract

3.1.3.1. Total phenolics determination

The total phenolic content was determined in the aqueous acetone and aqueous ethanol extracts by means of a modified Folin-Ciocalteau assay with slight modifications. Gallic acid standard solutions were prepared at 0.0, 0.1, 0.2, 0.3, 0.4 and 0.5 mg/ml. The extracts (0.025 ml) and the gallic acid standards (0.1 ml) were transferred to 15 ml test tubes and 0.075 ml distilled water added to each. Three ml of 0.2 N Folin-Ciocalteu reagent (Sigma-Aldrich Co.) were also added to each test tube followed by 2.0 ml of 9.0% (w/v) aq. Na_2CO_3. The tube was then vortexed and the absorbance at 765 nm taken after 60 min on a Beckman DU 650 UV-VIS spectrophotometer. The amount of total extractable phenolics as gallic acid equivalent was calculated from a calibration curve using standard gallic acid solution, and expressed on a dry matter basis. All samples were run in duplicate.

3.1.3.2. Tannin content determination

Tannin content was determined by the method of Roux (1951): For each sample, a mass of 800 mg were dissolved in 200 ml distilled water. Slightly chromated hyde powder (6 g) previously dried in vacuum for 24 hours over $CaCl_2$ was added and the mixture stirred for 1 hour at ambient temperature. The suspension was filtered under gravity through a sintered glass filter. The weight gain of the hyde powder expressed as a percentage of the weight of the starting material was equated to the percentage of tannin in the sample. All samples were analysed in duplicate.

3.1.3.3. Stiasny reaction

Reactive tannin content was determined by the method of Hillis and Urbach (1959): For each tannin sample, a mass of 200 mg were dissolved in 20 ml distilled water. 2 ml of 10M HCl and 4

ml of formaldehyde (37%) were added and the mixture heated under reflux for 30 min. The reaction mixture was filtered whilst hot through a sintered glass filter. The precipitate was washed with hot water (5 x 10 ml) and dried over $CaCl_2$. The yield was expressed as a percentage of the starting material. All samples were analyzed in duplicate.

3.1.4. Near Infrared Spectra Aquisition

Each of the 110 powdered un-extracted bark samples was placed in a NIR System micro sample cup. Near-infrared (NIR) spectra were recorded on a Bruker FT-IR spectrometer to measure diffuse reflected light in the range 800 nm to 2,600 nm from the sample held in the spinning sample holder. With a spectral resolution of 20 cm^{-1} (678 data points), sixty four scans per spectrum were acquired and averaged. After the spectrum had been obtained, the sample cup was emptied, repacked with the next sample and the spectrum obtained. The background was taken with a sintered gold standard.

3.1.5. Chemometric Calibration

Chemometric modelling was performed with the OPUS software package (version 5.5). For each sample, one reflectance measurement of monochromatic light was made from 800 to 2600 nm to produce a spectrum with 678 data points at 2-nm intervals over this range. Reflectance (R) was converted to absorbance (A) using the following equation: A= log (1/R). For spectra pre-processing, the algorithms of full multiplicative scatter correction, first derivative (smoothed and derived according to Savitzky and Golay, 1964), straight line subtraction and standard normal variant among others were applied. Wavelength selection was done manually as well as

automatically by means of the Martens Uncertainty test to eliminate unimportant variables to simplify the models and make them more reliable.

Once these preprocessing procedures were completed, partial least squares method (PLS) was used to develop calibration models for predicting the total phenolic content, tannin content and Stiasny number. For each model, the standard error of calibration (SEC) was calculated for the calibration samples and the standard error of cross validation was calculated for the predicted samples. The coefficient of determination (r^2) for each model was also calculated.

The standard error of calibration (SEC) and standard error of cross-validation (SECV), which represents the sensitivity of prediction, were used to measure the model's performance. The SEC and SECV are calculated as follows:

$$SEC = \sqrt{\frac{\sum_{i=1}^{n}(y_c - y_i)^2}{n-1}} \qquad \textbf{(3.1)}$$

$$SECV = \sqrt{\frac{\sum_{i=1}^{N}(y_i - y_p)^2}{N}} \qquad \textbf{(3.2)}$$

Where y_i is total phenolic content, tannin content or Stiasny number of sample i determined by wet chemical analysis, y_c is the NIR calibrated value, y_p is the NIR predicted value, n is the

number of samples used in calibration and *N* is the number of samples used in prediction (Miller, 1989).

3.2. Optimization of Extraction Process Parameters

3.2.1. Material

Pine bark were obtained from plantation stands and were dried at 40°C for 48 h in a convection oven, ground in a Wiley mill to 100 - 250 μm particle size, sealed in a plastic bag, and stored at room temperature until use. All chemicals used were of analytical grade, obtained from commercial suppliers (MRS Scientific representative in Kumasi, Ghana).

3.2.2. Experimental Design

The experimental design for this study was divided into two major parts. Firstly, single factor experiments were performed to determine the appropriate range of conditions for pine bark phenolics extraction, namely; extraction temperature, extraction time, solvent composition, solid-liquid ratio and number of extraction stages. Each independent variable was varied over a range whilst keeping the others constant. Secondly, the optimization of phenolic compounds extraction was carried out using Response Surface Methodology (RSM).

3.2.3. Extraction Process

The solvent extraction adopted in this study essentially consisted of refluxing 20g of powdered pine bark in an extracting solvent and filtering the extract from the bark through a sintered glass filter under vacuum, and drying the filtrate in an aerated oven at about 60°C till constant weight was achieved.

3.2.3.1. Single Factor Experiments

Effect of solvent composition on extraction of phenolic compounds

Extractions were conducted using the following solvents; aqueous ethanol and aqueous acetone each at concentrations of 10, 20, 40, 60 80 and 100% (v/v); aqueous NaOH at concentrations of 0.05, 0.1, 0.2, 0.5, 1.5 and 2% (wt/v) and finally water. The extractions were carried out according to the procedures as described in Section 3.2.3. The extraction time was fixed at 60 min, whilst the extraction temperatures were fixed at the boiling points of the solvents. For each solvent, the best solvent concentration was chosen based on the highest value of tannin content.

Effect of liquid-solid ratio on extraction of phenolic compounds

The effect of liquid-solid ratio was studied using aqueous extraction at 80°C extraction temperature for 60 min extraction time with ratios of 10:1, 20:1, 25:1, 30:1, 40:1 and 50:1 (v/wt). The extraction procedures were repeated as described in solvent composition. The most suitable solid-liquid ratio and range was selected based on the highest value of tannin content.

Effect of Extraction time on extraction of phenolic compounds

For each solvent except aq. NaOH, the impact of extraction times (30, 45, 60, 90, 105, 120, 150 and 180 min) on the tannin content was studied. Extraction time for aq. NaOH ranged from 15 to 120 min. Extraction was accomplished by applying the best solvent concentration and liquid-solid ratio. The extraction procedures were repeated as described in solvent extraction. The best extraction time and range was chosen based on the highest value of tannin content.

Effect of Extraction temperature on extraction of phenolic compounds

For aqueous acetone, the effect of extraction temperatures (35°C, 40°C, 45°C, 50°C, 55°C and 60°C) on tannin content was studied. Whilst the temperatures used for aqueous ethanol was 35, 40, 45, 50, 55, 60, 70 and 80°C. Temperatures of 40, 45, 50, 55, 60, 70, 80, 90 and 100°C were used for both aqueous NaOH and water extractions. The extraction was executed by using the best solvent composition, liquid solid ratio and extraction time. The extraction procedures were repeated as described above. The best extraction temperature and range was chosen based on the highest value of tannin content.

Effect of Extraction stages on extraction of phenolic compounds

The effect of extraction stages was studied using aqueous extraction at the best extraction conditions (temperature, time and liquid-solid ratio) under extraction stages of 1, 2, 3, 4 and 5. The extraction procedures were repeated as described above. The most suitable number of extraction stages was noted based on the highest value of tannin content.

Based on the results of the single factor experiments, the ranges of the four factors extraction temperature, extraction time, solvent concentration and solid-liquid ratio were determined and used for response surface methodology using the solvents water, aqueous acetone, aqueous ethanol, and aqueous NaOH.

3.2.3.2. Response Surface Methodology

a) Experimental design for the response surface procedure

Response surface methodology was used in this study. A four factor, five level central composite rotatable designs (CCRD) was employed using Design-Expert 8.0 (Stat Ease, USA) optimization software to examine the optimum conditions of extraction variables for the pine bark phenolics. For each of the solvents; aqueous acetone, aqueous ethanol and aqueous NaOH, the generated runs of the CCRD investigated in this work consisted of 28 experimental runs with twenty two factorial points, two star points and four replicates at the centre point. The low and high factor values were entered in terms of alpha as extreme points (star), thus all other design points were located within these extremes. The design variables were the extraction temperature, T, the extraction time, t, the solvent concentration, C and the liquid to solid ratio, V. For the aqueous extraction, the CCRD design comprised of 18 experimental runs with twelve factorial points, two axial points and four replicates at the centre point. The coded values with their corresponding real experimental values can be found in Table 3.1. In RSM designs, a variation in response is caused by changing the level of the factor considered, when the factors are kept constant (Box and Behnken, 1960). Response surface methodology has been used to study the optimization of chemical processes and products (Sudesh et al., 2010; Mane et al., 2007; Ven et al., 2002).

Table 3. 1: Coded and Real Values of Solvent Extractions

Solvent	Concentration		Temperature		Time		Liquid-Solid ratio	
	Coded	**Real (%)**	**Coded**	**Real (°C)**	**Coded**	**Real (min)**	**Coded**	**Real**
Aqueous Acetone	-2	20	-2	40	-2	30	-2	10:1
	-1	40	-1	45	-1	60	-1	15:1
	0	60	0	50	0	90	0	20:1
	1	80	1	55	1	120	1	25:1
	2	100	2	60	2	150	2	30:1
Aqueous Ethanol	-2	20	-2	40	-2	30	-2	10:1
	-1	40	-1	50	-1	60	-1	15:1
	0	60	0	60	0	90	0	20:1
	1	80	1	70	1	120	1	25:1
	2	100	2	80	2	150	2	30:1
Aqueous NaOH	-2	0.05	-2	40	-2	15	-2	10:1
	-1	0.1	-1	60	-1	30	-1	15:1
	0	0.5	0	80	0	45	0	20:1
	1	1	1	90	1	60	1	25:1
	2	1.5	2	100	2	90	2	30:1
Water			-1.68	40	-1.68	30	-1.68	10:1
			-1	60	-1	60	-1	15:1
			0	80	0	90	0	20:1
			1	90	1	120	1	25:1
			1.68	100	1.68	150	1.68	30:1

For all the solvents, the responses were the tannin content Y, sugar content S and Stiasny number N. The variables X_i (ie. T, t, C and V) were coded as x_i based on Equation (3.3):

$$x_i = (X_i - \bar{X}_i) / \Delta X_i \qquad \textbf{(3.3)}$$

where, x_i was the coded value ($-\alpha$, -1, 0, +1, $+\alpha$) of an independent variable, $\bar{X}$ was the real value of an independent variable at the center point, and ΔX_i was the step change value. Each experimental treatment was carried out in triplicate and the average value was taken as response, Z. Randomizing the order of experiments reduced the effects of unexplained inconsistency in the observed response due to irrelevant factors.

b) Determination of the optimum conditions

The Design-Expert 8.0. software was set to search the optimum desirability of the response variables, i.e., the maximum content of tannin, maximum of Stiasny number and minimum content of sugar. Experimental data were fitted to the following second-order polynomial model (Eq. 3.4) and the regression coefficients (β's) obtained.

$$Z = \beta_0 + \sum_{i=1}^{k} \beta_i X_i + \sum_{i=1}^{k} \beta_{ii} X_i^2 + \sum_{i=1}^{k-1} \sum_{\substack{j=2 \\ i<j}}^{k} \beta_{ij} X_i X_j \qquad \textbf{(3.4)}$$

where $X_1, X_2, \ldots, X_k$ are the independent variables affecting the responses Z's; $\beta 0$, βi (i=1, 2, . . ., k), βii(i=1, 2, . . ., k), and βij(i=1,2, . . ., k; j=1,2, . . ., k) are the regression coefficients for intercept, linear, quadratic, and interaction terms, respectively; k is the number of variables.

c) Verification of model and extraction for resin processing

Using the predictive models generated by the RSM, the various optimized conditions (Table 4.15-4.24) were separately used to extract phenolics from 80 g of bark samples and used for condensable phenol-formaldehyde resin processing. The tannin content and Stiasny number of the extracts were determined using the methods described in 3.1.3.2 and 3.1.3.3 respectively and

the sugar content determined as in 3.2.3.2.d. The contents were compared with the predicted values of the models in order to examine the validity of each model. Each set of experiment was conducted in duplicate.

d) *Total Sugars in Extractives*

Total sugars in extractives were measured according to the phenol-sulfuric acid method (Dubois *et al*., 1956) with a slight modification. Ten mg extract dissolved in 10 ml of water was transferred to a centrifuge tube, and then 10 ml of 1% lead acetate aqueous solution was added. After 20 min, the tube was centrifuged at 18 000 rpm for 20 min. To 2 ml of the supernatant transferred to a new centrifuge tube were added 0.05 ml of 80% phenol aqueous solution and 5 ml of concentrated sulfuric acid. After 35 min, the tube was centrifuged at 3500 rpm for 5 min, and the absorptivity of the supernatant was read at 490 nm. Total sugar content was reported as average per cent of oven-dried bark meal (w/w) and the experiment was carried out in duplicate. The calibration curve was determined using glucose as the standard sample.

e) Efficiencies of extraction

The "total" phenolic concentrations were measured by an accelerated solvent "total" extraction (ASE) protocol (described in 3.3). The concentrations of phenolics from the optimized extractions above were compared with the ASE phenolic concentrations in order to determine the efficiencies of the optimized models.

3.3. Accelerated Solvent Extraction (ASE)

Extractions were carried out using a pressurized liquid extractor (PLE, Model ASE 200, Dionex Corporation, Sunnyvale, California, USA). Powdered pine bark material was obtained by

grinding dried pine bark with a Cryo-grinder and passing the powdered material through a standard sieve number 20. Extractions were carried out by placing 2 g of dried powdered bark in an 11 ml stainless steel extraction cell with two circular cellulose filters (size 1.983 mm, Dionex Corporation) placed at the bottom of the extraction cell in order to prevent suspended particles from entering the collection vials. A total of four extraction cycles were performed for each sample and the purge time was set at 90 s with a flush of 100%, whilst the heating time and static time were set at 5 min apiece. The extraction solvent was 70% aq. ethanol and the extraction temperature and pressure were set at 80°C and 100 bar respectively. Both extraction cells and collection vials were arranged appropriately in the two designated carousels. The extracts were collected in 60 ml amber sample vials fitted with Teflon coated rubber caps. The extracts were bulked, concentrated in a rotary evaporator and dried in an aerated oven at 60°C till constant weight. The dried extract was used for tannin content analysis.

3.4. Formulation of Tannin-Formaldehyde Adhesive for Plywood Manufacture

3.4.1. Materials

Veneer used for plywood preparation was rotary cut *Ceiba pentandra* (ceiba) and *Antiaris toxicaria* (Kyenkyen). Industrial grade phenol-formaldehyde and urea-formaldehyde resins were obtained from a local plywood mill. The tannins were from the extractions in this study and all chemicals used were of analytical grade, obtained from commercial suppliers.

3.4.2. Resin Processing

Tannin-Formaldehyde resin was processed in a 2-L glass reactor following the cook procedure similar to that outlined previously by Pizzi (1983). Tannin was dissolved in water to prepare a

55-percent aqueous solution, and the solution was left overnight to ensure complete hydration of the tannin. 2.5 parts of 50-percent aqueous sodium hydroxide, 10 parts of paraformaldehyde, and 17 parts of water were added to 100 parts of tannin solution. The solution was refluxed for 1 h and cooled to room temperature, and the pH was lowered to 7.6 by adding 3 parts glacial acetic acid to obtain a resol resin. Each plywood adhesive mix was formulated by adding 20 parts cassava flour, 4 parts urea formaldehyde (as a modifier) and 60 parts water to 100 parts of the resin under agitation using a speed regulated stirrer. Once a homogenous solution was obtained, 1 part hexamine (hardener) was also added under agitation. Industrial grade phenol-formaldehyde adhesive was used as the standard.

3.4.3. Effect of Extraction Conditions on Resin Quality

To study the effect of extraction conditions on the resin quality, resins were processed (as described in 3.4.2) from tannins extracted at the following response parameters; i) only tannin was optimized, ii) only sugar was optimized, iii) only Stiasny number was optimized and iv) tannin, sugar and Stiasny number were optimized, for each of the 4 solvents; aqueous acetone, aqueous ethanol, aqueous NaOH and water (Table 3.2). The resins were characterized by viscosity, pot life and plywood bond strength. Each experiment was done in triplicate.

Table3. 2: Resins prepared from tannins extracted at various optimized conditions

Solvent	Optimization condition	Resin No.
Aqueous acetone	Only tannin optimized	1
	Only sugar optimized	2
	Only Stiasny optimized	3
	Tannin, sugar and Stiasny optimized	4
Aqueous ethanol	Only tannin optimized	5
	Only sugar optimized	6
	Only Stiasny optimized	7
	Tannin, sugar and Stiasny optimized	8
Aqueous NaOH	Only tannin optimized	9
	Only sugar optimized	10
	Only Stiasny optimized	11
	Tannin, sugar and Stiasny optimized	12
Water	Only tannin optimized	13
	Only sugar optimized	14
	Only Stiasny optimized	15
	Tannin, sugar and Stiasny optimized	16

3.4.4. Viscosity and Pot Life Determination

Viscosities of all resins and the pot life of the blends were measured according to American Society for Testing and Materials (ASTM) Method D 1084 (ASTM 1991 a), with a Brookfield Digital Viscometer Model LVTD (Brookfield Engineering Laboratory, Inc.) using LV-1, LV-2, and LV-3 spindles at various rotation speeds.

3.4.5. Panel Preparation

Three-ply plywood were prepared using veneer sheets from Kyenkyen (*Antiaris toxicaria*) as face and back and Ceiba (*Ceiba pentandra*) as core. Area dimensions of 25 cm x 40 cm were demarcated on the veneers. Each of the adhesives was applied on the demarcated areas with a laboratory roller at a spread rate of $2g/cm^2$ of single glue-line. The spread panels were then pressed at 120°C and a pressure of 1.0 MPa at pressing time of 8 minutes to obtain plywood of thickness 9 mm. The open assembly time was minimal since the veneers were mounted immediately after the adhesive was spread and closed assembly time was 5 minutes. Three panels were manufactured for each adhesive. The plywood panels were made in an industrial plywood mill.

3.4.6. Adhesive Bond Evaluation

Eighteen specimens were cut from each panel and tested in shear under wet and dry conditions (ASTM 1991c). For the dry testing, the specimens (six) were conditioned to equilibrium at 23°C ± 1°C and 50 ± 2 percent relative humidity. Wet testing involved soaking another six test

samples in water for 24 hours before testing. In the cyclic boil resistance (CBR) test, the last six samples were submerged in boiling water for 4 hours, dried at 60°C for 20 hours in an oven and the cycle repeated before testing. Both dry and wet specimens were tested under shear with an Instron Model 1000 testing machine (Instron Corporation). Bond quality was evaluated from the shear strength of each specimen. Delaminations of plywood specimens during CBR test were also recorded.

3.5. Statistical Analysis

Analysis of variance (ANOVA), at the 95% level was performed on shear strength of plywood test samples using SPSS statistical software. Least significant difference (LSD) was used to separate data into significantly different groupings.

CHAPTER FOUR

RESULTS AND DISCUSSIONS

4.1 Calibration of chemical properties

A statistical summary of the polyphenolic content, tannin content and Stiasny number of *Pinus caribaea* bark determined through wet chemical analysis is given in Table 4.1. A meaningful interpretation of calibration results depends to a large extent on the accuracy and precision of the wet chemical analysis of the samples. The polyphenol content of *P. caribaea* bark varied from 16% to 23.5% with a mean and standard deviation of 19.69% and 1.18% respectively. Similarly, the tannin content and Stiasny number varied from 9.2 – 15.4% and 64.36 – 86.12% with means of 11.82% and 74.97% respectively. The values determined for each of the chemical properties covered a large enough range, which was helpful for developing good calibration curves.

Table 4. 1: Descriptive statistics for polyphenol content, tannin content and Stiasny number of *P. caribaea* bark samples.

Parameter	Range	Mean	Standard deviation
Polyphenol content (%)	16 -23.5	19.69	1.18
Tannin content (%)	9.2 – 15.4	11.82	0.73
Stiasny number	64.36 – 86.12	74.97	4.91

The NIR diffuse reflectance spectra of *P. caribaea* bark samples (Fig. 4.1) demonstrated a high degree of variation, with wavelengths in the regions 7500 – 6200 cm^{-1} and 5500 – 4500 cm^{-1} showing the greatest variability. Bands in the region 6170 – 5800 cm^{-1} results from the first overtone of C – H stretch, while bands in the region 4760 – 4350 cm^{-1} mainly results from C – H, N – H and O – H combination bands (Shenk *et al*., 1992; Osborne *et al*., 1993). Michell and Schimleck (1996) in a study of *Eucalyptus globulus* Labill Woods, noted that the bands at 5995, 4800 and 4690 cm^{-1} were all very well correlated with hot water extractives and lignin content.
The best frequency intervals are in the region of the spectrum in which the reflected light intensity best correlates with the concentrations of the analyzed chemical species. Figures 4.3a and 4.3b show the relative reflectance spectra of the highest, lowest and two other intermediate values of tannin content and Stiasny number respectively. Since the spectral data below 800 nm and above 2600 nm contained considerable noise, the wavelengths of 800 nm to 2600 nm were used in this study. Several bands in these regions showed variations in absorbance that could be attributed to a general trend of increasing or decreasing Stiasny number as observed by Schimleck and Yazaki (2003).

The flexibility of NIRS makes it possible to manipulate a set of samples and to choose the best mathematical regression for obtaining the calibration equation (Mark**,** 1989). The most appropriate mathematical model should be used to predict the composition of samples that needs to be determined. In this study, the 'leave-one-out' cross validation of the PLS algorithm automatically contented regression models. Table 4.2 presents the results obtained in the calibration process for all the three models (polyphenol content, tannin content and Stiasny number) using the partial least-squares method. These results show that, for all the models, the

coefficient of determination was high. These values represent a reduction in the standard error of calibration (SEC) and the standard error of cross validation (SECV). These figures can thus be used as an indicator of validation (Stone, 1974).

The leave-one-out cross validation method was used to calculate the prediction residual error sum of squares (which calculates the lack of prediction accuracy) and to establish the number of PLS components for each model. A number of PLS components that contents the lowest prediction residual error sum of squares is usually chosen to establish a model (Geladi and Kowalski, 1986). In this study, a PLS component of 4 was found for each of the models.

Other criteria generally used to assess the quality of a model include the root mean square error of calibration (SEC), SECV and the correlation coefficient (r^2). A good model should have a low SEC, a low SECV and a high correlation coefficient (r^2) between the predicted and measured values, but also a small difference between SEC and SECV. The correlation coefficient r^2, the most commonly used, should be higher than 0.8 for quantitative predictions. For excellent models, the SEC-to-SD ratio should be ≤ 0.2, where SD is the standard deviation of the reference values. If $0.2 <$ SEC-to-SD ratio ≤ 0.5, quantitative predictions is possible (Couˆteaux *et al.,* 2003). The SD-to-SECV ratio should be ≥ 2 (Chang *et al*., 2001; Chang and Laird, 2002), SECV-to-SEC ≤ 1.2 and the SD-to-SECV ratio should be ≥ 2.5 (Mathison *et al*., 1999). The PLS regression calibrations developed for polyphenol content, tannin content and Stiasny number in this study are given in Table 4.2.

Table 4. 2: The PLS regression calibration developed for polyphenol content, tannin content and Stiasny number

Model	SEC	SECV	SEC/SD	SD/SECV	SECV/SEC	R^2
PhC (%)	0.21	0.23	0.17	5.13	1.09	0.96
TC (%)	0.12	0.14	0.16	5.21	1.16	0.97
SN	1.25	1.26	0.25	3.89	1.00	0.95

PhC: Polyphenol content TC: Tannin content SN: Stiasny number

Plots indicating the relationship between laboratory determined polyphenol, tannin contents and Stiasny number against their NIR fitted values are shown in Figures 4.5a – 4.5c respectively. All the plots show that over the range of calibration sets the data were well fitted by the PLS regression. Gielinger *et al*. (2002) have used NIR spectroscopy to estimate total soluble extractives and phenolic contents from Larch heartwood, recording good calibration models. Donkin and Pearce (1995) have also used NIR spectroscopy to estimate total soluble extractives from the bark of *Acacia mearnsii* reporting a correlation coefficient of 0.99. Their calibration was developed using 11 factors, which could be considered excessive. Schimleck and Yazaki (2003) used NIR spectroscopy to estimate hot water extractives and Stiasny number from the bark of *P. radiata* reporting a correlation coefficient of 0.88 and 0.96 respectively which are comparable to the values obtained in this study.

The three calibration models for polyphenol content, tannin content and Stiasny number were accurate with r^2 = 0.96, 0.97 and 0.95 respectively. In general, all the models showed good predictive ability as can be observed in Figures 4.4a – 4.4c. For each model, the slope of the calibration curve was close to 1.0 indicating a good calibration. However, the PLS model for tannin content showed the highest prediction performance according to SECV/SEC, SEC/SD,

SD/SECV and r^2 (Table 4.2). Values obtained for SEC and SECV were close for each model, indicating that the introduction of the given number of PLS components did not create an over-fitting effect and that the calibration model was valid. The NIRS fitted data points for the three calibration curves are given in appendix 1.

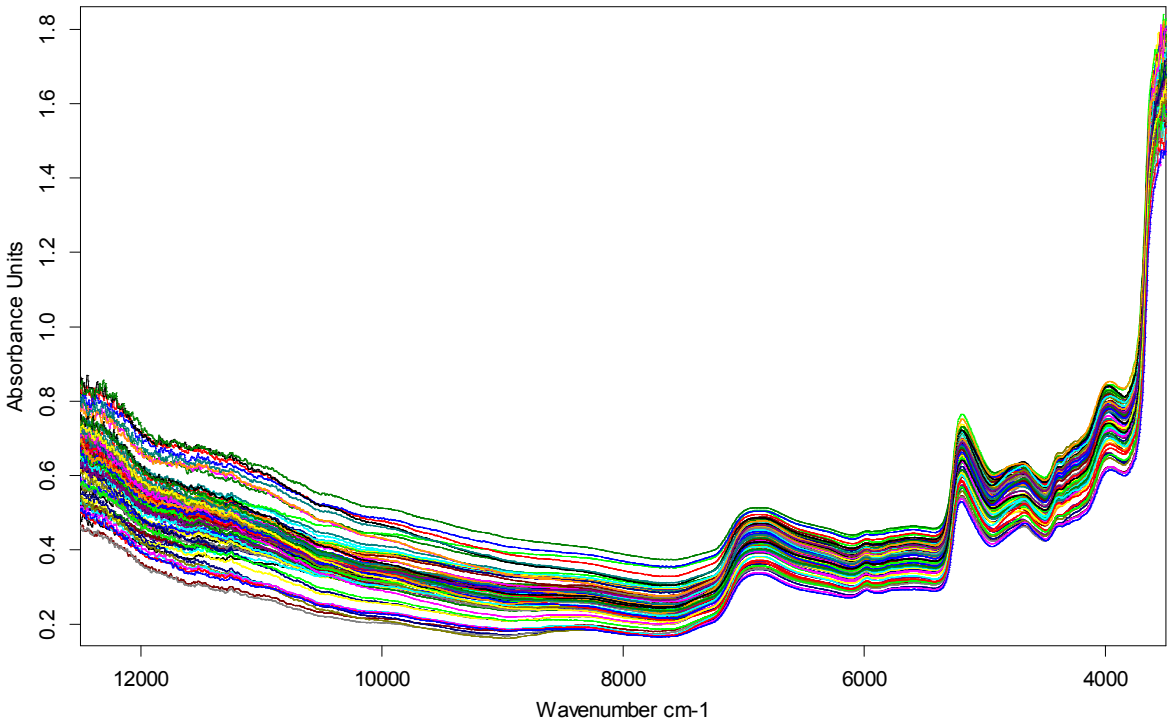


Figure 4. 1: Near infrared diffused reflectance spectra of *P. caribaea* bark

.

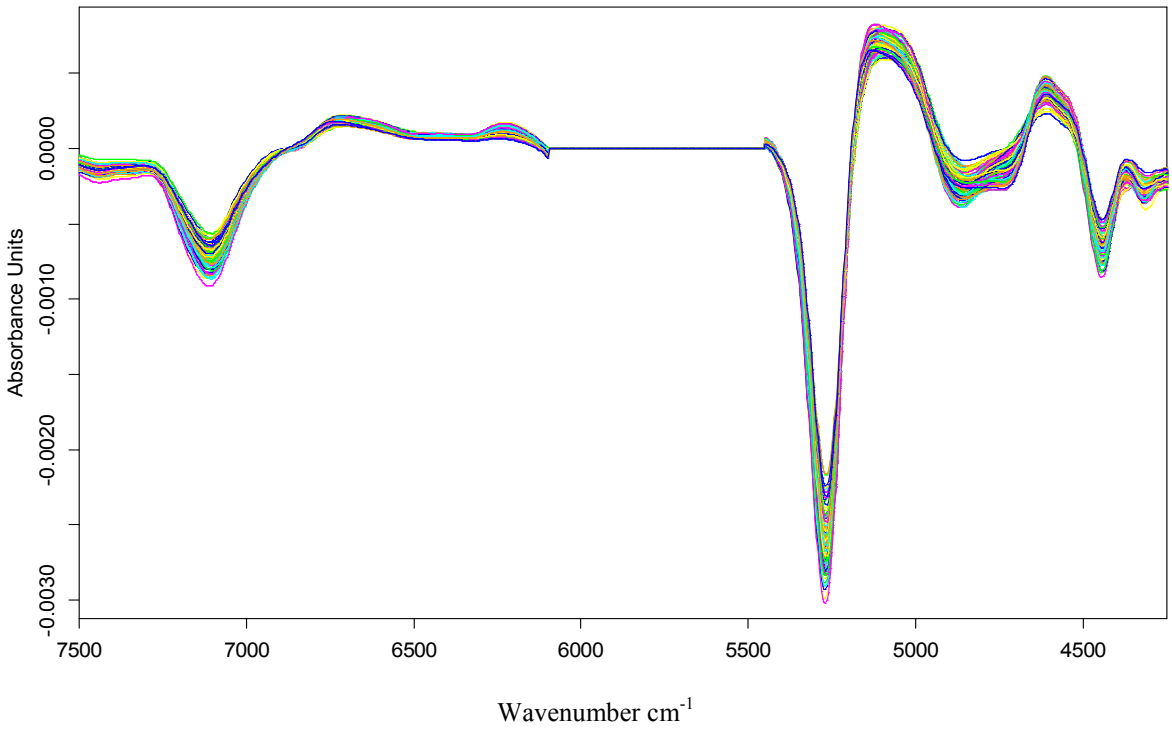


Figure 4. 2: First derivative spectra of *P. caribaea* bark in selected wavelength region

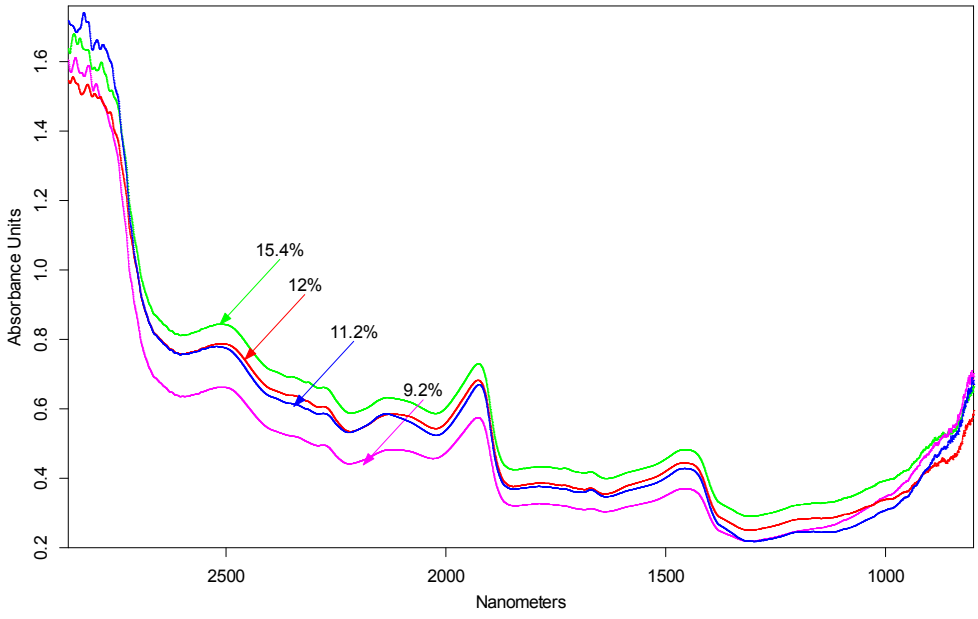


Figure 4. 3a: NIR spectra of four P. caribaea bark samples showing different tannin contents

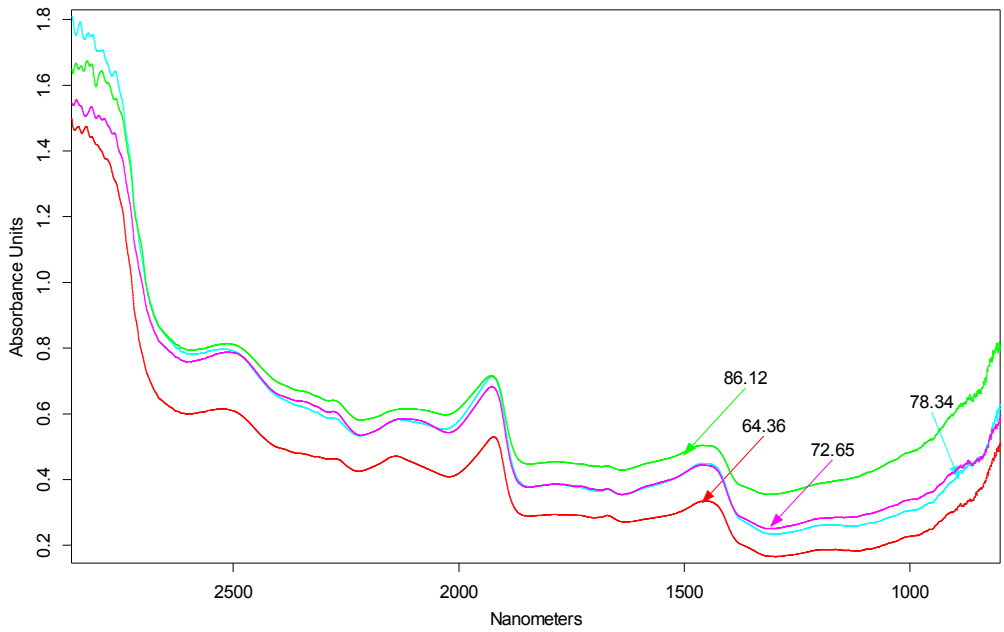


Figure 4. 3b: NIR spectra of four P. caribaea bark samples showing different Stiasny numbers.

The quality of the chemometric model depends on the choice of the correct number of factors (rank) used for the model. Choosing too small a rank, results in underfitting so that not all features can be explained by the model. On the other hand, including too many factors (rank too high) leads to overfitting and only adds noise, and in fact degrades the model. As a consequence, there is an optimum number of factors for every system (that is an optimum rank). A criteria for determining the optimum rank is to look at the root mean square error of cross validation resulting from an analysis of the cross validation. If the root mean square error of cross validation (RMSECV) is depicted against the rank used in each model, a minimum can be observed in this graph, indicating the optimum rank. In this study, the optimum rank for each of the models was 9 (Figure 4.5).

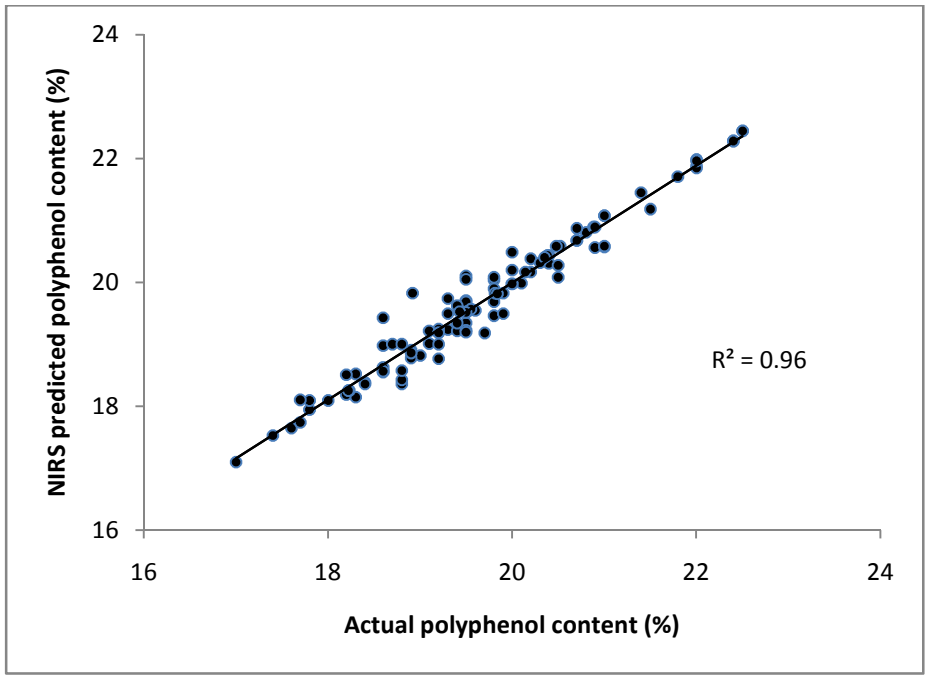


Figure 4. 4a: Actual versus predicted values for calibrations estimating a) polyphenol content.

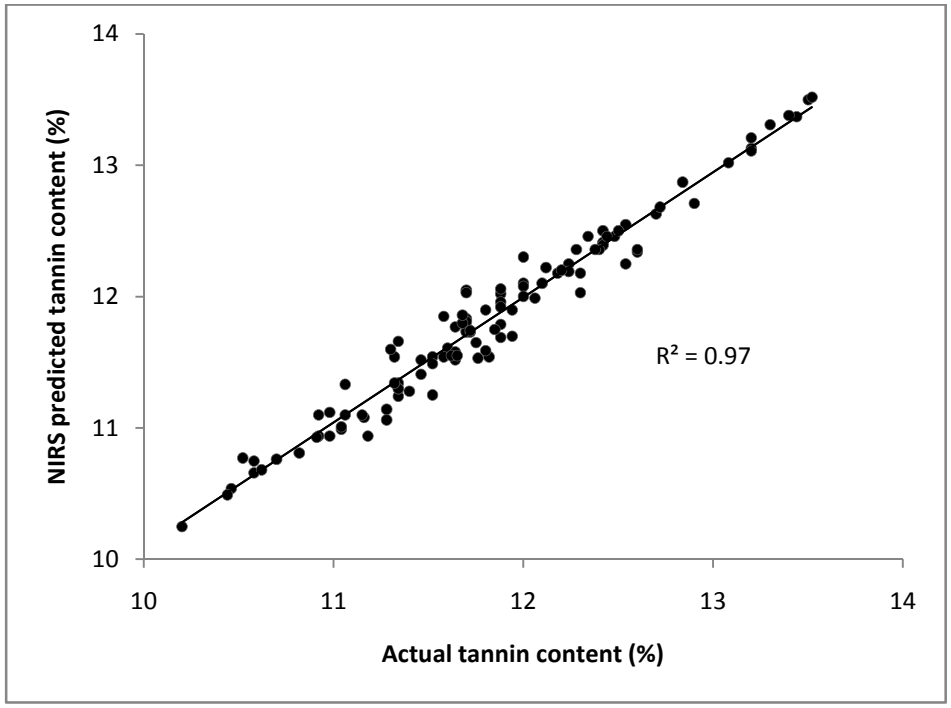


Figure 4. 4b: Actual versus predicted values for calibrations estimating tannin content.

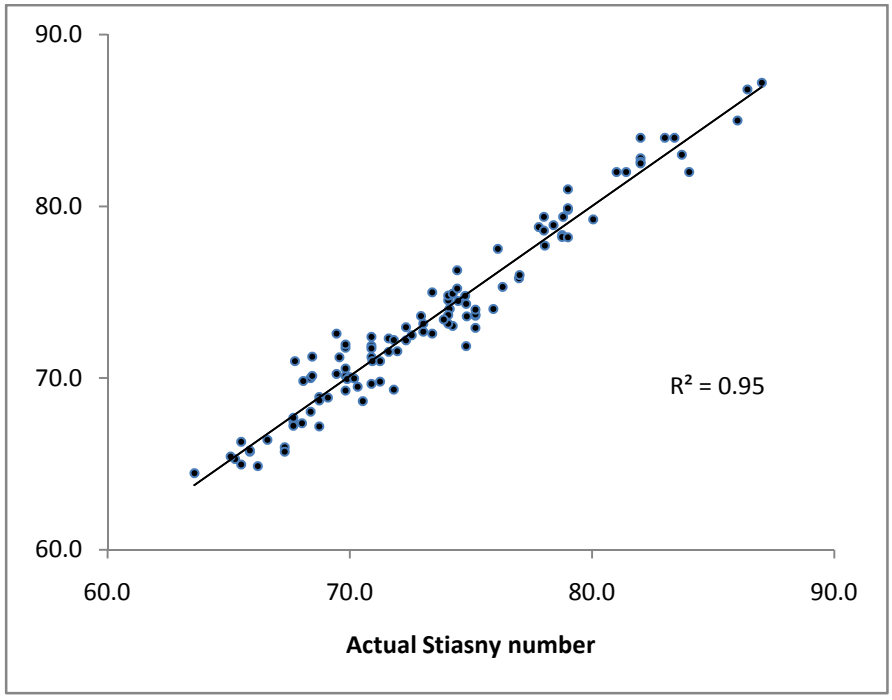


Figure 4. 4c: Actual versus predicted values for calibrations estimating Stiasny number.

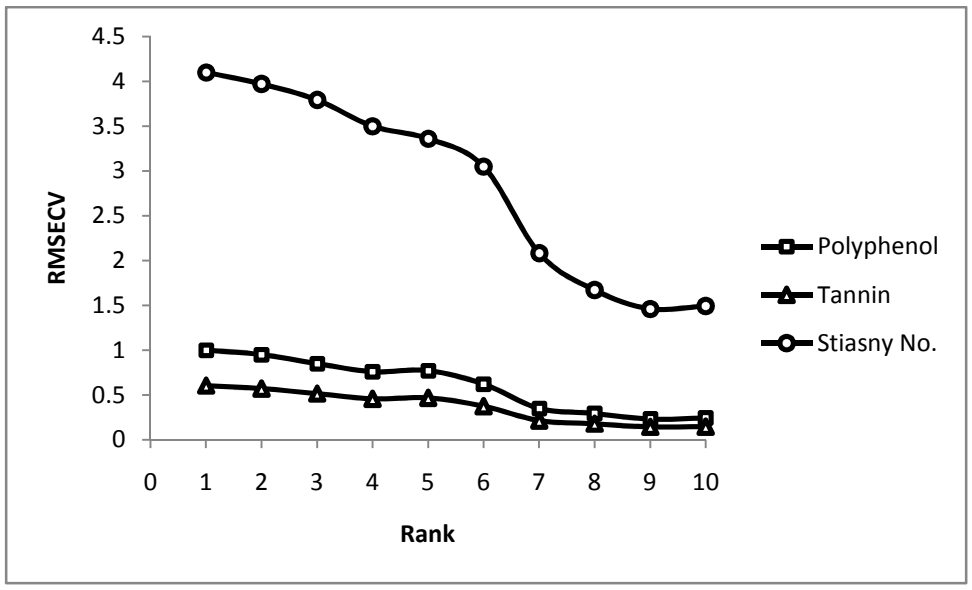


Figure 4. 5: RMSECV plotted against Rank for polyphenol content, tannin content and Stiasny number.

4.2 Optimization of Phenolic Extraction

4.2.1 Results from single factor extraction experiments

At the beginning of this study, the factors liquid-solid ratio, extraction temperature, solvent concentration and time of contact were investigated to determine the appropriate experimental ranges, which were then used for the optimization process.

4.2.1.1 Selection of solvent concentration range

For an efficient extraction, the solvent must be able to solubilize the target analytes while leaving the sample matrix intact. The polarity of the extraction solvent should closely match that of the target compounds. Mixing solvents of differing polarities can be used to extract a broad range of compound classes. In this study, the phenolics in the extracts increased with increasing concentration of organic solvent (in the case of aq. NaOH, solute) in water. The phenolic content reached a maximum when the acetone and ethanol concentrations were each 60% (Fig. 4.6).

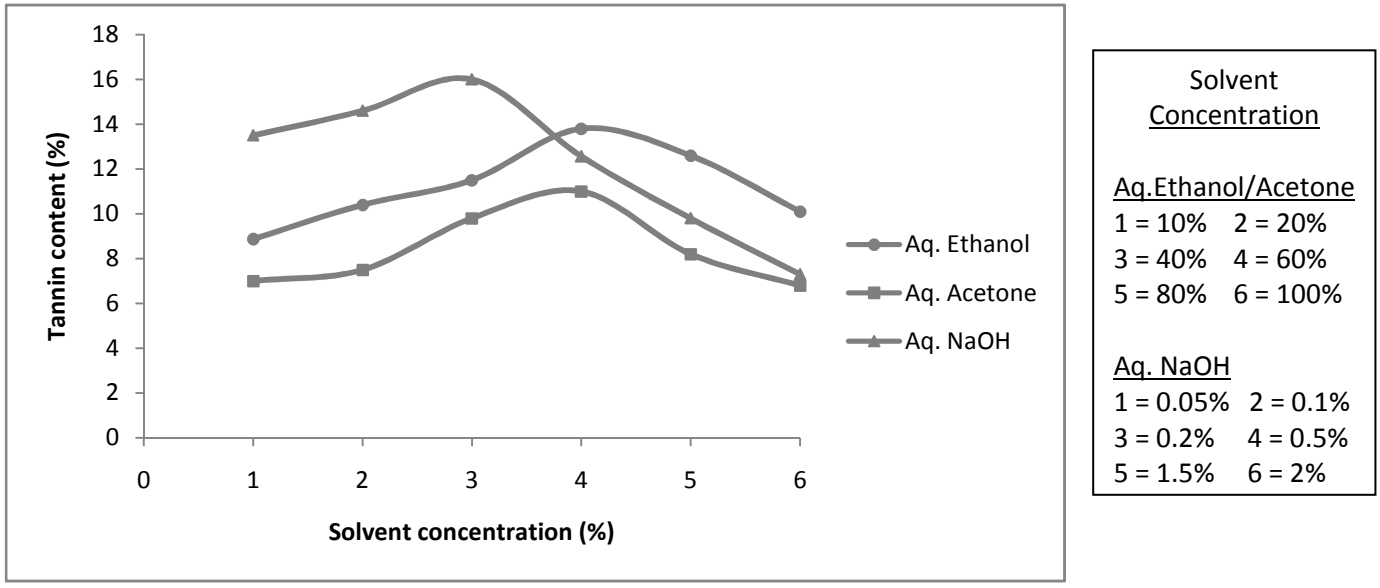


Figure 4. 6: Effect of extraction solvent concentration on tannin content.

At 10% acetone and ethanol concentrations, the phenolic content was minimal and therefore not selected for the optimization process. An important process in industrial extractions is solvent removal to obtain the extracted compound of interest. Low boiling solvents like acetone and ethanol are easier and cheaper to recover. Consequently, 80 and 100% concentrations for both solvents were included in the optimization process. In the case of aq. NaOH, concentrations beyond 1.5% contented lower amounts of phenolics than that obtained for the least concentrated solvent (Fig. 4.6). Hence the concentration range of 0.05 to 1.5 was selected for the optimization process.

4.2.1.2 Selection of liquid-solid ratio range

Using 60% aqueous ethanol as solvent at a temperature of 80°C for 60 min extraction time, the results (Fig. 4.7) show that if ratios were chosen above 30:1, where a maximum of 14.2% tannin content was obtained, then the quantity of phenolic compounds extracted remained the same or fell off.

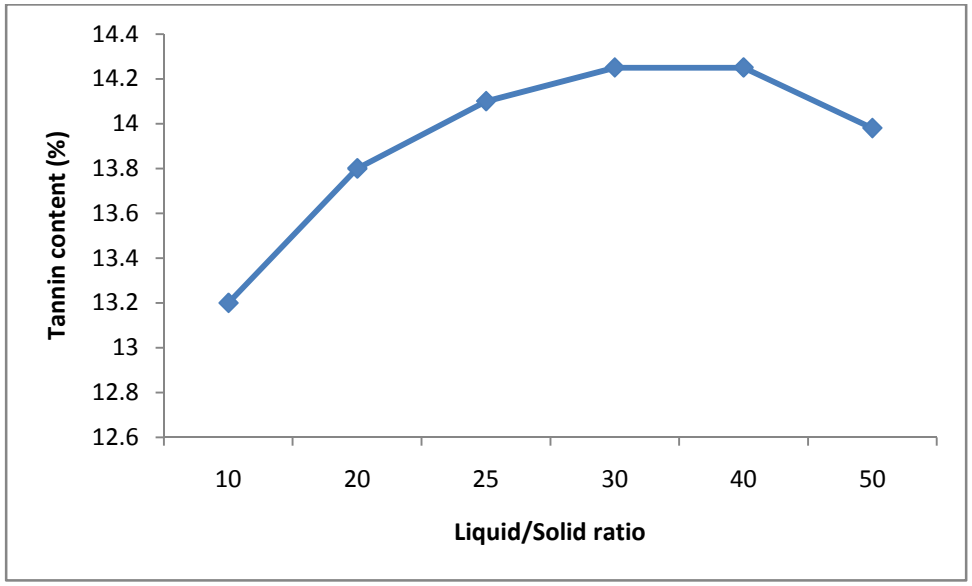


Figure 4.7: Effect of liquid-solid ratio on tannin content.

The high solubility of polyphenols in hydro-alcoholic solutions, especially in a glycosidic linkage (Knop and Scheib, 1979; Sellers, 2001), may explain the absence of significant variability at the higher ratios. Liquid-solid ratio from 10 to 30 was thus chosen for the optimization design.

4.2.1.3 Selection of extraction time range

Certain sample matrices can retain analytes within pores or other structures. Increasing the contact time at elevated temperatures can allow these compounds to diffuse into the extraction solvent. Figure 4.8 presents the amount of tannin extracted from pine bark using different extraction times. For all the solvents except aq. NaOH, an extraction time around 150 min resulted in the highest tannin content. However, an extraction time of 90 min was noted for aq. NaOH.

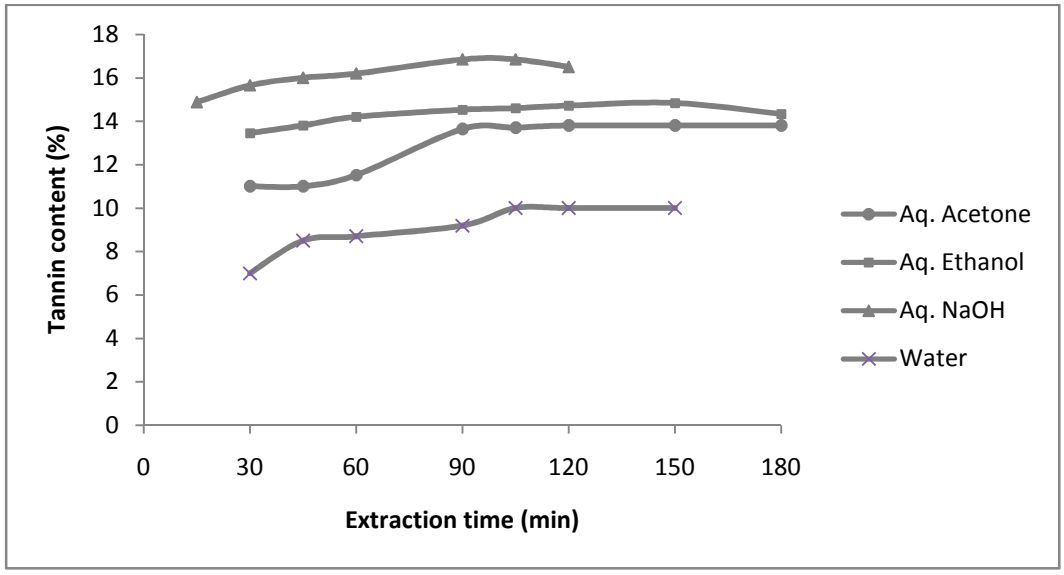


Figure 4.8: Effect of extraction time on tannin content.

Longer extraction time decreased the total tannin extracted, possibly because of some loss of phenolic compounds via oxidation and these products might polymerize into insoluble compounds. Again, Fick's second law of diffusion estimates that final equilibrium among the solute concentrations in the solid matrix and in the bulk solution will be attained after a certain period (Silva *et al.,* 2007). Hence the range of extraction time chosen for the optimization study was 30 to 150 min.

It must be noted that the tannin content from aqueous acetone extraction was significantly higher than that from water extraction. This could probably be due to the hydrolytic nature of water which aids the breaking of phenolic bonds and the acetone possibly being available to ensure effective contact with the phenolic compounds and extract them into solution. A similar reason could be given to aqueous ethanol which was also found to give higher tannin content than water (Fig. 4.8).

4.2.1.4 Selection of extraction temperature range

As the temperature is increased, the viscosity of the solvent is reduced, thereby increasing its ability to wet the matrix and solubilize the target analytes. The added thermal energy also assists in breaking analyte matrix bonds and encourages analyte diffusion to the matrix surface. In this study, increasing the aqueous acetone and aqueous ethanol extraction temperatures to 55°C and 70°C respectively resulted in the maximum amount of tannin extracted (Fig. 4.9). Similarly, temperatures of 90°C resulted in the maximum amount of tannins in the case of water and aqueous NaOH extractions. Heating might soften the plant tissue and weaken the phenol-protein and phenol-polysaccharide interactions in the powdered bark meal, thus more polyphenols would

migrate into the solvents. Hence for each solvent, the temperature range chosen for the optimization process, was from the minimum temperature in the study to the temperature where the maximum tannin content was obtained.

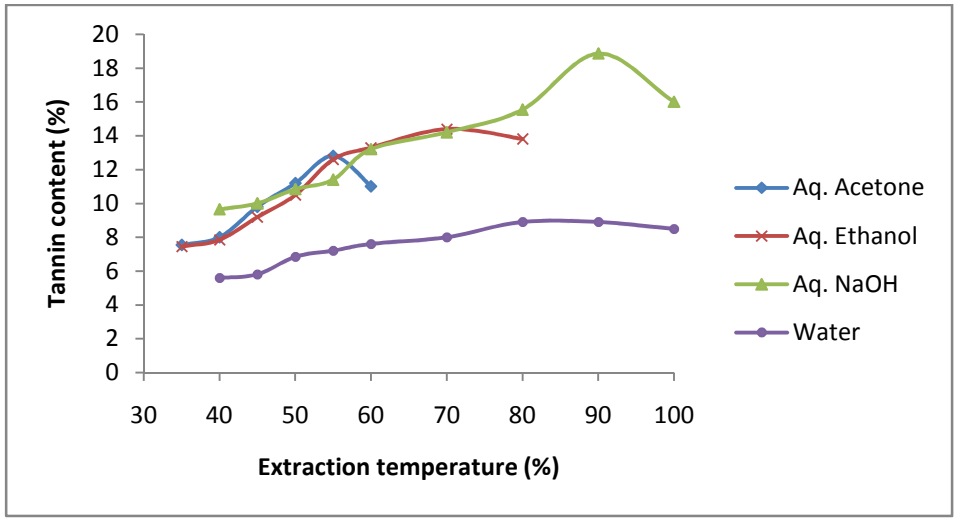


Figure 4.9: Effect of extraction temperature on tannin content.

4.2.1.5 Selection of Extraction stage

Using 60% aqueous ethanol as solvent with a liquid-to-solid ratio of 20 at a temperature of 80°C for 60 min extraction time, the maximum tannin content (18.2%) was obtained with a triple stage extraction which was not significantly different from the double stage extraction (18%) but significantly different from the single stage extraction (13.8%) (Fig. 4.10).

Operating single stage extractions in multiple cycle results in only limited content gains but substantial increases in cost and time. In this study, repeating the single stage extraction twice improves the extraction content from 13.8% to 17%, but doubles the running time and the solvent (or extract) volume. Higher extract volume in turn increases the cost of energy in

downstream extraction concentration operations. Hence single stage extraction was fixed for the optimization process.

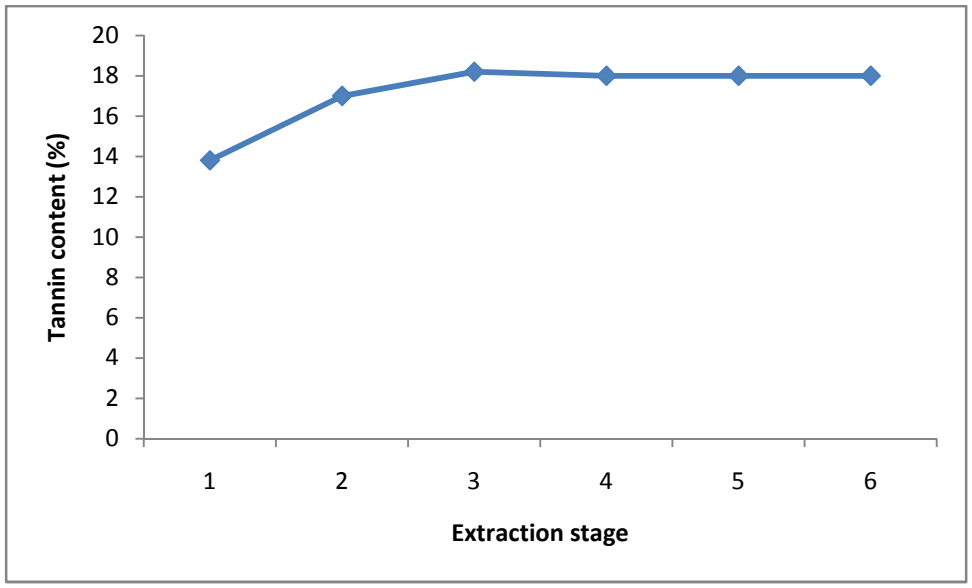


Figure 4. 10: Effect of extraction stage number on tannin content.

4.2.2 Optimization of extraction conditions by response surface methodology (RSM)

To determine the optimum operating conditions and to analyze the process of solvent extraction of phenolics, the response surface methodology was used to assess the optimum extraction conditions for each solvent when the objective function was to i) maximize the tannin content, ii) minimize the sugar content, iii) maximize the Stiasny number and iv) maximize the tannin content, minimize the sugar content and maximize the Stiasny number simultaneously. These optimal conditions are conducive for phenol-formaldehyde resin production.

4.2.2.1 Optimum extraction conditions based on maximizing tannin content

The polynomial equations for the estimation of tannin content (Y) in terms of extraction temperature (T), extraction time (t), solvent composition (C) and liquid-solid ratio (V) using aqueous acetone, aqueous ethanol, aqueous sodium hydroxide and water extractions were fitted as in equations 4.1 – 4.4. For each extraction, the objective function was to maximize the tannin content whilst the range of sugar content and that of Stiasny number were fixed as constraints.

$$Y_{acetone} = 1.64 + 0.03T + 0.02t - 0.52V + 0.01TV \quad \textbf{4.1}$$

$$Y_{ethanol} = -75.78 + 1.7T + 0.16t + 0.37C + 0.88V - 0.006TC - 0.006Vt - 0.009T^2 \quad \textbf{4.2}$$

$$Y_{hydroxide} = -12.1 + 0.42T - 5.21C + 1.46V - 0.02TV + 7.23C^2 \quad \textbf{4.3}$$

$$Y_{water} = 9.24 + 0.1T + 0.54t + 0.24V - 0.8Tt + 0.75Vt - 0.78T^2 \quad \textbf{4.4}$$

The analysis of variance for each of the approximating functions in equations 4.1 – 4.4 shows a Model F value to be 4.76, 12.92, 2.81 and 5.42 respectively (appendix 2) which implies that each model is significant. The Model R^2 of the approximating functions were different from each other, with $Y_{ethanol}$ function having the highest R^2 value of 0.82 followed by Y_{water}, $Y_{hydroxide}$ and $Y_{acetone}$ with respective R^2 values of 0.74, 0.62 and 0.45 (appendix 2). The predictive model graphs can be found in Appendix 4.

Aqueous acetone extraction

Table 4. 3: Comparism of experimental and predicted values using Box-Behnken design for the four independent variables on the content of tannin from aqueous acetone extraction.

Run no.	Extraction temperature (°C) T	Extraction time (min) t	Solvent composition (%) C	Liquid-Solid ratio V	Actual value (%)	Predicted value (%) using equation 4.1
1	50.00	90.00	20.00	20.00	9.00	9.61
2	50.00	90.00	100.00	20.00	10.50	10.23
3	50.00	90.00	60.00	20.00	13.00	10.11
4	45.00	120.00	40.00	25.00	13.00	12.57
5	50.00	150.00	60.00	20.00	13.00	13.57
6	50.00	90.00	60.00	20.00	10.00	10.23
7	55.00	120.00	40.00	25.00	9.00	8.61
8	55.00	120.00	80.00	15.00	12.00	14.19
9	50.00	90.00	60.00	10.00	7.00	10.11
10	55.00	60.00	40.00	25.00	8.00	9.61
11	45.00	120.00	40.00	15.00	8.00	10.23
12	45.00	120.00	80.00	15.00	7.00	8.52
13	60.00	90.00	60.00	20.00	9.00	7.90
14	45.00	60.00	80.00	25.00	14.00	14.19
15	50.00	30.00	60.00	20.00	10.00	8.52
16	55.00	60.00	80.00	25.00	13.00	11.11

17	55.00	60.00	40.00	15.00	12.00	10.23
18	45.00	120.00	80.00	25.00	11.00	11.73
19	55.00	60.00	80.00	15.00	9.00	8.61
20	50.00	90.00	60.00	30.00	7.00	8.73
21	40.00	90.00	60.00	20.00	13.00	12.69
22	50.00	90.00	60.00	20.00	15.00	12.69
23	45.00	60.00	40.00	15.00	12.00	10.23
24	45.00	60.00	40.00	25.00	7.00	7.02
25	45.00	60.00	80.00	15.00	11.00	10.23
26	55.00	120.00	40.00	15.00	7.00	7.02
27	55.00	120.00	80.00	25.00	11.00	11.11
28	50.00	90.00	60.00	20.00	6.00	6.90

The extraction design variables on the tannin content in actual and predicted values using aqueous acetone as extraction solvent is given in Table 4.3. The results of the ANOVA and model coefficients are presented in appendix 2. For the sake of simplicity, only some of the 3-D response surface plots with significant factors have been shown. The response surface plots between aqueous acetone extraction time and temperature are shown in Figure 4.11a. The percentage content of tannin increased at higher extraction temperatures and time at constant solvent concentration and liquid/solid ratio of 60% and 20:1 respectively. At a temperature of 51°C and 96 min extraction time, the tannin content was 11.4% and the maximum tannin content of 16% occurred at 60°C and 149 min extraction temperature and time respectively.

The effect of acetone concentration and extraction temperature on tannin content is illustrated in the response surface at constant extraction time and liquid-solid ratio of 90 minutes and 20:1 respectively (Figure 4.11b). It showed that an increase in acetone concentration at high extraction temperature resulted in a gradual increase in tannin content. At a solvent concentration of 52% and extraction temperature of 54°C, the percentage tannin content was found to be 12.2%. The responses observed for the effect of extraction time and solvent concentration at a fixed temperature of 60°C and liquid/solid ratio of 20 indicated that a general direction of increased time ensures maximum tannin content whilst concentration has no significant effect (Figure 4.11c). At a solvent concentration of 55% and extraction time of 71 min, the percentage tannin content was found to be 10.3%. Using numerical optimization, the maximum predicted tannin content of 17.57% was obtained under the optimum extraction conditions of 58°C extraction temperature, 78.5 min extraction time, 60% acetone concentration, and 29.8 liquid-solid ratio. The amount of total sugars extracted and the Stiasny number under these conditions were 4.4% and 76.96% respectively (Table 4.15).

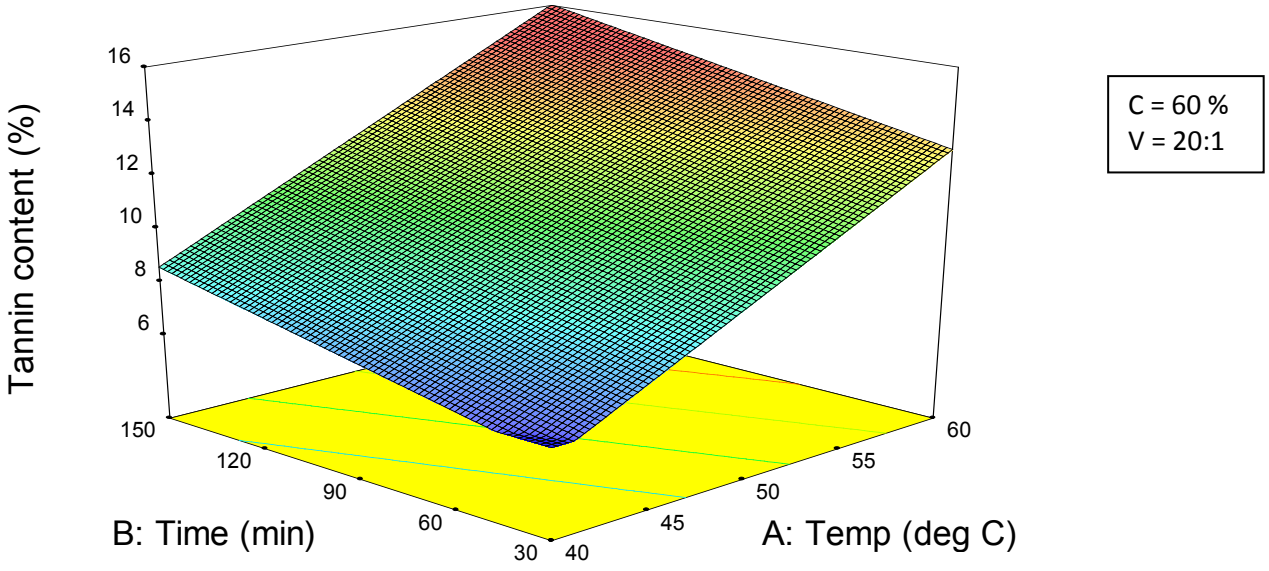


Fig. 4.11a Response surface plots showing percentage tannin content from aqueous acetone extraction at varying extraction temperature and extraction time.

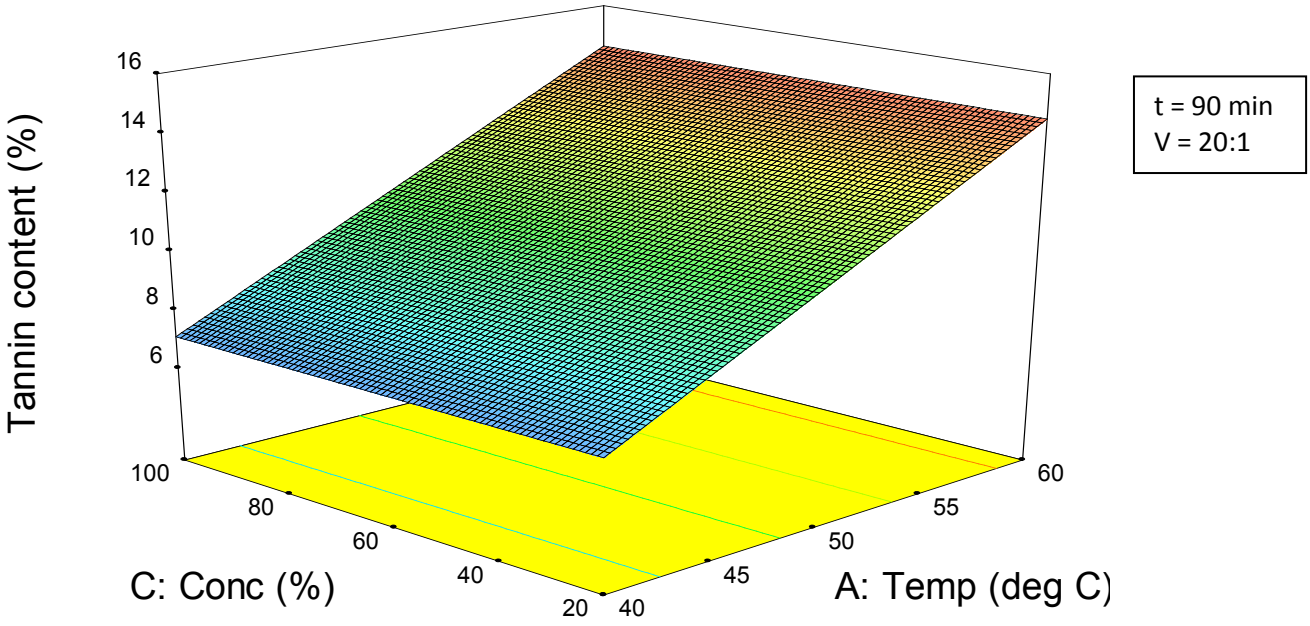


Fig. 4.11b Response surface plots showing percentage tannin content from aqueous acetone extraction at varying solvent concentration and extraction temperature.

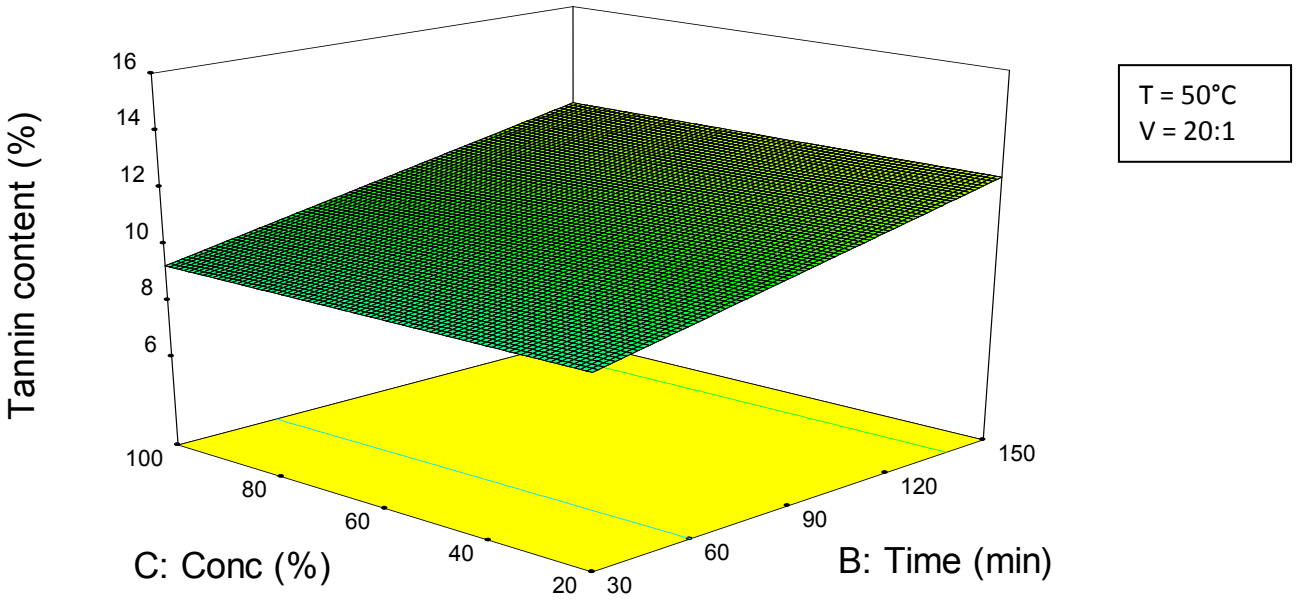


Fig. 4.11c Response surface plots showing percentage tannin content from aqueous acetone extraction at varying solvent concentration and extraction time.

Figure 4.12 is a factor plot between the tannin content with the extraction design variables in coded values. This plot shows how t he response moves as the level of one particular factor is changed. The plot shows that with an increase in extraction temperature from 40°C (coded value -1) to 60°C (coded value +1), the percentage tannin content increases. Similarly, increasing the extraction time from 30 min (coded value -1) to 150 min (coded value +1) increases the tannin content. Increasing the liquid/solid ratio from 10 (coded value -1) to 30 (coded value +1) also increases the tannin content. Varying the solvent concentration did not significantly affect the tannin content and therefore this factor did not appear in the factor plots. This can also be observed in Figure 4.11b and 4.11c. The factor plot shows that each of the design variables have their own individual effect as well as combined effect on the percentage tannin content in the design and optimization of tannin content from aqueous acetone extraction.

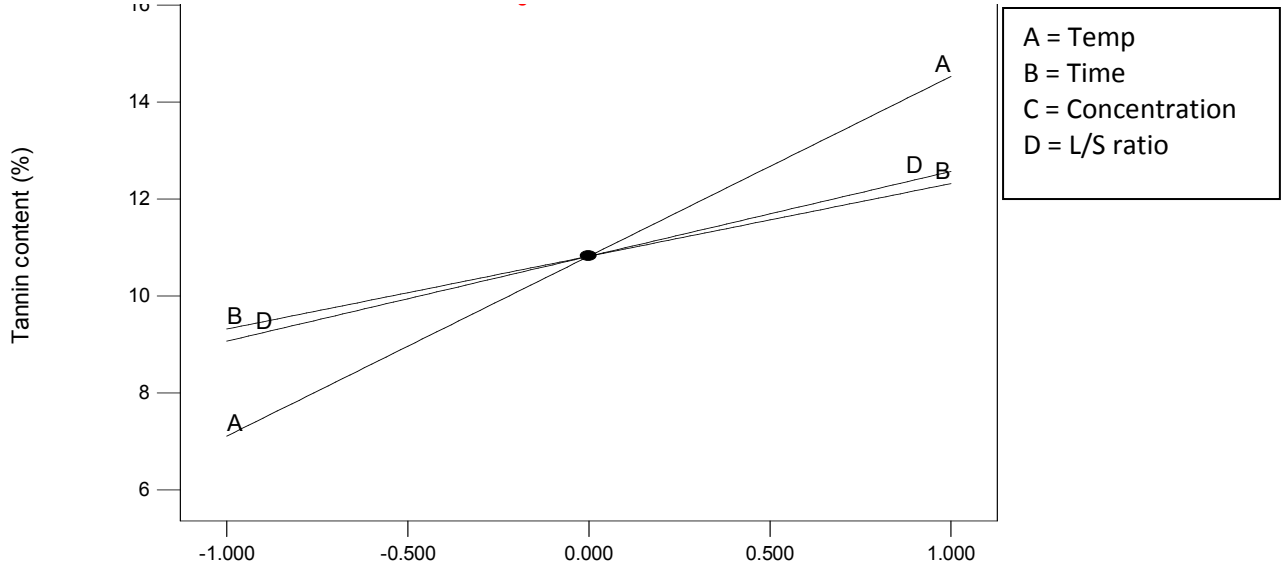


Fig. 4.12 Effect of individual variables on the content of tannin from aqueous acetone extraction.

Aqueous ethanol extraction

Table 4. 4: Comparison of experimental and predicted values using Box-Behnken design for the four independent variables on the content of tannin from aqueous ethanol extraction.

Run no.	Extraction temperature (°C) T	Extraction time (min) t	Solvent composition (%) C	Liquid-Solid ratio V	Actual value (%)	Predicted value (%) using equation 4.2
1	60.00	90.00	20.00	20.00	8.00	6.68
2	60.00	90.00	100.00	20.00	12.00	13.64
3	60.00	90.00	60.00	20.00	10.00	10.97
4	50.00	120.00	40.00	25.00	19.00	17.93
5	60.00	150.00	60.00	20.00	10.00	9.64
6	60.00	90.00	60.00	20.00	13.00	11.85
7	70.00	120.00	40.00	25.00	14.00	13.93
8	70.00	120.00	80.00	15.00	16.00	16.14
9	60.00	90.00	60.00	10.00	13.00	11.81
10	70.00	60.00	40.00	25.00	19.00	18.77
11	50.00	120.00	40.00	15.00	10.00	12.35
12	50.00	120.00	80.00	15.00	20.00	19.31
13	80.00	90.00	60.00	20.00	13.00	14.77
14	50.00	60.00	80.00	25.00	19.00	16.97
15	60.00	30.00	60.00	20.00	18.00	15.31
16	70.00	60.00	80.00	25.00	17.00	17.52
17	70.00	60.00	40.00	15.00	7.00	6.84
18	50.00	120.00	80.00	25.00	15.00	16.01

19	70.00	60.00	80.00	15.00	10.00	12.74
20	60.00	90.00	60.00	30.00	16.00	17.57
21	40.00	90.00	60.00	20.00	16.00	14.57
22	60.00	90.00	60.00	20.00	15.00	15.74
23	50.00	60.00	40.00	15.00	13.00	11.91
24	50.00	60.00	40.00	25.00	19.00	18.41
25	50.00	60.00	80.00	15.00	17.00	15.16
26	70.00	120.00	40.00	15.00	14.00	15.16
27	70.00	120.00	80.00	25.00	17.00	15.16
28	60.00	90.00	60.00	20.00	12.00	15.16

The extraction design variables on the tannin content in actual and predicted values using aqueous ethanol as extraction solvent is given in Table 4.4. The results of the ANOVA and model coefficients are presented in appendix 2. The response surface plots between aqueous ethanol extraction time and temperature are shown in Figure 4.13a. The percentage content of tannin increased at higher extraction temperatures and time at constant solvent concentration and liquid/solid ratio of 60% and 20:1 respectively. At a temperature of 53.2°C and 78.4 min extraction time, the tannin content was 12.7% and the maximum tannin content of 18.9% occurred at 74°C and 149 min extraction temperature and time respectively. The effect of ethanol concentration and extraction temperature on tannin content is illustrated in the response surface at constant extraction time and liquid-solid ratio of 50 minutes and 20:1 respectively (Figure 4.13b). It showed that an increase in ethanol concentration at high extraction temperature

resulted in a gradual increase in tannin content. At a solvent concentration of 61.2% and extraction temperature of 53.4°C, the percentage tannin content was found to be 13.3%.

The responses observed for the effect of extraction temperature and liquid-solid ratio at a fixed time of 90 min and solvent concentration of 60% indicated that a general direction of increased temperature and liquid solid ratio ensures maximum tannin content (Figure 4.13c). At a liquid-solid ratio of 20.3:1 and extraction temperature of 57°C, the percentage tannin content was found to be 14.5%. From the numerical optimization, the maximum predicted tannin content of 20.68% was obtained under the optimum extraction conditions of 71.46°C extraction temperature, 79.2 min extraction time, 21.9% ethanol concentration, and 26.4:1 liquid-solid ratio. The amount of total sugars extracted and the Stiasny number under these conditions were 4.94% and 80.47% respectively (Table 4.16).

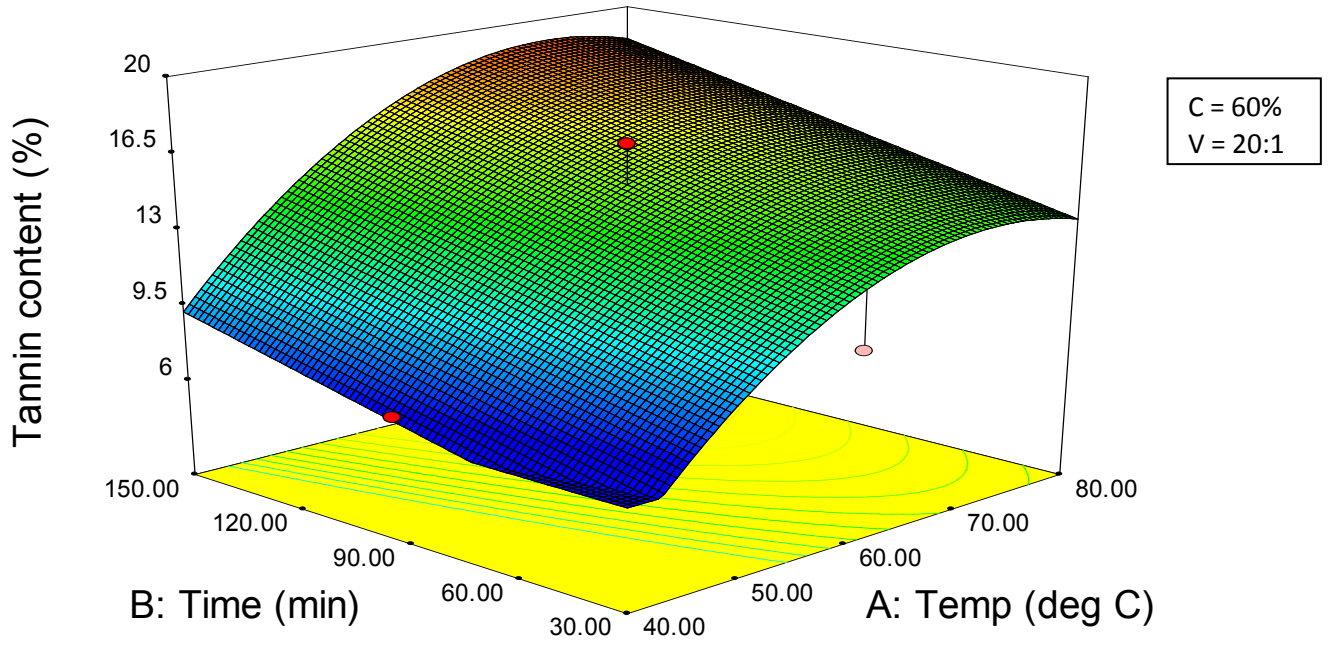


Fig. 4.13a Response surface plots showing percentage tannin content from aqueous ethanol extraction at varying extraction temperature and time.

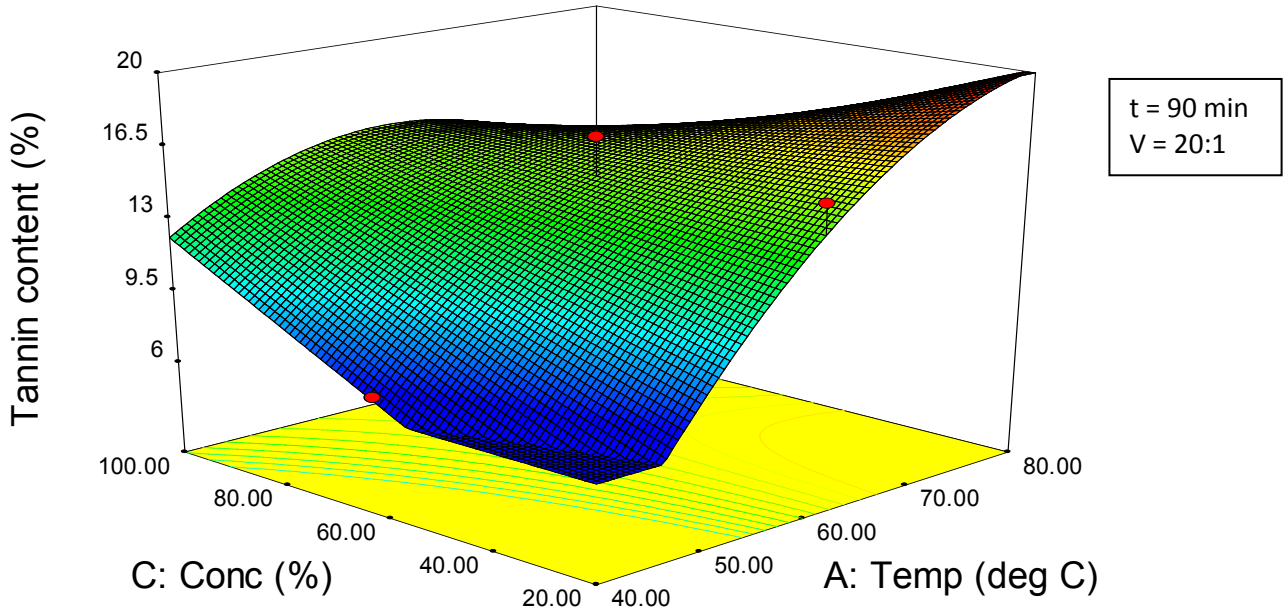


Fig. 4.13b Response surface plots showing percentage tannin content from aqueous ethanol extraction at varying solvent concentration and extraction temperature.

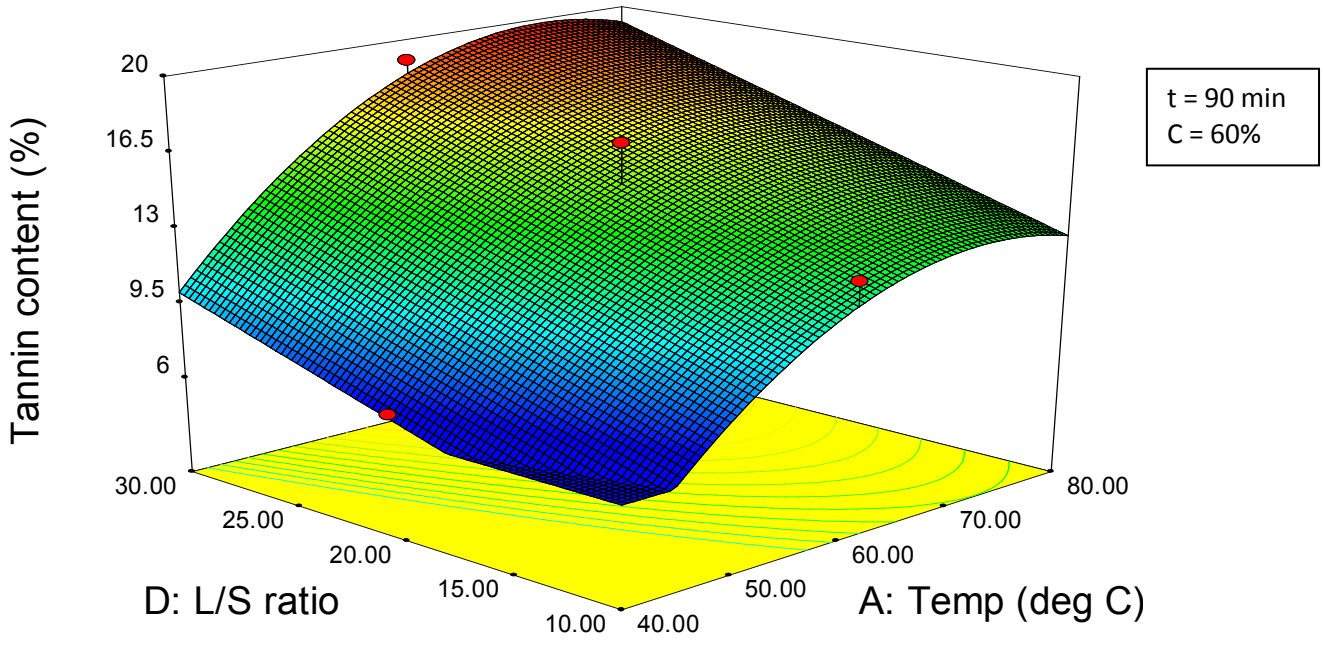


Fig. 4.13c Response surface plots showing percentage tannin content from aqueous ethanol extraction at varying liquid-solid ratio and extraction temperature.

Figure 4.14 is a factor plot between the percentage tannin content with the extraction design variables in coded values. The plot shows that with an increase in extraction temperature from 40°C (coded value -1) to 80°C (coded value +1), the percentage tannin content increases. Similarly, increasing the extraction time from 30 min (coded value -1) to 150 min (coded value +1) increases the tannin content. Increasing the liquid/solid ratio from 10 (coded value -1) to 30 (coded value +1) also increases the tannin content. Varying the solvent concentration did not significantly affect the tannin content and therefore this factor did not appear in the factor plots. The factor plot shows that each of the design variables have their own individual effect as well as combined effect on the percentage tannin content in the design and optimization of tannin content from aqueous ethanol extraction.

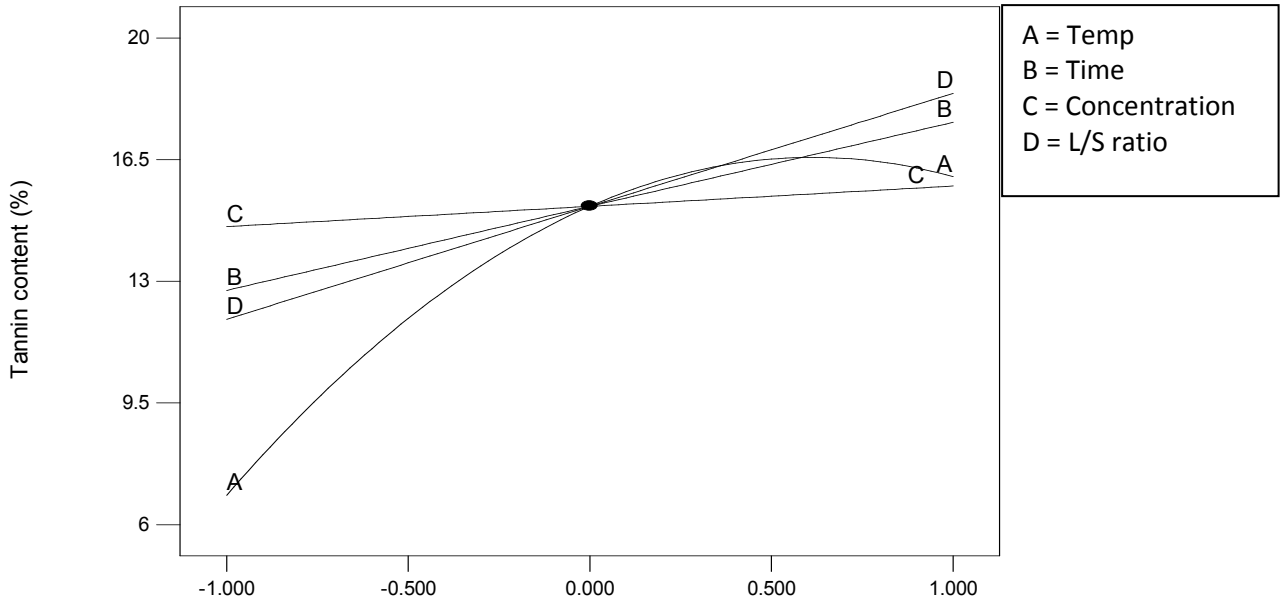


Fig 4.14 Effect of individual variables on the content of tannin from aqueous ethanol extraction.

Aqueous NaOH extraction

Table 4. 3: Comparison of experimental and predicted values using Box-Behnken design for the four independent variables on the content of tannin from aqueous NaOH extraction.

Run no.	Extraction temperature (°C) T	Extraction time (min) t	Solvent composition (%) C	Liquid-Solid ratio V	Actual value (%)	Predicted value (%) using equation 4.3
1	80.00	45.00	0.05	20.00	20.00	19.73
2	80.00	45.00	1.50	20.00	28.00	27.01
3	80.00	45.00	0.50	20.00	28.00	25.10
4	60.00	60.00	0.10	25.00	27.00	27.01
5	80.00	90.00	0.50	20.00	28.00	22.19
6	80.00	45.00	0.50	20.00	23.00	27.32
7	90.00	60.00	0.10	25.00	26.00	24.85
8	90.00	60.00	1.00	15.00	27.00	23.56
9	80.00	45.00	0.50	10.00	26.00	24.75
10	90.00	30.00	0.10	25.00	18.00	27.21
11	60.00	60.00	0.10	15.00	27.00	24.85
12	60.00	60.00	1.00	15.00	30.00	27.32
13	100.00	45.00	0.50	20.00	27.00	24.75
14	60.00	30.00	1.00	25.00	21.00	23.56
15	80.00	15.00	0.50	20.00	23.00	23.56
16	90.00	30.00	1.00	25.00	24.00	24.55
17	90.00	30.00	0.10	15.00	25.00	23.56

18	60.00	60.00	1.00	25.00	19.00	23.56
19	90.00	30.00	1.00	15.00	28.00	27.21
20	80.00	45.00	0.50	30.00	25.00	23.56
21	40.00	45.00	0.50	20.00	28.00	25.34
22	80.00	45.00	0.50	20.00	25.00	24.55
23	60.00	30.00	0.10	15.00	33.00	32.81
24	60.00	30.00	0.10	25.00	15.00	19.73
25	60.00	30.00	1.00	15.00	22.00	24.12
26	90.00	60.00	0.10	15.00	25.00	22.19
27	90.00	60.00	1.00	25.00	18.00	20.01
28	80.00	45.00	0.50	20.00	20.00	22.03

The extraction design variables on the tannin content in actual and predicted values using aqueous NaOH as extraction solvent is given in Table 4.5, with the results of the ANOVA and model coefficients presented in appendix 2. The response surface plots between aqueous NaOH concentration and extraction temperature are shown in Figure 4.15a. The percentage content of tannin increased at higher concentrations and extraction temperatures at constant extraction time and liquid/solid ratio of 52.5 min and 20:1 respectively. At a temperature of 69°C and 1.2% solvent concentration, the tannin content was 25.5% and the maximum tannin content of 34.5% occurred at 100°C and 1.5% extraction temperature and concentration respectively.

The effect of time and extraction temperature on tannin content is illustrated in the response surface at constant concentration and liquid-solid ratio of 0.78% and 20:1 respectively (Figure

4.15b). It showed that the content of tannin was less affected by time and slightly increased by increasing temperature when concentration and liquid-solid ratio were kept constant at 0.78% and 20 respectively. At an extraction temperature of 31°C, and time of 41 min, the percentage tannin content was found to be 20.3%. The responses observed for the effect of extraction time and solvent concentration at a fixed temperature of 60°C and liquid/solid ratio of 20 indicated that a general direction of increased concentration ensures maximum tannin content whilst time has less effect (Figure 4.15c). At an extraction time of 51min, and concentration of 1%, the percentage tannin content was found to be 24.8%. From the numerical optimization, the maximum predicted tannin content of 34.51% was obtained under the optimum extraction conditions of 96.4°C extraction temperature, 37.7min extraction time, 1.48% NaOH concentration, and 15.2:1 liquid-solid ratio. The amount of total sugars extracted and the Stiasny number under these conditions were 40.61% and 45.17% respectively (Table 4.17).

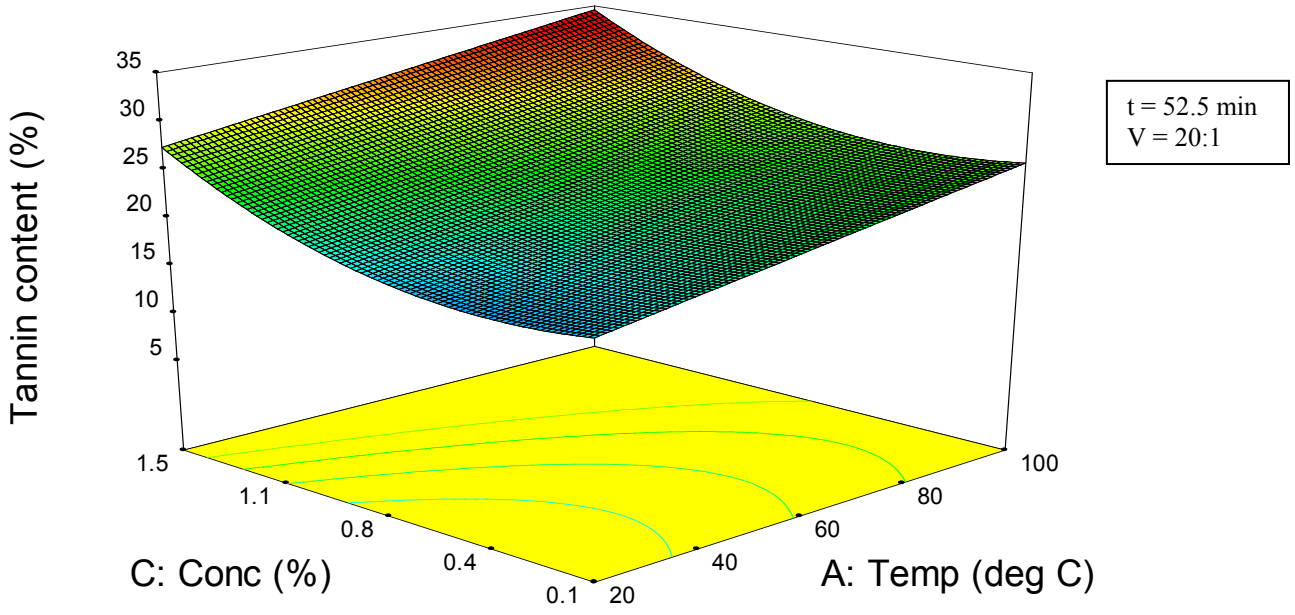


Fig. 4.15a Response surface plots showing percentage tannin content from aqueous NaOH extraction at varying solvent concentration and extraction temperature.

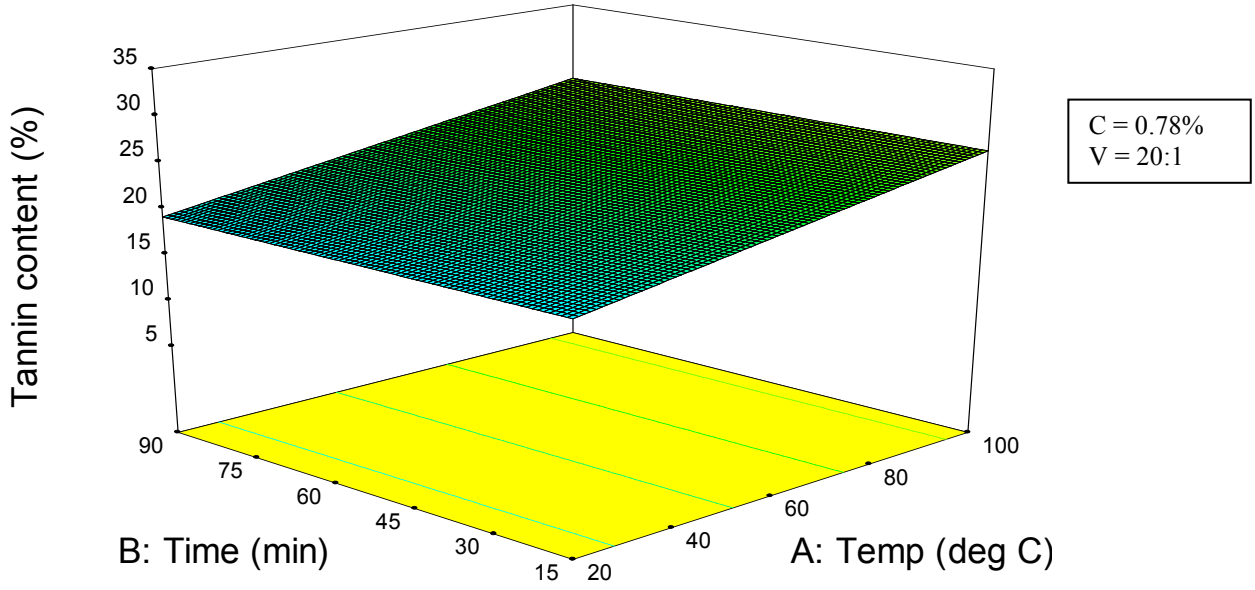


Fig. 4.15b Response surface plots showing percentage tannin content from aqueous NaOH extraction at varying extraction temperature and time.

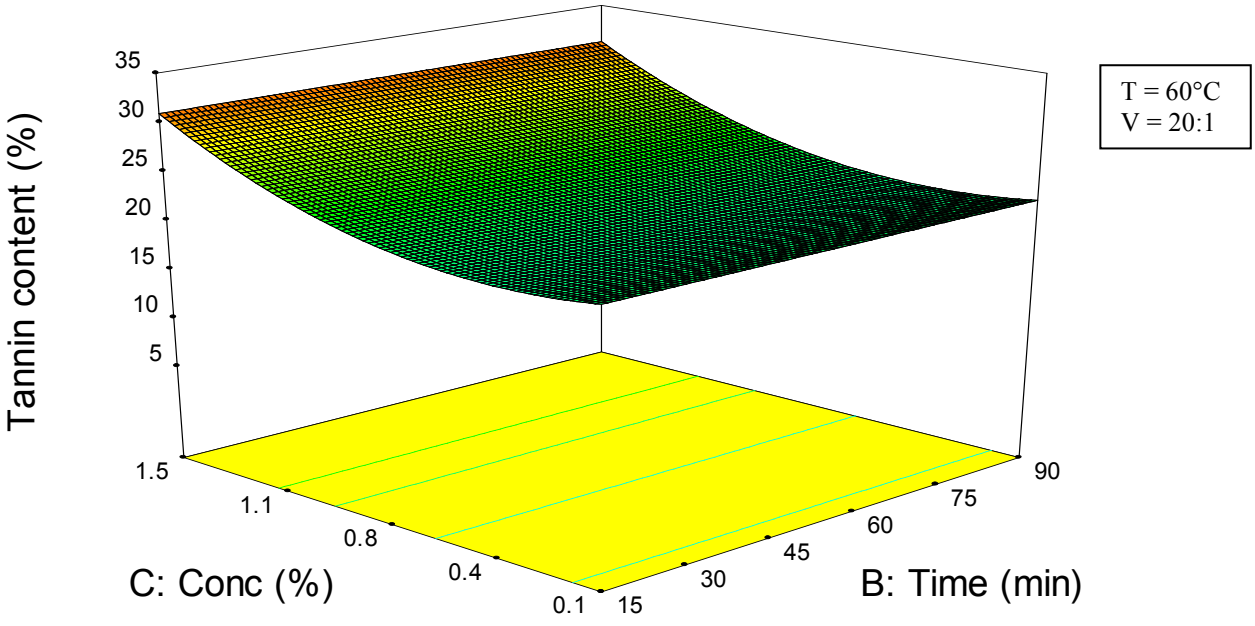


Fig. 4.15c Response surface plots showing percentage tannin content from aqueous NaOH extraction at varying solvent concentration and extraction time.

Figure 4.16 is a factor plot between the percentage tannin content with the extraction design variables in coded values. The plot shows that with an increase in extraction temperature from 40°C (coded value -1) to 100°C (coded value +1), the percentage tannin content increases. Similarly, increasing the liquid/solid ratio from 10 (coded value -1) to 30 (coded value +1) and concentration from 0.05% to 1.5% also increases the tannin content. Varying the extraction time did not significantly affect the tannin content and therefore this factor did not appear in the factor plots. The factor plot shows that each of the design variables have their own individual effect as well as combined effect on the percentage tannin content in the design and optimization of tannin content from aqueous NaOH extraction.

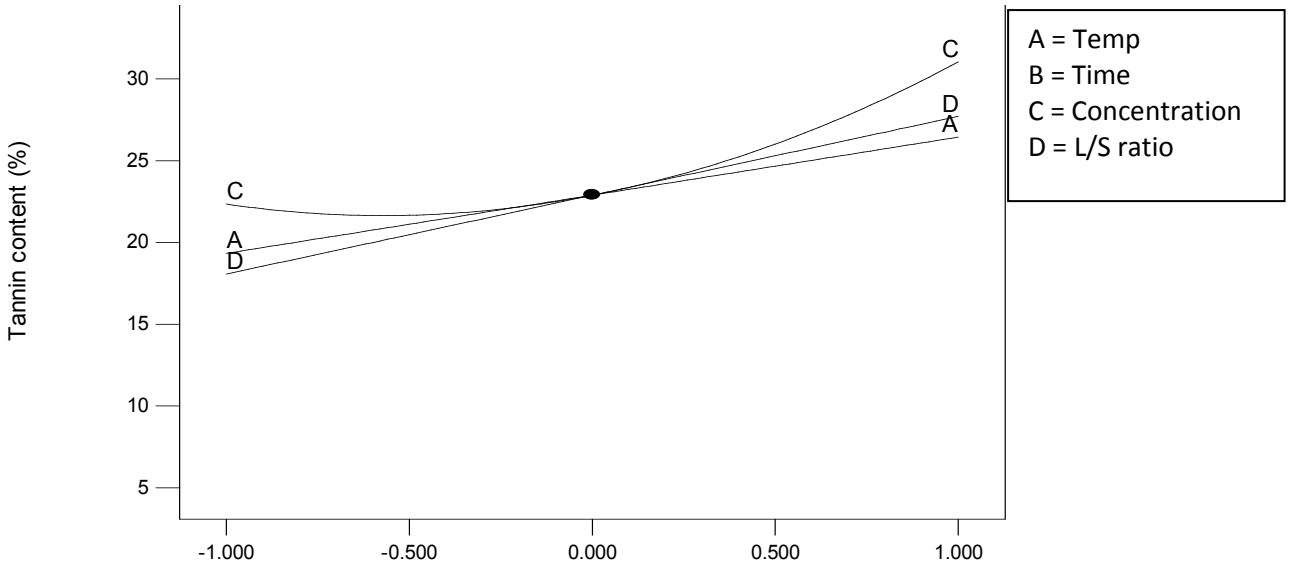


Fig 4.16 Effect of individual variables on the content of tannin from aqueous NaOH extraction.

Water extraction

Table 4. 4: Comparison of experimental and predicted values using Box-Behnken design for the four independent variables on the content of tannin from water extraction.

Run no.	Extraction temperature (°C) T	Extraction time (min) t	Liquid-Solid ratio V	Actual value (%)	Predicted value (%) using equation 4.4
1	80.00	90.00	20.00	9.50	9.83
2	90.00	120.00	25.00	9.50	9.43
3	80.00	90.00	10.00	9.40	9.19
4	90.00	60.00	15.00	8.60	8.79
5	90.00	90.00	30.00	8.60	8.65
6	80.00	90.00	20.00	9.40	9.19
7	90.00	60.00	25.00	8.50	8.57
8	60.00	60.00	15.00	8.90	8.95
9	100.00	90.00	20.00	8.80	8.89
10	90.00	120.00	15.00	8.80	8.92
11	80.00	30.00	20.00	9.80	9.46
12	40.00	90.00	20.00	8.40	8.66
13	60.00	120.00	15.00	9.20	9.03
14	80.00	90.00	20.00	9.40	9.19
15	60.00	120.00	25.00	9.00	9.22
16	80.00	150.00	20.00	9.40	9.19
17	80.00	90.00	20.00	9.00	9.27
18	60.00	60.00	25.00	8.60	8.36

The extraction design variables on the tannin content in actual and predicted values using water as extraction solvent is given in Table 4.6. The results of the ANOVA and model coefficients are presented in appendix 2. The response surface plots between extraction time and liquid-solid ratio are shown in Figure 4.17a. The percentage content of tannin increased at higher extraction temperatures and liquid-solid ratio at constant temperature of 70°C. At an extraction time of 73.6 min and 21.6:1, liquid-solid ratio, the tannin content was 9.1%, and the maximum tannin content of 10.7% occurred at 148 min and 30:1 liquid-solid ratio.

The effect of time and extraction temperature on tannin content is illustrated in the response surface plots at constant liquid-solid ratio of 20:1 (Figure 4.17b). It showed that an increase in extraction time and temperature resulted in increased tannin content. At an extraction temperature and time of 56.1°C and 75.8 min respectively, the tannin content was found to be 8.8%. The responses observed for the effect of extraction temperature and liquid-solid ratio at a fixed time of 90 min indicated that an increase in temperature ensures maximum tannin content. (Figure 4.17c). At an extraction temperature of 51.7°C and liquid-solid ratio of 16.4:1, the tannin content was found to be 8.8%. From the numerical optimization, the maximum predicted tannin content of 9.8% was obtained under the optimum extraction conditions of 69°C extraction temperature, 126 min extraction time and 23:1 liquid to solid ratio. The amount of total sugars extracted and the Stiasny number under these conditions were 1.76% and 93.82% respectively (Table 4.18).

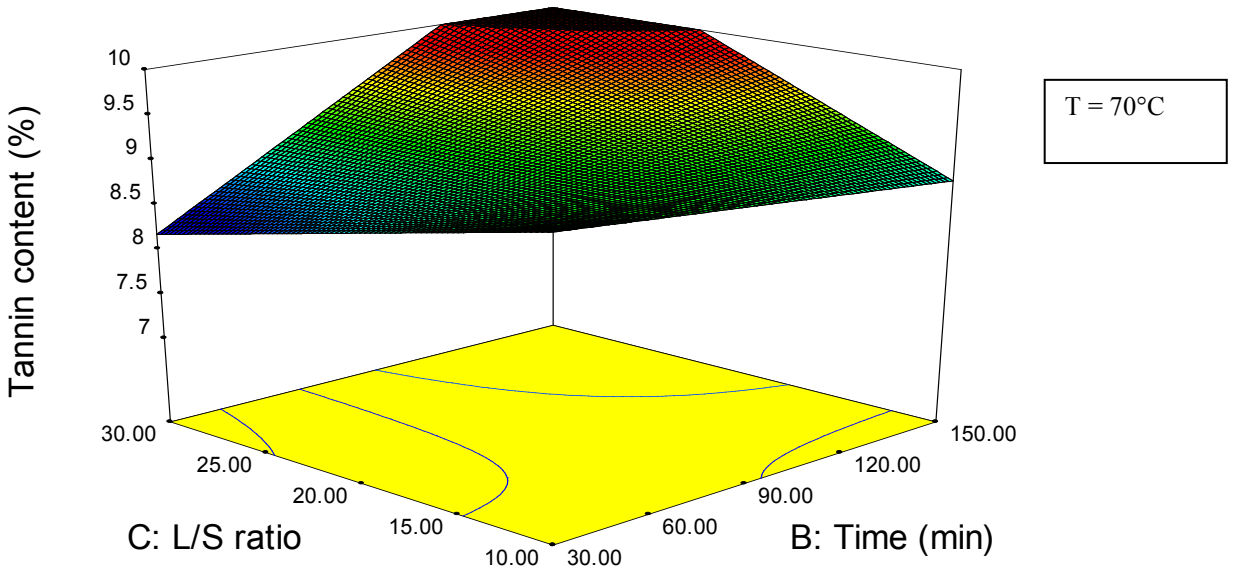


Fig. 4.17a Response surface plots showing percentage tannin content from water extraction at varying liquid-solid ratio and extraction time.

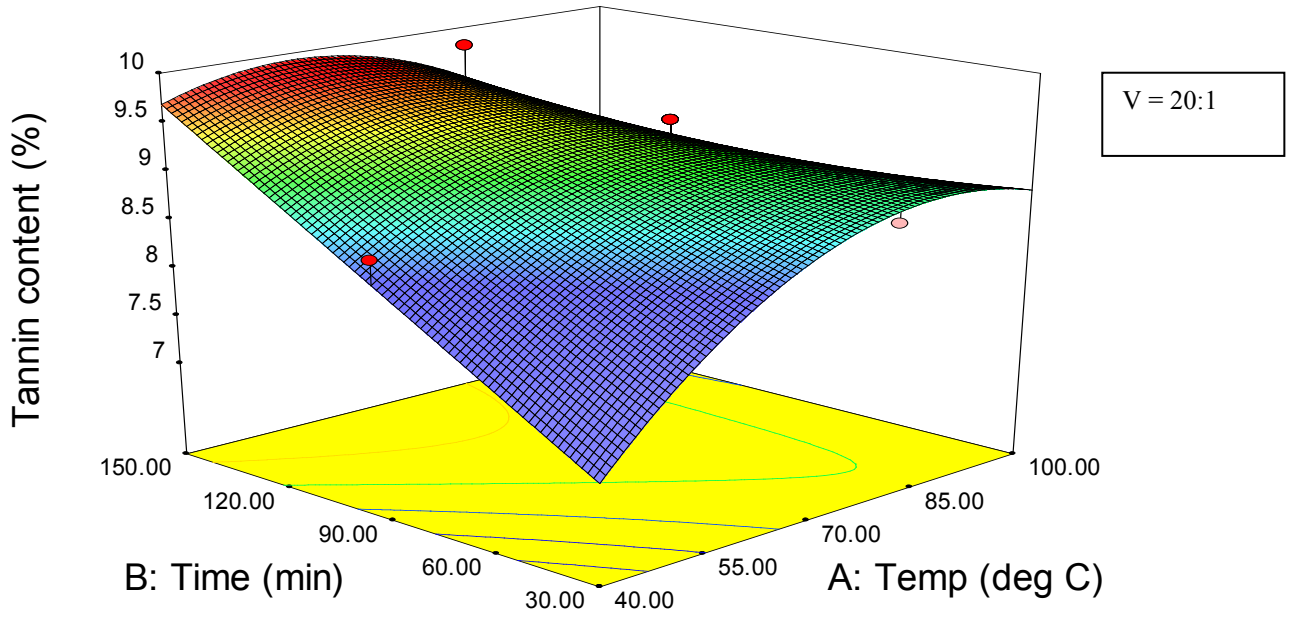


Fig. 4.17b Response surface plots showing percentage tannin content from water extraction at varying extraction temperature and time.

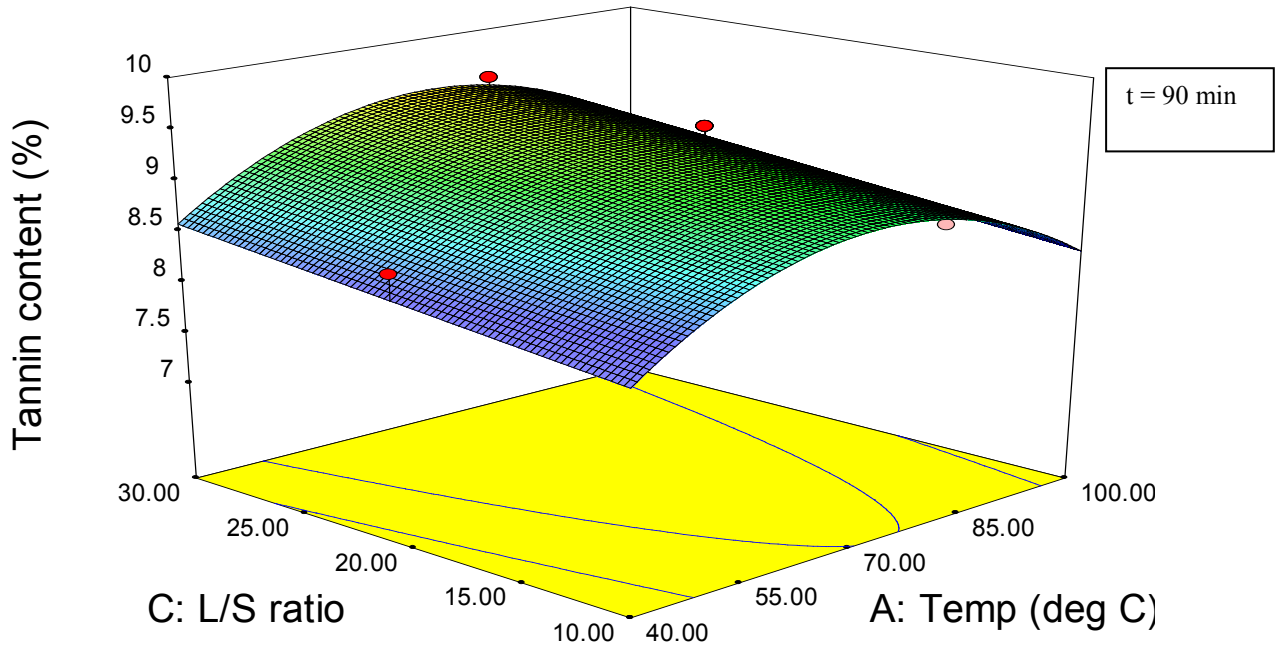


Fig. 4.17c Response surface plots showing percentage tannin content from water extraction at varying liquid-solid ratio and extraction temperature.

Figure 4.18 is a factor plot between the percentage tannin content with the extraction design variables in coded values. The plot shows that with an increase in extraction temperature from 40°C (coded value -1) to 80°C (coded value 0), the percentage tannin content increases and thereafter decreases as temperature increases to 100°C. Increasing the extraction time from 15min (coded value -1) to 90 min (coded value +1) increases the tannin content. Similarly, increasing the liquid-solid ratio from 10 (coded value -1) to 30 (coded value +1) also increases the tannin content. The factor plot shows that each of the design variables have their own individual effect as well as combined effect on the percentage tannin content in the design and optimization of tannin content from aqueous acetone extraction.

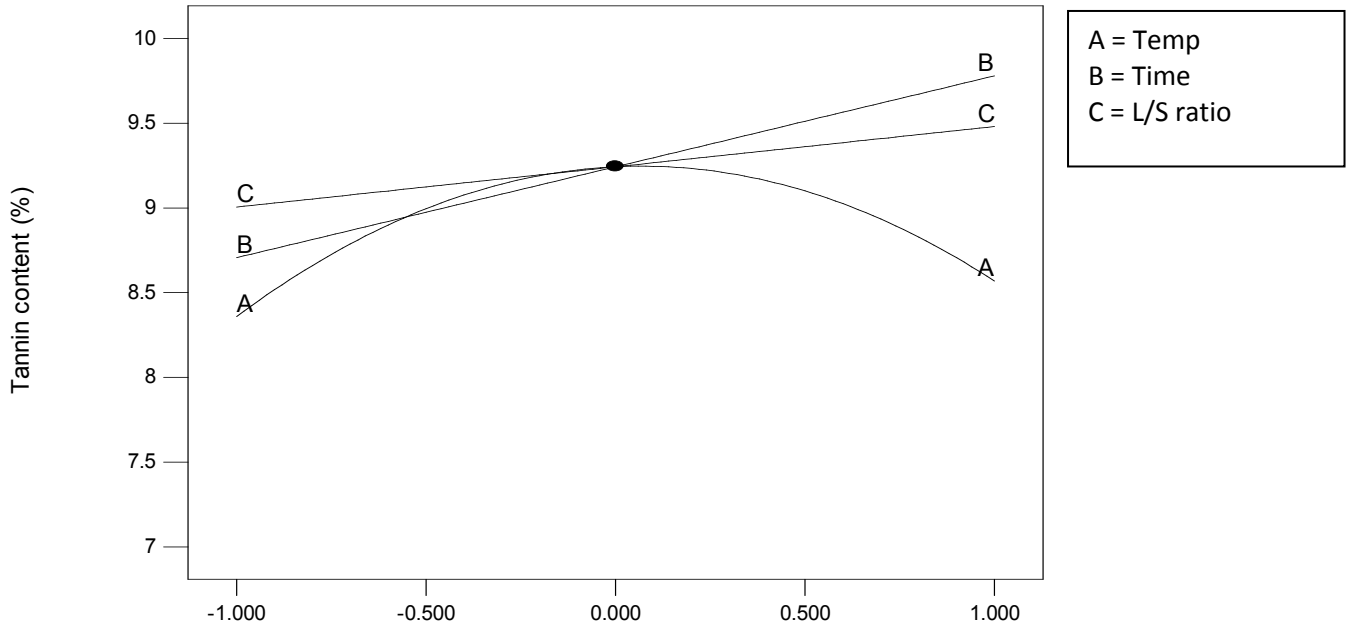


Fig 4.18 Effect of individual variables on the content of tannin from water extraction.

4.2.2.1 Optimum extraction conditions based on minimizing sugar content

The polynomial equations for the estimation of sugar content (S) in terms of extraction temperature (T), extraction time (t), solvent composition (C) and liquid-solid ratio (V) using aqueous acetone, aqueous ethanol, aqueous sodium hydroxide and water extractions were fitted as in equations 4.5 – 4.8. For each extraction, the objective function was to minimize the sugar content whilst the range of tannin content and that of Stiasny number were fixed as constraints.

$$S_{acetone} = -4.4 + 0.1T + 0.02t + 0.91V - (4.16 \times 10^{-4}Vt) \quad \textbf{4.5}$$

$$S_{ethanol} = -8.6 + 0.16T + 0.009t + 0.1C + 0.06V - 0.0017TC \quad \textbf{4.6}$$

$$S_{hydroxide} = -20.39 + 1.19T\ 0.05t - 1.19C + 0.23TC - (7.29 \times 10^{-3}T^2) \quad \textbf{4.7}$$

$$S_{water} = 1.63 + 0.52T + 0.19t + 0.09C + 0.52Tt - 0.79TC + 0.2Ct + 0.4T^2 - (6.27 \times 10^{-3}t^2) - 0.31C^2 \quad \textbf{4.8}$$

The analysis of variance for each of the approximating functions in equations 4.5 – 4.8 shows a Model F value to be 9.08, 12.14, 9.27 and 8.2 respectively (appendix 2) which implies that each model is significant. The Model R^2 of the approximating functions $S_{acetone}$, $S_{ethanol}$, $S_{hydroxide}$ and S_{water} were respectively 0.6, 0.73, 0.68 and 0.90 (appendix 2). The predictive model graphs can be found in Appendix 4.

Aqueous acetone extraction

Table 4. 7: Comparison of experimental and predicted values using Box-Behnken design for the four independent variables on the sugar content from aqueous acetone extraction.

Run no.	Extraction temperature (°C) T	Extraction time (min) t	Solvent composition (%) C	Liquid-Solid ratio V	Actual value (%)	Predicted value (%) using equation 4.5
1	50.00	90.00	20.00	20.00	3.30	3.06
2	50.00	90.00	100.00	20.00	3.50	3.13
3	50.00	90.00	60.00	20.00	3.40	3.07
4	45.00	120.00	40.00	25.00	4.00	3.66
5	50.00	150.00	60.00	20.00	3.70	4.13
6	50.00	90.00	60.00	20.00	2.80	3.13
7	55.00	120.00	40.00	25.00	3.20	2.72
8	55.00	120.00	80.00	15.00	4.10	4.07
9	50.00	90.00	60.00	10.00	2.00	3.07
10	55.00	60.00	40.00	25.00	2.80	3.06
11	45.00	120.00	40.00	15.00	2.50	3.13
12	45.00	120.00	80.00	15.00	2.00	2.67
13	60.00	90.00	60.00	20.00	3.00	2.60

14	45.00	60.00	80.00	25.00	4.50	4.07
15	50.00	30.00	60.00	20.00	3.30	2.67
16	55.00	60.00	80.00	25.00	4.00	3.67
17	55.00	60.00	40.00	15.00	3.00	3.13
18	45.00	120.00	80.00	25.00	4.00	3.61
19	55.00	60.00	80.00	15.00	2.60	2.72
20	50.00	90.00	60.00	30.00	2.00	2.65
21	40.00	90.00	60.00	20.00	3.80	3.72
22	50.00	90.00	60.00	20.00	4.00	3.72
23	45.00	60.00	40.00	15.00	3.50	3.13
24	45.00	60.00	40.00	25.00	2.80	2.06
25	45.00	60.00	80.00	15.00	3.00	3.13
26	55.00	120.00	40.00	15.00	2.00	2.06
27	55.00	120.00	80.00	25.00	3.00	3.67
28	50.00	90.00	60.00	20.00	1.80	2.13

The extraction design variables on the sugar content in actual and predicted values using aqueous acetone as extraction solvent is given in Table 4.7. The results of the ANOVA and model coefficients are presented in appendix 2. The response surface plots between aqueous acetone concentration and extraction temperature are shown in Figure 4.19a. The percentage sugar content decreased at lower extraction temperatures and solvent concentration at a fixed extraction time and liquid/solid ratio of 90 min and 20:1 respectively. At an extraction

temperature of 51°C and 57% solvent concentration, the sugar content was 3.4%, and the minimum sugar content of 2.2% occurred at 40°C and 82% solvent concentration.

The effect of acetone extraction time and temperature on sugar content is illustrated in the response surface plots at constant solvent concentration and liquid-solid ratio of 60% and 20:1 respectively (Figure 4.19b). It showed that a decrease in acetone concentration at low extraction temperature resulted in a gradual decrease in sugar content. At an extraction temperature of 54°C and time of 115 min, the sugar content was 3.8%. The responses observed for the effect of extraction time and liquid-solid ratio at a fixed temperature of 60°C and solvent concentration of 60% indicated that a general direction of decreased extraction time and liquid-solid ratio leads to low sugar content (Figure 4.19c). At an extraction time of 125 min and liquid-solid ratio of 24.8:1, the sugar content was 3.6%. From the numerical optimization, the minimum predicted sugar content of 1.69% was obtained under the optimum extraction conditions of 40.4°C extraction temperature, 64.7 min extraction time, 60% acetone concentration, and 15.8:1 liquid to solid ratio. The amount of tannin extracted and the Stiasny number under these conditions were 9.43% and 79.22% respectively (Table 4.15).

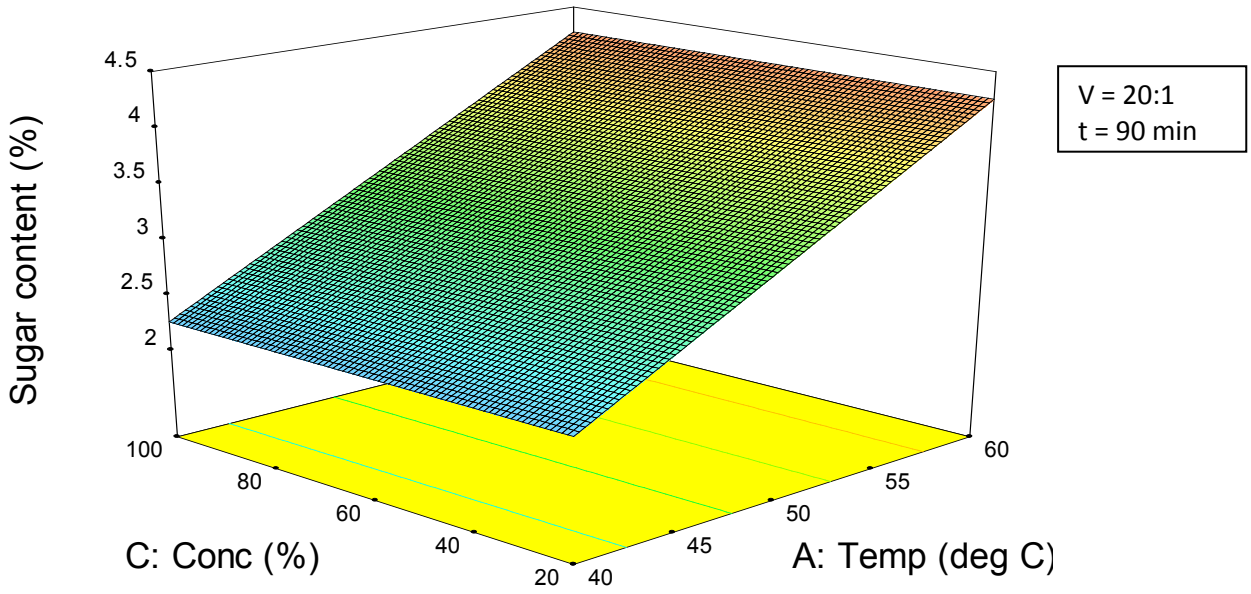


Fig. 4.19a Response surface plots showing percentage sugar content from aqueous acetone extraction at varying solvent concentration and extraction temperature.

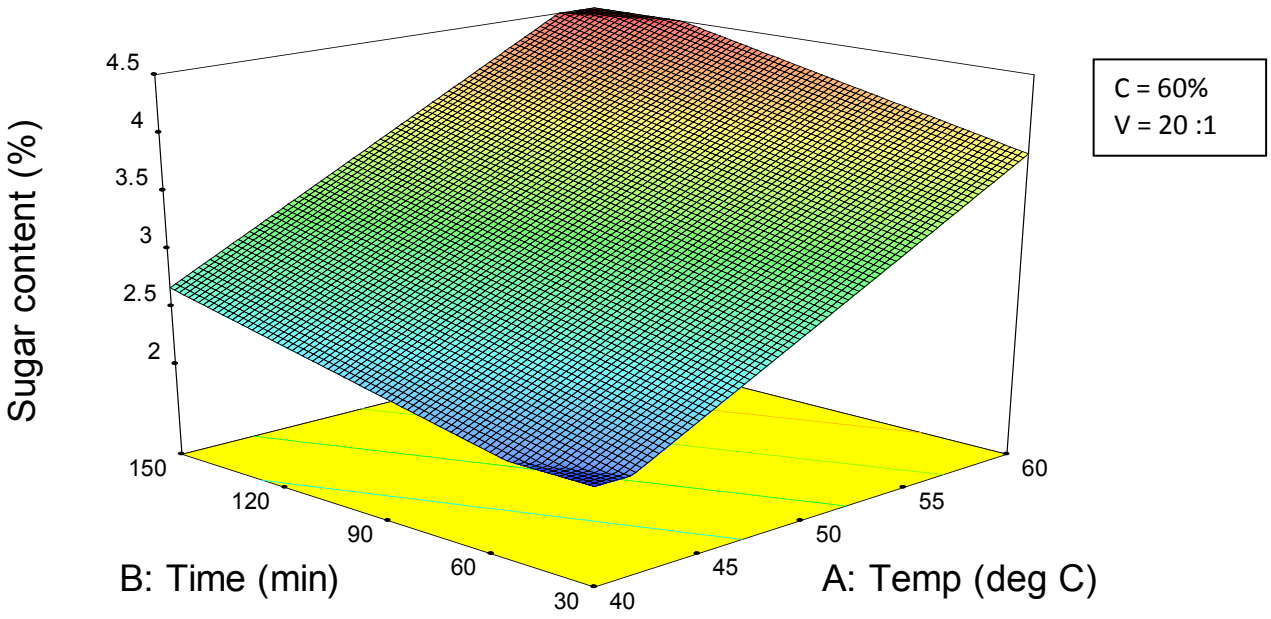


Fig. 4.19b Response surface plots showing percentage sugar content from aqueous acetone extraction at varying extraction temperature and time.

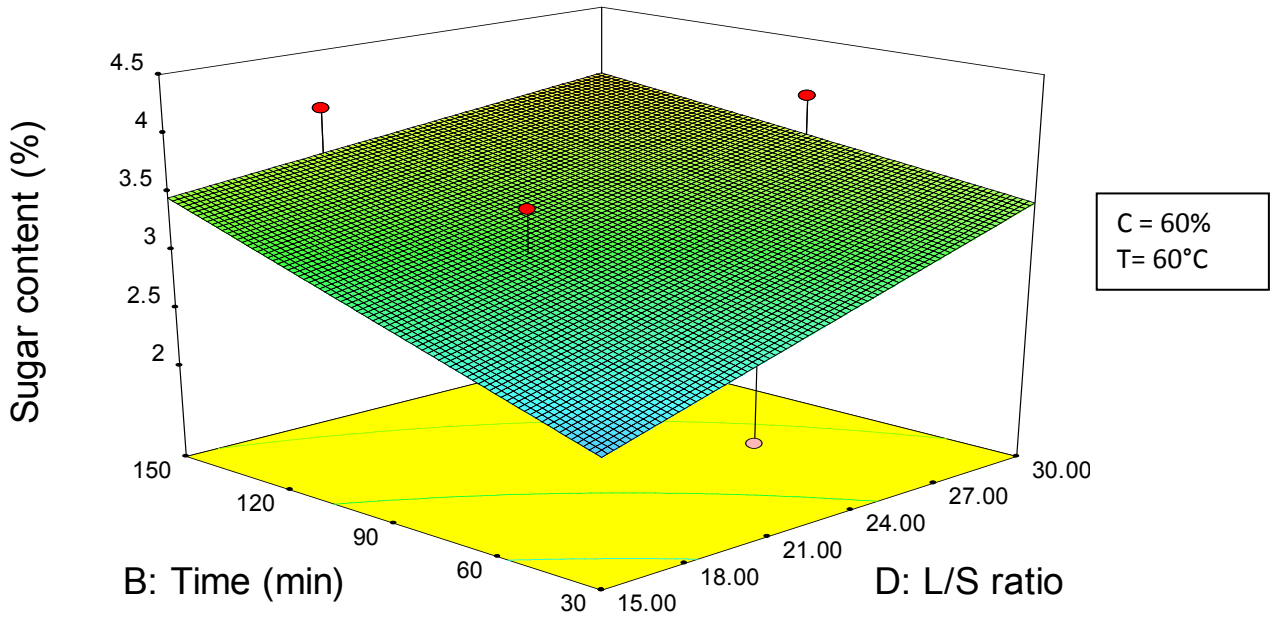


Fig. 4.19c Response surface plots showing percentage sugar content from aqueous acetone extraction at varying liquid-solid ratio and extraction time.

Figure 4.20 is a factor plot between the percentage sugar content with the extraction design variables in coded values. It can be observed that with an increase in extraction temperature from 40°C (coded value -1) to 60°C (coded value +1), the sugar content increases. Similarly, increasing the extraction time from 30 min (coded value -1) to 150 min (coded value +1) increases the sugar content. Increasing the liquid/solid ratio from 10 (coded value -1) to 30 (coded value +1) also increases the sugar content. Varying the solvent concentration did not significantly affect the sugar content and therefore this factor did not appear in the factor plots. The factor plot shows that each of the design variables have their own individual effect as well as combined effect on the percentage sugar content in the design and optimization of sugar content from aqueous acetone extraction.

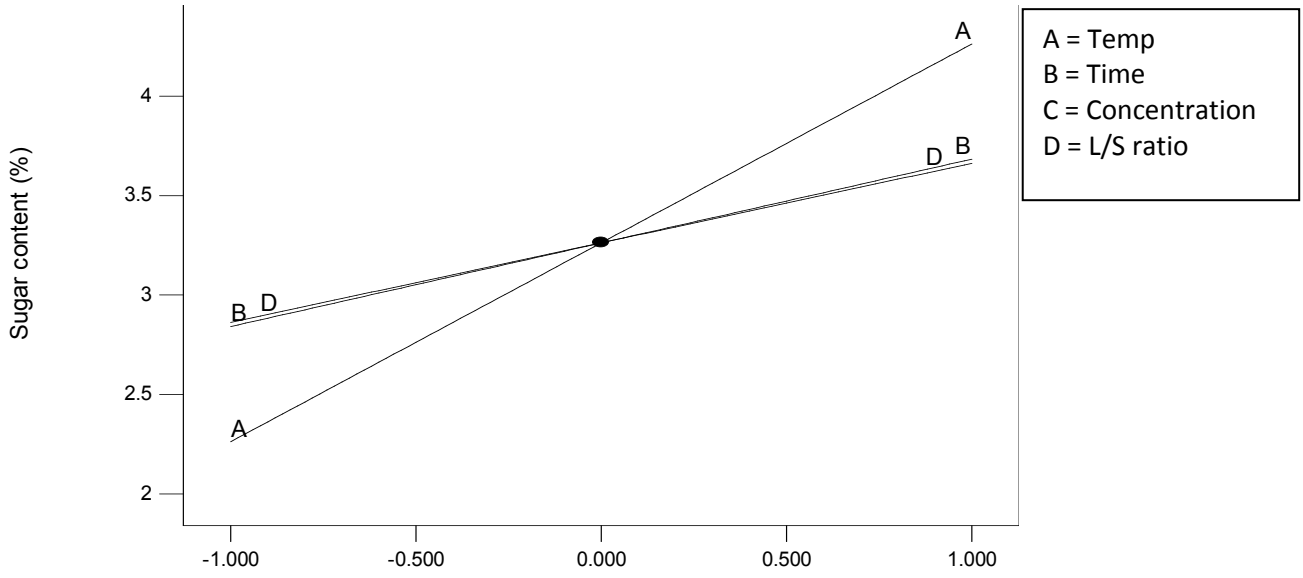


Fig 4.20 Effect of individual variables on the sugar content from aqueous acetone extraction.

Aqueous ethanol extraction

Table 4. 8: Comparison of experimental and predicted values using Box-Behnken design for the four independent variables on the sugar content from aqueous ethanol extraction

Run no.	Extraction temperature (°C) T	Extraction time (min) t	Solvent composition (%) C	Liquid-Solid ratio V	Actual value (%)	Predicted value (%) using equation 4.6
1	60.00	90.00	20.00	20.00	2.16	1.83
2	60.00	90.00	100.00	20.00	3.12	3.66
3	60.00	90.00	60.00	20.00	2.16	2.41
4	50.00	120.00	40.00	25.00	4.32	4.24
5	60.00	150.00	60.00	20.00	2.64	2.74
6	60.00	90.00	60.00	20.00	3.36	3.19
7	70.00	120.00	40.00	25.00	3.6	3.32
8	70.00	120.00	80.00	15.00	3.6	3.77

9	60.00	90.00	60.00	10.00	2.88	2.45
10	70.00	60.00	40.00	25.00	4.32	4.28
11	50.00	120.00	40.00	15.00	2.16	3.03
12	50.00	120.00	80.00	15.00	5.04	4.86
13	80.00	90.00	60.00	20.00	3.36	3.36
14	50.00	60.00	80.00	25.00	4.32	3.81
15	60.00	30.00	60.00	20.00	4.08	3.94
16	70.00	60.00	80.00	25.00	4.32	4.39
17	70.00	60.00	40.00	15.00	1.92	2.31
18	50.00	120.00	80.00	25.00	4.08	4.59
19	70.00	60.00	80.00	15.00	2.16	2.87
20	60.00	90.00	60.00	30.00	4.08	4.03
21	40.00	90.00	60.00	20.00	3.84	3.23
22	60.00	90.00	60.00	20.00	3.6	3.67
23	50.00	60.00	40.00	15.00	3.36	2.83
24	50.00	60.00	40.00	25.00	4.32	4.07
25	50.00	60.00	80.00	15.00	3.84	3.45
26	70.00	120.00	40.00	15.00	3.12	3.45
27	70.00	120.00	80.00	25.00	4.32	3.45
28	60.00	90.00	60.00	20.00	2.64	3.45

The extraction design variables on the sugar content in actual and predicted values using aqueous ethanol as extraction solvent is given in Table 4.8. The results of the ANOVA and model

coefficients are presented in appendix 2. The response surface plots between aqueous acetone concentration and extraction temperature are shown in Figure 4.21a. The percentage sugar content decreased at lower extraction temperatures and solvent concentration at constant extraction time and liquid/solid ratio of 90 min and 20:1 respectively. At an extraction temperature of 52.9°C and 56.8% solvent concentration, the sugar content was 3%, and the minimum sugar content of 0.75% occurred at 40°C and 20.6% solvent concentration.

The effect of extraction temperature and time on sugar content is illustrated in the response surface plots at constant solvent concentration and liquid-solid ratio of 60% and 20:1 respectively (Figure 4.21b). It showed that a decrease in extraction temperature and time resulted in a low sugar content. At an extraction temperature and time of 40.1°C and 31.3 min respectively, the sugar content was found to be 1.7%. The responses observed for the effect of liquid-solid ratio and solvent concentration at a fixed temperature of 60°C and time of 90 min indicated that a general direction of decreased temperature and time ensures minimum sugar content (Figure 4.21c). At a liquid-solid ratio of 17.7:1 and solvent concentration of 38.45 the sugar content was found to be 3.2%. From the numerical optimization, the minimum predicted sugar content of 1.86% was obtained under the optimum extraction conditions of 47.4°C extraction temperature, 92.9 min extraction time, 47.6% ethanol concentration, and 10.9:1 liquid - solid ratio. The amount of tannin extracted and the Stiasny number under these conditions were 7.01% and 75.2% respectively (Table 4.16).

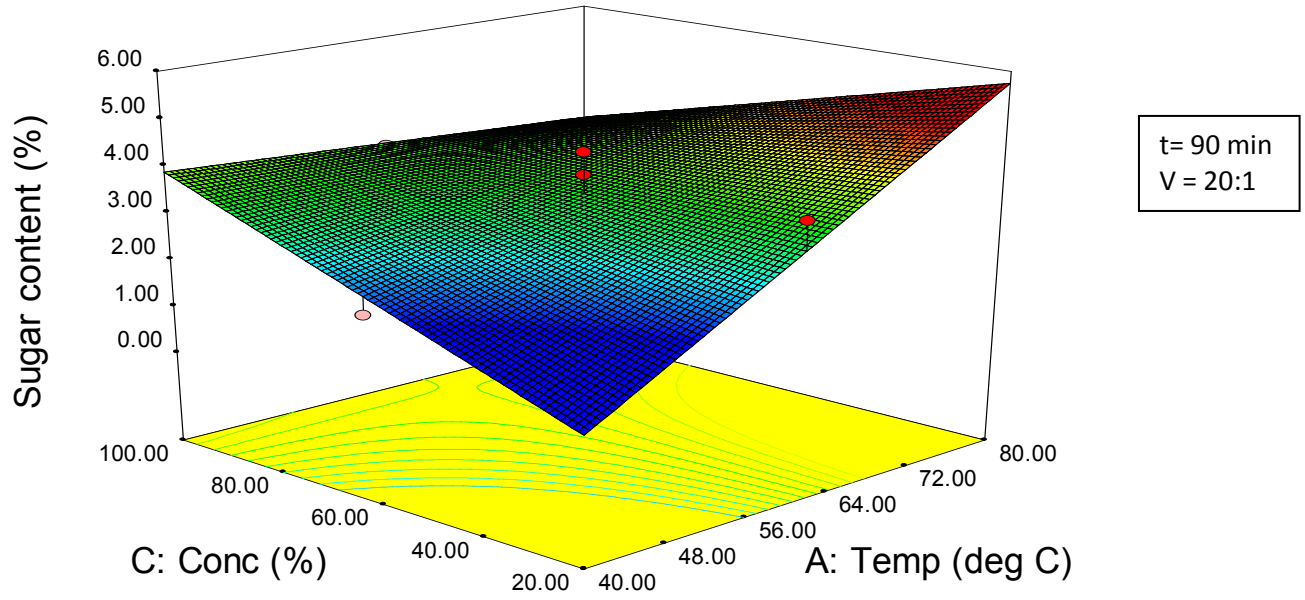


Fig. 4.21a Response surface plots showing percentage sugar content from aqueous ethanol extraction at varying solvent concentration and extraction temperature.

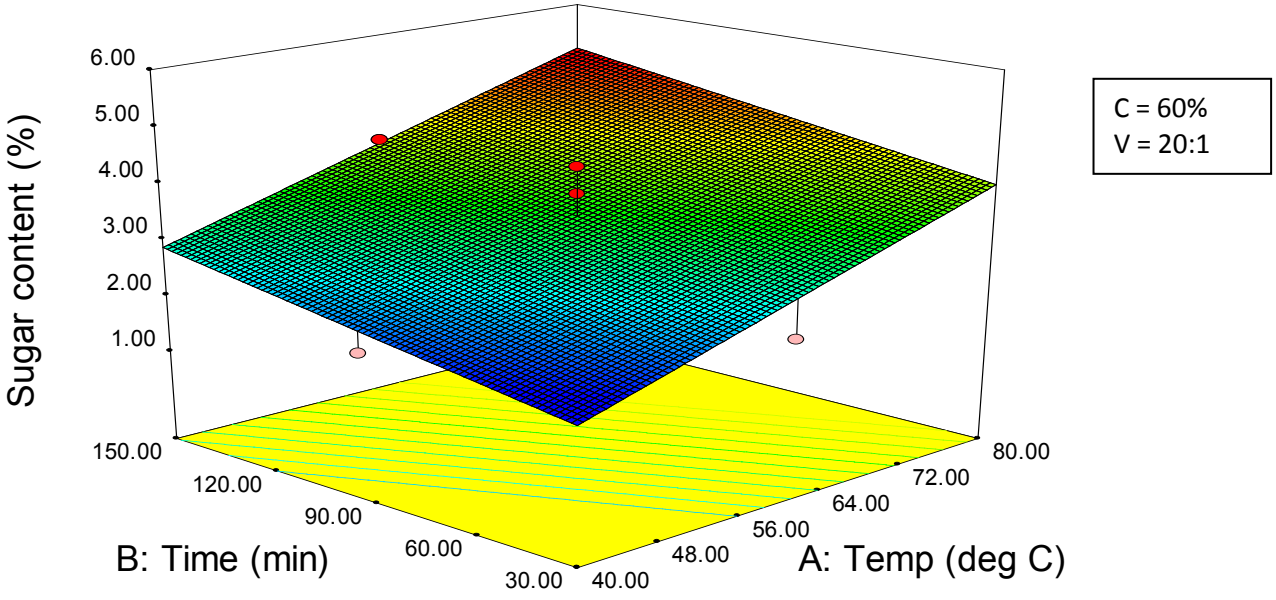


Fig. 4.21b Response surface plots showing percentage sugar content from aqueous ethanol extraction at varying extraction temperature and time.

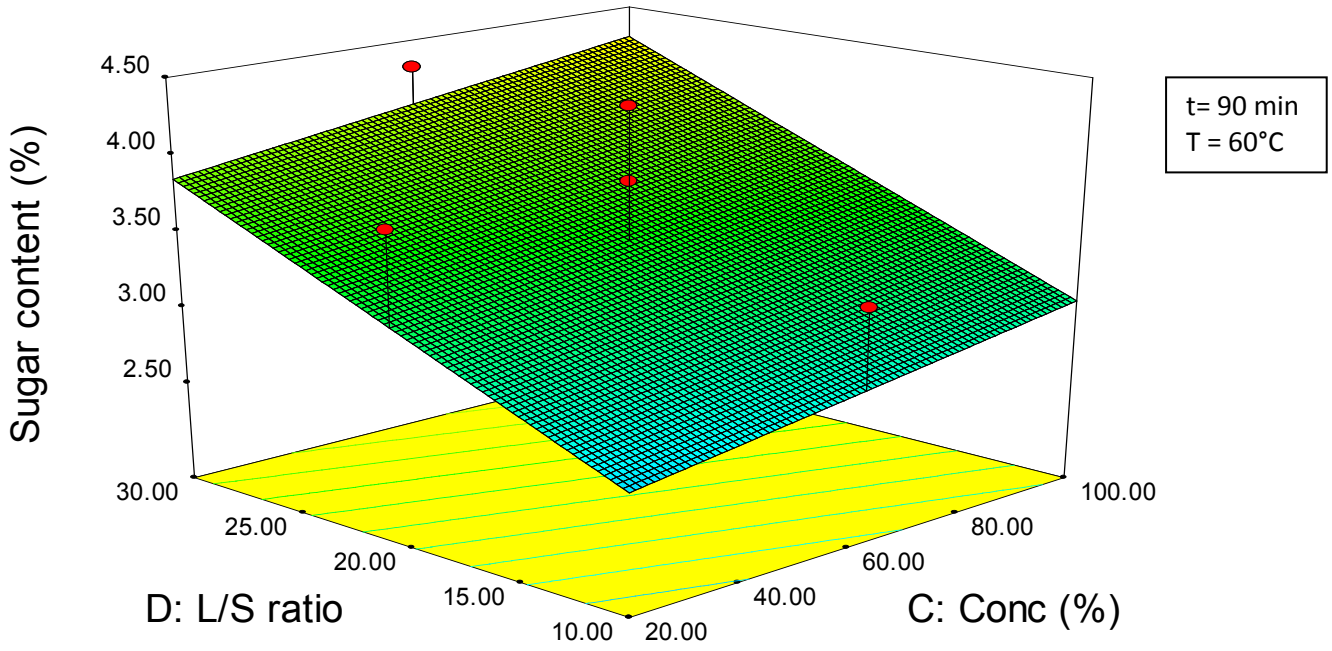


Fig. 4.21c Response surface plots showing percentage sugar content from aqueous ethanol extraction at varying solvent concentration and liquid-solid ratio.

Figure 4.22 is a factor plot between the percentage sugar content with the extraction design variables in coded values. The plot shows that with an increase in extraction temperature from 40°C (coded value -1) to 80°C (coded value +1), the sugar content increases. Similarly, increasing the extraction time from 30 min (coded value -1) to 150 min (coded value +1) increases the sugar content. Increasing the liquid/solid ratio from 10 (coded value -1) to 30 (coded value +1) also increases the sugar content. Varying the solvent concentration slightly increased the sugar content. The factor plot shows that each of the design variables have their own individual effect as well as combined effect on the sugar content in the design and optimization of sugar content from aqueous ethanol extraction.

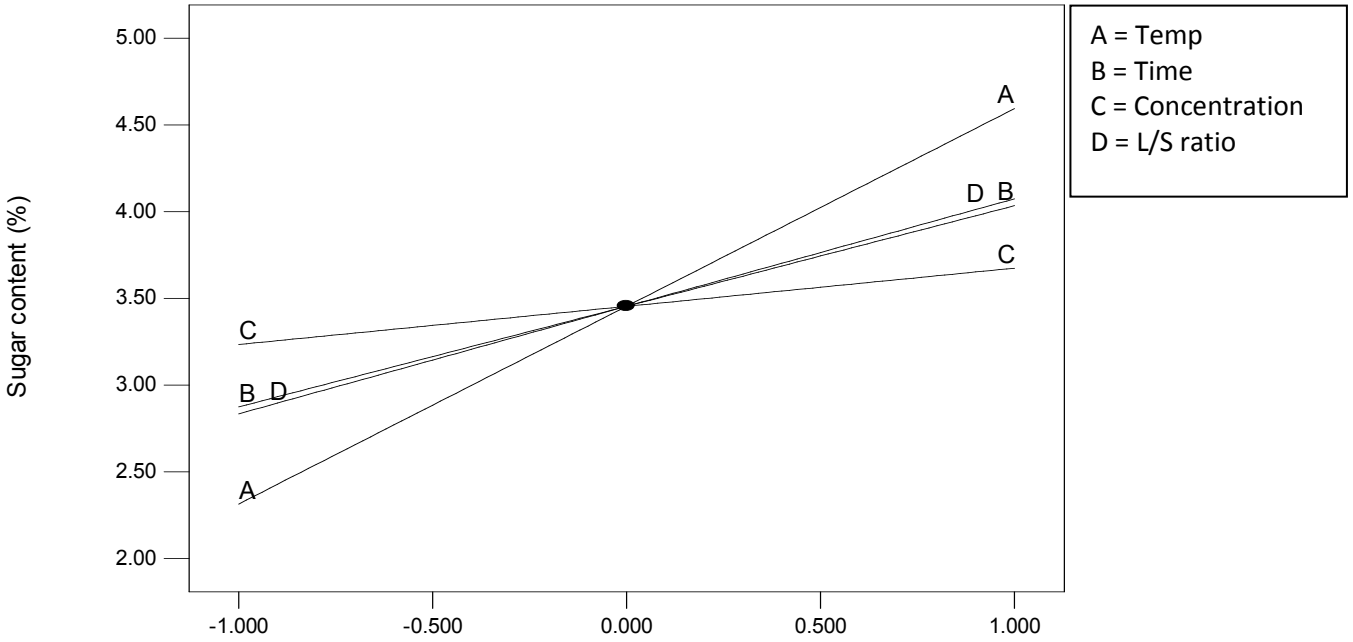


Fig 4.22 Effect of individual variables on the sugar content from aqueous ethanol extraction.

Aqueous NaOH extraction

Table 4. 9: Comparison of experimental and predicted values using Box-Behnken design for the four independent variables on the content of sugar from aqueous NaOH extraction.

Run no.	Extraction temperature (°C) T	Extraction time (min) t	Solvent composition (%) C	Liquid-Solid ratio V	Actual value (%)	Predicted value (%) using equation 4.7
1	80.00	45.00	0.05	20.00	25.00	27.33
2	80.00	45.00	1.50	20.00	39.00	32.64
3	80.00	45.00	0.50	20.00	38.00	35.76
4	60.00	60.00	0.10	25.00	47.00	41.33
5	80.00	90.00	0.50	20.00	30.00	32.64
6	80.00	45.00	0.50	20.00	42.00	44.40

7	90.00	60.00	0.10	25.00	35.00	32.69
8	90.00	60.00	1.00	15.00	36.00	35.76
9	80.00	45.00	0.50	10.00	37.00	32.69
10	90.00	30.00	0.10	25.00	38.00	35.72
11	60.00	60.00	0.10	15.00	30.00	30.40
12	60.00	60.00	1.00	15.00	39.00	35.72
13	100.00	45.00	0.50	20.00	37.00	30.40
14	60.00	30.00	1.00	25.00	36.00	35.76
15	80.00	15.00	0.50	20.00	33.00	35.76
16	90.00	30.00	1.00	25.00	33.00	27.33
17	90.00	30.00	0.10	15.00	30.00	35.76
18	60.00	60.00	1.00	25.00	25.00	30.63
19	90.00	30.00	1.00	15.00	40.00	44.40
20	80.00	45.00	0.50	30.00	47.00	43.46
21	40.00	45.00	0.50	20.00	30.00	33.43
22	80.00	45.00	0.50	20.00	25.00	29.62
23	60.00	30.00	0.10	15.00	42.00	45.22
24	60.00	30.00	0.10	25.00	25.00	29.62
25	60.00	30.00	1.00	15.00	28.00	31.51
26	90.00	60.00	0.10	15.00	42.00	41.33
27	90.00	60.00	1.00	25.00	22.00	22.91
28	80.00	45.00	0.50	20.00	39.00	35.76

The extraction design variables on the sugar content in actual and predicted values using aqueous NaOH as extraction solvent is given in Table 4.9. The results of the ANOVA and model coefficients are presented in appendix 2. The response surface plot between aqueous NaOH concentration and extraction temperature at fixed liquid-solid ratio and extraction time of 20:1 and 53.5 min respectively is shown in Figure 4.23a. The percentage sugar content decreased at lower extraction temperatures and solvent concentration. At an extraction temperature of 52°C and 0.8% solvent concentration, the sugar content was 33.6%, and the minimum sugar content of 4.6% occurred at 21°C and 0.06% solvent concentration.

Figure 4.23b shows the 3-D response surface plot of the effect of NaOH concentration and extraction time on sugar content at a fixed temperature and liquid-solid ratio of 60°C and 20:1 respectively. It showed that a decrease in NaOH concentration at low extraction time resulted in a decrease in sugar content. At an extraction time of 56 min and solvent concentration of 1%, the sugar content was found to be 40.1%. From the numerical optimization, the minimum predicted sugar content of 20.41% was obtained under the optimum extraction conditions of 31.6°C extraction temperature, 40.8 min extraction time, 0.97% NaOH concentration, and 18:1 liquid - solid ratio. The amount of tannin extracted and the Stiasny number under these conditions were 19.93% and 79.88% respectively (Table 4.17).

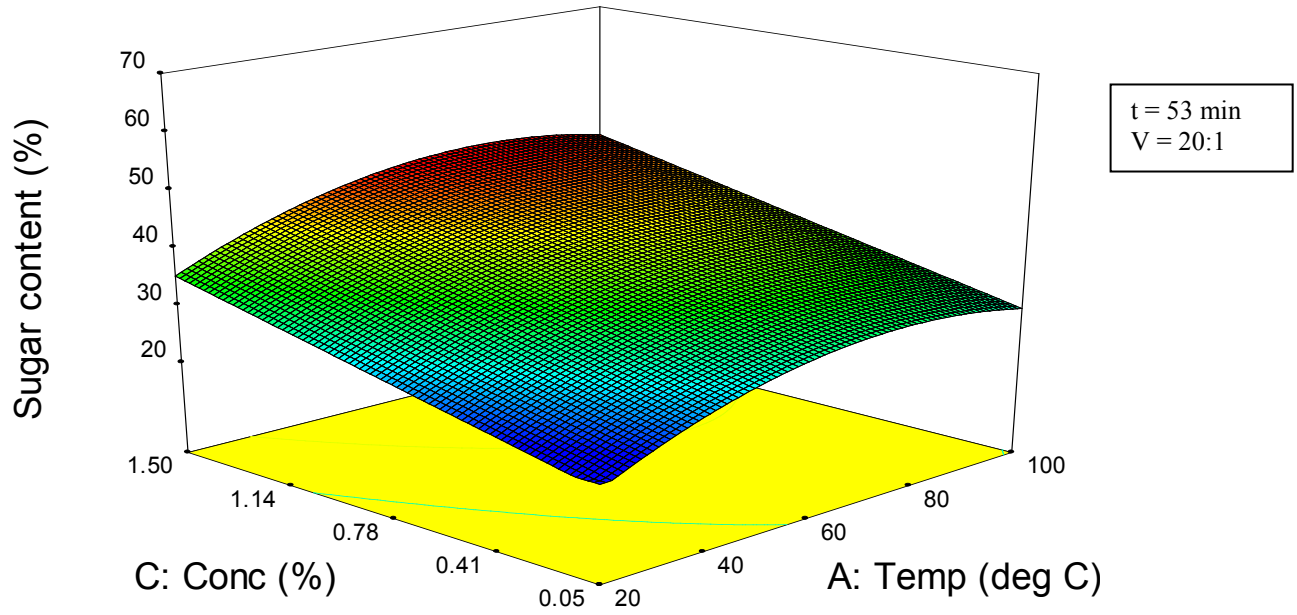


Fig. 4.23a Response surface plots showing percentage sugar content from aqueous NaOH extraction at varying solvent concentration and extraction temperature.

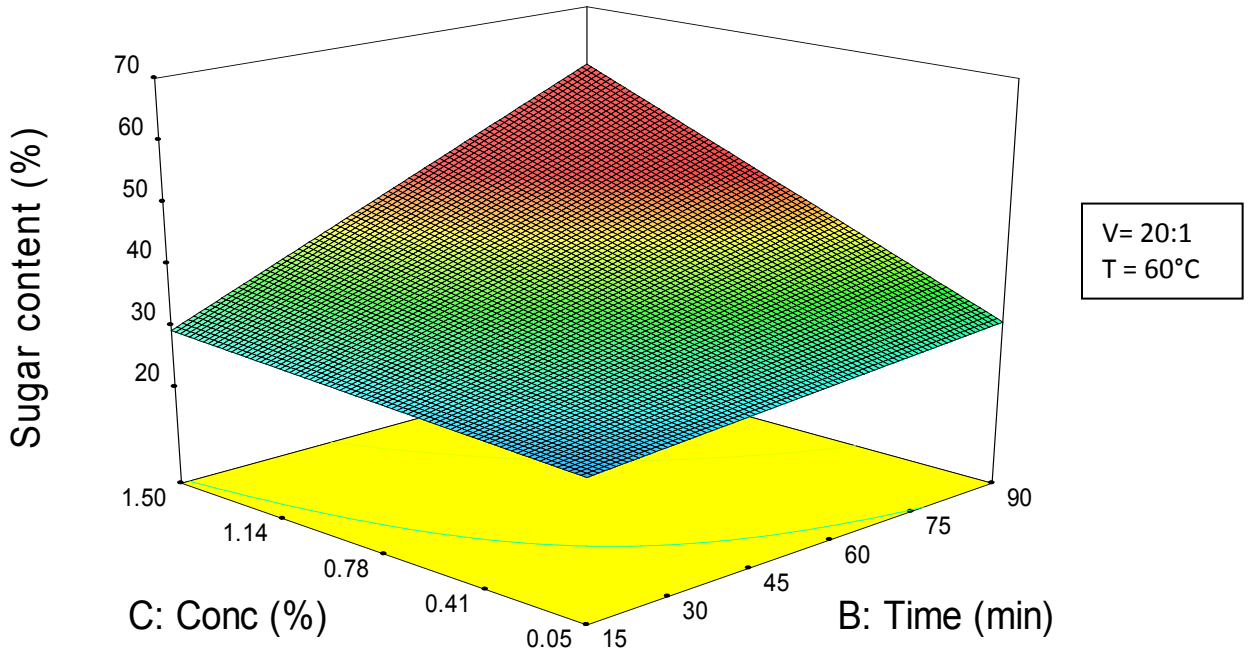


Fig. 4.23b Response surface plots showing percentage sugar content from aqueous NaOH extraction at varying solvent concentration and extraction time.

Figure 4.24 is a factor plot between the percentage sugar content with the extraction design variables in coded values. The plot shows that with an increase in extraction temperature from 40°C (coded value -1) to 100°C (coded value +1), the percentage sugar content increases. Similarly, increasing the extraction time from 15 min (coded value -1) to 90 min (coded value +1) increases the sugar content. Increasing the solvent concentration from 0.05% (coded value -1) to 1.5 (coded value +1) also increases the sugar content. Varying the liquid/solid ratio did not significantly affect the sugar content and therefore this factor did not appear in the factor plots. The factor plot shows that each of the design variables have their own individual effect as well as combined effect on the percentage tannin content in the design and optimization of sugar content from aqueous NaOH extraction.

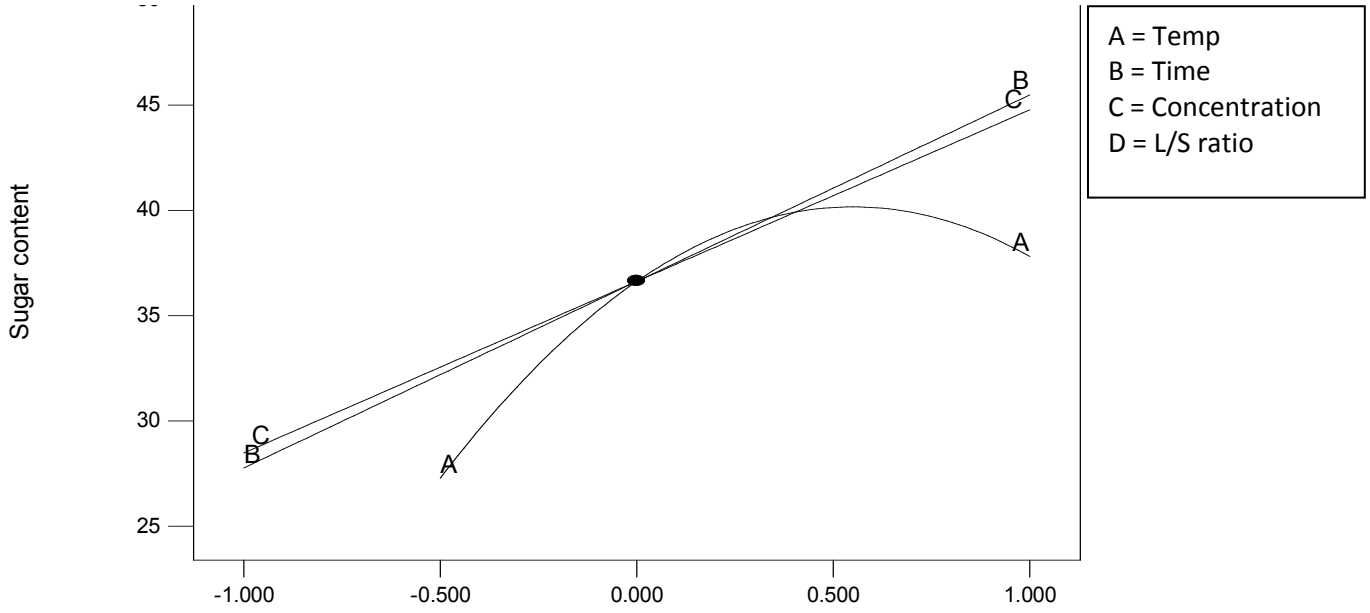


Fig 4.24 Effect of individual variables on the sugar content from aqueous NaOH extraction

Water extraction

Table 4. 10: Comparison of experimental and predicted values using Box-Behnken design for the four independent variables on the sugar content from water extraction.

Run no.	Extraction temperature (°C) T	Extraction time (min) t	Liquid-Solid ratio V	Actual value (%)	Predicted value (%) using equation 4.8
1	80.00	90.00	20.00	1.70	1.55
2	90.00	120.00	25.00	1.50	1.61
3	80.00	90.00	10.00	1.80	1.85
4	90.00	60.00	15.00	1.40	1.40
5	90.00	90.00	30.00	1.50	1.42
6	80.00	90.00	20.00	1.80	1.85
7	90.00	60.00	25.00	2.80	2.56
8	60.00	60.00	15.00	1.60	1.48
9	100.00	90.00	20.00	1.70	1.78
10	90.00	120.00	15.00	1.60	1.48
11	80.00	30.00	20.00	2.10	2.21
12	40.00	90.00	20.00	2.20	2.28
13	60.00	120.00	15.00	1.60	1.84
14	80.00	90.00	20.00	1.80	1.85
15	60.00	120.00	25.00	1.40	1.32
16	80.00	150.00	20.00	1.90	1.85
17	80.00	90.00	20.00	2.50	2.43
18	60.00	60.00	25.00	1.40	1.51

The extraction design variables on the sugar content in actual and predicted values using water as extraction solvent is given in Table 4.10. The results of the ANOVA and model coefficients are presented in appendix 2. The 3-D response surface plot between extraction time and temperature at constant liquid-solid ratio is shown in Figure 4.25a. The percentage sugar content decreased at lower extraction temperatures and time at constant solvent concentration and liquid/solid ratio of 60% and 20:1 respectively. At an extraction temperature and time of 84.5°C and 106 min respectively, the sugar content was 2.1%, and the minimum sugar content of 1.4% occurred at 61.9°C and 32.9 min.

The response surface plot between liquid-solid ratio and extraction temperature at a fixed extraction time of 90 min is shown in Figure 4.25b. The percentage sugar content decreased at lower extraction temperatures and liquid-solid ratio. At an extraction temperature of 74.4°C and liquid-solid ratio of 18.2:1, the sugar content was found to be 1.7%. Figure 4.25c shows the 3-D response surface plot of the effect of liquid-solid ratio and extraction time on sugar content at a fixed temperature of 70°C. It showed that a decrease in liquid-solid ratio at low extraction time resulted in a decrease in sugar content. At an extraction time of 133.8 min and liquid-solid ratio of 21.7:1, the sugar content was found to be 1.8%. From the numerical optimization, the minimum predicted sugar content of 1.29% was obtained under the optimum extraction conditions of 67.8°C extraction temperature, 61.4 min extraction time and 28.7:1 liquid - solid ratio. The amount of tannin extracted and the Stiasny number under these conditions were 8.84% and 89.15% respectively (Table 4.18).

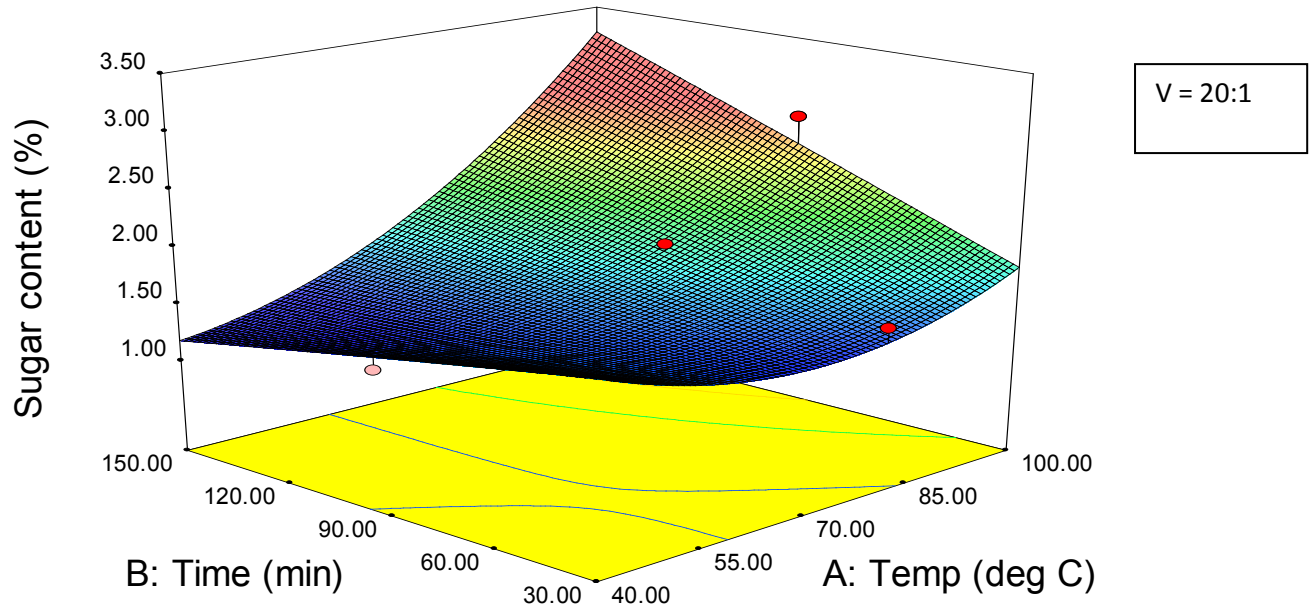


Fig. 4.25a Response surface plots showing percentage sugar content from water extraction at varying extraction temperature and time.

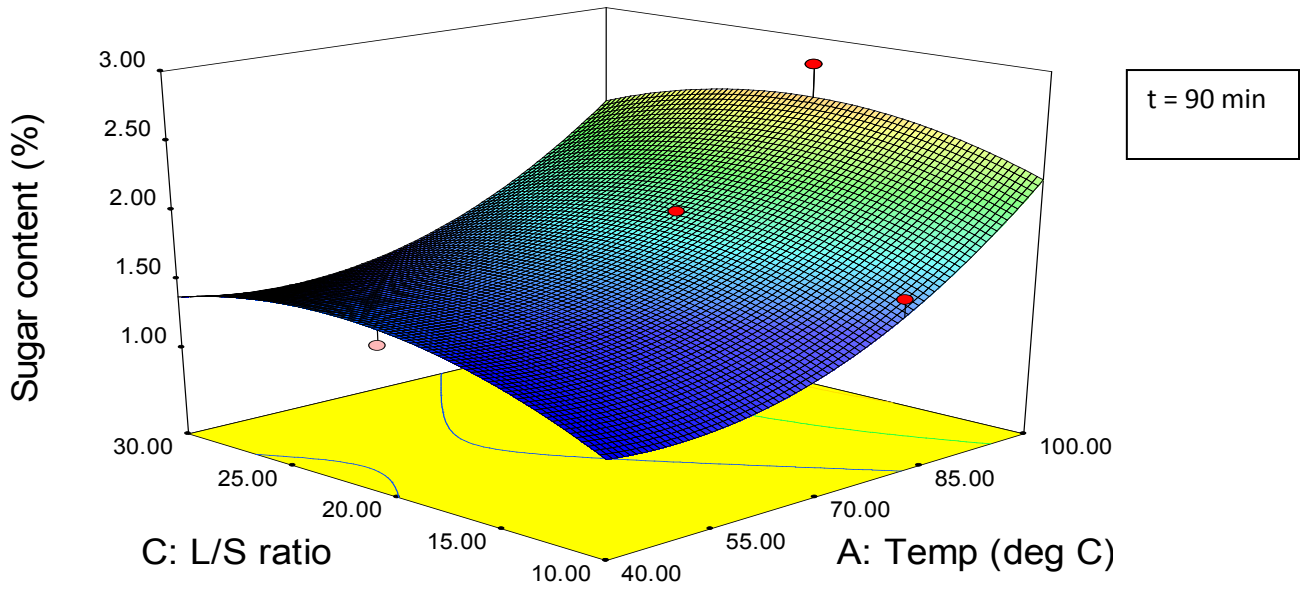


Fig. 4.25b Response surface plots showing percentage sugar content from water extraction at varying extraction temperature and liquid-solid ratio.

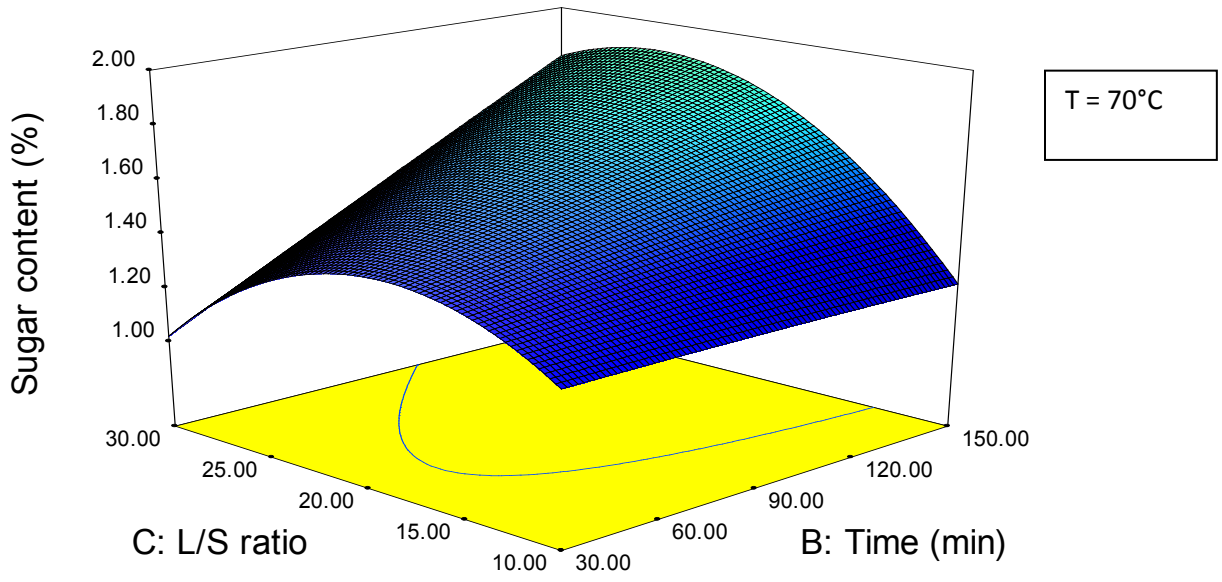


Fig. 4.25c Response surface plots showing percentage sugar content from water extraction at varying extraction time and liquid-solid ratio.

Figure 4.26 is a factor plot between the percentage sugar content with the extraction design variables in coded values. The plot shows that with an increase in extraction temperature from 40°C (coded value -1) to 100°C (coded value +1), the percentage sugar content increases. Similarly, increasing the extraction time from 30 min (coded value -1) to 150 min (coded value +1) increases the sugar content. Increasing the liquid/solid ratio from 10 (coded value -1) to 30 (coded value +1) also increases the sugar content, but falls off at higher ratios. The factor plot shows that each of the design variables have their own individual effect as well as combined effect on the percentage sugar content in the design and optimization of sugar content from water extraction.

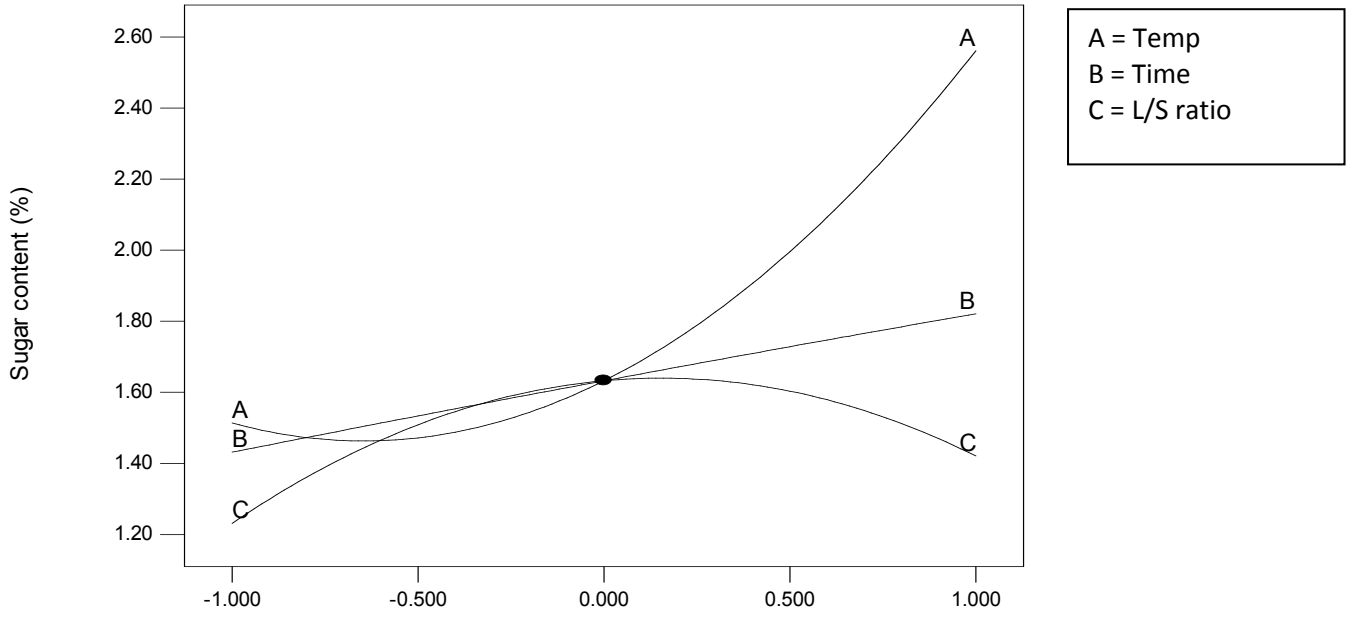


Fig. 4.26 Effect of individual variables on the sugar content from water extraction.

4.2.2.1 Optimum extraction conditions based on maximizing Stiasny number

The polynomial equations for the estimation of Stiasny number (N) in terms of extraction temperature (T), extraction time (t), solvent composition (C) and liquid-solid ratio (V) using aqueous acetone, aqueous ethanol, aqueous sodium hydroxide and water extractions were fitted as in equations 4.9 – 4.12. For each extraction, the objective function was to maximize the Stiasny number whilst the range of sugar content and that of tannin content were fixed as constraints.

$$N_{acetone} = 111 - 0.4t - 1.89V + 0.02Vt \quad \textbf{4.9}$$

$$N_{ethanol} = 5.31 + 0.88T + 0.72t + 0.49V - 0.01Tt \quad \textbf{4.10}$$

$$N_{hydroxide} = 144.74 - 1.86T - 0.02t + 2.62C - 0.47Ct + 0.01T^2 \quad \textbf{4.11}$$

$$N_{water} = 92.18 + 0.54T + 2.63t + 1.63V - 8.02T^2 - 4.11V^2 \quad \textbf{4.12}$$

The analysis of variance for each of the approximating functions in equations 4.1 – 4.4 shows a Model F value to be 3.45, 5.82, 10.52 and 4.23 respectively (appendix 2) which implies that each model is significant. The Model R^2 of the approximating functions $S_{acetone}$, $S_{ethanol}$, $S_{hydroxide}$ and S_{water} were respectively 0.3, 0.5, 0.7 and 0.64 (appendix 2). The predictive model graphs can be found in Appendix 4.

Aqueous acetone extraction

Table 4. 11: Comparison of experimental and predicted values uisng Box-Behnken design for the four independent variables on the Stiasny number from aqueous acetone extraction.

Run no.	Extraction temperature (°C) T	Extraction time (min) t	Solvent composition (%) C	Liquid-Solid ratio V	Actual value (%)	Predicted value (%) using equation 4.9
1	50.00	90.00	20.00	20.00	76.00	79.82
2	50.00	90.00	100.00	20.00	78.00	78.86
3	50.00	90.00	60.00	20.00	85.00	84.65
4	45.00	120.00	40.00	25.00	88.00	80.19
5	50.00	150.00	60.00	20.00	78.00	78.86
6	50.00	90.00	60.00	20.00	77.00	78.86
7	55.00	120.00	40.00	25.00	70.00	74.40
8	55.00	120.00	80.00	15.00	83.00	84.65
9	50.00	90.00	60.00	10.00	87.00	84.65
10	55.00	60.00	40.00	25.00	87.00	79.82
11	45.00	120.00	40.00	15.00	76.00	78.86
12	45.00	120.00	80.00	15.00	76.00	76.57

13	60.00	90.00	60.00	20.00	77.00	77.52
14	45.00	60.00	80.00	25.00	82.00	84.65
15	50.00	30.00	60.00	20.00	79.00	76.57
16	55.00	60.00	80.00	25.00	76.00	76.57
17	55.00	60.00	40.00	15.00	75.00	78.86
18	45.00	120.00	80.00	25.00	82.00	82.36
19	55.00	60.00	80.00	15.00	74.00	74.40
20	50.00	90.00	60.00	30.00	75.00	75.36
21	40.00	90.00	60.00	20.00	70.00	74.40
22	50.00	90.00	60.00	20.00	82.00	74.40
23	45.00	60.00	40.00	15.00	84.00	78.86
24	45.00	60.00	40.00	25.00	88.00	79.82
25	45.00	60.00	80.00	15.00	81.00	78.86
26	55.00	120.00	40.00	15.00	75.00	79.82
27	55.00	120.00	80.00	25.00	82.00	76.57
28	50.00	90.00	60.00	20.00	65.00	78.86

The extraction design variables on the Stiasny number in actual and predicted values using aqueous acetone as extraction solvent is given in Table 4.11. The results of the ANOVA and model coefficients are presented in appendix 2. The 3-D response surface plot between aqueous acetone extraction time and liquid-solid ratio is shown in Figure 4.27a. The Stiasny number increased at higher extraction time and liquid-solid ratio at constant solvent concentration and

and extraction temperature of 60% and 50°C respectively. At an extraction time of 98 min and 25:1 liquid-solid ratio, the Stiasny number was 80.8%, and the maximum Stiasny number of 97.1% occurred at 150 min and 30:1 liquid-solid ratio.

Figure 4.27b shows the response surface plot of effect of liquid-solid ratio and extraction temperature on Stiasny number at constant extraction time and solvent concentration of 90 minutes and 60% respectively. There was no significant effect on the Stiasny number. At an extraction temperature of 44°C and 19:1 liquid-solid ratio, the Stiasny number was found to be 78.75 whilst the maximum Stiasny number was only 80% which occurred at 53°C and 30:1 liquid-solid ratio. The responses observed for the effect of extraction time and temperature at a fixed concentration of 60% and liquid/solid ratio of 20 indicated that a general direction of increased temperature and time ensures high Stiasny number (Figure 4.27c). At an extraction temperature and time of 50°C and 90 min respectively, the Stiasny number was found to be 79.1%. From the numerical optimization, the maximum predicted Stiasny number of 88.92% was obtained under the optimum extraction conditions of 45°C extraction temperature, 125 min extraction time, 60% acetone concentration, and 15.8:1 liquid - solid ratio. The amount of total sugars and tannin extracted under these conditions were 3.25% and 9.26% respectively (Table 4.15).

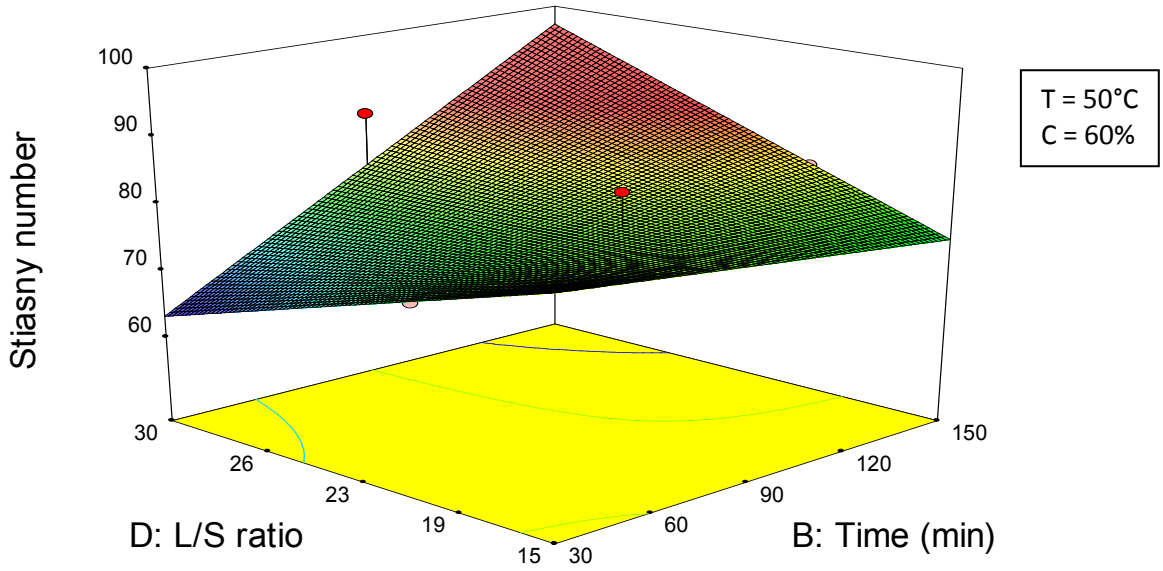


Fig. 4.27a Response surface plots showing percentage Stiasny number from aqueous acetone extraction at varying liquid-solid ratio and extraction time.

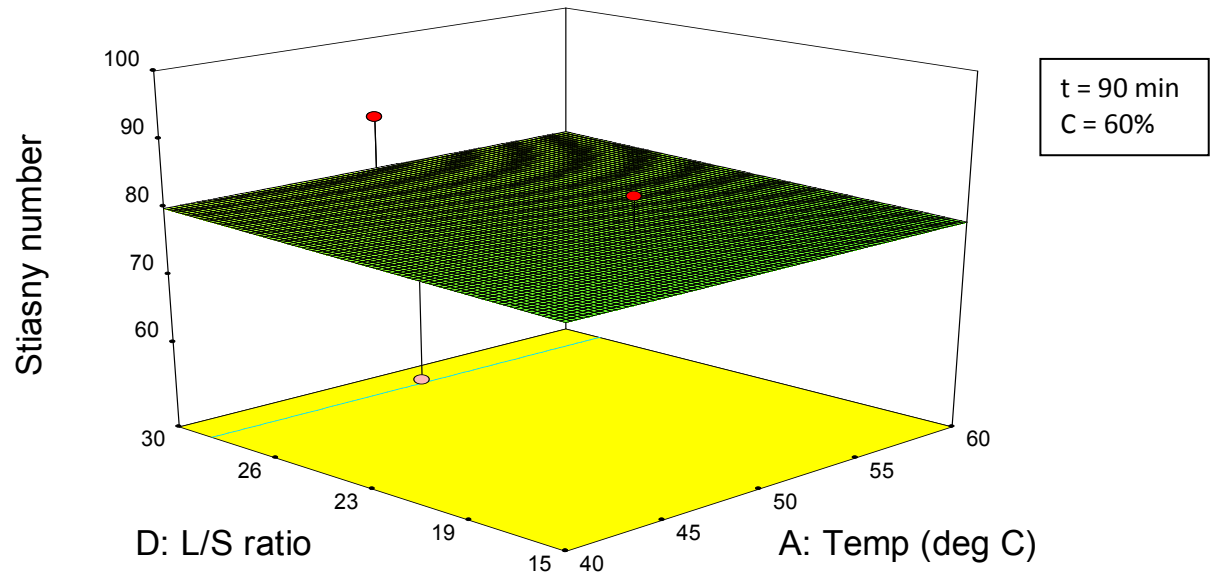


Fig. 4.27b Response surface plots showing percentage Stiasny number from aqueous acetone extraction at varying liquid-solid ratio and extraction temperature.

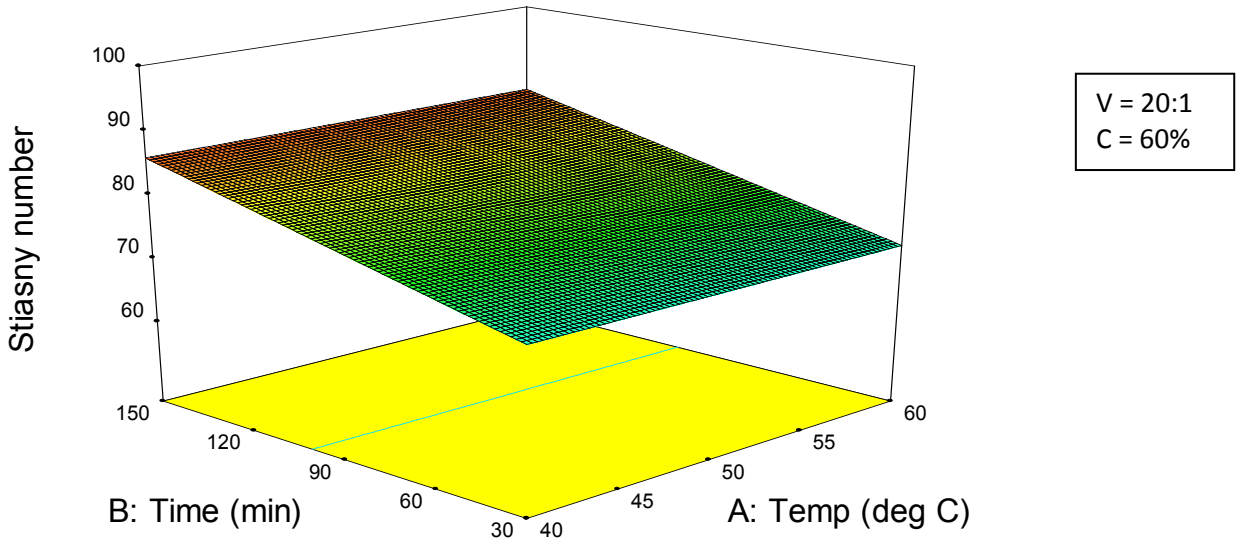


Fig. 4.27c Response surface plots showing percentage Stiasny number from aqueous acetone extraction at varying extraction temperature and time.

Figure 4.28 is a factor plot between the Stiasny number with the extraction design variables in coded values. The plot shows that only extraction time and liquid-solid ratio had significant effect on the Stiasny number, with time having the greater effect.

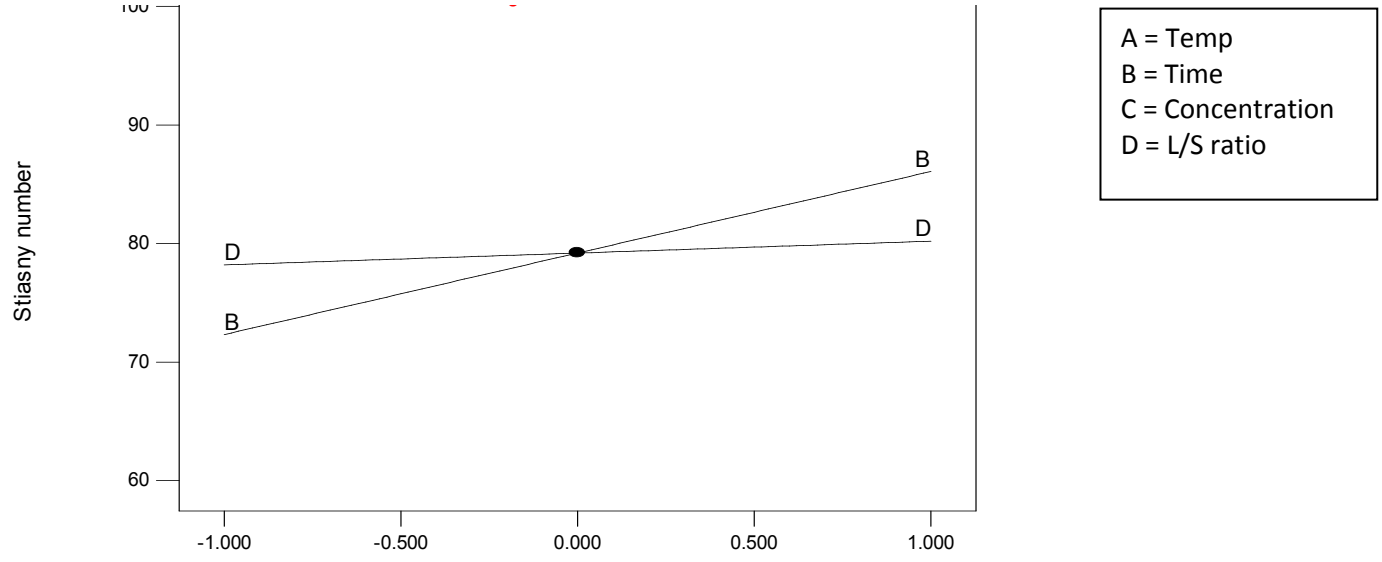


Fig 4.28 Effect of individual variables on the Stiasny number from aqueous acetone extraction.

Aqueous ethanol extraction

Table 4. 12: Comparison of experimental and predicted values using Box-Behnken design for the four independent variables on the Stiasny number from aqueous ethanol extraction

Run no.	Extraction temperature (°C) T	Extraction time (min) t	Solvent composition (%) C	Liquid-Solid ratio V	Actual value (%)	Predicted value (%) using equation 4.10
1	60.00	90.00	20.00	20.00	75.00	69.29
2	60.00	90.00	100.00	20.00	70.00	74.66
3	60.00	90.00	60.00	20.00	83.00	81.83
4	50.00	120.00	40.00	25.00	78.00	74.96
5	60.00	150.00	60.00	20.00	60.00	69.29
6	60.00	90.00	60.00	20.00	69.00	74.66
7	70.00	120.00	40.00	25.00	82.00	81.83
8	70.00	120.00	80.00	15.00	80.00	74.96
9	60.00	90.00	60.00	10.00	67.00	74.21
10	70.00	60.00	40.00	25.00	80.00	79.58
11	50.00	120.00	40.00	15.00	84.00	86.75
12	50.00	120.00	80.00	15.00	78.00	79.87
13	80.00	90.00	60.00	20.00	72.00	74.21
14	50.00	60.00	80.00	25.00	79.00	79.58
15	60.00	30.00	60.00	20.00	90.00	86.75
16	70.00	60.00	80.00	25.00	78.00	79.87
17	70.00	60.00	40.00	15.00	80.00	78.39
18	50.00	120.00	80.00	25.00	76.00	76.89

19	70.00	60.00	80.00	15.00	84.00	71.23
20	60.00	90.00	60.00	30.00	82.00	84.06
21	40.00	90.00	60.00	20.00	80.00	77.64
22	60.00	90.00	60.00	20.00	75.00	77.64
23	50.00	60.00	40.00	15.00	70.00	72.73
24	50.00	60.00	40.00	25.00	84.00	82.56
25	50.00	60.00	80.00	15.00	83.00	77.64
26	70.00	120.00	40.00	15.00	75.00	77.64
27	70.00	120.00	80.00	25.00	82.00	77.64
28	60.00	90.00	60.00	20.00	78.00	77.64

The extraction design variables on the Stiasny number in actual and predicted values using aqueous ethanol as extraction solvent is given in Table 4.12. The results of the ANOVA and model coefficients are presented in appendix 2. The response surface plot between aqueous ethanol extraction time and temperature is shown in Figure 4.29a. The Stiasny number increased at higher extraction temperatures and time at constant solvent concentration and liquid/solid ratio of 60% and 20:1 respectively. At an extraction temperature of 46.4°C and 93.5 min extraction time, the Stiasny number was 79%, and the maximum Stiasny number of 96.7% occurred at 40.2°C and 149 min.

The effect of ethanol concentration and liquid-solid ratio on Stiasny number at constant extraction time and temperature of 90 minutes and 60°C respectively is illustrated in the response surface plot (Figure 4.29b). It showed that an increase in ethanol concentration at high extraction

temperature resulted in a gradual increase in Stiasny number. At a solvent concentration of 66.7% and liquid-solid ratio of 16.6:1, the Stiasny number was found to be 76%. The responses observed for the effect of extraction temperature and liquid-solid ratio at a fixed extraction time of 90 min and solvent concentration of 60% indicated that a general direction of increased temperature ensures maximum Stiasny number whilst concentration has no significant effect (Figure 4.29c). At an extraction temperature of 54.2°C and liquid-solid ratio of 15.8:1, the Stiasny number was found to be 75.8%. From the numerical optimization, the maximum predicted Stiasny number of 91.17% was obtained under the optimum extraction conditions of 40.77°C extraction temperature, 134 min extraction time, 62.8% ethanol concentration, and 23.6:1 liquid-solid ratio. The amount of total sugars and tannin extracted under these conditions were 4.29% and 16.65% respectively (Table 4.16).

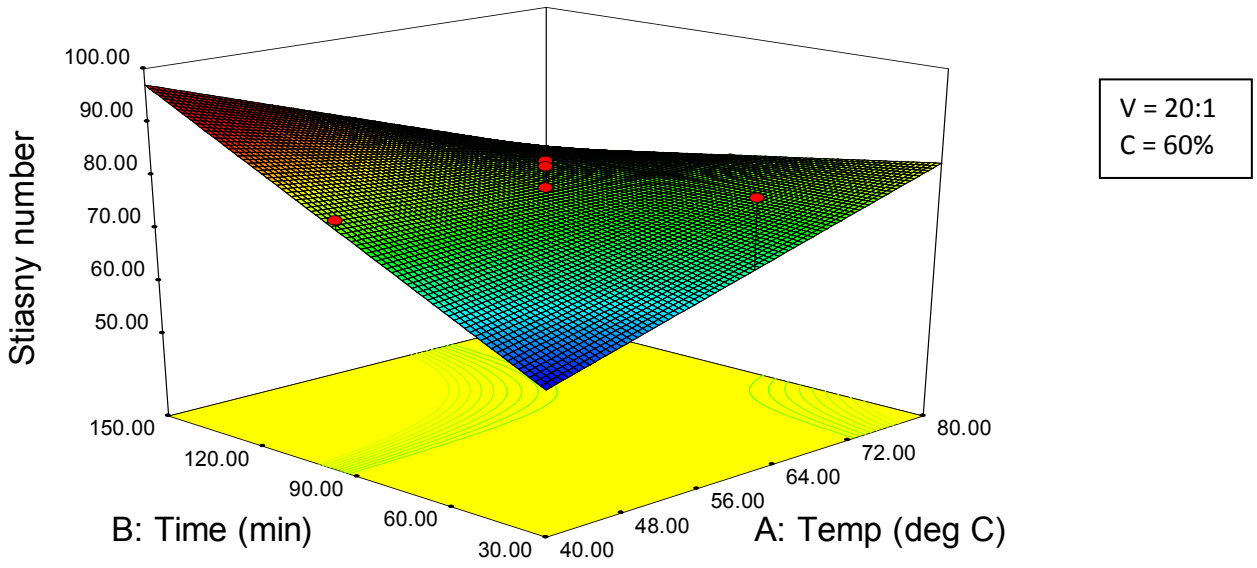


Fig. 4.29a Response surface plots showing percentage Stiasny number from aqueous ethanol extraction at varying extraction temperature and time.

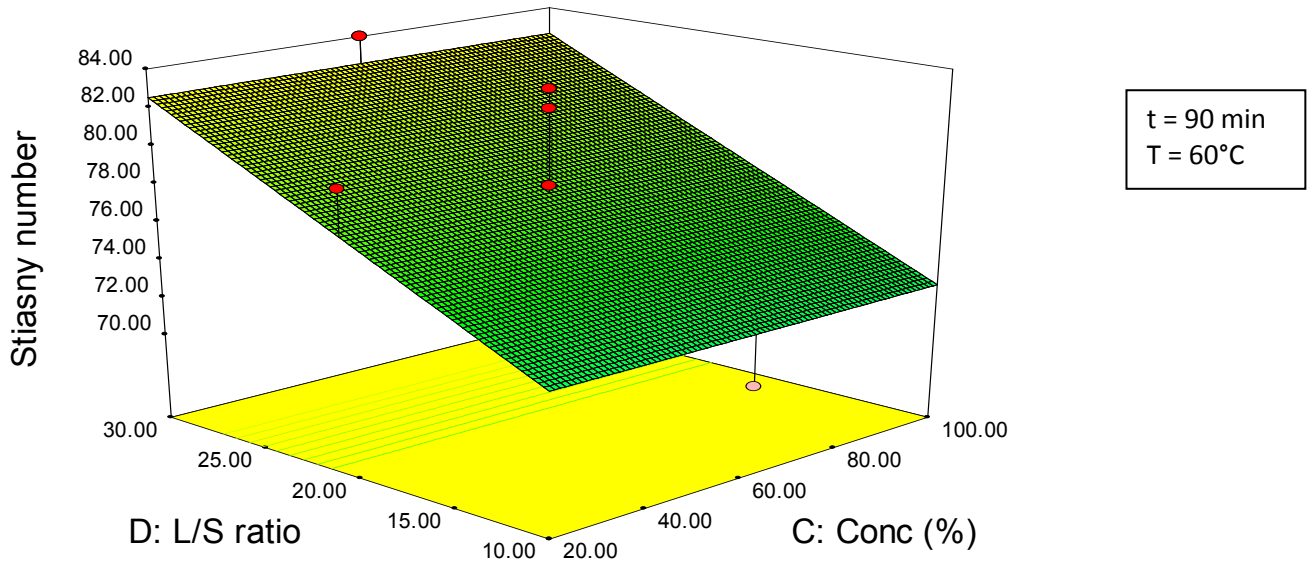


Fig. 4.29b Response surface plots showing percentage Stiasny number from aqueous ethanol extraction at varying extraction temperature and liquid-solid ratio.

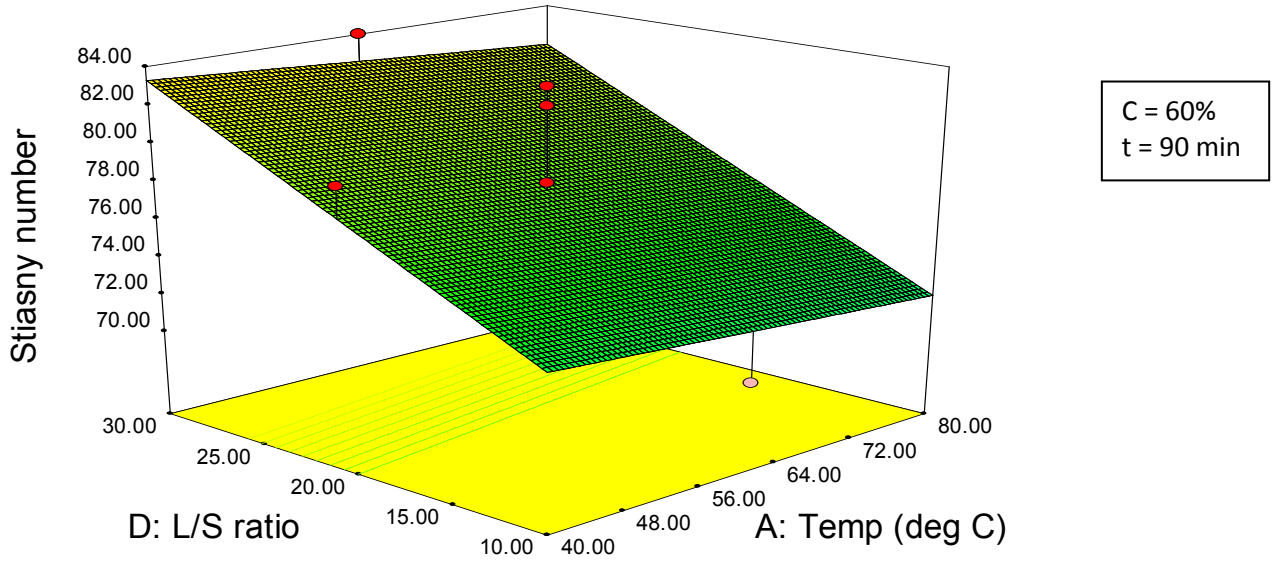


Fig. 4.29c Response surface plots showing percentage Stiasny number from aqueous ethanol extraction at varying solvent concentration and liquid-solid ratio.

Figure 4.30 is a factor plot between the Stiasny number with the extraction design variables in coded values. The plot shows that with an increase in extraction time and liquid-solid ratio, the

Stiasny number increases, whilst decreasing temperature increases the Stiasny number. The factor plot shows that each of the design variables have their own individual effect as well as combined effect on the Stiasny number in the design and optimization of Stiasny number from aqueous ethanol extraction.

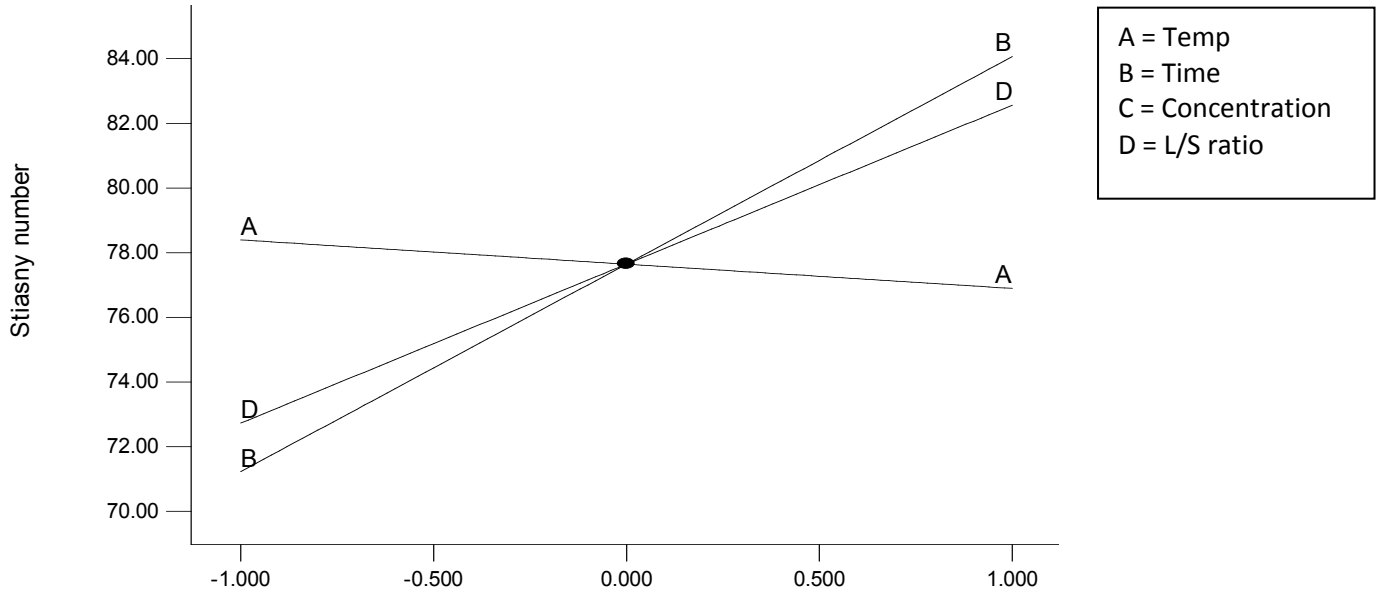


Fig 4.30 Effect of individual variables on the Stiasny number from aqueous ethanol extraction.

Aqueous NaOH extraction

Table 4. 13: Comparison of experimental and prdicted values using Box-Behnken design for the four independent variables on the Stiasny number from aqueous NaOH extraction

Run no.	Extraction temperature (°C) T	Extraction time (min) t	Solvent composition (%) C	Liquid-Solid ratio V	Actual value (%)	Predicted value (%) using equation 4.11
1	80.00	45.00	0.05	20.00	25.00	27.33
2	80.00	45.00	1.50	20.00	39.00	32.64
3	80.00	45.00	0.50	20.00	38.00	35.76
4	60.00	60.00	0.10	25.00	47.00	41.33
5	80.00	90.00	0.50	20.00	30.00	32.64

6	80.00	45.00	0.50	20.00	42.00	44.40
7	90.00	60.00	0.10	25.00	35.00	32.69
8	90.00	60.00	1.00	15.00	36.00	35.76
9	80.00	45.00	0.50	10.00	37.00	32.69
10	90.00	30.00	0.10	25.00	38.00	35.72
11	60.00	60.00	0.10	15.00	30.00	30.40
12	60.00	60.00	1.00	15.00	39.00	35.72
13	100.00	45.00	0.50	20.00	37.00	30.40
14	60.00	30.00	1.00	25.00	36.00	35.76
15	80.00	15.00	0.50	20.00	33.00	35.76
16	90.00	30.00	1.00	25.00	33.00	27.33
17	90.00	30.00	0.10	15.00	30.00	35.76
18	60.00	60.00	1.00	25.00	25.00	30.63
19	90.00	30.00	1.00	15.00	40.00	44.40
20	80.00	45.00	0.50	30.00	47.00	43.46
21	40.00	45.00	0.50	20.00	30.00	33.43
22	80.00	45.00	0.50	20.00	25.00	29.62
23	60.00	30.00	0.10	15.00	42.00	45.22
24	60.00	30.00	0.10	25.00	25.00	29.62
25	60.00	30.00	1.00	15.00	28.00	31.51
26	90.00	60.00	0.10	15.00	42.00	41.33
27	90.00	60.00	1.00	25.00	22.00	22.91
28	80.00	45.00	0.50	20.00	39.00	35.76

The extraction design variables on the Stiasny number in actual and predicted values using aqueous NaOH as extraction solvent is given in Table 4.13. The results of the ANOVA and model coefficients are presented in appendix 2. The response surface plot between aqueous NaOH concentration and extraction temperature is shown in Figure 4.31a. The Stiasny number increased at lower concentrations and lower extraction temperatures at constant extraction time and liquid/solid ratio of 45 min and 20:1 respectively. At an extraction temperature of 33°C and 0.98% solvent concentration, the Stiasny number was 72%, and the maximum Stiasny number of 79% occurred at 21°C and 1.36% solvent concentration.

The effect of NaOH extraction temperature and liquid-solid ratio at constant extraction time and concentration of 45 minutes and 0.78% respectively on Stiasny number is illustrated in the response surface plots (Figure 4.31b). It showed that decreasing the extraction temperature resulted in a gradual increase in Stiasny number. At and extraction temperature of 72°C and liquid-solid ratio of 23:1, the Stiasny number was found to be 48.9%. From the numerical optimization, the maximum predicted Stiasny number of 80% was obtained under the optimum extraction conditions of 46.9°C extraction temperature, 36 min extraction time, 0.06% NaOH concentration, and 22.5:1 liquid - solid ratio. The amount of total sugars and tannin extracted under these conditions were 22% and 22.89% respectively (Table 4.17).

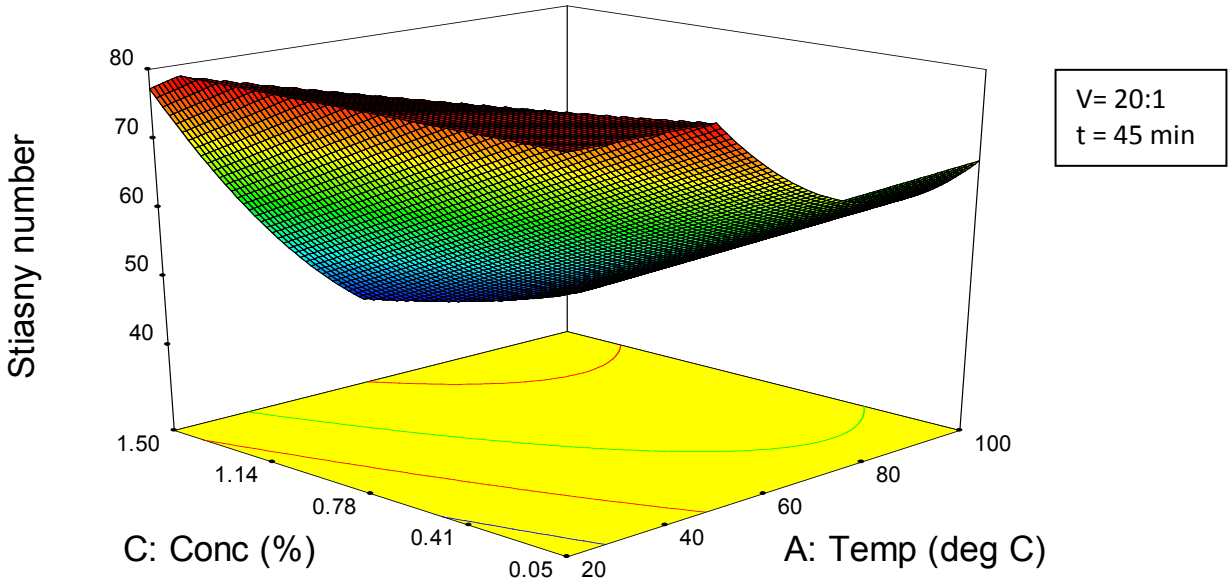


Fig. 4.31a Response surface plots showing percentage Stiasny number from aqueous NaOH extraction at varying extraction temperature and solvent concentration.

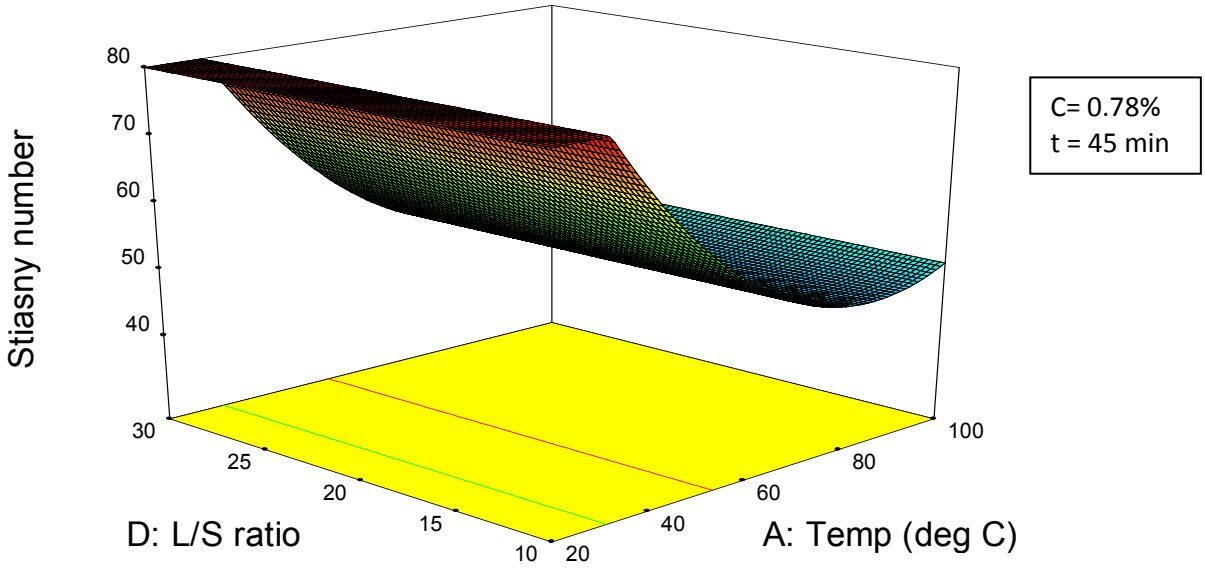


Fig. 4.31b Response surface plots showing percentage Stiasny number from aqueous NaOH extraction at varying extraction temperature and liquid-solid ratio.

Figure 4.32 is a factor plot between the Stiasny number with the extraction design variables in coded values. The plot shows that with an increase in extraction time and liquid-solid ratio, the Stiasny number increases, whilst decreasing temperature increases the Stiasny number. The factor plot shows that each of the design variables have their own individual effect as well as combined effect on the Stiasny number in the design and optimization of Stiasny number from aqueous NaOH extraction.

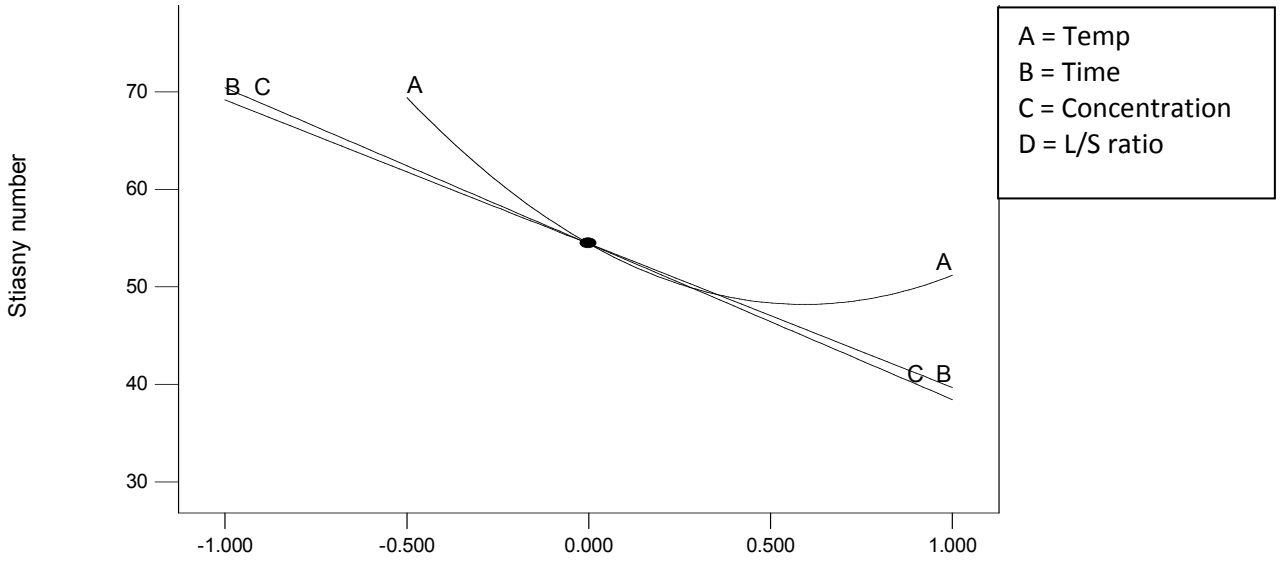


Fig 4.32 Effect of individual variables on the Stiasny number from aqueous NaOH extraction.

Water extraction

Table 4. 14: Comparison of experimental and predicted values using Box-Behnken design for the three independent variables on the Stiasny number from water extraction.

Run no.	Extraction temperature (°C) T	Extraction time (min) t	Liquid-Solid ratio V	Actual value (%)	Predicted value (%) using equation 4.12
1	80.00	90.00	20.00	93.00	92.21
2	90.00	120.00	25.00	90.00	88.98
3	80.00	90.00	10.00	93.00	91.47
4	90.00	60.00	15.00	84.00	87.96
5	90.00	90.00	30.00	88.00	89.59
6	80.00	90.00	20.00	93.00	91.47
7	90.00	60.00	25.00	83.00	84.70
8	60.00	60.00	15.00	87.00	85.73
9	100.00	90.00	20.00	86.00	87.45
10	90.00	120.00	15.00	88.00	88.85
11	80.00	30.00	20.00	95.00	94.10
12	40.00	90.00	20.00	86.00	88.45
13	60.00	120.00	15.00	90.00	85.82
14	80.00	90.00	20.00	93.00	91.47
15	60.00	120.00	25.00	88.00	90.59
16	80.00	150.00	20.00	93.00	91.47
17	80.00	90.00	20.00	88.00	90.07
18	60.00	60.00	25.00	86.00	83.63

The extraction extraction design variables on the Stiasny number in actual and predicted values using water as extraction solvent is given in Table 4.14. The results of the ANOVA and model coefficients are presented in appendix 2. The response surface plots between water extraction time and temperature at constant liquid/solid ratio of 20:1 are shown in Figure 4.33a. The Stiasny number increased at higher extraction time and temperature. However, further increase in temperature decreased the Stiasny number. At an extraction temperature of 50.7°C and 73.6 min extraction time, the Stiasny number was 87.8%, and the maximum Stiasny number of 94.8% occurred at 70°C and 149.7 min.

The effect of extraction temperature and liquid-solid ratio at constant extraction time of 90 minutes on Stiasny number is illustrated in the response surface plot (Figure 4.33b). It showed quadratic effects of the variables on the Stiasny number. At an extraction temperature of 44°C and liquid-solid ratio of 17.8:1, the Stiasny number was found to be 85.1%. The responses observed for the effect of extraction time and liquid-solid ratio at a fixed temperature of 70°C indicated that a general direction of increased extraction time and liquid-solid ratio ensures maximum Stiasny number with time indicating linear effects and liquid-solid ratio indicating quadratic effects (Figure 4.33c).

At an extraction time of 34.2 min and a liquid-solid ratio of 11:1, the Stiasny number was 85%. Using numerical optimization, the maximum predicted Stiasny number of 94.91% was obtained under the optimum extraction conditions of 72.5°C extraction temperature, 150 min extraction time and 20.8:1 liquid to solid ratio. The amount of total sugars and tannin extracted under these conditions were 1.93% and 9.8% respectively (Table 4.18).

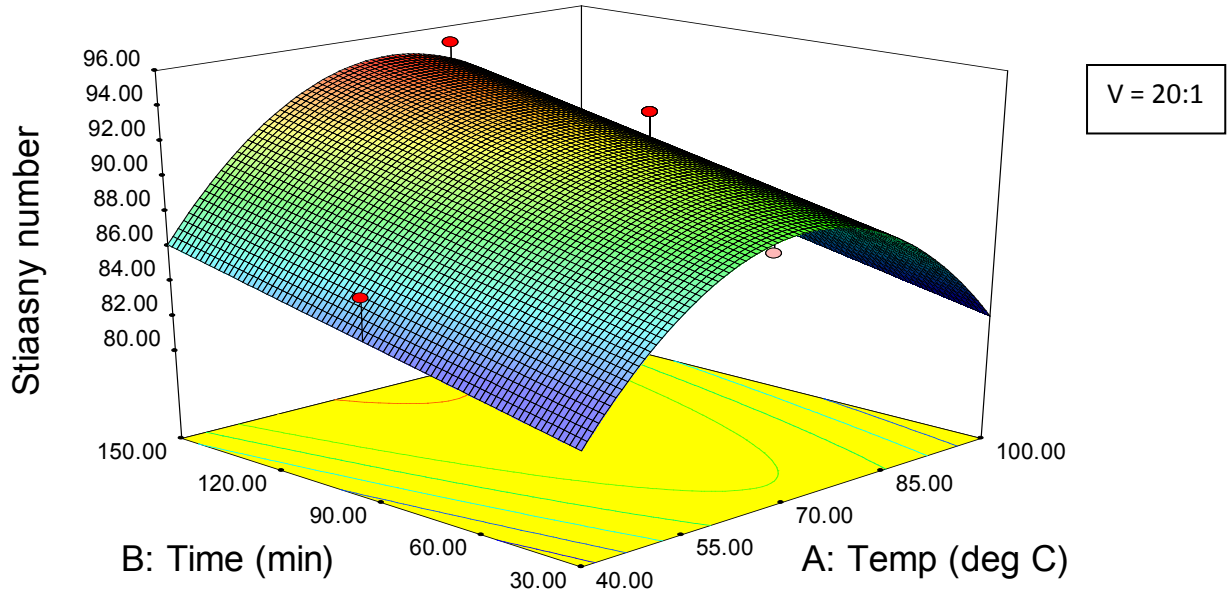


Fig. 4.33a Response surface plots showing percentage Stiasny number from water extraction at varying extraction temperature and time.

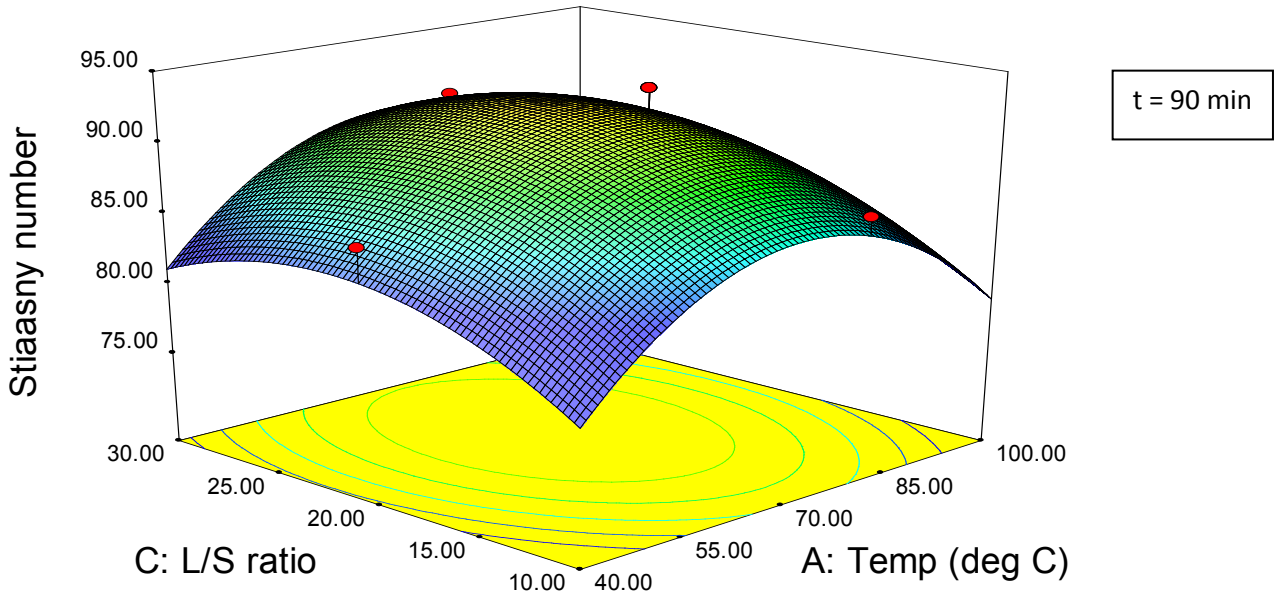


Fig. 4.33b Response surface plots showing percentage Stiasny number from water extraction at varying extraction temperature and liquid-solid ratio.

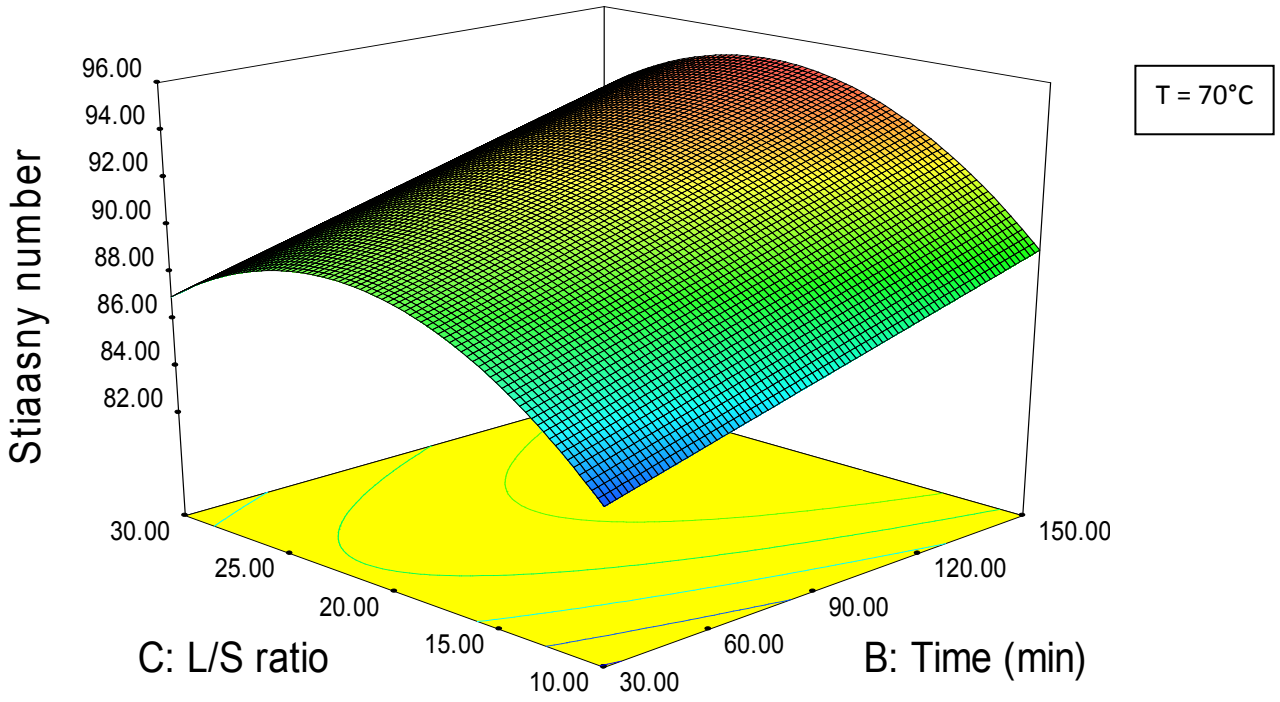


Fig. 4.33c Response surface plots showing percentage Stiasny number from water extraction at varying extraction time and liquid-solid ratio.

Figure 4.34 is a factor plot between the Stiasny number with the extraction design variables in coded values. The plot shows that the Stiasny number increases with extraction time from its low value to high value. However, Stiasny number increases and decreases as the extraction temperature and liquid-solid ratio go from their low values to high values. The factor plot shows that each of the design variables have their own individual effect as well as combined effect on the Stiasny number in the design and optimization of Stiasny number from water extraction.

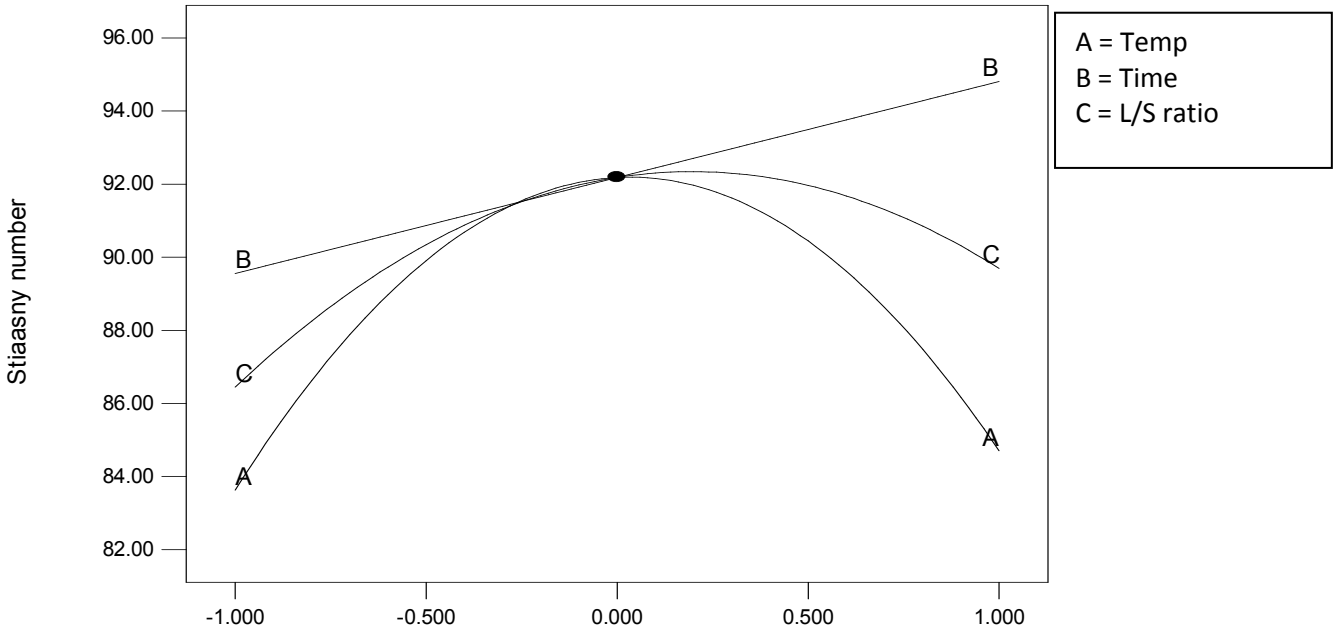


Fig 4.34 Effect of individual variables on the Stiasny number from water extraction.

4.2.2.4 Optimum extraction conditions based on optimizing tannin content, sugar content and Stiasny number simultaneously

For each solvent extraction, the objective function was to maximize the tannin content, minimize the sugar content and maximize the Stiasny number simultaneously. The optimum extraction conditions for each of the solvents as well as the predicted values can be found in Table 4.15 - 4.24. The optimum tannin content, sugar content and Stiasny number were respectively 14.68%, 2.65% and 84.26%, and occurred at extraction conditions of 52.13°C, 150 min, 10:1 liquid-solid ratio using 43.6% aqueous ethanol solvent concentration. In the case of aqueous NaOH extraction, the optimum tannin content, sugar content and Stiasny number were respectively 33.26%, 17.41% and 83.38%. These were obtained at 20.8°C, 56 min, 30:1 liquid-solid ratio and 1.1% solvent concentration. Using aqueous acetone, the optimum tannin content, sugar content and Stiasny number were respectively 10.37%, 0.8% and 87.5%, and occurred at extraction

conditions of 40°C, 30 min, 10:1 liquid-solid ratio and 60% solvent concentration. The optimum tannin content, sugar content and Stiasny number were respectively 9.8%, 1.46% and 93.38%, and occurred at extraction conditions of 59.6°C, 150 min and 18.7:1 liquid-solid ratio when water was used as the extraction solvent.

Generally in this study, the elevated extraction temperature, longer extraction times, increased solvent concentration and liquid-solid ratio that increased the tannin content might be attributed to the fact that these factors perhaps soften the tissues of the bark samples and weaken the phenol-protein and phenol-polysaccharide linkage, resulting in migration of more polyphenols into the extraction solvent. This reason was most likely the explanation to the positive linear effects of the parameters on the increased content of tannin content as also observed by Mane *et al.* (2007) and Wang *et al.* (2008).

Indeed, a higher temperature increases the solubility and diffusion coefficient of polyphenols, allowing higher extraction rate (Cacace and Mazza, 2003). An upper limit must however be respected to avoid degradation of heat-sensitive phenolics. According to Liyana-Pathirana and Shahidi (2005), a high coefficient of variation (CV) demonstrates that variation in the mean value is large and does not sufficiently generate an acceptable response model. Therefore, CV < 10% has been suggested suitable in predicting the response surface models.

Tannin content, sugar content and Stiasny number values obtained in the single factor experiments were somewhat different from the values acquired in the optimization process. This

was due to the interactive effects between the four extraction variables on the crude phenolic extracts as observed also by Yap *et al.* (2009).

In the work of Makino *et al.* (2009), it is noted that the extractability of polyphenolics and sugar components from tree barks is different at various temperature conditions and that water extraction at 80 ˚C from the bark of *A. mangium* and *L. leptolepis* is suitable for extraction of polyphenolics with the minimum possible presence of sugar components. In this study, the minimum sugar content obtainable from pine bark was found for water extraction at 68.3˚C with liquid-solid ratio of 24.9 at 30 min contact time (Table 4.18). However, the content of tannin at these conditions was appreciably low to be of industrial interest.

Total polyphenolics content is known to increase with increased temperatures. The total sugar content of some tree bark studied is in the range of 0.4–2.6%, and the amount was almost the same at 20–80 ˚C aqueous extraction but increased substantially at 100 ˚C (Makino *et al.,* 2009). This confirms the fact that an optimum extraction condition is needed to obtain tannins with minimal sugar presence in order to be used effectively as tannin-formaldehyde resin.

The optimum conditions used for the extraction of polyphenols from *Pinus pinaster* bark by Vazquez et al. (1986, 1987) is 15 min, 1% (w/w) NaOH solution at 95 ˚C with a solid/liquid ratio of 1:10. These conditions allow the extraction of 90% of polyphenols and only 5% of carbohydrates. Using aqueous NaOH at the optimal conditions of 60˚C, 60 min, 1% concentration and 25 liquid-solid ratio in this study, a tannin content of 25% was obtained. Obviously, the 90% polyphenols obtained by Vazquez *et al.* (1986, 1987) does not refer to

tannins since no tree bark has ever been found to contain even close to 50% tannins. Since tannins are the specific phenolics suitable for resin formulation, it presupposes that quite a sizeable amount of the 90% polyphenols reported by Vazquez *et al.* (1986, 1987) might be unimportant for resin formulation. The Stiasny number of 73% obtained for NaOH extraction in this study was close to 75% obtained by Vazquez *et al*. (1989) but rather different from the 50-60% quoted for pine bark by Pizzi (1983). The improvement might be due to the extraction conditions adopted which might have either enhanced the tannin content or reduced the extraction of impurities or both.

4.2.2.5 Verification of optimal extraction conditions

In this study, tannins were extracted based on the optimized extraction conditions for the formulation of tannin-formaldehyde resin in plywood application. The tannin content, sugar content and Stiasny number were determined for each extract and compared with the predicted values to confirm the validity of the models. The values determined agreed with the predicted values (Table 4.15 – 4.24) in the 95% confidence interval. This demonstrated that the response models were adequate to reflect the expected optimization processes.

4.2.2.6 Efficiencies of the models

The extraction efficiency of each model was indicated by comparing the tannin content, sugar content and Stiasny number of the extracted tannin to the quantified values from extracts obtained by employing pressurized accelerated solvent extraction. The accelerated solvent extraction is an effective method of extracting phenolics because of the short contact time and low temperatures employed, ensuring minimal degradation of the phenolic compounds, with the

high pressure enhancing removal of phenolics into solution. By this rapid procedure, it was possible to extract average 28.8% tannins with 96% Stiasny number and 1.5% sugar content from pine bark. The efficiencies of the optimization processes are presented in Table 4.25. It can clearly be observed that the very high model efficiency of aqueous NaOH extraction in terms of tannin content was offset by the poor model efficiency in terms of sugar content, which then gave low average model efficiencies. Though higher alkali concentrations give higher polyphenols content, they also increase the impurity content and lower stability, thus making the total extract less suitable for adhesive manufacture (Vazquez *et al*., 1989).

The presence of sugar derived from the hydrolysis of the polysaccharides lowered the potential formaldehyde condensable polyphenols content and would thus reduce the strength and water resistance of adhesives formulated with the tannin extracts (Pizzi and Mittal, 1994). The highest model efficiency of 78.98% (Table 4.25) was observed for water extraction when tannin content was maximized in the numerical optimization process. This corresponded to optimum extraction conditions of 69°C extraction temperature, 126 min extraction time and 23:1 liquid-solid ratio (Table 4.18).

Table 4. 15: Optimized conditions for Aqueous Acetone extraction with both predicted and actual values.

Optimized response	Temp (°C)	Time (min)	Conc. (%)	L/S ratio	Tannin (%)		Sugar (%)		Stiasny No.	
					Predicted	Actual	Predicted	Actual	Predicted	Actual
Tannin	58	78.5	60	29.8	17.57	14.62	4.40	4.25	76.96	90.20
Sugar	40.4	64.7	60	15.8	9.43	6.35	1.69	1.82	79.22	79.85
Stiasny No.	45	125	60	28.7	9.26	12.84	3.25	3.98	88.92	90.88
Tan, Sug, Sti	40	30	60	10	10.37	11.48	0.86	2.98	87.5	87.6

Table 4. 16: Optimized conditions for Aqueous Ethanol extraction with both predicted and actual values.

Optimized response	Temp (°C)	Time (min)	Conc. (%)	L/S ratio	Tannin (%)		Sugar (%)		Stiasny No.	
					Predicted	Actual	Predicted	Actual	Predicted	Actual
Tannin	71.46	79.2	21.9	26.4	20.68	17.95	4.94	5.20	80.47	88.25
Sugar	47.4	92.9	47.6	10.9	7.01	7.62	1.86	1.93	75.20	74.34
Stiasny No.	40.77	134	62.8	23.6	16.65	17.78	4.29	4.52	91.17	88.25
Tan, Sug, Sti	52.13	150	43.6	10	14.68	18.85	2.65	3.24	84.26	92.25

Table 4. 17: Optimized conditions for Aqueous NaOH extraction with both predicted and actual values.

Optimized response	Temp (°C)	Time (min)	Conc. (%)	L/S ratio	Tannin (%)		Sugar (%)		Stiasny No.	
					Predicted	Actual	Predicted	Actual	Predicted	Actual
Tannin	96.4	37.7	1.48	15.2	34.51	27.35	40.61	50.24	45.17	50.65
Sugar	31.6	40.8	0.97	18	19.93	25.23	20.41	30.52	79.88	78.28
Stiasny No.	46.9	36	0.06	22.5	22.89	19.82	22	28.45	80	74.95
Tan, Sug, Sti	20.8	56	1.1	30	33.26	26.50	17.41	26.32	83.38	76.65

Table 4. 18: Optimized conditions for Water extraction with both predicted and actual values

Optimized response	Temp (°C)	Time (min)	L/S ratio	Tannin (%)		Sugar (%)		Stiasny No.	
				Predicted	Actual	Predicted	Actual	Predicted	Actual
Tannin	69	126	23	9.8	11.25	1.76	1.52	93.82	95.23
Sugar	67.8	61.4	28.7	8.84	9.68	1.29	1.88	89.15	86.75
Stiasny No.	72.5	150	20.8	9.8	9.74	1.93	3.00	94.91	88.28
Tan, Sug, Sti	59.6	150	18.7	9.8	10.39	1.46	1.86	93.38	94.05

Table 4. 19: Optimization model efficiencies (Effi) of solvent extraction process

Solvent extraction	Optimized response	Tannin content		Sugar content		Stiasny number		Average efficiency (%)
		%	Model Effi (%)	%	Model Effi (%)	%	Model Effi (%)	
Aqueous acetone	Tannin	14.62	50.76	4.25	35.29	90.20	93.96	60.01
	Sugar	6.35	22.05	1.82	82.42	79.85	83.18	62.55
	Stiasny No.	12.84	44.58	3.98	37.69	90.88	94.67	58.98
	Tan, Sug, Sti	11.48	39.86	2.98	50.34	87.65	91.30	60.50
Aqueous ethanol	Tannin	17.95	62.33	5.2	28.85	88.25	91.93	61.03
	Sugar	7.62	26.46	1.93	77.72	80.74	84.10	62.76
	Stiasny No.	17.78	61.74	4.52	33.19	88.25	91.93	62.28
	Tan, Sug, Sti	18.85	65.45	3.24	46.30	92.25	96.09	69.28
Aqueous NaOH	Tannin	27.35	94.97	50.24	2.99	50.65	52.76	50.24
	Sugar	25.23	87.60	30.52	4.91	78.28	81.54	58.02
	Stiasny No.	19.82	68.82	28.45	5.27	74.95	78.07	50.72
	Tan, Sug, Sti	26.5	92.01	26.32	5.70	76.65	79.84	59.19
Water	Tannin	11.25	39.06	1.52	98.68	95.23	99.20	78.98
	Sugar	9.68	33.61	1.88	79.79	86.75	90.36	67.92
	Stiasny No.	9.74	33.82	3	50.00	88.28	91.96	58.59
	Tan, Sug, Sti	10.39	36.08	1.86	80.65	94.05	97.97	71.56

Tan: Tannin Sug: Sugar Sti: Stiasny number

4.3 Effect of phenolic extraction condition on resin quality

The viscosities and pot lives of the resins formulated from tannins obtained under different optimization processes are presented in Figure 4.35. The processing of thermosetting resins requires understanding of their rheological behavior. Rheological properties such as viscosity can be directly correlated to the evolving physical and mechanical properties during resin cure (Hu *et al*., 2001). The optimization processes adopted in this study indicated variable effects on the quality of the resins produced.

Considering extraction with water, the viscosities of all the tannin resins were not significantly different, but different from the control. However, the pot life of R4 (54 min) was significantly different from R1 and R2 (Fig. 4.35). The dry shear strength of R4 (1.9 MPa) was not significantly different from that of R2 (2.1 MPa), but significantly different from that of R1 (2.3 MPa) which was the only resin not significantly different from that of the control (2.52 MPa) (Fig. 4.36).

In the case of aqueous acetone extractions, there was no significant difference in viscosities, dry shear strengths, wet shear strengths and plywood delamination of the tannin-formaldehyde resins. The pot life of R4 (55 min) was however significantly different from R2 (42 min) and R3 (Fig.35).

In the case of aqueous ethanol extraction, the viscosity of R1 was different from that of all the other resins with the pot life of R2 (40 min) being significantly different from that of R4 (54 min). The dry shear strength of R4 (2.26 MPa) was significantly different from R1, (1.8 MPa),

R2 (1.83 MPa) and R3 (1.88 MPa) but similar to that of the control (2.52 MPa) (Fig. 4.30). The wet shear strength of R1 was significantly different from R4 and the control but similar to the others (Fig. 4.37). The percentage of plywood samples that passed the delamination test was similar for R1, R3 and R4 with only R4 not significantly different from the control (Fig. 38).

Considering aqueous NaOH, the viscosity of R1(2949 cP) was significantly different from all the resins, whilst R2 (2154 cP) and R3 (2056 cP) were not different. Similarly, R4 (1955 cP) and R3 (Fig. 4.35) were not significantly different. The dry shear strength of R1(1.87 MPa) was not significantly different from all the other resins except the control (2.52 MPa) (Fig. 4.36). However, the wet shear strength of R1(0.31 MPa) was significantly different from all the other resins (Fig. 4.37).

From the analysis of variance, the optimization method used to extract the tannins for the tannin-formaldehyde resin (all solvents considered together), did not significantly affect the viscosity of the resins. Similarly, the dry shear strength was also not significantly affected by the optimization method used. However, the wet shear strengths and plywood delaminations were significantly affected by the optimization method used for the extraction. For the wet shear strength, R1 (0.92 MPa) was significantly different from R2 (1.24 MPa) and R4 (1.19 MPa) whilst for the delamination test, R1 was significantly different from R3. All Anova tables are presented in appendix 3.

Pearson's correlation revealed that the mode of optimization used in the extraction of the phenolics from pine bark was significantly related to the viscosity, pot life, dry shear strength,

wet shear strength and plywood delamination of the resin, with correlation coefficients of -0.421, 0.860, 0.496, 0.477 and 0.401 respectively, at the 0.001 level of significance.

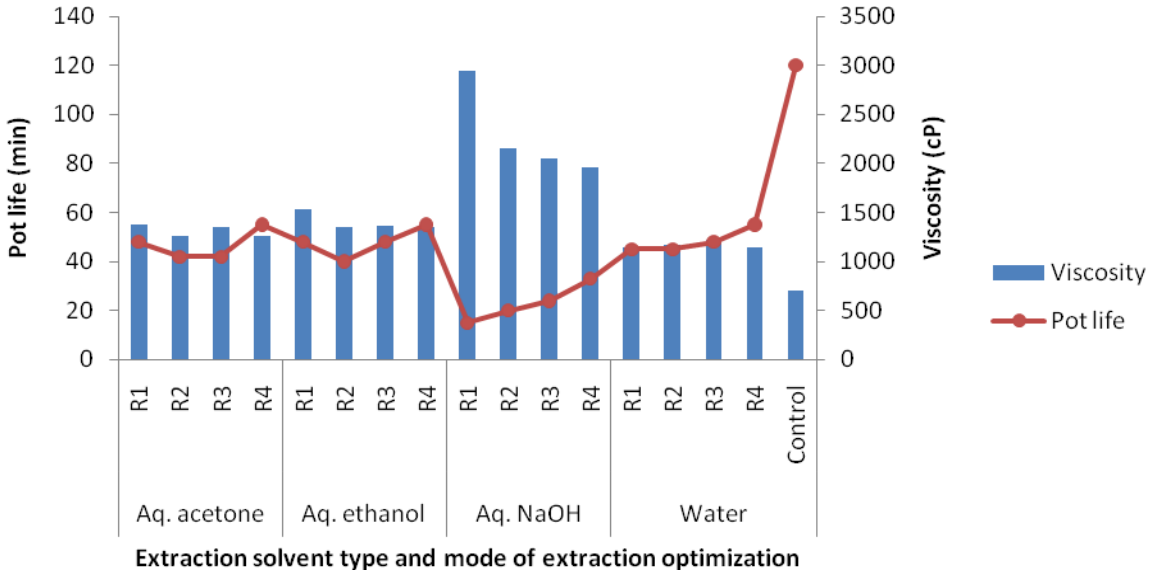
Due to the phenolic groups in tannin, tannin-formaldehyde resin tends to perform like a phenol–formaldehyde resin (Pizzi, 1994; Pizzi, 1983). According to several studies, pine tannin reacts very fast with formaldehyde and has a short pot life (Pizzi, 1994). High viscosity and short pot life are drawbacks of most tannin-formaldehyde resins and tannin-formaldehyde resins fortified with UF and PF resins (Santana et al, 1995). In this study, R4 from each of the solvents considered gave the lowest viscosity and highest pot life (Fig 4.35). Thus, optimizing tannin extraction conditions based on simultaneously minimizing sugar content, maximizing tannin content and maximizing Stiasny number contented good extracts in terms of viscosity and pot life. Considering all the resins, R1 of aqueous NaOH gave the highest viscosity (2949 cP) and the shortest pot life of 15 min (Fig. 4.35). Tannin-based resins harden very fast and tannins extracted by using alkali are found to produce highly viscous resins. Highly viscous resins are difficult to apply, whilst low viscosity resins penetrate the wood causing starved glue joints leading to poor bonding.

Condensation of tannins with small amounts of urea-formaldehyde resins can prevent the water deterioration normally experienced by the latter resins. Conversely, urea-formaldehyde resins improve crosslinking and strength of wood tannin-formaldehyde networks (Pizzi, 1978). In this study, urea-formaldehyde was used in the tannin-formaldehyde resins formulation. Urea-formaldehyde is not water resistant and this could explain the low water resistance of the tannin resins compared with the industrial phenol-formaldehyde control. The viscosities of the tannin

resins and shear strengths of plywood reported in this study are comparable to the work done by Santana et al. (1995) and Sellers and Miller (2004).

Because of its high reactivity and slow solubility, the processing of pine tannin for commercialization has been a slow process. Pine tannins are considerably more reactive toward hardeners than *Acacia mearnsii* (mimosa) because of their more reactive phloroglucinolic A-ring in their monomeric flavonoid structure. Pine tannins have a much higher average degree of polymerization than mimosa tannins. The adhesive property of a tannin compound has been found to be dependent on the reactive tannin groups present. The higher the number of reactive tannin groups, the greater the crosslinking capacity and therefore the greater the strength of the cured glue line (Panamgama, 2006).

The quality properties of the resins produced from the tannins obtained under optimized conditions were generally in close agreement with the optimized models. For instance, the highest model efficiency attributed to aqueous extraction under numerical optimization of tannin can be verified by the relatively high shear strengths of plywood bonded with this tannin-formaldehyde resin (Figs. 4.36 and 4.37).



R1, R2, R3 and R4 are resins prepared by using extracted tannins based on maximizing tannin content, minimizing sugar content, maximizing Stiasny number and simultaneously optimizing tannin content, sugar content and Stiasny number respectively.

Figure 4. 35: Pot life against viscosity of resins.

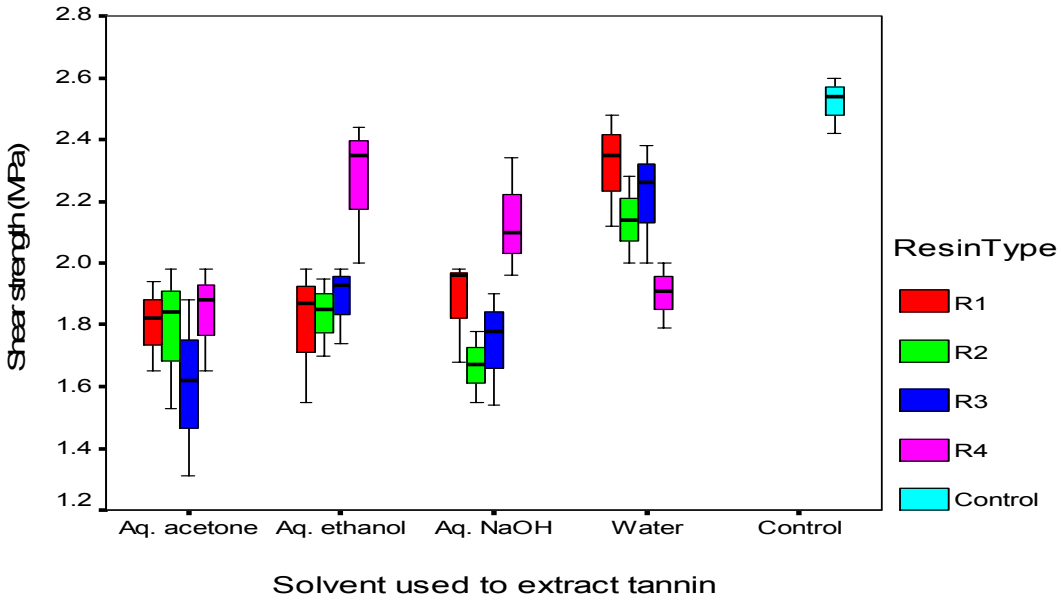


Figure 4. 36: Effect of extraction solvent type and mode of extraction optimization on dry shear strength of plywood bond.

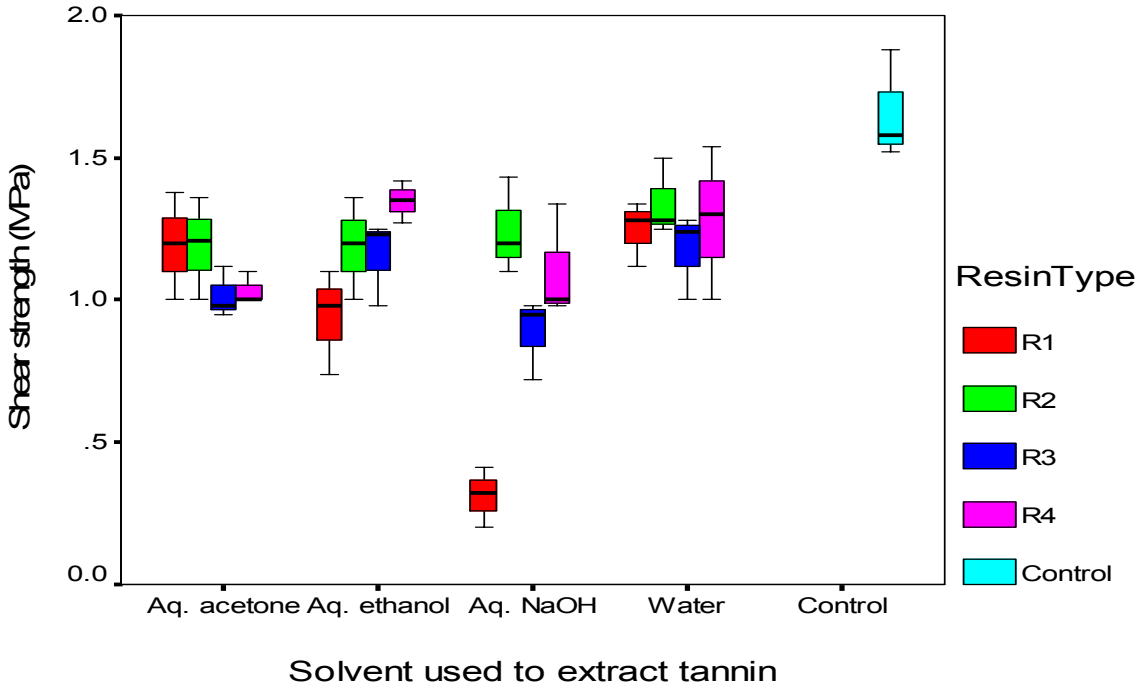


Figure 4. 37: Effect of extraction solvent type and mode of extraction optimization on wet shear strength of plywood bond.

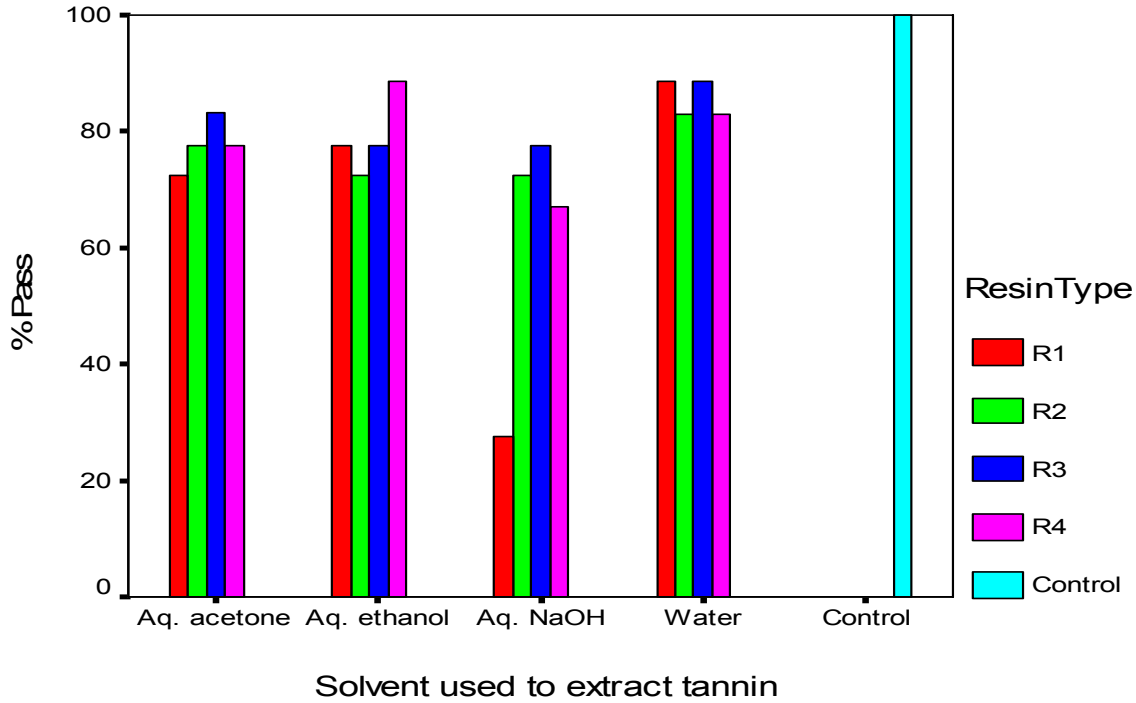


Figure 4. 38: Effect of extraction solvent type and mode of extraction optimization on three-cycle soak/dry tests for plywood bond delamination

CHAPTER FIVE

CONCLUSIONS AND RECOMMENDATIONS

5.1 Conclusions

The potential of near infrared reflectance spectroscopy (NIRS) for rapidly and accurately determining the polyphenolic content in *Pinus caribaea* bark was assessed by means of multivariate calibration techniques. The Box-Behnken design of experiments was found to adequately represent the extraction of the polyphenols from the pine bark using aqueous acetone, aqueous ethanol, aqueous NaOH and water as the extracting solvents. A true functional relationship between the response namely, tannin content, Stiasny number and sugar content along with the extraction design variables namely, temperature, time, solvent concentration and liquid-solid ratio have been studied in an attempt to optimize the tannin content that will be suitable for tannin-formaldehyde resins.

In the near infrared spectroscopy calibration of the quantities of phenolic compounds available in pine bark, the first derivative spectra with PLS regression were found to provide the best predictions for the polyphenol and tannin contents as well as Stiasny number of *Pinus caribaea* bark with a standard error of cross validation (SECV) of 0.23, 0.14 and 1.26 respectively, and coefficient of determination (r^2) of 0.96, 0.97 and 0.95 respectively. The polyphenol content of *P. caribaea* bark varied from 16% to 23.5% with a mean and standard deviation of 19.69% and 1.18% respectively. Similarly, the tannin content and Stiasny number varied from 9.2 – 15.4%

and 64.36 – 86.12% with means of 11.82% and 74.97% respectively. The non-destructive FT-NIR predicted values were highly correlated with destructively measured values of polyphenol content, tannin content and Stiasny number.

In the optimization of extraction process to get the phenolic compounds (suitable for tannin-formaldehyde adhesives) out of the pine bark, twelve different approximating functions were obtained. The model with the highest predictive ability (r^2 = 0.9) was found for the approximating function estimating minimum sugar content using water as extraction solvent. The model with the least predictive ability (r^2 = 0.3) was found for aqueous acetone extraction with the objective function of maximizing the Stiasny number. The highest model efficiency (78.98%) was observed for aqueous extraction when only tannin content was maximized in the numerical optimization process. This corresponded to optimum extraction conditions of 69°C extraction temperature, 126 min extraction time and 23:1 liquid-solid ratio. The RSM model that gave a high tannin content (18.85%) with a corresponding good quality resin (shear strength = 2.4 MPa, 10% delamination) was found for aqueous ethanol extraction when the objective function was to maximize both the tannin content and Stiasny number and minimize the sugar content simultaneously. This corresponded to optimum extraction conditions of 51.4°C extraction temperature, 150 min extraction time, 48.6% solvent concentration and 10:1 liquid-solid ratio.

5.2 Recommendations

Interesting follow-up on this research work for further studies would consist of the following recommendations:

1. In the current study, equal weights were given to the tannin content response, sugar content response and Stiasny number response during the simultaneous optimization of these response factors. Further studies could be undertaken to ascertain the appropriate weights for each response factor when optimizing the factors simultaneously.

2. The effect of plywood production process variables (press time, temperature and pressure) on plywood bond strength could be investigated using adhesives prepared from the extracted tannins.

3. Industrial production of tannin-based adhesives is non-existent in Ghana. Therefore, studies concerning pilot plant extraction of tannins which could then be upgraded to use in feasibility study for a small-scale tannin extraction plant in Ghana could be carried out. The results will then have a solid technological foundation from the current study.

REFERENCES

Aguilera, J. M. and Stanley, D. W. (1999). Microstructural Principles of Food Processing and Engineering. Aspen Publishers, Gaithersburg, MD.

Antti, H. (1999). Multivariate Characterization of Wood Related Materials. Department of Chemistry, Umea University, Dissertation. pp. 86

Association of Official Analytical Chemists, 1995. Official Methods of Analysis of AOAC International. 16th ed. P. A. Cunniff, ed. Association of Analytical Chemists International, Washington, DC.

ASTM, Annual Book of ASTM Standards, D 1084 – 88, vol 15.06, American Society for Testing and materials, Philadephia, Pennsylvania, 1991.

ASTM, Annual Book of ASTM Standards, D 4426 – 84 vol 15.06, American Society for Testing and materials, Philadephia, Pennsylvania, 1991.

Austin, A. G. (1994). Shreve's Chemical Process Industries, 5th ed. McGraw Hill, New York.

Bas, D. and Boyac, I. H. (2007). Modeling and optimization I: usability of response surface methodology, *J. Food Eng*. **78**: 836-845.

Bate-Smith, E. C. and Swain, T. (1962). Flavanoid compounds. Comparative Biochemistry vol 3A (Mason and Florkin eds). Academic Press.

Beebe, K.R. and Kowalski, B. (1987). An introduction to multivariate calibration and analysis. *Anal. Chem*. **59**: 1007 – 1017.

Box, G. E. P. and Behnken, D. W. (1960). Three level design for the study of quantitative variables. *Tecnometrics*. **2:** 455 – 475.

Box, G. E. P., Hunter, W.G. and Hunter. J.S. (1978). Statistics for Experimenters: An Introduction to Design, Data Analysis and Model Building. John Wiley &Sons Inc.

Cacace, J. E. and Mazza, G. (2003). Mass transfer process during extraction of phenolic compounds from milled berries, J. *Food Eng*. **59**: 379-389.

Caesar P. D. and Sachanen, A.N.(1948). Thiophene-formaldehyde Condensation, *Ind. Eng. Chem.*, **40**, 922.

Chang, C.W. and Laird, D.A., (2002). Near-infrared reflectance spectroscopic analysis of soil C and N. *Soil Science* **167**: 110-116.

Chang, C.W., Laird, D.A., Mausbach, M.J. and Hurburgh, C.R.. (2001). Nearinfrared reflectance spectroscopy-principal components regression analyses of soil properties. *Soil Science Society of America Journal* **65**: 480-490

Christiansen, A. W. and Gillespie, R.H. (1986). Potential of carbohydrates for exterior type adhesives. *For. Prod. J.*. **36** (7/8): 20-28

Conner, A. H., River B.H. and Lorenz. L.F. (1986). Carbohydrate modifiedphenol-formaldehyde resins. *J. Wood Chem. Tech*. **6** (4): 591-613.

Couˆteaux, M.M., Rovira, P. and Berg, B. (2003). Near infrared reflectance spectroscopy for determination of organic matter fractions including microbial biomass in coniferous forest soils. *Soil Biology and Biochemistry* **35**: 1587-1600.

Crammond, P. C. and Wilcox, M. E. (1992). Tannin adhesives from pine bark. Proc. Wash. St. Uni. Int. Particleboard/Comp. Materials Symp **26**: 172-188.

Cussler E.L. (1997). Diffusion, mass transfer in fluid systems. In: Cambridge University Press New York, NY:Cambridge University Press

Dalton, L. K. (1950). Tannin-formaldehyde resins as adhesives for wood. *Aust. J. Appl. Sci*. **1**: 54-70.

Dalton, L. K. (1953). Resins from sulphited tannins as adhesives for wood. *Aust. J. Appl. Sci.* **4**: 136-145.

Dionex Technical Note 208, (1998). Methods Optimization in Accelerated Solvent Extraction. Dionex Corporation, Sunnyvale, CA, USA.

Donkin, M.J. and Pearce, J. (1995). Tannin analysis by near infrared spectroscopy. *J. Soc. Leather Technol. Chem.* **79**: 8 - 11.

Drlje, R. M. (1975). El extracto de quebracho como material para adhesivo de paneles baseados en Madera. FAO World Consultation on Wood Based Panels, New Delhi, India. Feb. p 6.

Dubois M, Giles KA, Hamilton JK, Rebers PA, Smith F (1956) Colorimetric method for determination of sugar and related substances. Anal Chem 28:350–356

Easty, D. B., Berben, S. A., DeThomas, F.A. and Brimmer, P. J. (1990). Near-infrared spectroscopy for the analysis of wood pulp: quantifying hardwood-softwood mixtures and estimating lignin content. *Tappi Journal* **73** (4): 257-261

Escribano-Bailon, M. T. C. and Santos-Buelga, C. (2003). Polyphenol extraction from foods, in: C. Santos-Buelga, G.Williamson (Eds.), Methods in Polyphenol Analysis, pp. 1-16.

Freeman J. H. and Lewis, C.W. (1954). Alkaline-Catalyzed Reaction of Formaldehyde and the Methylols of Phenol*, J. Am. Chem. Soc*., **76**: 2080.

Geankopolis, C. J. (1993). Transport Processes and Unit Operations. 4th Edition, Prentice International.

Gekkas, V. (1992). Transport Phenomena of Foods and Biological Materials. CRC Press, Boca Raton, FL.

Geladi, P. (2003). Chemometrics in spectroscopy. Part 1. Classical chemometrics. Spectrochimica *Acta* Part B **58**: 767-782

Geladi, P. and Kowalski, B.R. (1986). Partial least squares regression: A tutorial. *Anal. Chim. Acta.* **185**: 1 - 17.

Gierlinger, N., Schwanninger, M., Hinterstoisser, B. and Wimmer, R. (2002). Rapid determination of heartwood extractives in Larix sp. By means of Fourier transform near infrared spectroscopy. J. Near Infrared Spectrosc. 10: 203 - 214.

Godwin, T. W. and Mercier, E. I. (1983). Introduction to Plant Biochemistry, 2nd ed., Pergamon Press, Oxford, UK.

Hagerman, A. E., (1988). Extractions of tannin from fresh and preserved leaves. *Journal of Chemical Ecology* **14**: 453-461.

Hall, J.W. and Pollard, A. (1992). Near infrared spectrophotometry: A new dimension in clinical chemistry. *Clin. Chem*. **38**:1623-1631.

Haaland, D.M. and Thomas, E.V. (1998). Partial least squares methods for spectral analyses. 1. Relation to other quantitative calibration methods and extraction of qualitative information. *Anal. Chem*. **60:** 1193 – 1208.

Haslam, E. (1998). Practical polyphenolics: from structure to molecular recognition and physiological function. Cambridge University Press. Cambridge, U.K.

Hathway, D. E. (1958). *Biochem. J* **70**:34

Hemingway, R. W. (1981). Bark: its chemistry and prospects for chemical utilization. In I.S. Goldstein, (ed.) Organic Chemicals From Biom888, CRC Pre88 Boca Raton, Fla., pp. 190-248.

Hillis, W.E. and Urbach, G. (1959). Reaction of phenols with formaldehyde. J. Appl. Chem. 9: 665-673.

Hu, X., Fan, J. and Yue, C. Y. (2001). Rheological study of crosslinking and gelation in bismaleimide/cyanate ester interpenetrating polymer network. *J. Appl. Polym. Sci*. **80**: 2437-2445.

Irvine, F. R. (1961). Woody Plants of Ghana. Oxford Univ. Press, London.

Jingge, L. and Maplesden, F. (1998). Commercial production of tannins from radiata pine bark for wood adhesives. *IPENZ Transactions*, **25**: 1

Kim, M.G., Tiedeman, G.T. and Amos, L.A. (1980). Weyerhaeuser Science Symposium. 2: 263-289

Kim, M.G., Wu, Y., and L. Amos, W. (1997). Journal of Polymer Science. Part A: Polymer Chemistry. 35: 3275-3285

Knop A. and Pilato, L. A. (1985). Phenolic resins, chemistry applications and performance. Springer-Verlag, New York.

Knop, A. and Pilato, L.A. (1993). Phenolic resins, chemistry applications and performance, Springer-Verlag, New York, Taylor and Krishna, Multicomponent Mass Transfer, Wiley, New York,

Knop, A. and Scheib W. (1979). Chemistry and application of phenolic resins. Springer, New York

Kraus, T. E. C., Dahlgren, R. A.and Zasoski, R. J. (2003). Tannins in nutrient dynamics of forest ecosystems - a review. *Plant and Soil* **256**: 41-66.

Liyana-Pathirana, C. and Shahidi, F. (2005). Optimization of extraction of phenolic compounds from wheat using response surface methodology, *Food Chem*. **93**: 47-56.

Lu X. and Pizzi, A. (1998). Curing conditions effects on the characteristics of thermosetting adhesives-bonded wood joints, Holz-als Roh-Werkstoff, 56: 393.

Maciel G. E., Chuang, I. S. A and Gollob, L. (1984). Solid-State Carbon-13 NMR Study of Resol-Type Phenol-Formaldehyde Resins, *Macromolecules*, **17**: (5) 1081- 1087.

Mafart, P. and B´eliard, E. (1992). G´enie Industriel Alimentaire, Tome II: Techniques S´eparatives.

Mahalanobis, P.C., 1936. On the generalized distance in statistics. Proceedings of the National Institute of Science India **2:** 49–55.

Makino, R., Ohara, S. and Hashida, K. (2009). Efficient extraction of polyphenolics from the bark of tropical tree species. *Journal of Tropical Forest Science* **21**(1): 45-49

Mane, C., Souquet, J. M., Olle, D., Verries, C., Veran, F., Mazerolles, G., Cheynier, V. and Fulcrand, H. (2007). Optimization of simultaneous flavanol, phenolic acid, and anthocyanin extraction from grapes using an experimental design: Application to the characterization of champagne grape varieties. *Journal of Agricultural and Food Chemistry* **55**: 7224-7233.

Mark, H. 1989. Chemometrics in near-infrared spectroscopy. *Anal. Chim. Acta*. **223**: 75 – 93.

Marra J., Pinelo, M., Sineiro, J. and Nu´n˜ez, M. J. (2006). Influence of extraction conditions on phenolic contents from pine bark: assessment of procyanidins polymerization degree by thiolysis. *Food Chemistry* **94**: 406-414

Marra G. G. 1984. The role of adhesion and adhesives in the wood industry. In: Gillespie R. H. (ed) Adhesives for Wood. Noyes, Park Ridge, NJ, pp. 2-9

Marra, A. A. (1992). Technology of Wood Bonding: Principles in Practice. New York: Van Nostrand Reinhold

Mathison, G.W., Hsu, H., Soofi-Siawash, R., Recinos-Diaz, G., Okine, E.K., Helm, J. and Juskiw, P., (1999). Prediction of composition and ruminal degradability characteristics of barley straw by near infrared reflectance spectroscopy. *Canadian Journal of Animal Science* **79**: 519-523.

McCabe, W. Smith, J. and Harriott, P. (1993). Unit Operations of Chemical Engineering, 5th ed., McGraw-Hill, New York.

Michell, A. J. (1995) Pulpwood quality estimation by near-infrared spectroscopic measurements on eucalypt wood. *Appita* 48: 425-428

Michell, A.J. and Schimleck, L.R. (1996). NIR spectroscopy of woods from Eucalyptus globulus. *Appita* J. 49: 23 - 26.

Miller, C.E. (1989). Analysis of synthetic polymers by near-infrared spectroscopy. Ph.D. thesis, University of Washington, Seattle, Wash.

Montgomery, D. C. (2005). Design and analysis of Experiments: Response surface method and designs. New Jersey. John Wiley and Sons Inc.

Nimz, H. (1983). Lignin-based wood adhesives. Wood Adhesives: Chemistry and Technology, In: Wood Adhesives. Chemistry and Technology, Vol. 1. Ed. A. Pizzi. Chapter 5. Marcel Dekker Inc. New York. pp. 248-288.

Norris, K.H., 1989. Definition of NIRS analysis. In: Near Infrared Reflectance Spectroscopy (NIRS): Analysis of Forage Quality. Agriculture Handbook. USDA, Washington, DC.

Norris, K.H., Barnes, R.F., Moore, J.E. and Shenk, J.S., 1976. Predicting forage quality by infrared reflectance spectroscopy. *Journal of Animal Science* **43**: 889-897.

Oehlert, G. W. (2000). Design and analysis of experiments: Response surface design. New York: W.H. Freeman and Company

Ohunyon, P. E. (1992). Fortified mangrove tannin-based plywood adhesive. PhD. thesis. Faculty of Science, Ahmadu Bello University, Zaria.

Ohunyon, P. E. and Ebewele R. O. (1992). Differential scanning calorimetry of hydrolysed mangrove tannin. *Adhesives age* **35** (3): 35- 40

Ono, H. K. and Inoue A. (1994). Phenolated bark as plywood adhesives. In: Adhesives and Bonded Wood Products. Eds. C.Y.Hse., B. Tomita, S.J. Branham, Forest Products Society Proceedings No. 4735: 330-343.

Orwa C., Mutua, A., Kindt, R., Jamnadass R. and Anthony, S. (2009). Agroforestree Database:a tree reference and selection guide version 4.0 (http://www.worldagroforestry.org/sites/treedbs/treedatabases.asp)

Osborne, B.G., Fearn, T. and Hindle, P.H., (1993). Practical NIR Spectroscopy with Applications in Food and Beverage Analysis. Longman Scientist and Technical, Harlow, UK. 277.

Panamgama, L. A. (2007). Polyphenolic extracts of *Pinus radiata* bark and networking mechanisms of additive-accelerated polycondensates. *Journal of Applied Polymer Science*, Vol. 103, 2487-2493.

Pease, D. A. in J. A. Sowle, ed., (1994). Panels: Products, Applications and Production Trends. *A Special Report from Wood Technology*, Miller Freeman Publications, Inc., San Francisco, pp. 272.

Perry's Chemical Engineers' Handbook, Seventh Edition, 1999.

Pinelo, M., Rubilar, M., Jerez, M., Sineiro, J. and Nunez, M.J. (2005). Effect of solvent, temperature, and solvent-to-solid ratio on the total phenolic content and antiradical activity of extracts from different components of grape pomace, *J. Agric. Food Chem*. **53**: 2111-2117.

Pizzi A., (1994). Handbook of Adhesive Technology, Marcel Dekker Ed., New York.

Pizzi A., Lu X. and Garcia, R. (1999). Lignocellulosic substrates influence on TTT and CHT curing diagrams of polycondensation Resins *J. Appl. Polym.* Sci, **71**: 915.

Pizzi A., Mtsweni, B. and Parsons, W. (1994). Wood-induced catalytic activation of PF adhesives autopolymerization vs. PF/ wood covalent bonding, J. Appl. Polym. Sci., 52, 1847.

Pizzi, A. (1978). The chemistry and development of tannin/urea-formaldehyde condensates for exterior wood adhesives. *Journal of Applied Polymer Science* **23** (9): 2777 - 2792.

Pizzi, A. and Stephanou, A. (1992). A comparative C^{13} NMR study of polyflavonoid tannin extracts for phenolic polycondensates. *Holzforsch Holzverwert* no. **4**

Pizzi, A. (1983). Tannin-based wood adhesives. Chapter 4 in: Wood adhesives chemistry and technology, Pizzi, A. (Ed.): New York: Marcel Dekker Inc.

Pizzi, A. (1994). Advanced Wood Adhesives Technology, Marcel Dekker, Inc., New York, p89-151.

Pizzi, A. (1994). Tannin-based wood adhesives. Advanced wood adhesives Technology. Marcel Dekker, Inc. New York, Basel, Hong Kong. Chapter. 5.

Pizzi, A. and Mittal, K.L. (1994). Handbook of adhesives technology. Marcel Dekker Inc., New York.

Pizzi, A. and Scharffeter, H. O. (1981). Adhesives and techniques open new possibilities for the wood processing industry. Part 1: Experiment with tannin based adhesives. *Holz Roh-Werkstoff* **39**: 85-89.

Plomley, K. F. (1966). Tannin-formaldehyde adhesives for wood. II. Wattle tannin adhesives. CSIRO Div. *For. Prod. Technol*. No. **39**.

Plomley, K. F. 1959. The effect of soluble salts on the gelation of tannin formaldehyde. *Aust. J. Appl*. *Sci*. **10**: 494-497.

Pu, S., Yoshioka M. and Shiraishi. N. (1994). Liquefaction of wood in phenol and its application to adhesives. In: Adhesives and Bonded Wood Products. Eds. C. Y. Hse., B. Tomita and S. J. Branham, Forest Products Society Proceedings No. **4735**: 344-355.

Rodriguez-Nogales, J. M., Ortega N, Perez-Mateos, M. and Busto M. D. (2007). Experimental design and response surface modeling applied for the optimization of pectin hydrolysis by enzymes from A. niger CECT 2088. *Food Chem* **101** (2): 634-642.

Roffael, E. and Dix, B. (1991). Lignin and ligninsulfonate in non-conventional bonding - an overview. *Holz Roh- Werkstoff* **49**: 199-205.

Roldan, E., Sanchez-Moreno, C., de Ancos, B. and Cano, M. P. (2008). Characterization of onion (Allium cepaL.) by-productsas food ingredients with antioxidant and antibrowning properties. *Food Chem*. **108** (3): 907 – 916.

Roux, D. G. 1951. Photometric methods of tannin analysis for black wattle tannin. J. Soc. Leather Trades' Chem. 35: 322.

Santana, A. E., Baumann, M. G. D. and Conner, A. H. (1995). Resol Resins Prepared with Tannin Liquified in Phenol. *Holzforschung* **49**: 146 – 152

Santana, M. A. E. and Filho, M. S. (1983). Desenvolvimento de adesivos tanio formaldeido: efeito da quantidade de carga na qualidade de colagem. *Silvicultura* **28**: 863-867.

Savitzky, A. and Golay, J. E. (1964). Smoothing and differentiation of data by simplified least squares procedures. *Anal Chem*. 36(1): 1627 – 1639.

Schimleck, L. R., Michell, A. J., Raymond, C. A. and Muneri, A. (1998). Assessment of the pulpwood quality of standing trees using near infrared spectroscopy. *Journal of Near Infrared Spectroscopy* **6**: 117-123

Schimleck, L. R., Wright, P. J., Michell, A. J. and Wallis, A. F. A. (1997). NIR Infrared spectra and chemical compositions of E.globulus and E.nitens wood. *Appita* **50**: 40-46

Schimleck, L.R. and Yazaki; Y. (2003). Analysis of Pinus radiata D. Don Bark by Near Infrared Spectroscopy. *Holzforscchung* **57**: 520 - 526.

Schwanninger, M. and Hinterstoisser, B. (2001) Determination of the lignin content in wood by FT- NIR. 11th ISWPC, International Symposium on Wood and Pulping Chemistry, Nice, France, Vol. III, 641-644

Sellers, T. Jr. (2001). Wood Adhesive Innovations and Applications in North America. *Forest Products Journal*. **51**(6): 12-22

Sellers, T. Jr.(1985). Plywood and Adhesive Technology. New York: Marcel Dekker, Inc.

Sellers, T., Jr. (1990). Lignins from organic solvent pulped wood and brown-rotted wood have successfully replaced a portion of phenol in phenol-formaldehyde resins. *Panel World* **31**(5): 26-29.

Sellers, T.Jr. and Miller, M. D. Jr. (2004). Laboratory manufacture of high moisture southern pine strandboard bonded with three tannin adhesive types. *Forest Products Journal*. **54** (12): 296 – 301

Shenk, J.S. and Westerhaus, M.O., (1991). Population definition, sample selection, and calibration procedures for near infrared reflectance spectroscopy. *Crop Sci*. **31**: 469-474.

Shenk, J.S., and Westerhaus, M.O. (1995). Analysis of Agriculture and Food Products by Near Infrared Reflectance Spectroscopy. Infrasoft International, Port Matilda, PA.

Shenk, J.S., Westerhaus, M.O. and Abrams, S.M. (1989). Protocol for NIRS calibration: Monitoring analysis results and recalibration. In: Near Infrared Reflectance Spectroscopy (NIRS): Analysis of Forage Quality. Agriculture Handbook. USDA, Washington, DC.

Shenk, J.S., Workman, J.J. and Westerhaus, M.O. (1992). Application of NIR spectroscopy to agricultural products. In: Handbook of Near Infrared Analysis. Burns, D.A. and Ciurczak, E.W. (eds). Marcel Dekker, new York.

Shiraishi, N., Itoh, H. and Lonikar, S.V. (1987). Adhesives prepared from hydroxyethylated wood with or without explosion pre-treatment. *J. Wood Chem. Tech*. **7** (3): 405-426.

Silva, E. M., Souza, J. N. S., Rogez, H., Rees, J. F. and Larondelle, Y.(2007). Antioxidant activities and polyphenolic contents of fifteen selected plant species from the Amazonian region, *Food Chem* 101: 1012-1018.

So, S. and Rudin, A. (1990). Analysis of the Formation and Curing Reactions of Resole Phenolics, *J. Appl. Polym. Sci*, 41 (1-2) 205 - 232,

Sowunmi, S. Corner, A. H., River, B. H. and Ebwele, R. O. (1996). *J Appl Polym Sci* **62**: 577

Stone, M., (1974). Cross-validatory choice and assessment of statistical predictions. *J. R. Stat. Soc*. **36**:111-133.

Sudesh, S., Meenakshi, M., Sheeja, R. Y. and Thanapalan, M. (2010). Optimization studies on biosorption of copper (II) by crab shell using response surface methodology. *Chemical Product and Process Modeling* **5:**1

Treybal, R. E. (1980). Mass Transfer Operations, 3rd ed., McGraw-Hill, New York.

Vazquez, G., Antorrena, G., Parajo, J. C, and Francisco, J. L. (1989). Preparation of wood adhesives by polycondensation of phenolic acids from Pinus pinaster bark with resoles, *Holz Rob- Werkstoff* **47**: 491 494

Vazquez, G., Antorrena, G. and Parajo, J. C. (1986). Selection of operational conditions in alkaline lixiviation of Pinus pinaster bark. *Holz Roh- Werkstoff* **44** 415 418

Vazquez, G., Antorrena, G. and Parajo, J. C. (1987). Studies on utilization of Pinus pinaster bark. Part 2: Kinetics and contents of alkaline extractions. *Wood Sci. Technol.* **44**: 155 166

Vazquez, G., Gonzalez-Alzarez, J., Freire, S., Lopez-Suevos, F. and Antorrena, G. (2001). Characteristics of Pinus pinaster bark extracts obtained under different extraction conditions. *Holz als Roh-und Werkstoff* **59**: 451-456.

Ven, C. V. D., Gruppen, H., Bont, D. B. A. and Voragen, A. G. J. (2002). Optimization of the angiotensin converting enzyme inhibition by whey protein hydrolysates using response surface methodology. *International Dairy Journal* **12**: 813-820.

von Leyser, E.and Pizzi, A. (1990). The formulation and commercialisation of glulam pine tannin adhesives in Chile. *Holz als Roh-und Werkstoff* **48**: 25-29.

Walker, J. F. (1964). Formaldehyde. ACS Monograph No. 159. 3 Ed. New York: Reinhold Publication Co.

Wang, J., Sun, B., Cao, Y.P., Tian, Y. & Li, X.H. (2008). Optimization of ultrasound-assisted extraction of phenolic compounds from wheat bran. *Food Chemistry* **106**: 804-810.

Werstler, D.D. (1986). Quantitative ^{13}C n.m.r. characterization of aqueous formaldehyde resins: 1. Phenol-formaldehyde resins. Polymer. 27(5): 750-756

Wright, J.A., Birkett M.D. and Grambino, M.J.T. (1990). Prediction of pulp content and cellulose content from wood samples using near infrared reflectance spectroscopy. *Tappi J*. 164 - 166.

Williams, P.C., (1975). Applications of near-infrared spectrometry to analysis of cereal grains and oilseeds. Cereal Chemistry **52**: 561-576.

Yap, C.F., Ho, C.W., Wan Aida, W.M., Chan, S.W., Lee C.Y. and Leong, Y. S. (2009) Optimization of Extraction Conditions of Total Phenolic Compounds from Star Fruit (Averrhoa carambola L.) Residues. *Sains Malaysiana.* **38**(4): 511–520

Yazaki, Y. (1983). Ultrafiltration of extracts from *Pinus radiata* bark. *Holzforschung* **52**:185-190

Yazaki, Y. (1985). Improved ultrafiltration of Extracts from *Pinus radiata* bark. *Holzforschung*, **39**: 79-83.

Yazaki, Y. and Collins, P. J. (1994). Wood adhesives based on tannin extracts from barks of some pine and spruce species. *Holz als Roh Werkstoff* **52**: 307-310.

Yazaki, Y. and Hillis, W. E. (1980). Molecular size distribution of radiata pine bark extracts and its effect on properties. *Holzforschung*. **34**: 125 – 130.

APPENDICES

Appendix 1: NIRS fitted calibration data for Stiasny number and polyphenol and tannin content.

Polyphenolic content		Tannin content		Stiasny number	
Actual value	NIRS predicted value	Actual value	NIRS predicted value	Actual value	NIRS predicted value
17.8	17.95	10.58	10.66	82.0	82.80
17.8	18.09	10.58	10.75	69.8	71.78
18	18.09	10.7	10.76	78.8	79.40
18.6	18.63	11.06	11.1	82.0	84.00
18.2	18.19	10.82	10.81	75.2	73.64
18.6	18.98	11.06	11.33	75.2	73.71
17.6	17.65	10.46	10.54	77.0	75.82
17.7	18.1	10.52	10.77	71.2	69.81
18.4	18.38	11.04	10.99	79.0	79.80
18.8	18.36	11.18	10.94	79.0	81.00
19.5	19.35	11.6	11.61	83.0	84.00
18.9	18.91	11.34	11.34	84.0	82.00
19	18.82	11.4	11.28	69.5	70.24
19.3	19.24	11.58	11.54	68.7	67.20
20.9	20.56	12.54	12.25	78.8	78.33
20.4	20.44	12.24	12.25	72.3	72.96
18.9	18.78	11.34	11.24	78.8	78.22
18.3	18.52	10.98	11.12	78.0	77.72
19.8	20.04	11.88	12.02	81.0	82.00
20.1	19.99	12.06	11.99	73.4	75.00
18.3	18.15	10.98	10.94	81.4	82.00
19.4	19.22	11.64	11.52	86.0	85.00
19.1	19.01	11.46	11.41	68.4	68.06
19.4	19.34	11.64	11.58	69.5	72.60
19.2	19.25	11.52	11.54	68.7	68.92
19.8	19.69	11.88	11.79	70.9	72.40
19.1	19.22	11.46	11.52	68.4	70.00
20.7	20.68	12.42	12.41	74.1	74.03
19.9	19.83	11.94	11.9	71.2	70.99
19.8	19.46	11.88	11.69	70.9	69.67

20	20.2	12	12.1	71.6	72.32
19.5	20.1	11.7	12.05	69.8	71.96
20.4	20.31	12.24	12.19	73.0	72.71
19.8	20.08	11.88	12.06	70.9	71.89
19.5	19.59	11.7	11.77	69.8	70.13
19.2	19.19	11.52	11.49	68.7	68.70
19.8	19.9	11.88	11.96	70.9	71.24
19.5	19.71	11.7	11.83	69.8	70.56
17.4	17.53	10.44	10.49	77.8	78.80
17.7	17.74	10.62	10.68	79.0	79.90
17	17.1	10.2	10.25	83.4	84.00
20.8	20.81	12.48	12.46	74.5	74.50
18.9	18.86	11.34	11.3	67.7	67.52
18.8	18.43	11.28	11.06	67.3	65.98
18.4	18.36	11.04	11.01	65.9	65.73
20.7	20.87	12.42	12.5	83.7	83.00
19.5	20.05	11.7	12.03	78.0	79.40
18.2	18.51	10.92	11.1	82.0	82.60
21.4	21.45	12.84	12.87	78.0	78.60
21	20.57	12.6	12.34	77.0	76.00
21	20.59	12.6	12.36	82.0	82.50
21.5	21.18	12.9	12.71	79.0	78.20
19.9	19.5	11.94	11.7	78.4	78.90
18.8	18.58	11.28	11.14	65.9	65.80
19.5	19.69	11.7	11.81	67.3	65.73
18.9	18.86	11.34	11.3	69.8	69.27
19.3	19.74	11.58	11.85	67.7	67.70
19.4	19.62	11.64	11.77	68.0	67.38
19.2	18.77	11.52	11.25	69.1	68.88
22	21.88	13.2	13.13	74.8	73.60
20.2	20.38	12.12	12.22	73.0	73.18
22	21.85	13.2	13.11	67.7	67.23
21.8	21.71	13.08	13.02	65.5	66.30
20.3	20.32	12.18	12.18	70.9	71.74
20.5	20.08	12.3	12.03	72.0	71.56
20	20.49	12	12.3	65.5	64.98
20.5	20.28	12.3	12.18	73.4	72.60
19.7	19.18	11.82	11.54	70.5	68.66
20.88	20.89	12.54	12.55	74.8	74.79
19.81	19.83	11.88	11.92	70.9	70.99
20.2	20.17	12	12.08	72.3	72.21
20	19.98	12	12	71.6	71.53
19.55	19.57	11.7	11.74	70.0	70.06

18.23	18.25	10.92	10.94	65.3	65.30
20.7	20.68	12.42	12.39	74.1	74.03
18.6	18.55	11.16	11.08	66.6	66.41
18.92	19.83	11.34	11.66	67.7	70.99
19.52	19.54	11.7	11.73	69.9	69.95
19.6	19.55	11.76	11.53	70.2	69.99
22	21.98	13.2	13.21	74.1	74.54
22.5	22.45	13.5	13.5	75.2	74.00
22.4	22.28	13.44	13.37	68.4	70.14
21	21.08	12.7	12.63	72.6	72.50
19.2	19.19	11.62	11.55	74.8	71.86
19.5	19.52	11.8	11.59	75.9	74.03
19.3	19.5	11.68	11.8	75.2	72.93
20.52	20.58	12.34	12.46	74.1	73.68
20.38	20.44	12.28	12.36	74.2	73.04
18.7	19	11.32	11.54	76.1	77.53
20.9	20.89	12.5	12.5	74.4	76.28
19.84	19.82	11.8	11.9	74.1	73.17
20.14	20.17	12.1	12.1	74.8	74.33
20	19.98	12.2	12.2	86.4	86.80
19.55	19.57	11.72	11.73	76.3	75.32
18.22	18.25	10.91	10.93	74.1	74.82
20.7	20.68	12.4	12.36	69.6	71.21
18.6	18.57	11.15	11.1	71.8	72.22
18.6	19.43	11.3	11.6	73.9	73.42
19.5	19.52	11.72	11.74	68.4	71.25
19.5	19.23	11.75	11.65	65.1	65.45
22	21.96	13.3	13.31	66.2	64.89
22.5	22.45	13.52	13.52	63.6	64.48
22.4	22.28	13.4	13.38	74.2	74.93
21	21.08	12.72	12.68	71.8	69.34
19.2	19	11.65	11.55	70.3	69.51
19.5	19.2	11.85	11.75	87.0	87.20
19.43	19.53	11.68	11.86	74.4	75.20
20.48	20.58	12.44	12.46	72.9	73.60
20.35	20.4	12.38	12.36	68.0	69.80
18.8	19	11.32	11.34	80.0	79.20

Appendix 2: Analysis of variance of optimization models.

Aqueous acetone extraction when tannin content is maximized.

Source	Sum of Squares	df	Mean Square	F Value	p-value Prob > F
Model	78.17	4	19.54	4.76	0.0061
A-Temp	*5.63*	*1*	*5.63*	*1.37*	*0.254*
D-L/S ratio	*8.35*	*1*	*8.35*	*2.03*	*0.1673*
AD	*10.56*	*1*	*10.56*	*2.57*	*0.1225*
A^2	*3.86*	*1*	*3.86*	*0.94*	*0.3427*
Residual	94.5	23	4.11		
Lack of Fit	*94.5*	*20*	*4.72*		
Pure Error	*0*	*3*	*0*		
Cor Total	172.67	27			
Std. Dev.	2.03		R-Squared	0.4527	
Mean	10.45		Adj R-Squared	0.3575	
C.V. %	19.4		Pred R-Squared	0.1758	
PRESS	203.02		Adeq Precision	7.005	

Aqueous acetone extraction when sugar content is minimized.

Source	Sum of Squares	df	Mean Square	F Value	p-value Prob > F
Model	9.17	4	2.29	9.08	0.0001
A-Temp	*6*	*1*	*6*	*23.77*	*< 0.0001*
B-Time	*0.23*	*1*	*0.23*	*0.92*	*0.3476*
D-L/S ratio	*0.34*	*1*	*0.34*	*1.35*	*0.2568*
BD	*0.063*	*1*	*0.063*	*0.25*	*0.6235*
Residual	5.81	23	0.25		
Lack of Fit	*5.28*	*20*	*0.26*	*1.49*	*0.4194*
Pure Error	*0.53*	*3*	*0.18*		
Cor Total	14.98	27			
Std. Dev.	0.5		R-Squared	0.6123	
Mean	3.13		Adj R-Squared	0.5449	
C.V. %	16.06		Pred R-Squared	0.3955	
PRESS	9.05		Adeq Precision	9.753	

Aqueous acetone extraction when Stiasny number is maximized.

Source	Sum of Squares	df	Mean Square	F Value	p-value Prob > F
Model	266.42	3	88.81	3.45	0.0323
B-Time	*132.54*	*1*	*132.54*	*5.16*	*0.0324*
D-L/S ratio	*148.07*	*1*	*148.07*	*5.76*	*0.0245*
BD	*182.25*	*1*	*182.25*	*7.09*	*0.0136*
Residual	617.01	24	25.71		
Lack of Fit	*567.01*	*21*	*27*	*1.62*	*0.3885*
Pure Error	*50*	*3*	*16.67*		
Cor Total	883.43	27			
Std. Dev.	5.07		R-Squared	0.3016	
Mean	78.86		Adj R-Squared	0.2143	
C.V. %	6.43		Pred R-Squared	0.0705	
PRESS	821.19		Adeq Precision	5.348	

Aqueous ethanol extraction when tannin content is maximized.

Source	Sum of Squares	df	Mean Square	F Value	p-value Prob > F
Model	286.97	7	41	12.92	< 0.0001
A-Temp	*126.04*	*1*	*126.04*	*39.72*	*< 0.0001*
B-Time	*35.04*	*1*	*35.04*	*11.04*	*0.0034*
C-Conc	*2.04*	*1*	*2.04*	*0.64*	*0.4319*
D-L/S ratio	*63.38*	*1*	*63.38*	*19.97*	*0.0002*
AC	*22.56*	*1*	*22.56*	*7.11*	*0.0148*
BD	*14.06*	*1*	*14.06*	*4.43*	*0.0481*
A_2	*23.84*	*1*	*23.84*	*7.51*	*0.0126*
Residual	63.46	20	3.17		
Lack of Fit	*45.46*	*17*	*2.67*	*0.45*	*0.8797*
Pure Error	*18*	*3*	*6*		
Cor Total	350.43	27			
Std. Dev.	1.78		R-Squared	0.8189	
Mean	14.36		Adj R-Squared	0.7555	
C.V. %	12.41		Pred R-Squared	0.6669	
PRESS	116.72		Adeq Precision	13.259	

Aqueous ethanol extraction when sugar content is minimized.

Source	Sum of Squares	df	Mean Square	F Value	p-value Prob > F
Model	14.32	5	2.86	12.14	< 0.0001
A-Temp	*7.8*	*1*	*7.8*	*33.05*	*< 0.0001*
B-Time	*2.02*	*1*	*2.02*	*8.55*	*0.0078*
C-Conc	*0.29*	*1*	*0.29*	*1.23*	*0.2792*
D-L/S ratio	*2.31*	*1*	*2.31*	*9.78*	*0.0049*
AC	*1.9*	*1*	*1.9*	*8.07*	*0.0095*
Residual	5.19	22	0.24		
Lack of Fit	*3.52*	*19*	*0.19*	*0.33*	*0.944*
Pure Error	*1.67*	*3*	*0.56*		
Cor Total	19.51	27			
Std. Dev.	0.49		R-Squared	0.7339	
Mean	3.45		Adj R-Squared	0.6734	
C.V. %	14.06		Pred R-Squared	0.5975	
PRESS	7.85		Adeq Precision	13.476	

Aqueous ethanol extraction when Stiasny number is maximized.

Source	Sum of Squares	df	Mean Square	F Value	p-value Prob > F
Model	545.52	4	136.38	5.82	0.0022
A-Temp	*3.38*	*1*	*3.38*	*0.14*	*0.7078*
B-Time	*247.04*	*1*	*247.04*	*10.54*	*0.0036*
D-L/S ratio	*145.04*	*1*	*145.04*	*6.19*	*0.0205*
AB	*150.06*	*1*	*150.06*	*6.4*	*0.0187*
Residual	538.91	23	23.43		
Lack of Fit	*497.91*	*20*	*24.9*	*1.82*	*0.3454*
Pure Error	*41*	*3*	*13.67*		
Cor Total	1084.43	27			
Std. Dev.	4.84		R-Squared	0.503	
Mean	77.64		Adj R-Squared	0.4166	
C.V. %	6.23		Pred R-Squared	0.2267	
PRESS	838.54		Adeq Precision	8.535	

Aqueous NaOH extraction when tannin content is maximized.

Source	Sum of Squares	df	Mean Square	F Value	p-value Prob > F
Model	288.31	10	28.83	2.81	0.0296
A-Temp	*23.07*	*1*	*23.07*	*2.24*	*0.1524*
B-Time	*38.08*	*1*	*38.08*	*3.71*	*0.0711*
C-Conc	*68.59*	*1*	*68.59*	*6.67*	*0.0193*
D-L/S ratio	*7.79*	*1*	*7.79*	*0.76*	*0.396*
AB	*9.13*	*1*	*9.13*	*0.89*	*0.3591*
AC	*48.54*	*1*	*48.54*	*4.72*	*0.0442*
AD	*25.8*	*1*	*25.8*	*2.51*	*0.1315*
BC	*1.04*	*1*	*1.04*	*0.1*	*0.7543*
BD	*39.06*	*1*	*39.06*	*3.8*	*0.0679*
CD	*25.14*	*1*	*25.14*	*2.45*	*0.1362*
Residual	174.69	17	10.28		
Lack of Fit	*154.69*	*14*	*11.05*	*1.66*	*0.3765*
Pure Error	*20*	*3*	*6.67*		
Cor Total	463	27			
Std. Dev.	3.21		R-Squared	0.6227	
Mean	24.5		Adj R-Squared	0.4008	
C.V. %	13.08		Pred R-Squared	-0.1405	
PRESS	528.04		Adeq Precision	7.805	

Aqueous NaOH extraction when Stiasny number is maximized.

Source	Sum of Squares	df	Mean Square	F Value	p-value Prob > F
Model	2780.23	5	556.05	10.52	< 0.0001
A-Temp	*221.8*	*1*	*221.8*	*4.2*	*0.0526*
B-Time	*1.54*	*1*	*1.54*	*0.029*	*0.8659*
C-Conc	*2.3*	*1*	*2.3*	*0.044*	*0.8365*
BC	*162.07*	*1*	*162.07*	*3.07*	*0.0939*
A_2	*166.13*	*1*	*166.13*	*3.14*	*0.0901*
Residual	1162.74	22	52.85		
Lack of Fit	*1127.74*	*19*	*59.35*	*5.09*	*0.1026*
Pure Error	*35*	*3*	*11.67*		
Cor Total	3942.96	27			
Std. Dev.	7.27		R-Squared	0.7051	
Mean	58.04		Adj R-Squared	0.6381	
C.V. %	12.53		Pred R-Squared	0.5254	
PRESS	1871.22		Adeq Precision	11.769	

Aqueous NaOH extraction when sugar content is minimized.

Source	Sum of Squares	df	Mean Square	F Value	p-value Prob > F
Model	853.42	5	170.68	9.27	< 0.0001
A-Temp	*91.51*	*1*	*91.51*	*4.97*	*0.0363*
B-Time	*5.2*	*1*	*5.2*	*0.28*	*0.6005*
C-Conc	*0.48*	*1*	*0.48*	*0.026*	*0.8735*
BC	*41.08*	*1*	*41.08*	*2.23*	*0.1494*
A_2	*71.28*	*1*	*71.28*	*3.87*	*0.0618*
Residual	405.01	22	18.41		
Lack of Fit	*380.26*	*19*	*20.01*	*2.43*	*0.2539*
Pure Error	*24.75*	*3*	*8.25*		
Cor Total	1258.43	27			
Std. Dev.	4.29		R-Squared	0.6782	
Mean	34.64		Adj R-Squared	0.605	
C.V. %	12.39		Pred R-Squared	0.4673	
PRESS	670.4		Adeq Precision	11.235	

Water extraction when tannin content is maximized.

Source	Sum of Squares	df	Mean Square	F Value	p-value Prob > F
Model	2.22	6	0.37	5.42	0.0078
A-Temp	*0.046*	*1*	*0.046*	*0.68*	*0.4278*
B-Time	*0.78*	*1*	*0.78*	*11.49*	*0.006*
C-L/S ratio	*0.23*	*1*	*0.23*	*3.31*	*0.096*
AB	*0.34*	*1*	*0.34*	*4.93*	*0.0484*
BC	*0.28*	*1*	*0.28*	*4.13*	*0.067*
A_2	*0.9*	*1*	*0.9*	*13.19*	*0.0039*
Residual	0.75	11	0.068		
Lack of Fit	*0.75*	*8*	*0.094*		
Pure Error	*0*	*3*	*0*		
Cor Total	2.96	17			
Std. Dev.	0.26		R-Squared	0.7474	
Mean	9.04		Adj R-Squared	0.6096	
C.V. %	2.88		Pred R-Squared	0.2809	
PRESS	3.8		Adeq Precision	9.036	

Water extraction when sugar content is minimized.

Source	Sum of Squares	df	Mean Square	F Value	p-value Prob > F
Model	2.3	9	0.26	8.2	0.0035
A-Temp	*1.14*	*1*	*1.14*	*36.46*	*0.0003*
B-Time	*0.1*	*1*	*0.1*	*3.3*	*0.1067*
C-L/S ratio	*0.024*	*1*	*0.024*	*0.78*	*0.4025*
AB	*0.14*	*1*	*0.14*	*4.6*	*0.0644*
AC	*3.29E-03*	*1*	*3.29E-03*	*0.11*	*0.7536*
BC	*0.02*	*1*	*0.02*	*0.64*	*0.4463*
A_2	*0.21*	*1*	*0.21*	*6.63*	*0.0329*
B_2	*5.38E-05*	*1*	*5.38E-05*	*1.73E-03*	*0.9679*
C_2	*0.13*	*1*	*0.13*	*4.11*	*0.0771*
Residual	0.25	8	0.031		
Lack of Fit	*0.24*	*5*	*0.048*	*19.35*	*0.0172*
Pure Error	*7.50E-03*	*3*	*2.50E-03*		
Cor Total	2.55	17			
Std. Dev.	0.18		R-Squared	0.9022	
Mean	1.79		Adj R-Squared	0.7921	
C.V. %	9.84		Pred R-Squared	0.1988	
PRESS	2.04		Adeq Precision	9.392	

Water extraction when Stiasny number is maximized.

Source	Sum of Squares	df	Mean Square	F Value	p-value Prob > F
Model	136.4	5	27.28	4.23	0.0189
A-Temp	*1.2*	*1*	*1.2*	*0.19*	*0.6737*
B-Time	*27.56*	*1*	*27.56*	*4.27*	*0.061*
C-L/S ratio	*10.56*	*1*	*10.56*	*1.64*	*0.2248*
A_2	*89.75*	*1*	*89.75*	*13.92*	*0.0029*
C_2	*25.68*	*1*	*25.68*	*3.98*	*0.0692*
Residual	77.38	12	6.45		
Lack of Fit	*77.38*	*9*	*8.6*		
Pure Error	*0*	*3*	*0*		
Cor Total	213.78	17			
Std. Dev.	2.54		R-Squared	0.638	
Mean	89.11		Adj R-Squared	0.4872	
C.V. %	2.85		Pred R-Squared	0.4817	
PRESS	316.75		Adeq Precision	7.14	

Appendix 3: Analysis of variance of resin properties.

Table A.1 Effect of resin parameters from aqueous extracted tannins.

ANOVA

		Sum of Squares	df	Mean Square	F	Sig.
Viscosity	Between Groups	530407.600	4	132601.900	29.926	.000
	Within Groups	44309.333	10	4430.933		
	Total	574716.933	14			
Pot life	Between Groups	12804.667	4	3201.167	126.362	.000
	Within Groups	253.333	10	25.333		
	Total	13058.000	14			
Dry shear strength	Between Groups	.625	4	.156	7.092	.006
	Within Groups	.220	10	.022		
	Total	.845	14			
Wet shear strength	Between Groups	.427	4	.107	3.241	.060
	Within Groups	.330	10	.033		
	Total	.757	14			
Delamination	Between Groups	578.000	4	144.500	3.750	.041
	Within Groups	385.333	10	38.533		
	Total	963.333	14			

Table A.2 Effect of resin parameters from aqueous acetone extracted tannins.

ANOVA

		Sum of Squares	df	Mean Square	F	Sig.
Viscosity	Between Groups	36203.667	3	12067.889	1.455	.298
	Within Groups	66364.000	8	8295.500		
	Total	102567.667	11			
Pot life	Between Groups	344.250	3	114.750	21.857	.000
	Within Groups	42.000	8	5.250		
	Total	386.250	11			
Dry shear strength	Between Groups	.098	3	.033	.712	.572
	Within Groups	.369	8	.046		
	Total	.467	11			
Wet shear strength	Between Groups	.084	3	.028	1.389	.315
	Within Groups	.161	8	.020		
	Total	.245	11			
Delamination	Between Groups	181.583	3	60.528	.458	.719
	Within Groups	1056.667	8	132.083		
	Total	1238.250	11			

Table A.3 Effect of resin parameters from aqueous ethanol extracted tannins.

ANOVA

		Sum of Squares	df	Mean Square	F	Sig.
Viscosity	Between Groups	1227274.267	4	306818.567	62.337	.000
	Within Groups	49219.333	10	4921.933		
	Total	1276493.600	14			
Pot life	Between Groups	12881.733	4	3220.433	145.065	.000
	Within Groups	222.000	10	22.200		
	Total	13103.733	14			
Dry bond strength	Between Groups	1.209	4	.302	10.484	.001
	Within Groups	.288	10	.029		
	Total	1.498	14			
Wet bond strength	Between Groups	.860	4	.215	8.168	.003
	Within Groups	.263	10	.026		
	Total	1.123	14			
Delamination	Between Groups	1474.267	4	368.567	5.230	.016
	Within Groups	704.667	10	70.467		
	Total	2178.933	14			

Table A.4 Effect of resin parameters from aqueous NaOH extracted tannins.

ANOVA

		Sum of Squares	df	Mean Square	F	Sig.
Viscosity	Between Groups	7790534.933	4	1947633.733	430.321	.000
	Within Groups	45260.000	10	4526.000		
	Total	7835794.933	14			
Pot life	Between Groups	23057.733	4	5764.433	181.271	.000
	Within Groups	318.000	10	31.800		
	Total	23375.733	14			
Dry shear strength	Between Groups	1.446	4	.362	15.026	.000
	Within Groups	.241	10	.024		
	Total	1.687	14			
Wet shear strength	Between Groups	2.963	4	.741	26.818	.000
	Within Groups	.276	10	.028		
	Total	3.239	14			
Delamination	Between Groups	8278.933	4	2069.733	40.424	.000
	Within Groups	512.000	10	51.200		
	Total	8790.933	14			

Table A.5 Effect of resin parameters resulting from optimization method used to extract tannins.

ANOVA

		Sum of Squares	df	Mean Square	F	Sig.
Viscosity	Between Groups	2712339.583	4	678084.896	2.973	.029
	Within Groups	10490099.750	46	228045.647		
	Total	13202439.333	50			
Pot life	Between Groups	18614.260	4	4653.565	35.771	.000
	Within Groups	5984.250	46	130.092		
	Total	24598.510	50			
Dry bond strength	Between Groups	1.257	4	.314	4.853	.002
	Within Groups	2.979	46	.065		
	Total	4.236	50			
Wet bond strength	Between Groups	1.615	4	.404	6.303	.000
	Within Groups	2.947	46	.064		
	Total	4.562	50			
Delamination	Between Groups	3219.755	4	804.939	3.566	.013
	Within Groups	10384.167	46	225.743		
	Total	13603.922	50			

Table A.6 Effect of resin parameters resulting from type of solvent used to extract tannins.

ANOVA

		Sum of Squares	df	Mean Square	F	Sig.
Viscosity	Between Groups	11020913.083	4	2755228.271	58.097	.000
	Within Groups	2181526.250	46	47424.484		
	Total	13202439.333	50			
Pot life	Between Groups	22750.926	4	5687.732	141.610	.000
	Within Groups	1847.583	46	40.165		
	Total	24598.510	50			
Dry bond strength	Between Groups	1.976	4	.494	10.052	.000
	Within Groups	2.260	46	.049		
	Total	4.236	50			
Wet bond strength	Between Groups	1.776	4	.444	7.330	.000
	Within Groups	2.786	46	.061		
	Total	4.562	50			
Delamination	Between Groups	5583.422	4	1395.855	8.006	.000
	Within Groups	8020.500	46	174.359		
	Total	13603.922	50			

Appendix 4: Graphs of the different predictive extraction models.
The colours indicate low (blue) to high (red) values.

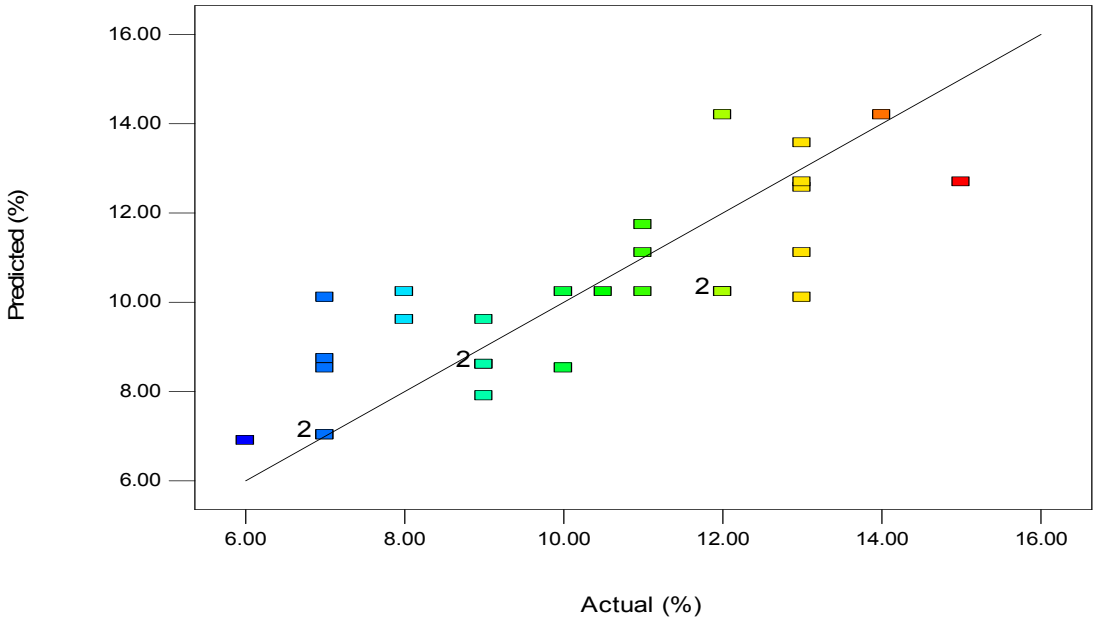


Figure A1: Actual experimental values versus predicted values for tannin content using aqueous acetone as extraction solvent (Equation 4.1).

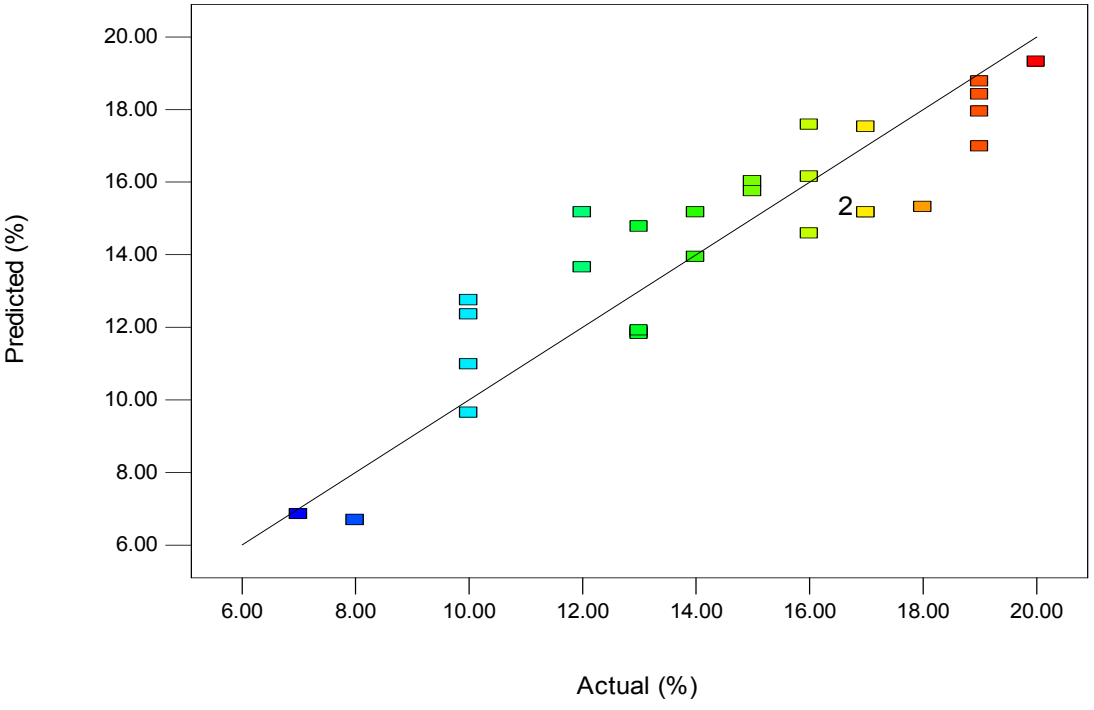


Figure A2: Actual experimental values versus predicted values for tannin content using aqueous ethanol as extraction solvent (Equation 4.2)

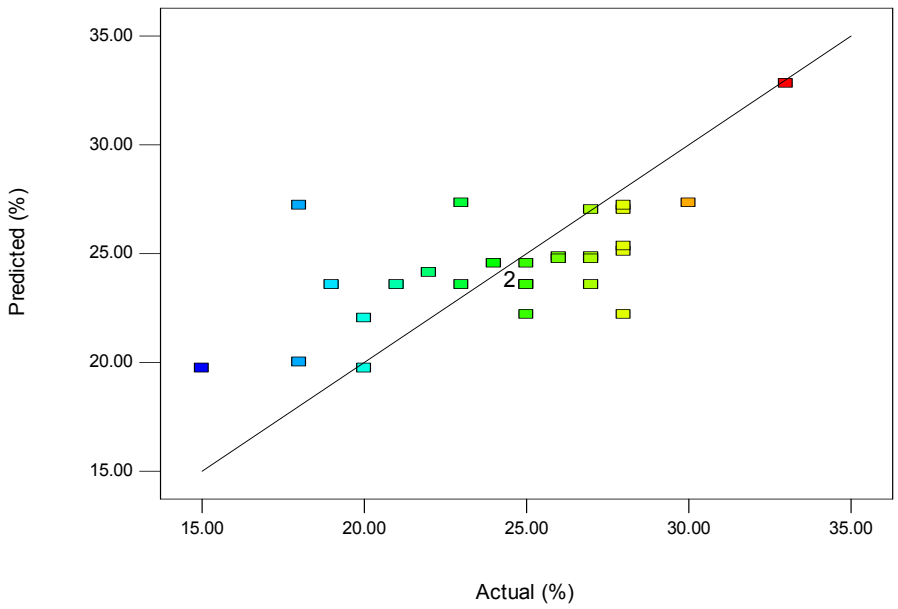


Figure A3: Actual experimental values versus predicted values for tannin content using aqueous NaOH as extraction solvent Equation (4.3).

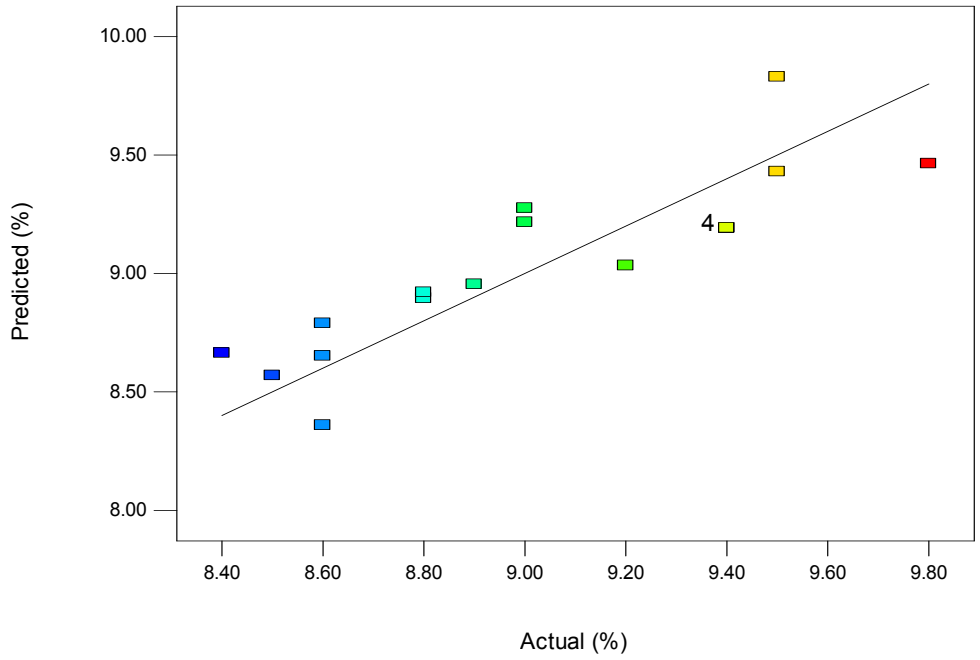


Figure A4: Actual experimental values versus predicted values for tannin content using water as extraction solvent (Equation 4.4)

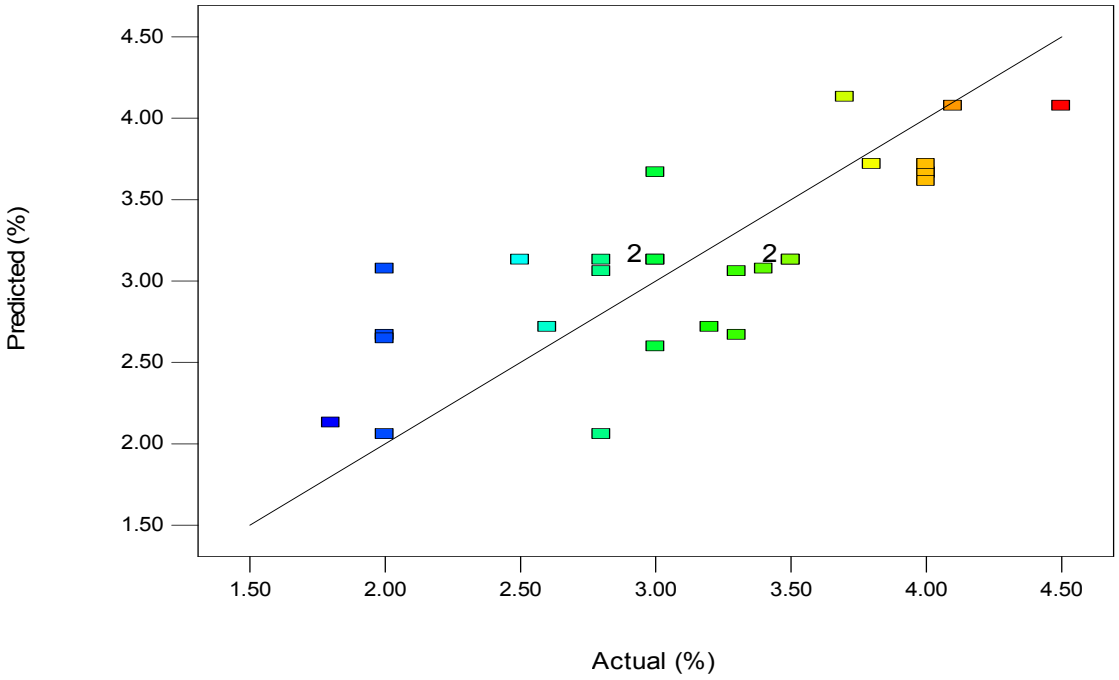


Figure A5: Actual experimental values versus predicted values for sugar content using aqueous acetone as extraction solvent Equation (4.5).

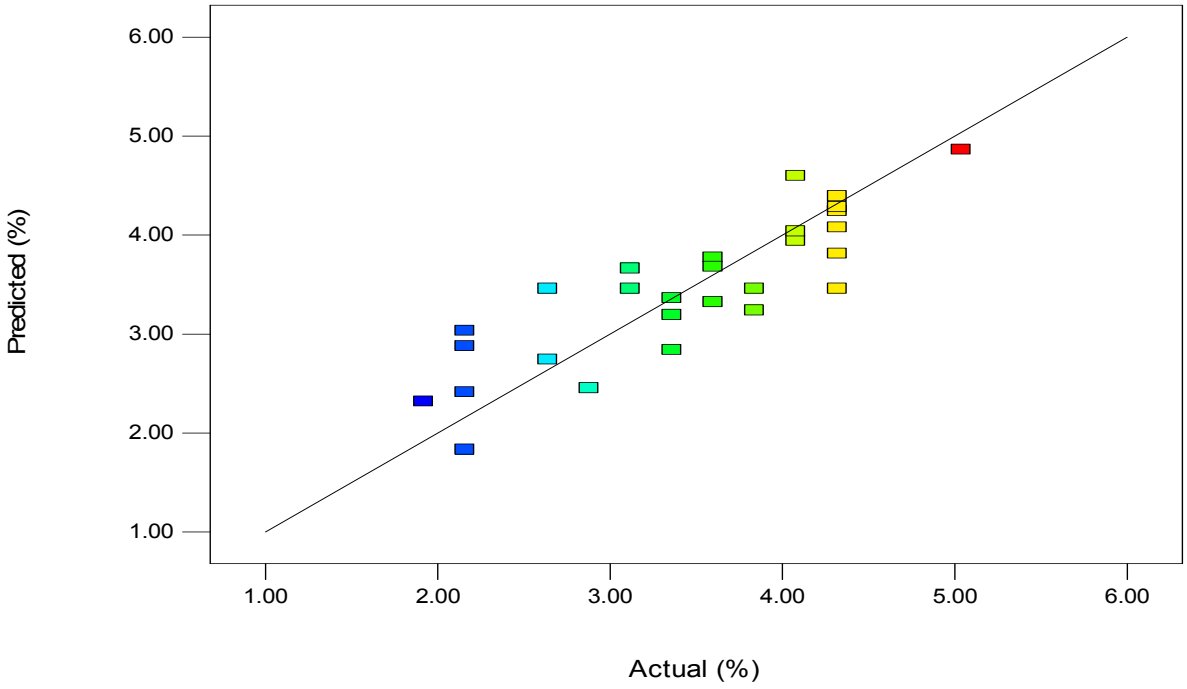


Figure A6: Actual experimental values versus predicted values for sugar content using aqueous ethanol as extraction solvent (Equation 4.6)

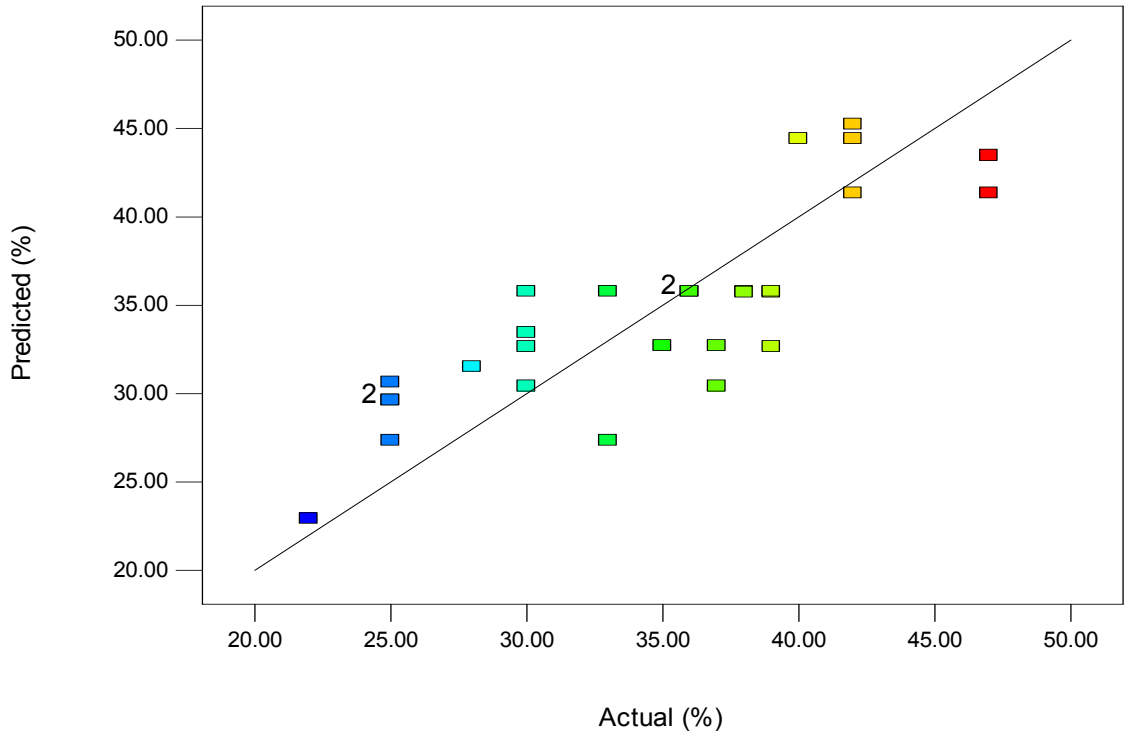


Figure A7: Actual experimental values versus predicted values for sugar content using aqueous NaOH as extraction solvent (Equation 4.7).

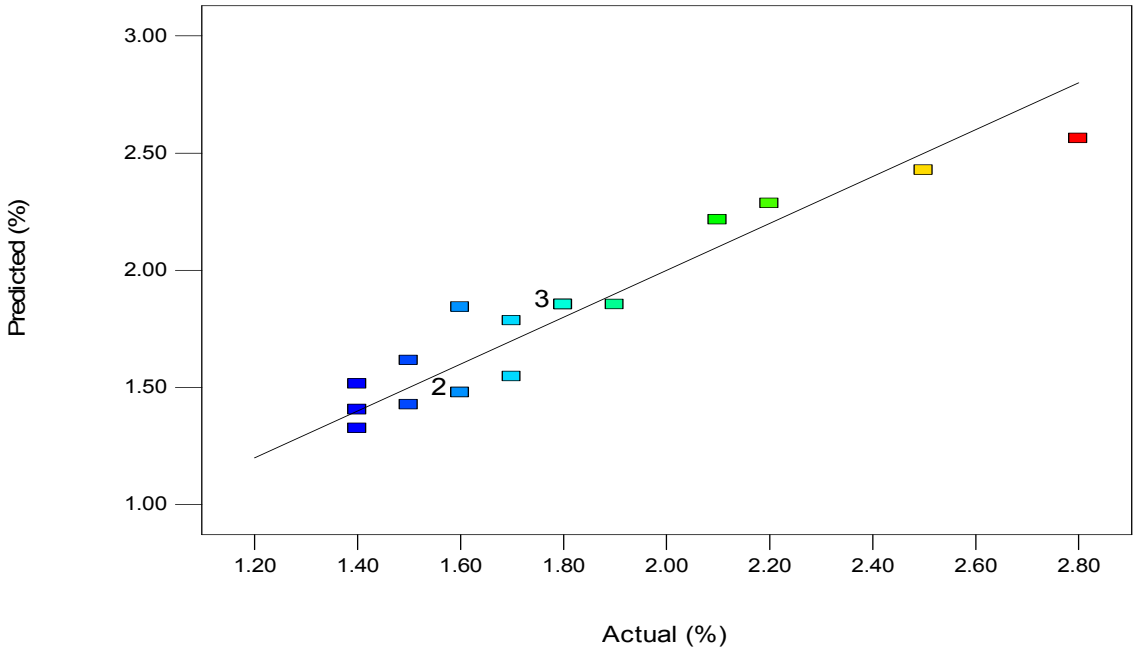


Figure A8: Actual experimental values versus predicted values for sugar content using water as extraction solvent (Equation 4.8)

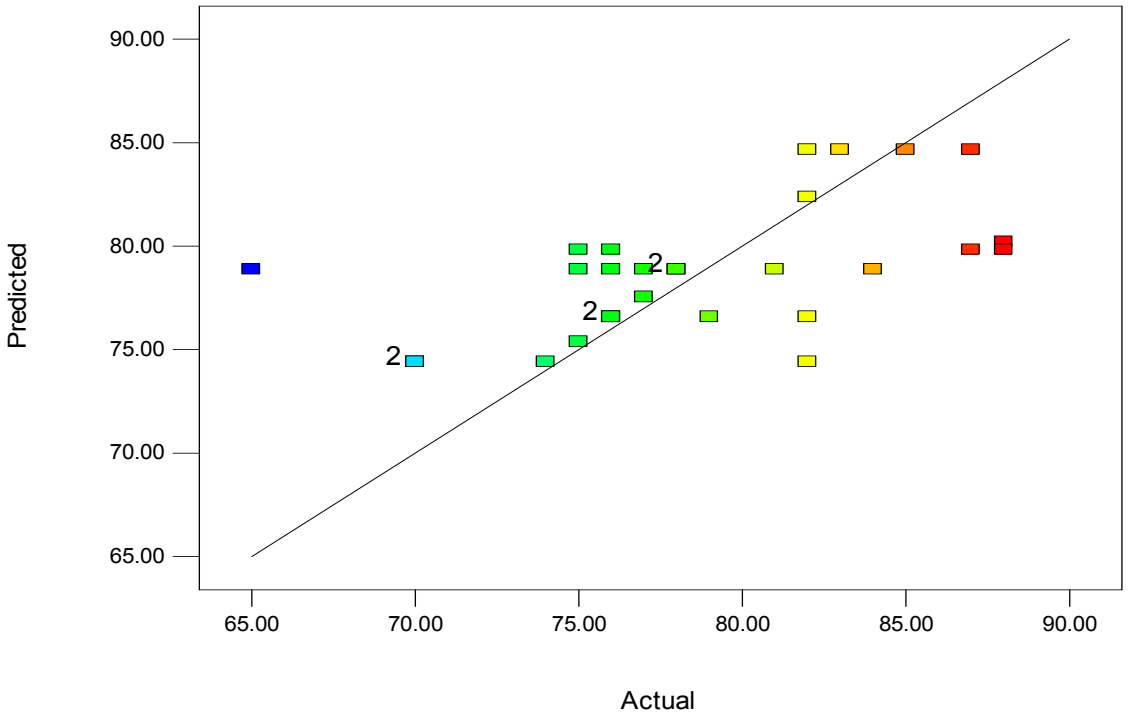


Figure A9: Actual experimental values versus predicted values for Stiasny number using aqueous acetone as extraction solvent Equation 4.9

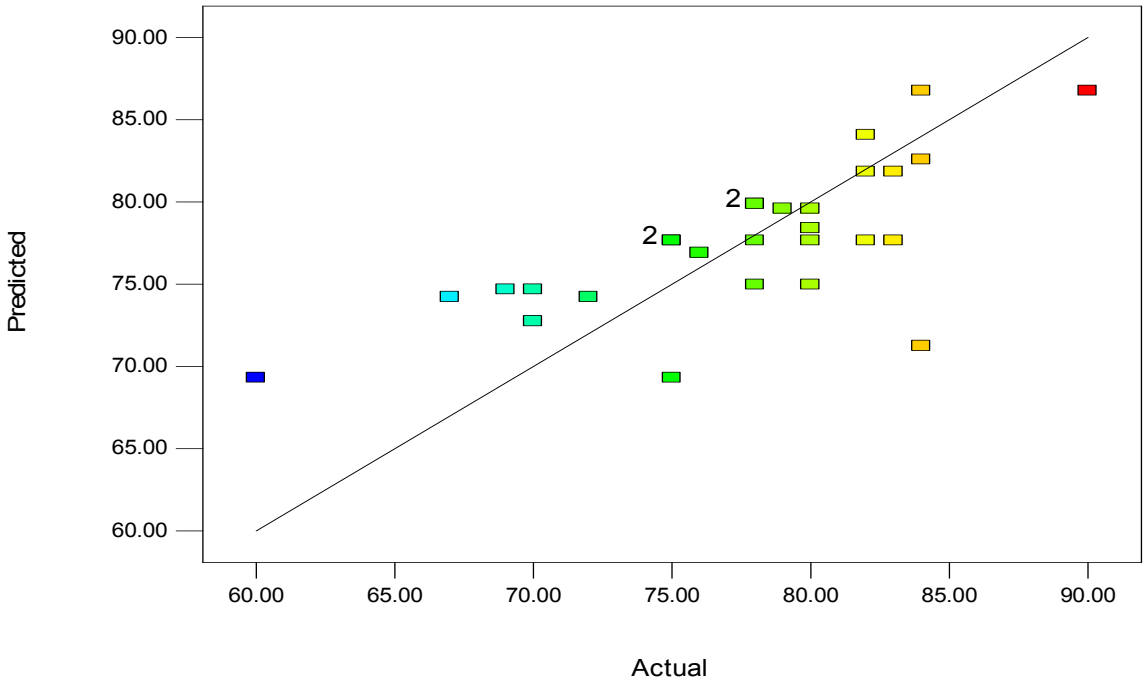


Figure A10: Actual experimental values versus predicted values for Stiasny number using aqueous ethanol as extraction solvent (Equation 4.10).

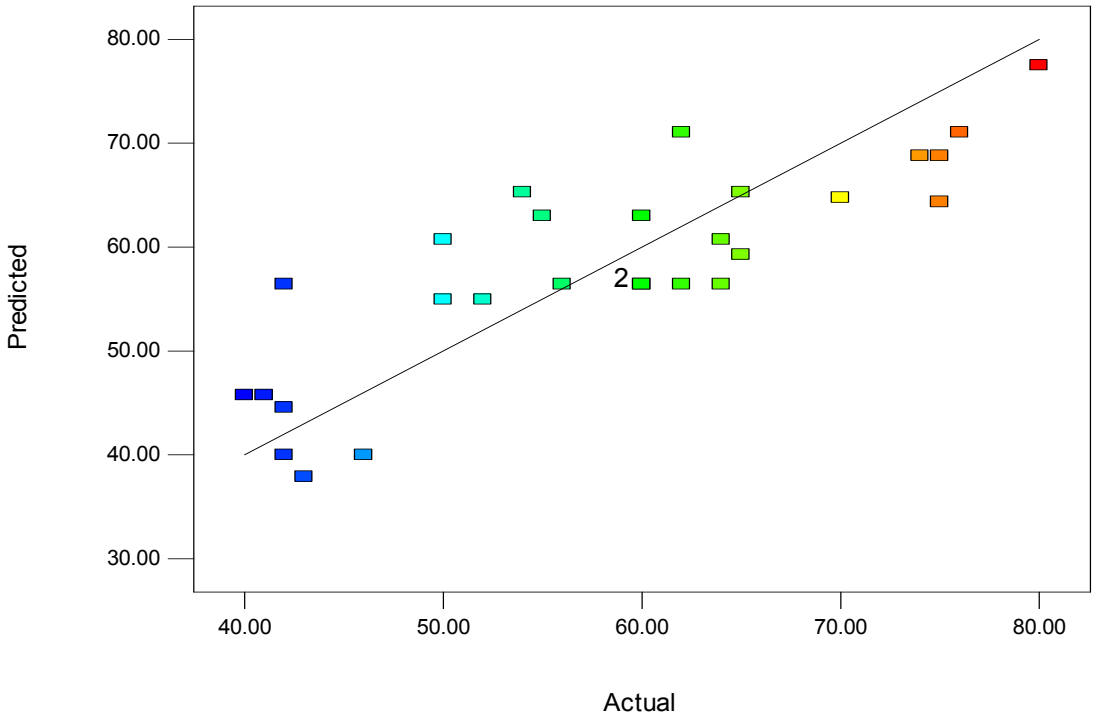


Figure A11: Actual experimental values versus predicted values for Stiasny number using aqueous NaOH as extraction solvent Equation 4.11

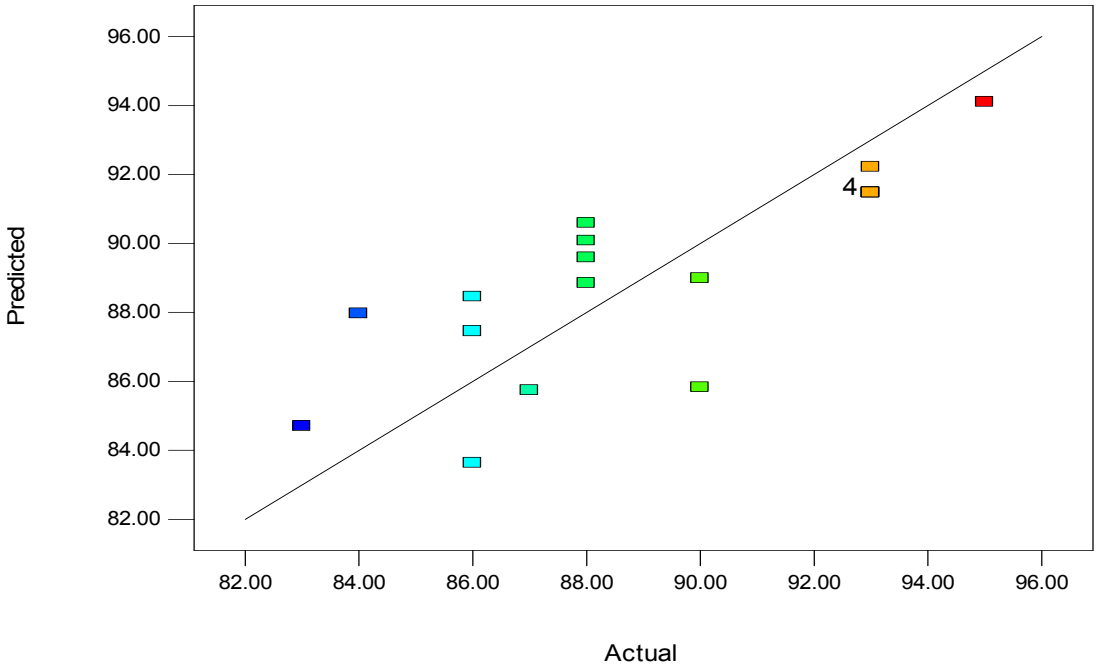


Figure A12: Actual experimental values versus predicted values for Stiasny number using water as extraction solvent (Equation 4.12).

Appendix 5: *Pinus caribaea* Morelet Description (Orwa et al. 2009)

BOTANIC DESCRIPTION

Pinus caribaea is a fine tree to 20-30 m tall, often 35 m, with a diameter of 50-80 cm and occasionally up to 1 m; trunk generally straight and well formed; lower branches large, horizontal and drooping; upper branches often ascending to form an open, rounded to pyramidal crown; young trees with a dense, pyramidal crown. Leaves needlelike, crowded and spreading at ends of twigs, remaining attached for 2 years, in fascicles of 3-5, mostly 15-25 cm long, 1.5 mm broad or less, rigid serrulate, dark or yellowish-green, slightly shiny, with stomata in whitish lines on all surfaces.

ECOLOGY

This species grows best in frost-free areas up to about 700 m in more fertile sites with good subsoil drainage and annual rainfall of 2000-3000 mm. Generally at elevations of 600-800 m it is associated with *P. oocarpa* var. hondurensis and *P.oocarpa* var. ochoterenai. *P. caribaea* is rated as moderately fire resistant. It tolerates salt winds and hence may be planted near the coast.

DOCUMENTED SPECIES DISTRIBUTION

Native: Bahamas, Colombia, Cuba, Guatemala, Honduras, Mexico, Nicaragua, Panama
Exotic: Australia, Brazil, Canada, Costa Rica, Gambia, Ghana, Guyana, India, Indonesia, Jamaica, Kenya, Madagascar, Malawi, Malaysia, Mozambique, Nigeria, Philippines, Puerto Rico, Sierra Leone, South Africa, Sri Lanka, Sudan, Surinam, Tanzania, Trinidad and Tobago, Uganda, United States of America, Venezuela, Zambia, Zimbabwe



P. Caribaea, young seedlings in nursery.

(David Boshier)



Extensive natural stands of *P. caribaea*, Peten, Guatemala

(Colin E. Hughes)



P. caribaea plantation stand, Kumasi, Ghana
(Derkyi, N. S. A.)

Appendix 6: List of Publications

1. **Derkyi Nana S.A.**, Adu-Amankwa Benjamin, Sekyere Daniel and Darkwa Nicholas A. (2011) Optimum Acetone and Ethanol Extraction of Polyphenols from *Pinus caribaea* Bark: Maximizing Tannin Content Using Response Surface Methodology. *Chemical Product and Process Modeling*: Vol. 6: Iss. 1, pp. 24.

2. **Derkyi N. S.A,** Adu-Amankwa B, Sekyere D, and Darkwa N. A. (2011). Optimization of Process Parameters Using Response Surface Methodology for the Extraction of Formaldehyde-Condensable Phenolics from Pine Bark. *Journal of Emerging Trends in Engineering and Applied Sciences* (JETEAS) 2 (1): 64-69.

3. **Derkyi N. S.A,** Adu-Amankwa B, Sekyere D, and Darkwa N. A. (2011). Application of Near Infrared Spectroscopy in Chemometric Modeling of Tannin Content and Stiasny Number of *Pinus caribaea* Bark. *Journal of Emerging Trends in Engineering and Applied Sciences* (JETEAS) 2 (1): 132-136.

4. **Derkyi N. S.A,** Adu-Amankwa B, Sekyere D, and Darkwa N. A. (2011). Rapid Prediction of Extractives and Polyphenolic Contents in *Pinus caribaea* Bark Using Near Infrared Reflectance Spectroscopy. *International Journal of Applied Sciences* (IJAS), Vol. 2: (1): 1 – 11.

5. **Derkyi, Nana S. A**.; Sekyere, Daniel; Darkwa, Nicholas A.; and Boakye, Nana B. (2011). Modeling and Optimization of Polyphenol Extraction for Tannin-Formaldehyde Resin Synthesis. *International Journal of Chemical Reactor Engineering* (IJCRE) Vol. 9: pp. 21.

6. **Derkyi N. S.A,** Adu-Amankwa B, Sekyere D, and Darkwa N. A. (2011). Rapid Prediction of Extractives Contents in *Pinus caribaea* Bark Using Near Infrared Reflectance Spectroscopy. *International Journal of Pure and Applied Chemistry* (IJPAC) Vol 6 (3): 377-383.